Octopus and dendrimer molecules with silsesquioxane cores

Thesis

Octopus and Dendrimer Molecules with Silsesquioxane Cores

A Thesis Presented to The Open University
for the Degree of Doctor of Philosophy

By

Theresa Eileen Gentle, B.Sc. (Educ.), B.Sc. (Chem.), M.Sc. (Chem.)

Department of Chemistry
The Open University
January, 1995

To my husband, Tom
and children, Tommy and Cecilia

DECLARATION

I grant the powers of discretion to the University Librarian to allow the thesis to be copied in whole or in part without further reference to me. This permission covers only single copies made for study purposes, subject to the normal condition of acknowledgement.

Signed

Theresa E. Gentle

January, 1995

STATEMENT

The work embodied in this thesis was carried out by the author during the period April 1991 to December 1994 in the Department of Chemistry at the Open University and at the Dow Corning Corporation, under the supervision of Dr. A. R. Bassindale.

Signed

Theresa E. Gentle

January, 1995

ACKNOWLEDGEMENTS

I would like to express my appreciation to Dow Corning Corporation for the financial support of this work.

I am especially grateful to my advisor, Dr. Alan Bassindale for his technical guidance in this work and his encouragement throughout these studies.

I could not have taken on this challenge without the support and encouragement of my husband, Tom. Throughout the past four years of this work, his understanding and patience has been immeasurable.

I am grateful to my parents for instilling in me the appreciation of the importance of education and the motivation to strive for higher goals.

I would like to acknowledge several of my Dow Corning colleagues for their technical assistance including Robin Hickerson for running GPC samples, Sharon Grienke for help obtaining GC/MS analyses, Jenny Starrine, Justin Clayman, and Jeff Janowicz for general lab assistance, Dr. Tom Lane, Dr. Steve Snow, Maris Ziemilis and Mike Lutz for their helpful technical discussions, and John Blizzard for his evaluation of materials for scratch resistant coatings. The support and encouragement of Dr. Michael Owen, my Dow Corning work supervisor, was also instrumental in the completion of this work.

ABSTRACT

OCTOPUS AND DENDRIMER MOLECULES WITH SILSESQUIOXANE CORES

The interest in materials with designed physical properties and controlled molecular formula is increasing. Octopus molecules, or materials with pendent groups from a core, and dendrimer molecules, or materials with a defined pattern of branching from a core are means of obtaining molecules of designed architecture. The work presented here involves the synthesis and characterization of octopus and dendrimer molecules of defined shape with molecular weights well into the thousands.

These designed molecular materials have been synthesized by placing pendant groups symmetrically about a silsesquioxane [$(SiO_{3/2})_8$] core. A facile, one-step route to hydrocarbon and siloxane functional octopus molecules via H_2PtCl_6 catalyzed hydrosilylation of 1-alkenes and vinyl-functional siloxanes by T_8 hydrogen silsesquioxane, $(HSiO_{3/2})_8$, has been demonstrated. The chemistry of addition was studied, and it was found that while the addition of the 1-alkenes to T_8 was regioprecise with only α-addition being observed, both α- and β-addition occurred with vinyl siloxanes. In addition, H/vinyl exchange on silicon was observed to occur with addition of vinyl-siloxane to T_8. The effect of the hydrosilylation catalyst, homogeneous and heterogeneous, on the regioselectivity of addition and on the

extent of exchange on silicon has been evaluated via GPC and ^{13}C and ^{29}Si NMR.

Investigations into the feasibility of placing a number of other moieties on the silsesquioxane core to show the almost limitless types of functional octopus molecules that can be made and to expand into dendritic molecules were also accomplished. For example polyether functional and mixed polyether/siloxane functional octopus molecules were synthesized and found to have interesting surface activity. The synthesis of an acrylate functional octopus molecule was accomplished and the product used to produce an ultra-violet curable coating.

Finally, routes other than hydrosilylation to produce octopus and dendrimer molecules with silsesquioxane cores, for instance, the reaction of ROH with SiH of $(HSiO_{3/2})_8$, were developed and used to increase the types of functional octopus possible and to produce dendrimer molecules with silsesquioxane cores. The synthesis, characterization, and possible applications of silsesquioxane-based octopus and dendrimer molecules will be discussed.

TABLE OF CONTENTS

LIST OF FIGURES

LIST OF TABLES

GLOSSARY OF TERMS

Me	$-CH_3$
Et	$-CH_2CH_3$
Pr^i	$-CH_2(CH_3)_2$
Bu	n-C_4H_9 (n-butyl unless otherwise specified)
M	Me_3Si-O-
D	$-O-SiMe_2-O-$
T	
Q	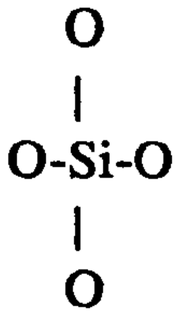
NMR	Nuclear Magnetic Resonance Spectroscopy
GPC	Gel Permeation Chromatography (also called Size Exclusion Chromatography)
FTIR	Fourier Transform Infrared Spectroscopy
GC	Gas Chromatography
GC/MS	Gas Chromatography/Mass Spectroscopy

Chapter One

General Introduction and Background

1.1 Octopus and Dendrimer Molecules

The desire for materials with designed physical properties and controlled molecular formula is increasing as will become apparent in this review of macromonomers. Star polymers, octopus molecules, and dendrimers are some types of designed molecular materials with potentially unique physical properties. Throughout this work, the terms star, octopus, and dendrimer will be used to define a particular type of design as shown in the schematics in Figure 1.1 show. A star polymer generally refers to a molecule with pendent groups off a single central atom or short linear chain. An octopus molecule is differentiated by being a molecule with pendant groups originating from a more complex core species. Materials with sequential and patterned branching from a core, whether a single atom core or more complex core, are considered dendrimers, sometimes called cascade polymers or starburst polymers.

Term	Configuration
Star	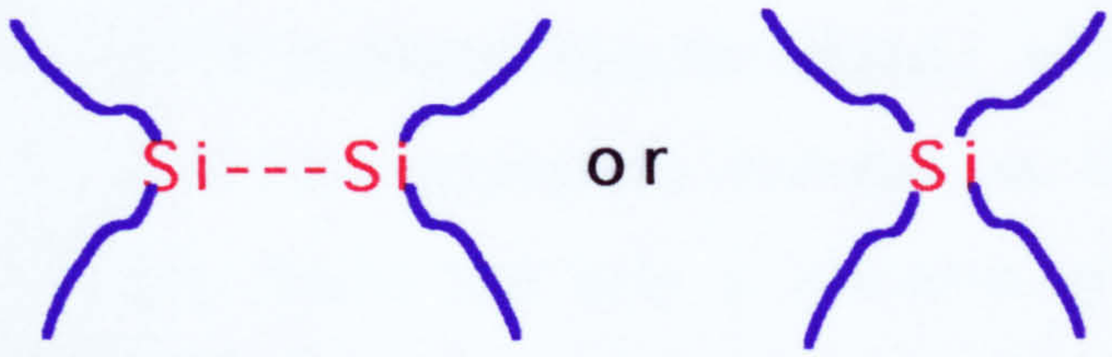
Octopus	
Dendrimer Starburst Cascade	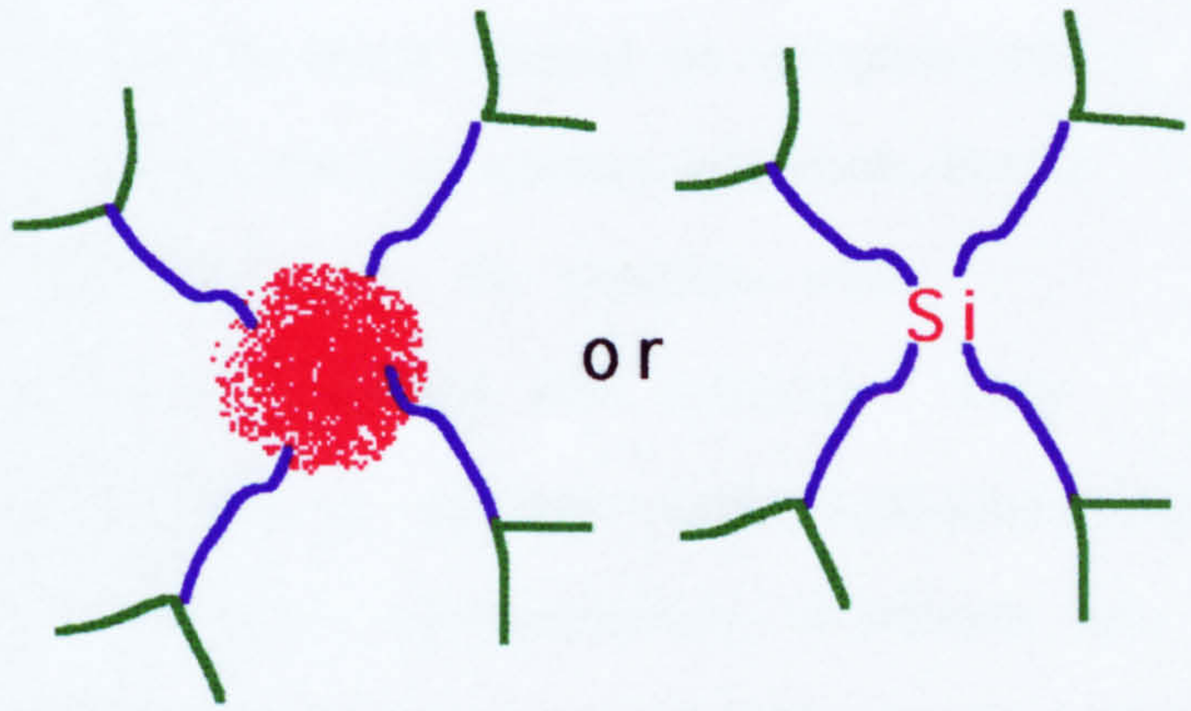

Figure 1.1 Star, octopus, and dendrimer configurations of macromolecules as defined in this work.

The considerable interest in these types of molecules is apparent from the growing literature on these materials[1-74]. A number of different strategies have been used to make molecules with these unusual architectures. In looking specifically at silicon containing materials, as far back as 1966, there was research on star polymers reported by Gervasi and Gosnell[1]. They were interested in preparing branched polystyrene with the ultimate aim of studying the effect of branching on the properties of polystyrene. They reacted $PhCHCH_2(PhCHCH_2)_n PhCHCH_2Li$ with $Cl_3SiCH_2CH_2SiCl_3$ hoping to place six polystyrene branches on the $SiCH_2CH_2Si$ core. However, they found that only a maximum of four branches could be added to the $Cl_3SiCH_2CH_2SiCl_3$. Roovers and Toporowski later found that all six polystyrene branches could be placed on the $SiCH_2CH_2Si$ core if the styryllithium ends of $PhCHCH_2(PhCHCH_2)_n PhCHCH_2Li$ were converted to isoprenyllithium ends[2].

In 1971 Roovers and Bywater similarly aimed to prepare star polystyrene molecules[3]. They used a similar approach but started with $MeCl_2SiCH_2CH_2SiMeCl_2$ in the reaction with $R(PhCHCH_2)_n Li$ to obtain a four branched star material. They later reported on characterization by osmotic and light-scattering techniques, intrinsic viscosities, and sedimentation coeffients of these star polymers[4].

Masuda, Ohta, and Onogi also prepared four branched star polystyrene but used $SiCl_4$ as the core[5]. They reacted $R(PhCHCH_2)_n Li$ with $SiCl_4$ and found that they could get on

average between 2.6 and 3.8 of the four chlorines replaced with polystyrene branches after prolonged reaction times.

Even more highly branched materials were made by Hadjichristidi *et al*[6]. Using octachlorosilane [$Si(CH_2CH_2SiCl_2R)_4$] and dodecachlorosilane [$Si(CH_2CH_2SiCl_3)_4$] as the cores, the authors claimed to have made eight- and twelve-armed polyisoprenes. Hadjichristidi[7] later reported obtaining a 18-armed polyisoprene by using dicaoctachlorosilane, $(CH_2Si(CH_2CH_2SiCl_3)_3)_2$, as the linking agent and sec- or tert-butyllithium as the initiator.

Pearson, Mueller, Fetters, and Hadjichristida compared physical properties of linear versus star-branched polyisoprenes[8]. They found that the branched polymers showed increased tensile viscosities relative to the linear polymers of the same molecular weight. Roovers, Hadjichristida, and Fetters investigated the dilute solution properties of these star polymers and found that these highly branched polymers behaved hydrodynamatically like hard spheres in dilute solution[9].

Long *et al*[10] prepared star polymers having styrene branches terminated with phenyltrimethoxysilyl functionality. These star polymers were useful as well-defined precursors for a controlled sol-gel process. Further branching of the trimethoxysilyl terminated ends of the arms of the star polymer could lead to starburst or dendrimer molecules.

The star polymers discussed above are ones with entirely or mostly organic branches. Examples of star polymers with siloxane arms are also known[11-18]. Tverdokhlebova *et al*[11] synthesized three- and four-armed star poly(dimethylsiloxane) polymers via the reaction of $BuMe_2Si(OSiMe_2)_nOLi$ with $MeSiCl_3$ for the three-armed star and with $SiCl_4$ for the four-armed star polymer.

Kazama *et al*[12] used monofunctional carboxy-terminated siloxanes in a reaction with $Al(OPr^i)_3$ or $Ti(OPr^i)_4$ to make three- and four-armed siloxane star molecules.

Another unusual siloxane-containing star polymer was one prepared by Fujimoto *et al*[13]. This star-shaped polymer had three branches, each of a different composition. The three branches were a polystyrene branch, a poly(dimethylsiloxane branch), and a poly(t-butylmethacrylate) branch. This molecule was prepared from coupling the polystyryl anion with end-reactive monofunctional siloxane, followed by anionic propagation of t-butyl methacrylate.

Sinyagina *et al*[14] have also prepared siloxane star polymers. Base catalyzed ring-opening polymerization of cis-2,4,6-trimethyl-2,4,6-triphenylcyclotrisiloxane in methanol formed the arms which were then reacted with a core of $GeCl_4$ or $SnCl_4$ to form the star polymers.

Dickstein and Lillya[15] synthesized star-shaped poly(dimethylsiloxanes) of defined structure using a blocked

amine functional anionic initiator, the reaction product of *p*-[N,N-Bis(trimethylsilyl)amino]styrene and sec-butyllithium[16]. Once initiated, a living anionic polymerization of hexamethylcyclotrisiloxane (D_3) was done to form the arms that were terminated with tetrachlorosilane to form the blocked, star polymer, each branch of which had a multifunctional terminus[15].

Using the same technique as described above, Bhattacharya, Smith, and Dickstein synthesized rigid-rod star-block copolymers with varying numbers of arms[17]. These copolymers consisted of flexible poly(dimethylsiloxane) cores with two to six arms, at the ends of which 4-[(methoxybenzoyl)oxy]benzoic acid segments were attached through amide linkages[17]. With these molecules, the authors found clear evidence of phase separation between the flexible siloxane segment and the rigid blocks and the polymers showed nematic liquid-crystalline texture in optical microscopy[17].

Morikawa *et al*[18] prepared three-armed siloxane star polymers trimethyl-terminated via anionic ring opening polymerization of hexamethylcyclotrisiloxane (D_3) initiated by 1,3,5-benzenetri(lithium dimethylsilanolate) and terminated by trimethylchlorosilane. They also terminated with 3-benzyloxypropyldimethylchlorosilane, which upon hydrogenation, a hydroxy-terminated star polymer was obtained. When ε-caprolactone was reacted with the lithium salt of the terminal alcohol, a three-armed polysiloxane-poly-ε-caprolactone star block copolymer was obtained.

In looking specifically at the octopus type of molecular design, the approach of using a planar, but highly functionalized hydrocarbon core from which polyether ligands extend outward has been reported[19-25]. An example of one such molecule is shown in Figure 1.2. These molecules were originally named 'octopus" because they were used to encase a metal ion in their 'tentacle' pendant groups[19]. Examples of the hydrocarbon cores used for the above octopus molecules are benzene, napthalene, biphenyl, and calix[n]arenes[19-25].

Conner, Kudelka, and Regen[26] made a series of polyether functional calix[6]arene octopus molecules via the alkylation of 37,38,39,40,41,42-hexahydroxycalix[6]arene with a series of brominated poly(ethylene glycol) monomethyl ethers [i.e., $CH_3O(CH_2CH_2O)_n CH_2CH_2Br$, where n = 0, 1, 2, and 3]. They studied the orientation of the polyether "tentacles" of these octopus molecules at the air/water interface upon surface compression.

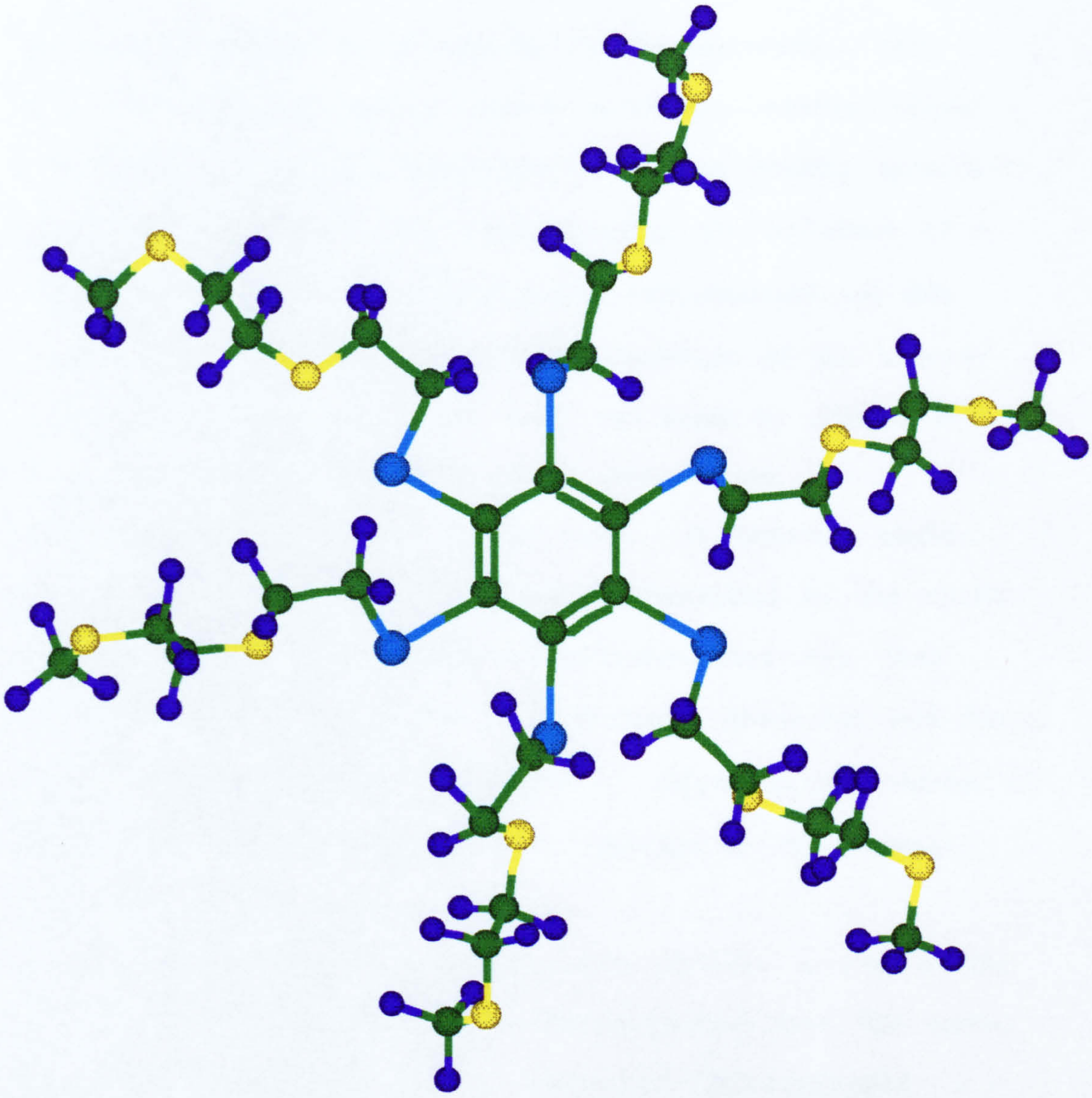

a.

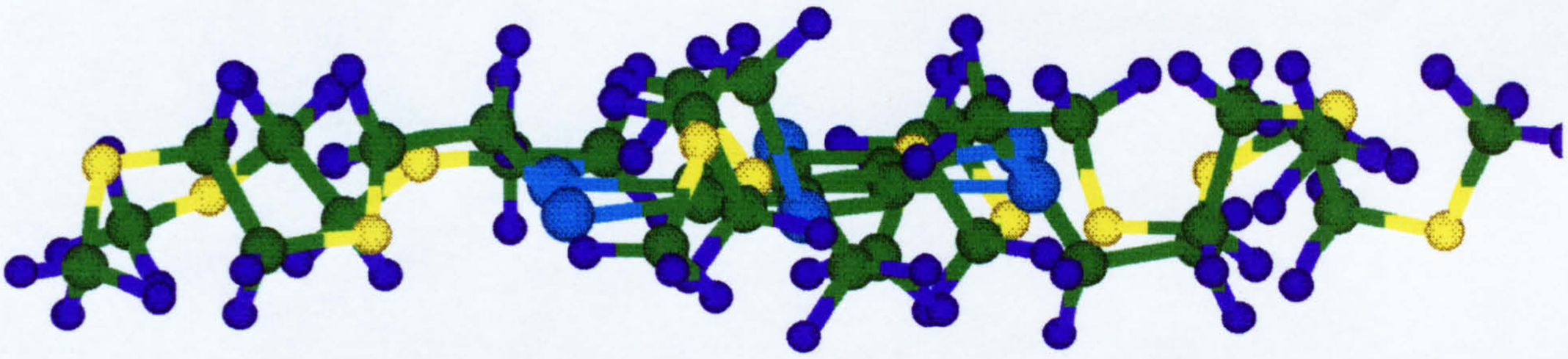

b.

Figure 1.2 Planar octopus molecule with benzene core, a. view from above, b. cross-sectional view.
From: Conner, M.; Kudelka, I.; Regen, S.L. *Langmuir* **1991**, 7, 982-987.
Green=Carbon, Yellow=Oxygen, Cyan=Sulfur, Blue=Hydrogen.

The above examples are of organic octopus molecules. Our search of silicon containing octopus molecules, whether silicon was in the core or the appendages, turned up nothing specifically termed "octopus" molecules, however, using the definition of a more complex core with appendages, a few examples of this configuration were found. A siloxane molecule of the 'octopus' configuration as defined in this work was made by Zhu, *et al*[27]. They used the SiH containing cyclic tetrasiloxane, tetramethylcyclotetrasiloxane as the core. A terminal olefin bearing silyl acetal group was then hydrosilylated by the cyclic siloxane and methyl methacrylate polymerization was then initiated using the acetate ion as a catalyst. Molecules with the cyclic core and arms of d.p. (degree of polymerization, number of repeat units) 20-150 per arm were obtained in this manner.

An octopus molecule of sorts with silica particles serving as the cores and poly(dimethylsiloxane) chains grafted onto the cores was made by Edwards *et al*[28]. Silanol (Si-OH) terminated poly(dimethylsiloxane) was grafted onto the silica in a heptane/EtOH mixture. The interest in these materials was for studying the stability of colloidal dispersions.

The next level of complexity of design beyond an octopus molecule with chains extending from the core is a dendrimer, often called starburst or cascade polymers, in which concentric branched 'layers' are built up from a core. In a classic paper on starburst dendrimers, Tomalia, *et al*[29] help define dendrimers by stating that "dendrimers differ from classical monomers/oligomers by their extraordinary symmetry, high

branching and maximized (telechelic) terminal functionality density."[29] The authors differentiate dendrimers from starburst polymers by stating that "chemically bridging these dendrimers leads to the new class of macromolecules - starburst polymers."[29] However, in the literature these two terms, dendrimers and starburst polymers, are often used interchangeably.

Many different approaches to producing dendrimer materials have been reported. The terms divergent synthesis and convergent synthesis are often used when discussing dendrimers. Divergent synthesis is used to describe an approach whereby the the macromolecule is built from the core outward. Convergent synthesis generally refers to building the arms or branches and then connecting them to the core.

Tomalia and coworkers have been one of the most active groups on the research of starburst or dendrimer molecules[29-35]. In a series of papers[29, 31-35], Tomalia and coworkers reported on the preparation of polyamido-amine dendrimers starting from an amine initiator core such as ammonia. Michael addition of the core with methyl acrylate and then exhaustive amidation of the resulting esters with ethylenediamine yielded what they called the zero generation compound. This compound was then reacted with methyl acrylate through the Michael reaction, and subsequent amidation with ethylenediamine resulted in the first generation dendrimer which had six amino functionalities on the branch ends. With repetition of the above procedures, a

dendrimer of the tenth generation with 3072 amine groups at the exterior layer was obtained.

Newkome and coworkers have also been particularly active in the field of dendrimers. They have used a number of different cores and branched building blocks to make a wide variety of organic dendrimers as outlined in a recent review article[36]. One of the first cores Newkome *et al* used to make dendrimers was pentaerythrityl bromide and homologs of it (additional CH_2 spacer groups from center point)[37-38]. The reaction of these four branched Br terminated cores with triethyl methanetricarboxylate gave a dodecaester which upon reaction of the esters with $H_2NC(CH_2OH)_3$ gave a spherical dendrimer (or arborol, the term meaning tree-like that Newkome and coworkers use) possessing 36 surface hydroxyl groups[39-42].

Newkome also reported on the synthesis of other highly branched cascade polymers using a single quaternary carbon center as the core[43-44]. With the aim of obtaining organic, spherical unimolecular micelles, Newkome and coworkers also worked out conditions to make a variety of different highly branched appendages, or dendrons[45] many of which were amine functional, that could then be placed on a core such as the tetrabromide core described above to obtain the dendrimers of interest[46-47]. For example, Newkome *et al*[44] prepared a symmetrical, four-directional (four dendrons off the central core), saturated hydrocarbon cascade polymer containing 36 carboxylic acid moieties equidistant from a neopentyl core as shown in Figure 1.3.

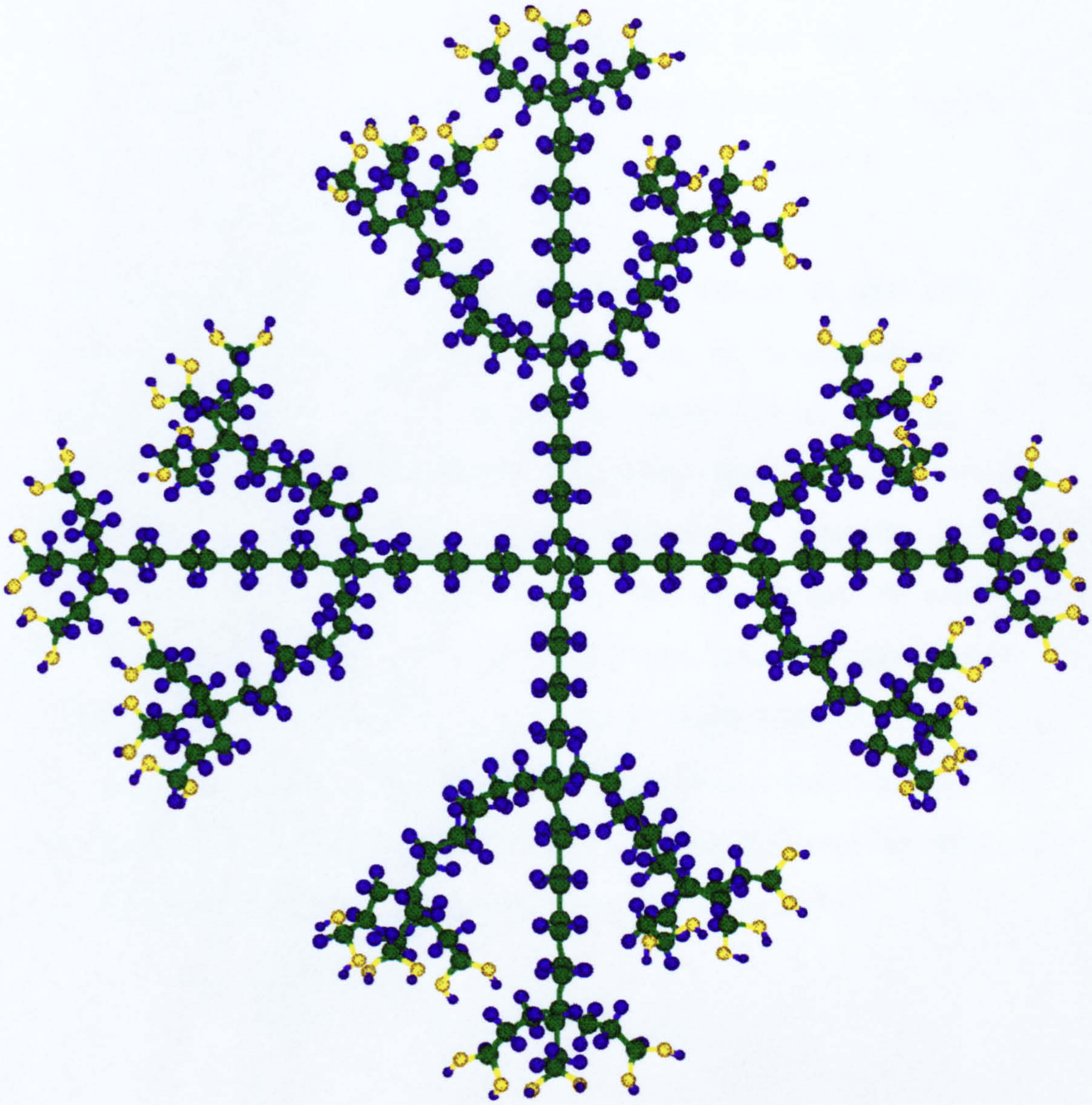

Figure 1.3 Quaternary carbon based dendrimer.
From: Newkome, G.R.; Moorefield, C.N.; Baker, G.R.; Saunders, M.J.; Grossman, S.H. *Angew. Chem., Int. Ed. Engl.* **1991**, 30, 1178.
Green=Carbon, Yellow=Oxygen, Blue=Hydrogen.

The carboxylic acid groups of the dendrimer were then converted to ammonium and tetramethylammonium carboxylate derivatives to study aggregation of these dendrimers[44].

In addition to the single quaternary carbon center as the core, Newkome *et al*[36] have reported on the use of functionalized adamantanes such as the one shown in Figure 1.4 to provide a four-armed core with tetrahedral symmetry for the construction of dendritic macromolecules. Amide groups are typically used[48] to give the functionality necessary for the attachment of chains or branches to the core to make dendrimers like the one shown in Figure 1.5. For example, the building block (dendron), 4-amino-4-(3-acetoxypropyl)-1,7-diacetoxyheptane, was added to a core based on 1,3,5,7-adamantanetetracarboxylic acid to form a four-directional spherical dendritic macromolecule[48].

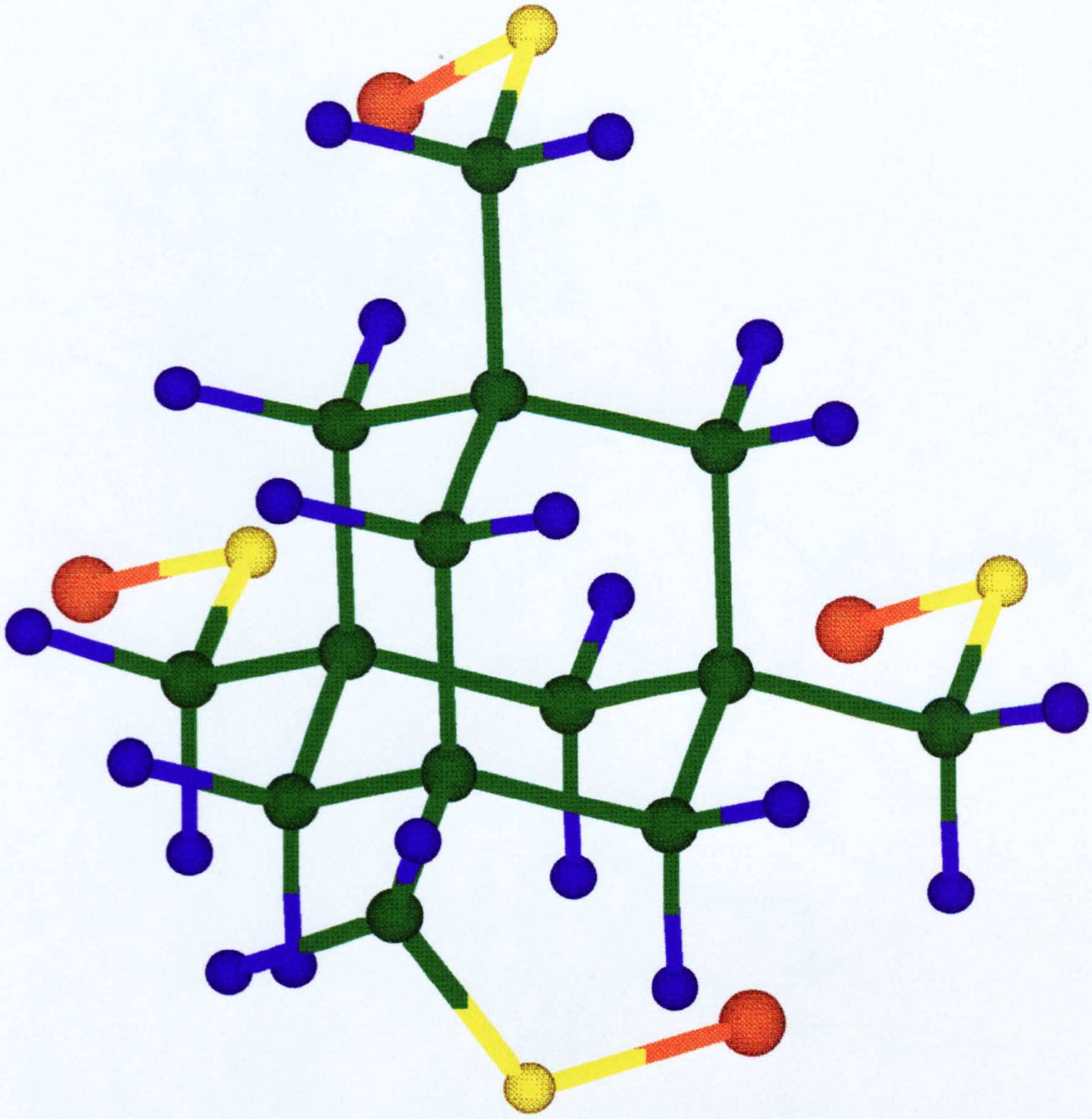

Figure 1.4 Functionalized adamantane core.
From: Newkome, G.R.; Nayak, A.; Behera, R.K.; Moorefield, C.N.; Baker, G.R. *J. Org. Chem.* 1992, 57, 358.
Green=Carbon, Yellow=Oxygen, Orange=Chlorine, Blue=Hydrogen.

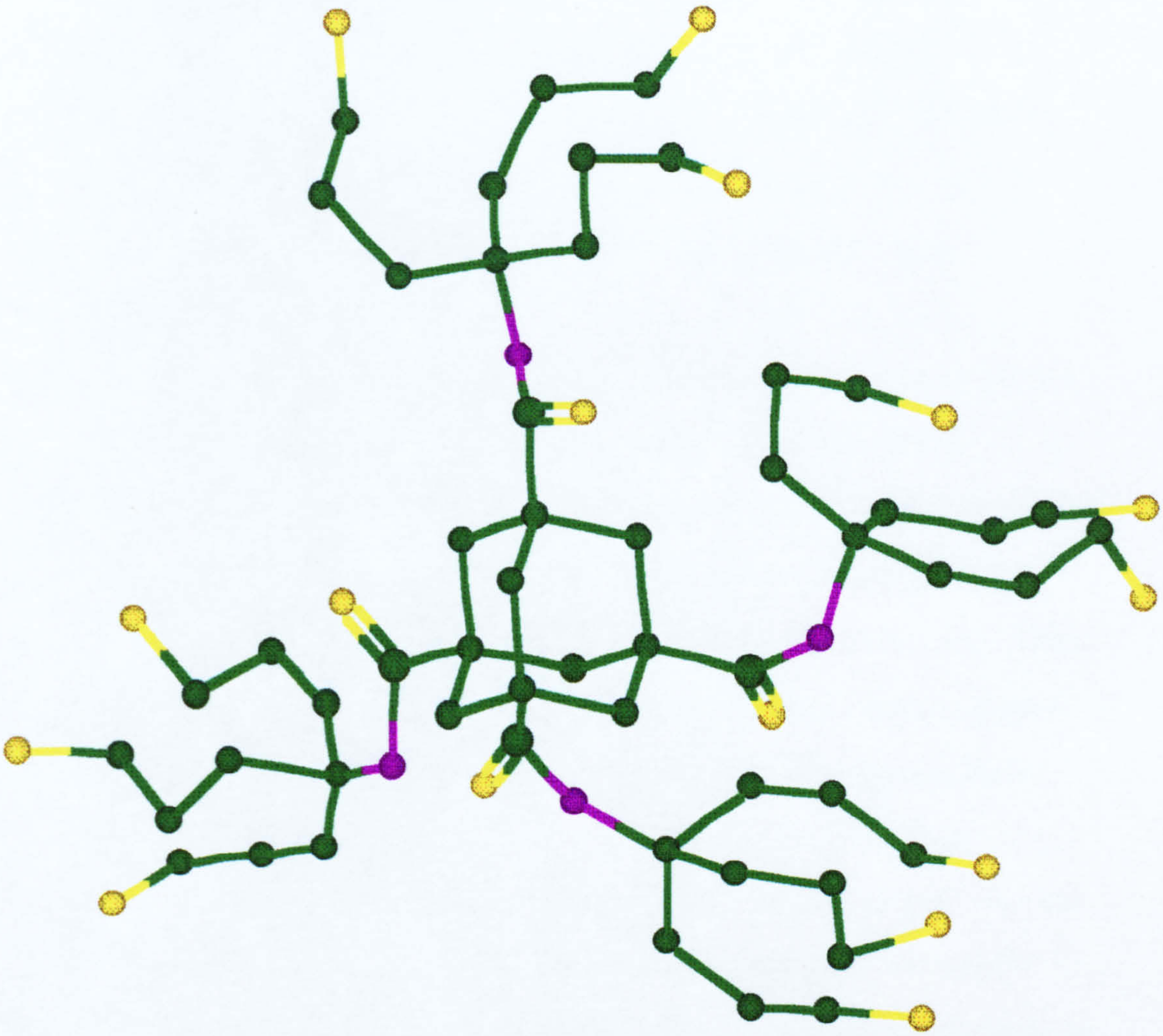

Figure 1.5 Adamantane-based dendrimer.
From: Newkome, G.R.; Nayak, A.; Behera, R.K.; Moorefield, C.N.; Baker, G.R. *J. Org. Chem.* **1992**, 57, 358.
Green=Carbon, Yellow=Oxygen, Purple=Nitrogen (Hydrogens are hidden).

Miller and coworkers have made a number of dendrimers based on trisubstituted benzenes as the core[49-52]. These dendrimers consisted of 4, 10, 22, and 46 benzene rings connected symmetrically. The preparation of these dendrimers involved first building the dendrons, followed by the attachment of 3 dendrons to a core. In one example[49], the dendron arm preparation started with 5-(tert-butyldimethylsiloxy)isophthaloyl dichloride which was reacted with phenol. Removal of the silyl protecting group led to formation of a new substituted phenol, two equivalents of which were reacted with 5-(tert-butyldimethylsiloxy)isophthaloyl dichloride. After repeating this process several times, the arms were formed. Three of these dendron arms were then coupled to 1,3,5-benzenetricarbonyl trichloride to form the dendrimer[49].

A number of silicon-containing dendrimers, either silicon in the core or with siloxane branches, have been reported as well[53-63]. An example of a dendrimer molecule with a silicon atom core as well as siloxane branches is one reported by Masamune and coworkers[53]. A core constructed from methyltrichlorosilane to which small, branched siloxanes were added sequentially resulted in a 24-armed siloxane dendrimer isolated in an acceptable yield. The $MeSiCl_3$ core reacted with three equivalents of $HSiMe_2(OSiMe_2)_4SiMe_2OH$ led to $MeSi[(OSiMe_2)_5SiMe_2H]_3$ that served as the core unit. An elongation unit, $ClMeSi[(OSiMe_2)_3SiMeH]_2$, was made from the $MeSiCl_3$ core reacted with two equivalents of $HSiMe_2(OSiMe_2)_4SiMe_2OH$. Coupling of the trifunctional core, $MeSi[(OSiMe_2)_5SiMe_2H]_3$, with the elongation unit,

$ClMeSi[(OSiMe_2)_3SiMeH]_2$, provided the first generation dendrimer with six functional sites. Repetition of the reaction of the dendrimer with elongation units led to second generation dendrimers with 12 branches and third generation siloxane dendrimers with 24 branches.

Using both divergent and convergent synthesis approaches, Mathias and coworkers[54-59] have made dendrimers with siloxane branches, or hyperbranched poly(siloxysilanes) as they termed them. One divergent route they studied involved use of hydrosilylation of $CH_2=CHCH_2Si(OSiHMe_2)_3$ as shown in Figure 1.6. As the figure indicates and as was determined by ^{29}Si NMR, polymerization was found to go through an initial cyclization of $CH_2=CHCH_2Si(OSiHMe_2)_3$ to form a cyclic core with two SiH functionalities[57]. Linear additions of the $CH_2=CHCH_2Si(OSiHMe_2)_3$ then took place to form the dendrimer[57] shown in Figure 1.6. Use of longer alkene-containing monomers such as 6-hex-1-enyltris(dimethylsiloxy)silane or the 8-oct-1-enyl analogue was found to entropically disfavor the undesired cyclization reaction[58]. They found non-uniform branching using the divergent approach[58].

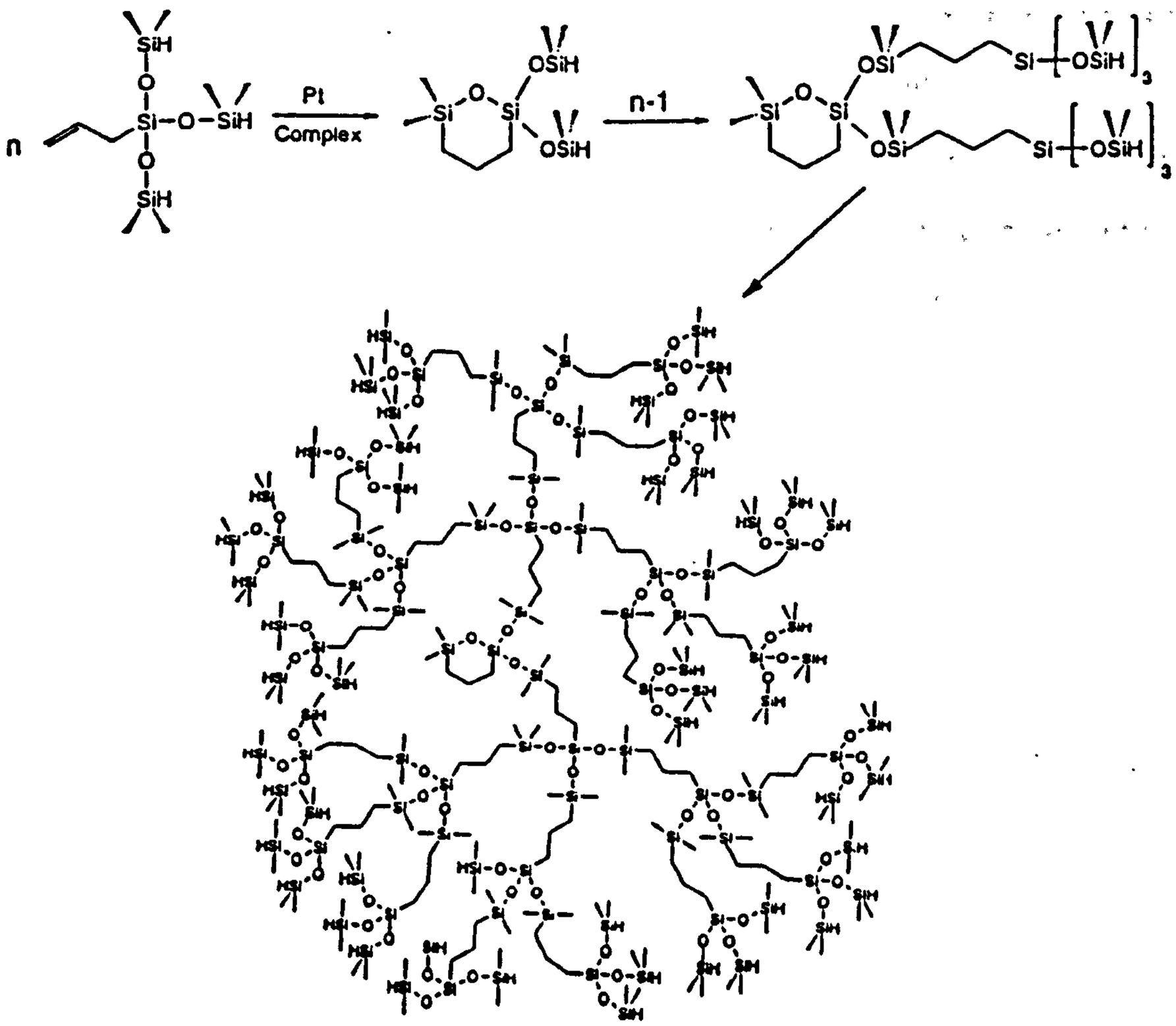

Figure 1.6. Divergent synthesis of hyperbranched poly(siloxysilanes).
From: Carothers, T.W.; Mathias, L.J. *Polym. Prepr., Am. Chem. Soc., Div. Polym. Chem.* **1993**, 34(1), 503-4.

Using a convergent synthetic route as shown in Figure 1.7, Carothers and Mathias[58] made uniformly branched siloxane dendrimers. What is shown in the figure is two different first generation dendrimers. The two-armed dendrimer polymer was made from the hydrosilylation reaction of $CH_2=CHCH_2Si(OSiHMe_2)_3$ by $HSiMe_2OSiMe_2H$ (1,1,3,3-tetramethyldisiloxane). The four-armed dendrimer shown in Figure 1.7 was prepared from the hydrosilylation reaction of $CH_2=CHCH_2Si(OSiHMe_2)_3$ by $Si(OSiMe_2H)_4$ [tetrakis-(dimethylsiloxy)silane]. The authors encountered difficulties continuing the dendrimer to a second generation due to cyclic compound formation that occurs with the use of $CH_2=CHCH_2Si(OSiHMe_2)_3$[58].

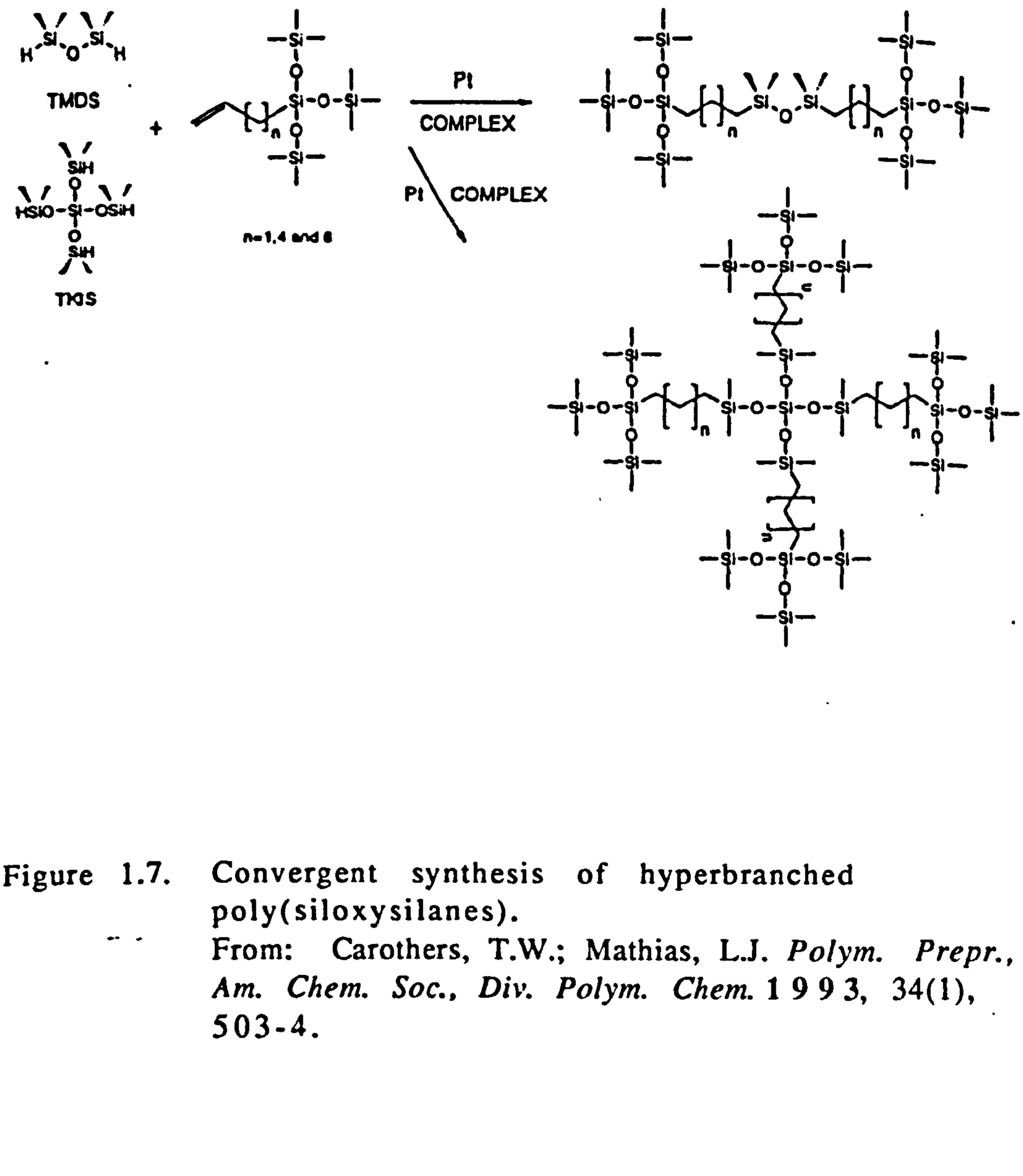

Figure 1.7. Convergent synthesis of hyperbranched poly(siloxysilanes).
From: Carothers, T.W.; Mathias, L.J. *Polym. Prepr., Am. Chem. Soc., Div. Polym. Chem.* 1993, 34(1), 503-4.

Morikawa, Kakimoto, and Imai have reported on the synthesis of a polysiloxane starburst polymer[60]. This molecule was started with tris[(phenyldimethylsiloxy)dimethylsiloxy]methylsilane (GO-Ph in Figure 1.8) as the core molecule which contained three phenylsilane-terminated disiloxane branches to minimize steric hindrance in later reactions. The branches added to the core were based on bis[(phenyldimethylsiloxy)methylsiloxy]dimethylsilanol (molecule 8 in Figure 1.8). The phenyl containing core molecule was reacted with bromine to generate the bromosilane (G0-Br in Figure 1.8), followed by diethylamine to make the the diethylamino functional core (G0-DEA in Figure 1.8). Reaction of the silanol functional building block (molecule 8 in Figure 1.8) with the amino functional core led to the first generation dendrimer bearing six phenylsilyl groups (G1-Ph in Figure 1.8). Second (12 phenylsilyl groups) and third generation (24 phenylsilyl groups) dendrimers were also prepared by continuation of the sequence of bromination, amination, and reaction with the silanol functional building block[60].

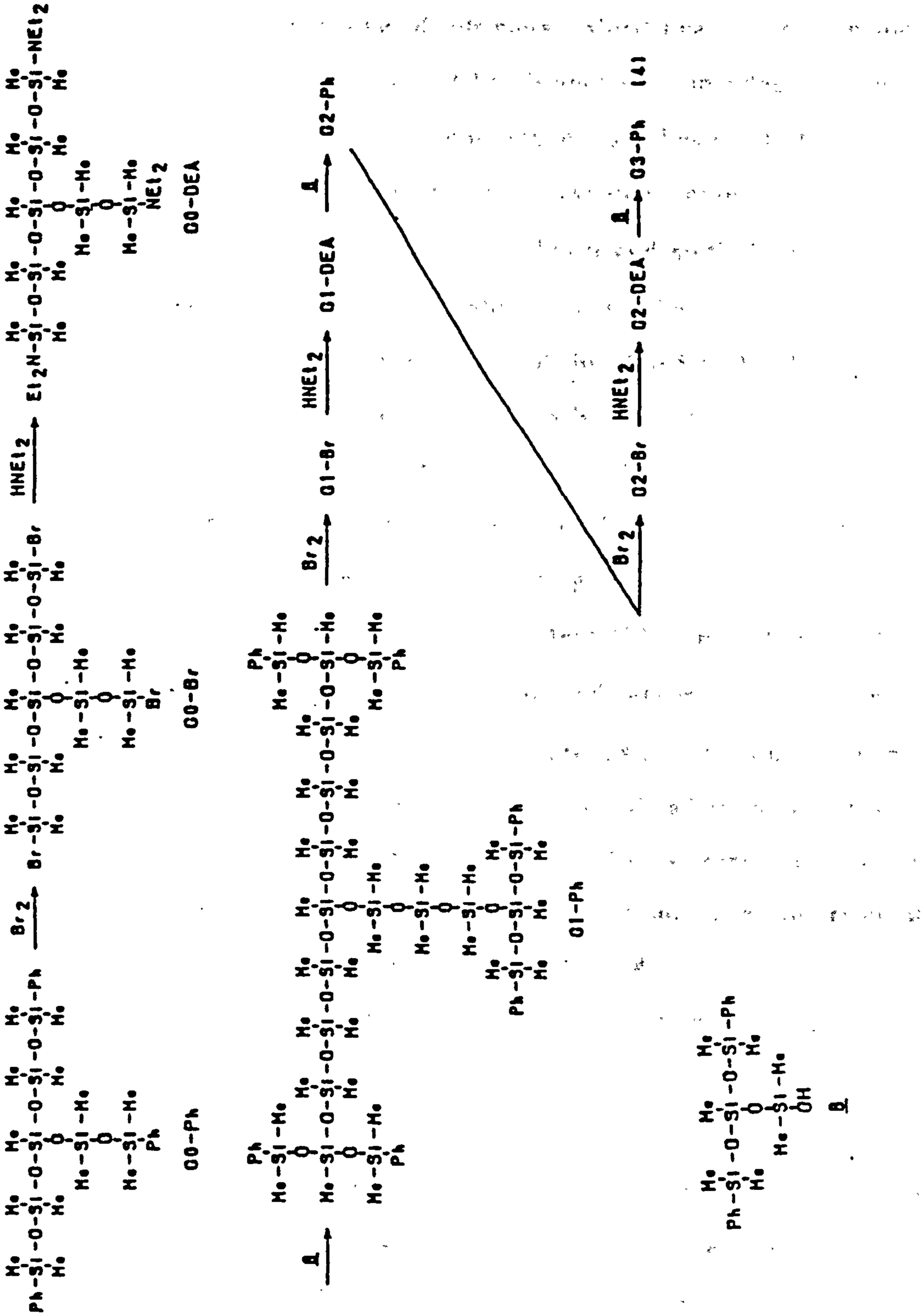

Figure 1.8 Siloxane dendrimer with tris[(phenyldimethylsiloxy)dimethylsiloxy]-methylsilane core.
From: Morikawa, A.; Kakimoto, M.; Imai, Y. *Macromolecules* 1991, 24(12), 3469-74.

In addition to the above dendrimers, Morikawa, *et al*[61] made siloxane starburst dendrons (the branched appendages) via hydrosilylation followed by convergent synthesis of the dendrimer. For the dendrons, allyl cyanide served as the starting material and allylbis[4-(hydroxydimethylsilyl)-phenyl]silane as the building block to synthesize the dendrons. The allyl cyanide was hydrosilylated by Me_2SiClH. Following amination with Et_2NH of the hydrosilylation reaction product, the resulting aminosilane was reacted with the allylbis[4-(hydroxydimethylsilyl)phenyl]silane building block to produce the first generation dendron containing two cyano groups. Repetition of hydrosilylation with Me_2SiClH, amination, and reaction with the building block, second generation (4 cyano groups), third generation (8 cyano groups), and fourth generation (16 cyano groups) dendrons were obtained after purification by silica gel column chromatography. Finally a spherical starburst dendrimer was made by reacting the aminosilane intermediate of the third generation dendron with tris[4-(hydroxydimethylsilyl)phenyl]methylsilane having three reactive OH groups.

A wide variety of silane dendrimers with up to 972 end groups were made by Van der Made *et al*[62]. They used repetitive alkenylation-hydrosilylation cycles. Starting with $SiCl_4$, the tetraallylsilane was made via treatment with allylmagnesium bromide. The allylsilane was then hydrosilylated with $HSiCl_3$ to obtain a core with four arms, each arm of which had one $SiCl_3$ functional group. The four $SiCl_3$ groups were then treated with allylmagnesium bromide to obtain 12 allyl end groups. The

alkenylation-hydrosilylation cycle was repeated up to a fifth generation dendrimer. The authors found that continuation beyond the fifth generation was not possible due to surface congestion[62].

Using a similar approach to the above, Roovers, Toporowski, and Zhou[63] reported making carbosilane dendrimers by hydrosilylating tetravinylsilane (the core) with $HSiMeCl_2$ to form the first generation dendrimer with four arms, each arm with two silicon chloride functional groups. All the chlorine groups were replaced by vinyl magnesium bromide to obtain a first generation vinyl functional dendrimer. By repetition of the hydrosilylation and conversion of silicon chloride groups with vinyl magnesium bromide, second (16 functional groups), third (32 functional groups) and fourth generation (64 functional groups) dendrimers were made[63].

Well-defined macromonomers, whether of the star, octopus, or dendrimer configuration have captured commercial interest in addition to academic interest. Meshke and Hoy of Union Carbide demonstrated and obtained a patent on the use of star polymers in making copolymers with alternating star and linear portions[64]. Using this approach, copolymers were designed by choice of components to allow superior morphological properties to be obtained. They noted in particular, the advantage of reduced viscosity at given molecular weights relative to polymers containing only linear segments.

Storey and George[65-66] obtained a patent on star-branched thermoplastic polymers consisting of a central linking moiety (preferably a silane) with at least 3 branches off the core. The block copolymer branches consisted of an elastic inner block and an outer block of polystyrene or polyisoprene endcapped with ionic moieties such as sulfonate, carboxylate, and phosphates. These materials were of interest as elastomeric binders in high energy compositions such as propellants and explosives.

Roovers and coworkers[67-69] reported on and obtained a patent for the synthesis and use of the carbosilane based hybrid star polymers. This molecule consisted of a central silane core with multiple carbosilane branches formed by anionic polymerization. They claimed molecules with at least 48 arms and preferably 64 or 128, each having peripheral Si-Cl or -Br reactive sites. They envisioned the use of these materials as viscosity modifiers in lubricating oils or in an extrusion or injection molding composition, as shear resistance improvers, flocculants, and as emulsifiers or deemulsifiers.

There is a Japanese patent[70] on the use of starburst dendrimers in a process to make porous silica with pores of a controlled and uniform size. The process consists of making a sol-gel based silica composite (hydrolysis and condensation of tetraalkoxysilanes) in which the starburst polymer is uniformly dispersed. Then upon sintering the composite, the starburst polymer decomposes and evaporates leaving the uniform sized pores. The process enables the formation of high quality filter materials, absorbers, and catalyst carriers[70].

Singh *et al*[71] report the use of the Tomalia's polyamido-amine dendrimers[29, 31-35] to which they coupled several specific antibodies to investigate their potential use in radial partition immunoassay. They found enhanced performance and flexibility for immunoassays using the dendrimer-coupled antibody.

It has been reported in Chemical & Engineering News[72] that DSM in the Netherlands is producing a poly(propylenimine) dendrimer on the multikilogram scale. DSM points out two key properties of these particular dendrimers that should be of commercial interest, their solubility and viscosity. They are reported to be easy to dissolve unlike linear polymers of this size. The instrinsic viscosity of these dendrimers passes through a maximum as a function of the size of the dendrimer, a property that also distinguishes them from linear polymers and a property that implies easier processibility of dendrimer containing materials[72].

Another fact indicating the increased commercial interest in dendrimers is the startup of a company focusing on only dendrimers, Dendritech, Inc., a subsidiary of Michigan Molecular Institute in Midland, Michigan[73]. One area of research and development at Dendritech involves polyamidoamine (PAMAM) dendrimers. They have made PAMAM dendrimers in a variety of sizes ranging from 10 to 124 Å in diameter. By appropriately modifying the chain ends of these dendrimers, they have shown that well behaved monolayer films can be formed[74].

Many of the reported routes to octopus and dendritic molecules involve multiple steps and purifications at each step before obtaining macromonomers of any size. Other strategies have worked well for a particular functionalization but are limiting in the types of functional groups that can be put on any one type of core. A route to octopus and dendrimer molecules that would have greater general utility than previously reported routes, that would be facile and high yielding, that would involve a limited number of steps to a highly branched macromonomer, and that could lead to any number of different functional groups being placed on a single type of core was of interest.

1.2 Silsesquioxanes

Silsesquioxanes are compounds with the general formula $(RSiO_{3/2})_n$. These compounds have also been called "spherosiloxanes" due to their polyhedral structures being topologically similar to a sphere, as the ball and stick model for $(HSiO_{3/2})_8$ shown in Figure 1.9 illustrates.

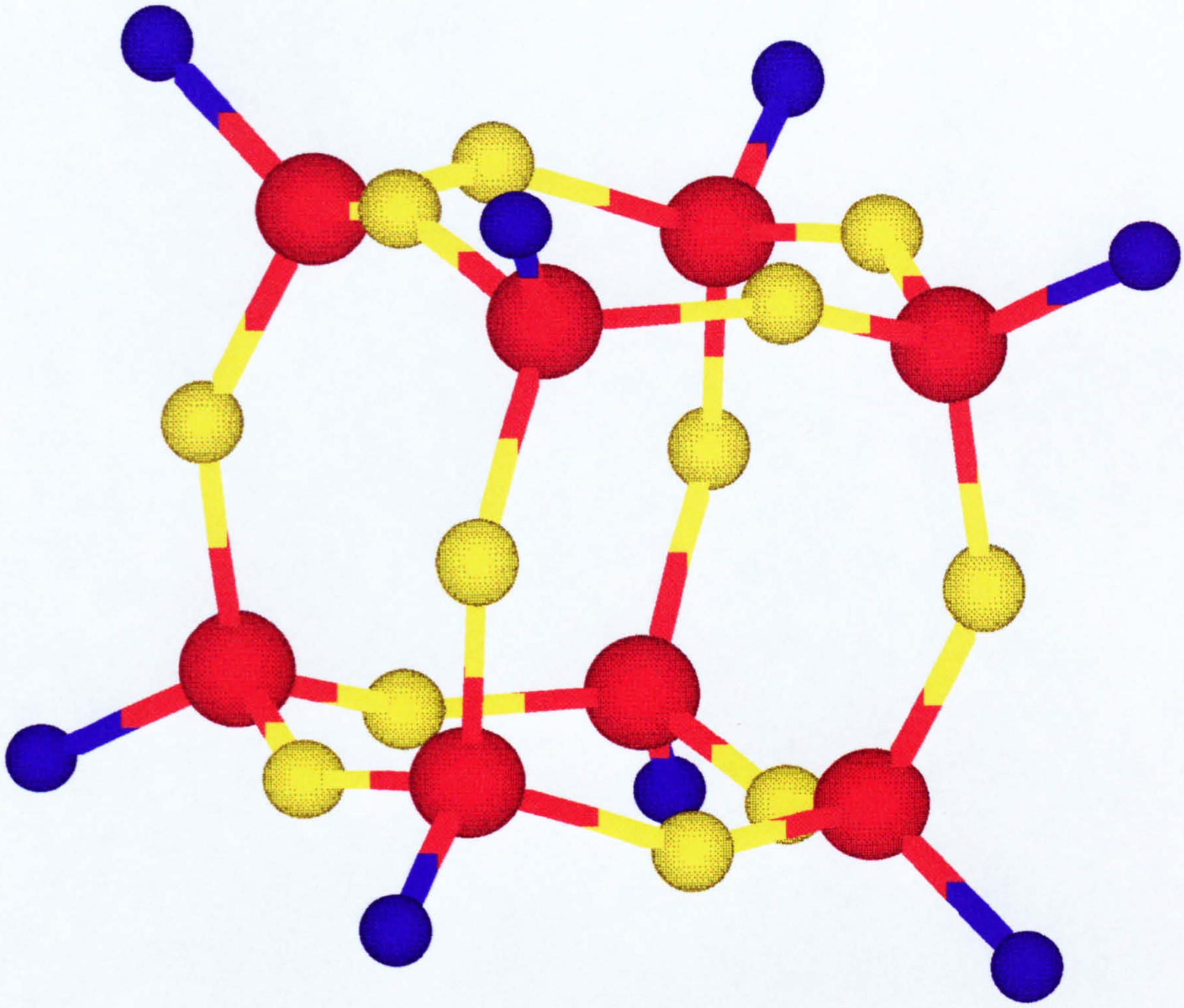

Figure 1.9 T_8 hydrogen silsesquioxane, $(HSiO_{3/2})_8$.
Yellow = Oxygen, Red = Silicon, Blue = Hydrogen.

An excellent review has been written by Voronkov, *et al*[75] on the general class of materials, the polyhedral oligosilsesquioxanes. Included in this review is information on the nomenclature, methods of synthesis, mechanisms of formation, structure and physical properties, chemical properties, and applications of this "rather versatile class of three-dimensional organosilicon oligomers which are of considerable theoretical and practical interest"[75]. In this section, a review of silsesquioxanes, and in particular T_8 hydrogen silsesquioxane and functionalized T_8 molecules, will be given.

The earliest reports on hydrogen silsesquioxane go back as far as 1950 and dealt with a completely insoluble, nonvolatile, crosslinked version of the material[76-79]. Vapour and solution hydrolysis of trichlorosilane[76-77] and trialkoxysilanes[77] were used to produce the gels that were described as "a high polymer white powder which is amorphous under X-ray"[77]. Their chemical and physical properties and possible industrial uses were envisioned[76-79].

The first reportably soluble hydrogen silsesquioxane was described in 1956 by Wiberg and Simmler[80]. It was made by the hydrolysis of $HSiCl_3$ in ether containing a stoichiometric amount of water in a vacuum apparatus at -40 °C. The material they made was soluble in the reaction solvent (ether) but became insoluble upon evaporation of the solvent. The authors proposed that they had most likely produced an incompletely condensed, silanol-containing material in which condensation of

the silanols, upon solvent evaporation, produced the insoluble gel of hydrogen silsesquioxane.

The first isolation of fully condensed $(HSiO_{3/2})_n$ was reported by Müller *et al*[81]. They recovered at an approximately 0.2% yield the octameric species, T_8 or $(HSiO_{3/2})_8$, as an unexpected by product of the reaction of $HSiCl_3$ and hexamethyldisiloxane in 80% H_2SO_4. They found the T_8 species to be sparingly soluble in benzene and hexane and proposed the cubic structure as shown in Figure 1.9. Larsson[82] later confirmed the cubic structure of T_8 by X-ray crystallography.

Nearly ten years after the initial isolation of T_8 by Müller, Collins and Fyre[83-84] reported on higher yielding methods of preparing T_8 and other volatile low molecular species as well as higher molecular weight nonvolatile soluble $(HSiO_{3/2})_{n>16}$ resin. The procedure they employed involved slowly adding a benzene solution of $HSiCl_3$ to a stirring solution of benzene and H_2SO_4 (*reaction scheme 1.1) under carefully controlled conditions* (i.e., slow addition, rapid agitation, dilute reaction medium).

$$HSiCl_3 \xrightarrow[C_6H_6]{H_2SO_4} \underset{\text{Volatile}}{(HSiO_{3/2})_{8-16}} + \underset{\text{Nonvolatile}}{(HSiO_{3/2})_{n>16}} \qquad (1.1)$$

The H_2SO_4 and benzene react to form benzenesulfonic acid hydrate as shown in reaction scheme 1.2. It is the arylsulfonic acid hydrate that provides water for a "scarce water hydrolysis" of the $HSiCl_3$, as Collins and Fyre described it, and allows for fully condensed soluble hydrogen silsesquioxane.

$$H_2SO_4 + C_6H_6 \rightarrow C_6H_5SO_3 \cdot H_2O \qquad (1.2)$$

By the H_2SO_4/benzene/$HSiCl_3$ route, Collins and Fyre[83-84] found that the volatile portion of hydrogen silsesquioxane resin which was generally between 15 and 36% of the total resin contained only trace amounts of the T_8 species while T_{12} and T_{14} made up the majority of the volatiles.

However. Collins and Frye[83-84] developed another preparation from which they were able to isolate the octamer, T_8, species in respectable yields (13%). In this procedure, they added a cyclohexane solution of $HSi(OMe)_3$ to a solution of cyclohexane, glacial acetic acid (previously saturated with HCl) and aqueous HCl.

In more recent years, industrial interest in soluble hydrogen silsesquioxane as a possible ceramic coating precursor has grown. Hydrogen silsesquioxane has found utility as a coating applied from solution and subsequently oxidized, for example, via thermal cure in air[85], cure with high intensity radiation (Rapid Thermal Processing)[86], cure in O_2 plasma[87], and ammonia[88-89] and amine[90] catalyzed cures, to form a ceramic or ceramic-like coating. Coatings derived from hydrogen silsesquioxane have been applied to microelectronic devices to form protective barriers[85] and are also being commercialized as an interlayer dielectric material in the assembly of multilayer microcircuits[91].

Commercialization of hydrogen silsesquioxane as a coating material for the above electronic applications has required development of means for large scale production of the material. Procedures for large scale production of a broad distribution of molecular weights of hydrogen silsesquioxane have been developed[92]. The procedure of Collins and Fyre[83-84] involving the use of the arylsulfonic acid hydrate to provide water for a "scarce water hydrolysis" of the $HSiCl_3$, modified for instance by use of toluene rather than benzene, faster addition times, and improved mixing have allowed for the production of hydrogen silsesquioxane in batches of up to 1000 gallons. Means of separating the various molecular weights of interest via supercritical fluid fractionation[93-94] and solvent fractionation for different applications have also been developed. For instance, the low molecular weight volatile portions (T_8 - T_{22}) have been found to be useful for deposition of silica films from vaporized hydrogen silsesquioxane[95-97], whereas the intermediate solid molecular weight species that melt at reasonable temperatures have good coating characteristics for applying a coating that flows out and planarizes a detailed topography on a microscale such as on a microelectronic device[91].

In addition to the industrial development of silsesquioxanes for applications in electronic coatings, there has been considerable research activity recently concerning silsesquioxanes[98-128]. However, unlike the above industrial applications, these research efforts have been primarily involved use of single species, most commonly T_8 for ease of characterization.

Much of the research involving silsesquioxanes has largely been related to sol-gel technology[98], studies of supported catalysts[99-108], use of silsesquioxanes as models to study the chemistry of silica surfaces[99, 109-110] and use of functionalized silsesquioxanes as precursors to ceramic materials[98] and silicate/organic hybrids[111].

Day, Klemperer, Mainz, and Millar[98] synthesized a functionalized T_8 molecule, the polysilicic acid ester, $[SiO_{3/2}]_8[OCH_3]_8$. They planned to use this molecule as a precursor to ceramic materials in which structural features could be more easily controlled by starting with tailor-made building blocks that could then be polymerized in subsequent reactions. They were able to make the $[SiO_{3/2}]_8[OCH_3]_8$ by using a two step reaction. The first step involved photochemical chlorination of $(HSiO_{3/2})_8$ and sublimation of the product to obtain $(ClSiO_{3/2})_8$. This was then reacted with neat methyl nitrite (CH_3ONO) in a sealed tube. The desired $[SiO_{3/2}]_8[OCH_3]_8$ was then obtained in a 45% yield via sublimation and crystallization from toluene. In a later paper, Klemperer, Mainz, and Millar[112] demonstrated the use of $[SiO_{3/2}]_8[OCH_3]_8$ as a building block in hydrolysis and condensation reactions or the sol-gel process to form ceramic or ceramic-like materials. They showed using ^{29}Si NMR that at least in the early stages of hydrolysis/condensation that the polysilicate framework is retained.

Agaskar, Day and Klemperer[113] described the synthesis and structure characterization of T_{12} and T_{14} trimethylsilylated silsesquioxanes from the reaction of the corresponding hydrogen

silsesquioxanes obtained using the Collins and Fyre preparation[83-84] with the agent $Me_3NOSiMe_3Cl$ which converts the SiH groups directly to $SiOSiMe_3$ groups. They were interested in obtaining these molecular polyhedral silicates with anionic oxygen atoms protected by trimethylsilyl groups to study the properties of isolated polysilicate cage frameworks.

Agaskar continued research into functionalized silsesquioxanes proposing the use of the polyhedral, polyreactive oligomers as molecular building blocks for organolithic macromolecular materials (OMM's) which are hybrids composed of an organic component and a well-defined silicate component[111, 114]. In one paper, Agaskar[111] gave details of procedures for making a) $[SiO_{3/2}]_8[Si(CH_3)_3]_8$, b) $[SiO_{3/2}]_8[Si(CH_3)_2CHCH_2]_8$, and c) $[SiO_{3/2}]_8[Si(CH_3)_2CH_2Cl]_8$ through silylation procedures. He started with the spherosilicate anion, $[Si_8O_{20}]^{8-}$, that is produced from mixing H_2O, $(H_3C)_4NOH$ (25% aqueous), $(H_3CO)_4Si$, and $(H_3C)_2SO$ as first described by Groennen *et al*[115]. The spherosilicate anion-containing solution was then added dropwise to a solution of $(H_3CO)_2C(CH_3)_2$, HCl, and $YSi(CH_3)_2OSi(CH_3)_2Y$ where Y is $-CH_3$ for a), $-CHCH_2$ for b), and $-CH_2Cl$ for c). The mixing of these two solutions led to the partially silylated $[Si_8O_{20}]^{8-}$ anion. After removal of volatiles under vacuum, the silylation reaction was completed by using a modified Tamas *et al*[116] silylating mixture composed of $(H_3C)_2NCHO$, $YSi(CH_3)_2OSi(CH_3)_2Y$, and $Y(CH_3)_2SiCl$ where Y is $-CH_3$ for a), $-CHCH_2$ for b), and $-CH_2Cl$ for c). Final products were obtained via a recrystalization process.

In another paper, Agaskar[114] reported on the synthesis of silsesquioxanes (T_8 and T_{10}) capped with $-Si(CH_3)_2Y$ groups, where Y is either a vinyl or a chloromethyl group resulting in some of the same molecules as above but in this case the syntheses started with hydrogen silsesquioxane. These molecules were made by mixing hydrogen silsesquioxane with $(H_3C)_3NO$ and $ClSi(CH_3)_2CHCH_2$ for the vinyl-capped silsesquioxane, and mixing with $(H_3C)_3NO$ and $ClSi(CH_3)_2CH_2Cl$ for the chloromethyl-capped silsesquioxane.

Using the $[SiO_{3/2}]_{10}[Si(CH_3)_2CHCH_2]_{10}$ prepared as described earlier[114], Agaskar made organolithic macromolecular materials by reacting the $[SiO_{3/2}]_{10}[Si(CH_3)_2CHCH_2]_{10}$ with a stoichiometric amount of the bifunctional compound, $(HSi(CH_3)_2C_6H_4O_{1/2})_2$, in the presence of a platinum catalyst, $PtCl_2(C_6H_5CN)_2$[117]. He obtained a solid that was hard, clear, resilant, and thermally stable (no weight change until >350 °C). Using ^{13}C CP/MAS and ^{29}Si CP/MAS, Agaskar found that the cross-linking reaction had gone almost to completion (>95%) and that the silsesquioxane cores of the OMM had retained its structural integrity[117].

Bürgy, Calzaferri, Herren, and Zhdanov[118] have published a review of their work and others concerning the synthesis and properties of functionalized silsesquioxanes as well as spherometallosiloxanes or silsesquioxanes in which some of the Si atoms of the cage framework have been replaced by other metal atoms. Their interest in these molecules stems from their resemblance of the T_8 framework to the double four ring of zeolites, and therefore they felt they could serve as models for

investigating zeolites. One approach they discussed basically involved the methods of Collins and Fyre[83-84] in which the hydrolysis and condensation of $RSiX_3$ leads to $(RSiO_{3/2})_n$ and isolation of the T_8 species is accomplished via crystallization. Bürgy *et al*[118] reported that silsesquioxanes carrying alkyl, allyl, and aryl substituents were obtained using this approach when starting with the appropriate silanes. Heterosubstituted products are also possible using mixtures of trifunctional silanes although the rate, degree of oligomerization, and yield depends on a large number of variables and it would seem that a particular arrangement of the different substituents on the silsesquioxane core would be difficult to achieve[117].

Feher and coworkers have been very active in the field of structurally well-defined silsesquioxanes and their applications. Feher and Budzichowski[119] described the hydrolytic condensation of *p*-$ClCH_2C_6H_4SiCl_3$ in aqueous acetone to obtain *p*-$[ClCH_2C_6H_4SiO_{3/2}]_8$ with the purpose of making highly functionalized silsesquioxanes. The yield of *p*-$[ClCH_2C_6H_4SiO_{3/2}]_8$ was found to be modest (6-15%) and the compound was found to be surprisingly inert. However, Feher and Budzichowski demonstrated that the eight chlorides of the *p*-$[ClCH_2C_6H_4SiO_{3/2}]_8$ could be replaced by iodides by refluxing of the *p*-$[ClCH_2C_6H_4SiO_{3/2}]_8$ with NaI in THF in the dark and that the *p*-$[ICH_2C_6H_4SiO_{3/2}]_8$ was sufficiently reactive enough to be used as a precursor to other functionalized silsesquixoanes of the formula, *p*-$[XCH_2C_6H_4SiO_{3/2}$ (X=I, OH, ONO_2, OAc, *p*-nitobenzoyl, and methylterephthaloyl)[119]. Feher and Budzichowski described these syntheses as "far from trivial" but believed that the *p*-

$[ClCH_2C_6H_4SiO_{3/2}]_8$ was a synthetically versatile precursor to highly functionalized silsesquioxanes[119].

In addition to the above work, Feher and coworkers have done extensive studies involving the use of silsesquioxanes as models for silica and silica surfaces[99-110, 120-121]. Feher and coworkers hoped to gain insight into modified silicas used in a number of applications such as stationary phases in chromatography, ion collection, heterogeneous catalysts, inorganic polymer fillers, and drug delivery agents[121]. Because detailed structural characterization and mechanistic studies of SiO_2-supported complexes are inherently difficult to do, Feher and coworkers have taken an approach of using the incompletely condensed silsesquioxanes for modeling of the chemistry of silica-supported transition metal complexes due to their similarity to hydroxylated silica surface sites. In a number of papers, Feher has described the synthesis and characterization of a variety of incompletely condensed silsesquioxanes (Figure 1.10) as models for hydroxylated silica surface sites[99, 109-110].

The synthesis of the trisilanol compound, $Cy_7Si_7O_9(OH)_3$ (1a in Figure 1.10, Cy = cyclohexyl), was first described by Brown and Vogt in 1965[122]. More recently, Feher and coworkers optimized the procedures and used this compound in a number of their studies of silica surfaces. The $Cy_7Si_7O_9(OH)_3$ was prepared via the kinetic hydrolytic condensation of cyclohexyltrichlorosilane ($CySiCl_3$) in aqueous acetone. Product precipitated over a 2-36 month period and was isolated from a mixture of products. In one study, Feher and Newman[109] studied the silylation of silica

using the $Cy_7Si_7O_9(OH)_3$ as their model for silica. They compared silylation of isolated silanols to intramolecularly hydrogen-bonded silanols. They found that in the presence of Et_3N or pyridine, the rates of silylation of all types of silanols were increased compared to the rates in the absence of amine bases. They found selectivity for the monosilylation of $Cy_7Si_7O_9(OH)_3$ in the presence of Et_3N and a slight kinetic preference for the silylation of vicinally hydrogen-bonded silanols over isolated, non hydrogen-bonded silanols. They proposed that their results suggested that the most reactive sites for silylation of hydroxylated silica surfaces were those possessing at least three mutually hydrogen-bonded hydroxy groups.

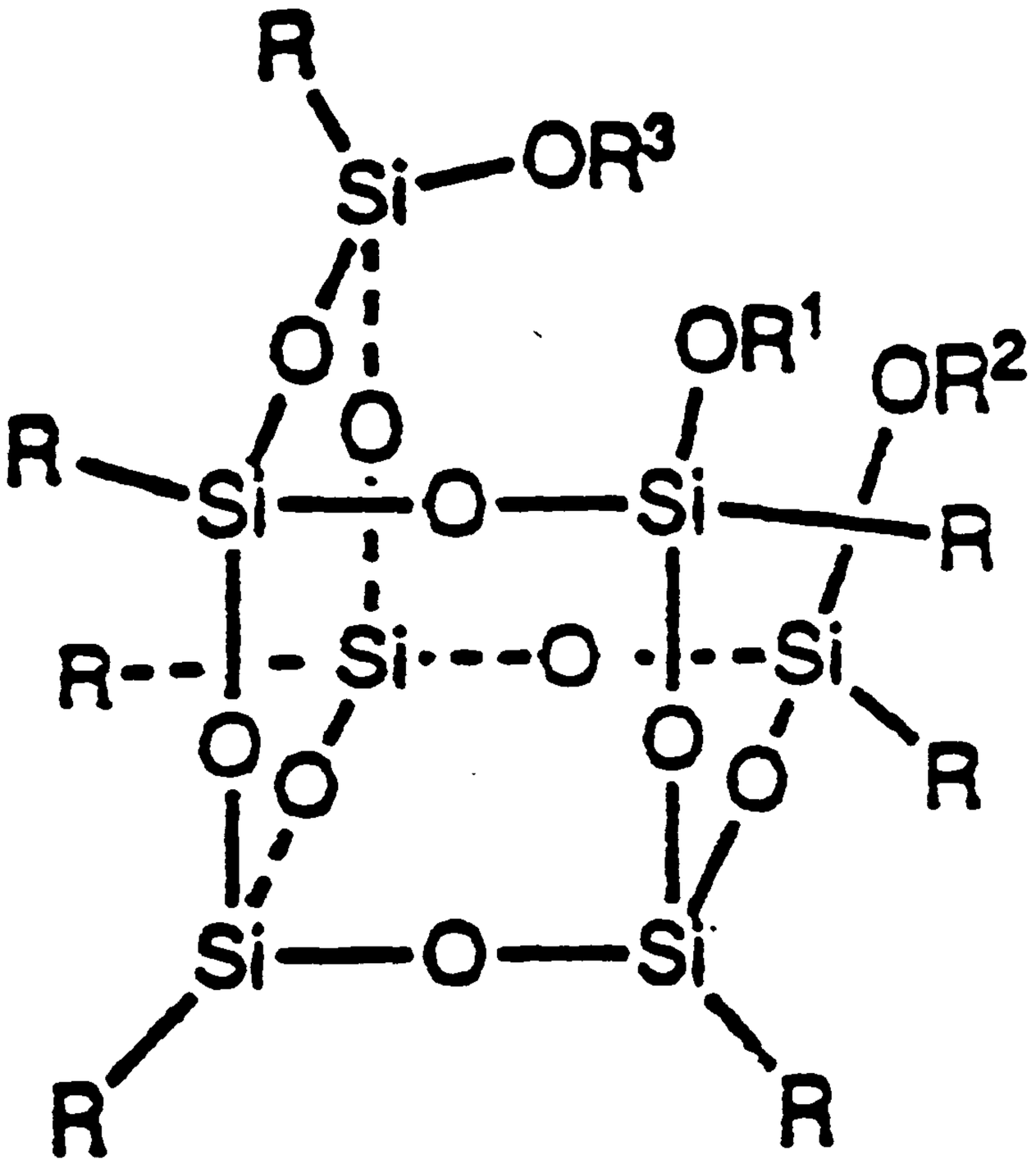

$(R = c\text{-}C_6H_{11})$

1a $R^1 = R^2 = R^3 = H$

b $R^1 = R^2 = R^3 = SbMe_4$

c $R^1 = R^2 = H;\ R^3 = SbMe_4$

d $R^1 = H;\ R^2 = R^3 = SbMe_4$

Figure 1.10 Incompletely condensed silsesquioxanes as models for hydroxylated silica surface sites.
From: Feher, R.J.; Budzichowski, T.A.; Rahimian, K.; and Ziller, J.W. *J. Am. Chem. Soc.* 1992, 114(10), 3859-3866.

Feher has also used the incompletely condensed silsesquioxane compounds as ligands in homogeneous models for silica-supported transition-metal complexes[101-108, 121]. Reactions leading to the formation of heteroatom- and metal-containing silsesquioxanes were described in a number of papers[100-108, 120-121] In one study[100], a number of incompletely condensed silsesquioxanes [one of which was $Cy_7Si_7O_9(OH)_3$] were reacted with excess Me_5Sb to form the corresponding stibonium-substituted silsesquioxanes [i.e., $Cy_7Si_7O_9(OSbMe_4)_3$ resulted from the starting with $Cy_7Si_7O_9(OH)_3$].

In the course of investigating silsesquioxane, Feher and Weller[124] became interested in the possibility of building immense aluminosilcate frameworks from linking aluminosilsesquioxanes and structurally well-defined polysilicate anions. With the purpose of obtaining polysilicate anions, Feher and Weller[124] began exploring routes to silsesquioxanes with labile functional groups. They demonstrated the synthesis of $(Me_3SnO)_8(SiO_{3/2})_8$ and $(Me_4SbO)_8(SiO_{3/2})_8$ to be used as labile sources of anhydrous, aprotic $[(Si_8O_{20})^{8-}]$. They obtained the $(Me_3SnO)_8(SiO_{3/2})_8$ by adding $Me_3SnOSnMe_3$ to a suspension of $(HSiO_{3/2})_8$, stripping volatiles and obtaining the product from crystallization. The reaction of the $(Me_3SnO)_8(SiO_{3/2})_8$ with $Me_4SbOSiMe_3$ or $Me_4SbOCMe_3$ afforded the desired $(Me_4SbO)_8(SiO_{3/2})_8$.

Herren *et al*[125] reported making a hydrocarbon functional silsesquioxane from the hydrosilylation of 1-hexene by T_8 hydrogen silsesquioxane. The authors considered that yields of

at least 90% could be regarded as proof that hydrosilylation proceeded with retention of the cage structure although they did not report ^{29}Si NMR data to support this[125].

Calzaferri and Imhof also recently reported on another unusually functionalized T_8 molecule, the first organometallic monostituted T_8 also made via hydrosilyation[126]. The ferrocene functionalized silsesquioxane was made via the H_2PtCl_6 catalyzed hydrosilylation of vinylferrocene by $(HSiO_{3/2})_8$. A 1:1 mole ratio of $(HSiO_{3/2})_8$:vinylferrocene was dissolved in toluene and the catalyst was added. The reaction mixture was heated at reflux for 20 hours. After solvent removal and redissolving in hexanes, the monosubstituted product $\{[(\eta\text{-}C_5H_5)Fe(\eta\text{-}C_5H_4CH_2CH_2)]H_7Si_8O_{12}\}$ was isolated in a 14% yield from a mixture of mono- and polysubstituted silsesquioxanes using gel permeation chromatography (GPC, also known as size exclusion chromatography).

Although there has been quite a lot of interest in silsesquioxanes as is apparent from the above summaries, research on silsesquioxanes had in the past been somewhat limited by the inefficiency of the synthesis and the difficult isolation of single species. Agaskar, Day, and Klemperer[113] worked on modifications of the original Collins and Fyre arylsulfonate "scarce water" hydrolysis route to come up with a more reproducible yield of volatile species (>30%) and reported on purification protocol to obtain gram quantities of four pure species, T_8, T_{10}, T_{12}, and T_{14}. Even so, yields were still low especially for the T_8 species (0.5%).

This situation changed when Agaskar[127] revealed a new synthesis and isolation of T_8 and T_{10} hydrogen silsesquioxane species in higher yield than the originally reported process by Collins and Frye. His approach was similar to the original Collins and Fyre "scarce water" hydrolysis but with use of a partially hydrated metal salt solution ($HSiCl_3$ added to a biphastic mixture of hexane and toluene and $FeCl_3$ in MeOH and HCl). By this route Agaskar was able to obtain pure T_8 in a 17.5% yield, while pure T_{10} could also be isolated from the same reaction mixture using procedures Agaskar, Day, and Klemperer reported on earlier[113].

In addition to T_8, the synthesis and isolation of T_{10}, T_{12}, and T_{14} in gram quantities has been reported[113] as well as the separation of the oligomeric silsesquioxanes, T_8 through T_{18}, by size exclusion chromatography[128].

1.3 Thesis Statement

As the ball and stick model of hydrogen silsesquioxane in Figure 1.9 (R=H and n=8) shows, there are eight SiH groups arranged symmetrically on the surface of a sphere. This unusual geometry is ideal for the development of highly functionalized molecules in which eight chains are symmetrically attached to a single $(SiO_{3/2})_8$ core for an octopus design and further branching beyond the first layer of chains for a dendrimer design. These three dimensional octopus and dendrimer configurations should lead to novel materials having unusual physical properties and morphologies. In addition, building on the regular geometry of

silsesquioxanes (spherical or cage-like) opens the possibility of making monodispersed molecules of defined shape and size. Accordingly, the rest of this thesis describes experiments to produce and characterize such molecules.

1.4 References

1. Gervasi, J.; Gosnell, A. *J. Polym. Sci.* **1966**, 4(6), 1391.

2. Roovers, J.; Toporowski, P. *Appl. Polym. Symp.* **1974**, 18(6), 1685.

3. Roovers, J.; Bywater, S. *Polym. Prepr., Am. Chem. Soc., Div. Polym. Chem.* **1971**, 12(1). 290.

4. Roovers, J.; Bywater, S. *Macromolecules* **1972**, 5(4), 384.

5. Masuda, T.; Ohta, Y.; Onogi, S. *Polym. Prepr., Am. Chem. Soc., Div. Polym. Chem.* **1971**, 12(1). 346.

6. Hadjichristidi, N.; Guyot, A.; Fetters, L.J. *Macromolecules* **1978**, 11(4), 668.

7. Hadjichristida, N.; Fetters, L.J. *Macromolecules* **1980**, 13(1), 191.

8. Pearson, D.S.; Mueller, S.J.; Fetters, L.J.; Hadjichristidi, N. *Polym. Prepr., Am. Chem. Soc., Div. Polym. Chem.* **1982**, 23(2), 21.

9. Roovers, J.; Hadjichristidi, N.; Fetters, L.J. *Macromolecules* **1983**, 16(2), 214.

10. Long, T.E.; Kelts, L.W.; Turner, S.R.; Wesson, J.A.; Mourey, T.H. *Macromolecules* **1991**, 24(6), 1431-4.

11. Tverdokhlebova, I.I.; Larina, T.A.; Mamaeva, I.I.; Pertsova, N.V.; Wilczak, L.; Rubinsztajn, S.; Chojnowski, J. *Vysokomol. Soedin., Ser. B* **1990**, 32(4), 292-6.

12. Kazama, H.; Tezuka, Y.; Imai, K. *Macromolecules* **1991**, 24(1), 122-5.

13. Fujimoto, T.; Zhang, H.; Kazama, T.; Isono, Y.; Hasegawa, H.; Hashimoto, T. *Polymer* **1992**, 33(10), 2208-13.

14. Sinyagina, M.A.; Vasetchenkova, T.V.; Polyakova, M.V.; Ivaschenko, D.A.; Stepanova, E.E.; Buzyreva, N.M.; Chernyshev, E.A. *Zh. Obshch. Khim.* **1993**, 63(7), 1591-5.

15. Dickstein, W.H.; Lillya, C.P. *Macromolecules* **1989**, 22, 3886-3888.

16. Dickstein, W.H.; Lillya, C.P. *Macromolecules* **1989**, 22, 3882-3885.

17. Bhattacharya, S.K.; Smith, C.A.; Dickstein, W.H. *Macromolecules* **1992**, 25(5), 1373-6.

18. Morikawa, A.; Kakimoto, M.; Imai, Y. *Polym. Prepr. Jpn.* **1991**, 40, 359.

19. Vogtle, F.; Weber, E. *Angew. Chem., Int. Ed.*, **1974**, 13, 814.

20. MacNicol, D.; Wilson, D. *J. Chem. Soc., Chem. Commun.* **1976**, 494

21. Fornasier, R.; Montanari, F.; Podda, G.; Tundo, P. *Tetrahedron Lett.*. **1976**, 17, 1381.

22. Bocchi, V.; Foina, D.; Pochini, A.; Ungaro, R. *Tetrahedron* **1982**, 38, 373.

23. Ungaro, R.; Pochino, A.; Andreetti, G.D.; Ugozzoli, F. *J. of Inclusion Phenom.* **1985**, 3, 409.

24. Taniguchi, H.; Nomura, E. *Chem. Lett.* **1988**, 1773.

25. Wooley, K.L.; Hawker, C.J.; Frechet, J.M.J. *J. Chem. Soc., Perkin Trans. 1* **1991**, 1059.

26. Conner, M.; Kudelka, I.; Regen, S.L. *Langmuir* **1991**, 7, 982-987.

27. Zhu, Z.; Rider, J.; Yang, C.Y.; Gilmartin, M.E.; Wnek, G.E. *Macromolecules* **1992**, 25(26), 7330-3.

28. Edwards, J.; Lenon, S.; Toussaint, A.F.; Vincent, B. *Am. Chem. Soc. Symp. Ser.* **1984**, 240, 281.

29. Tomalia, D.A.; Baker, H.; Dewald, J.; Hall, M.; Kallos, G.; Martin, S.; Roeck, J.; Ryder, J.; Smith, P. *Polym. J.* **1985**, 17, 117.

30. Tomalia, D.A.; Naylor, A.M.; Goddard, W.A. III *Angew. Chem., Int. Ed. Engl.* **1990**, 29, 138.

31. Tomalia, D.A.; Baker, H.; Dewald, J.; Hall, M.; Kallos, G.; Martin, S.; Roeck, J.; Ryder, J.; Smith, P. *Macromolecules* **1986**, 19, 2466.

32. Tomalia, D.A.; Hall, M.; Hedstrand, D.M. *J. Am. Chem. Soc.* **1987**, 109, 1601.

33. Tomalia, D.A.; Berry, V.; Hall, M.; Hedstrand, D.M. *Macromolecules* **1987**, 20, 1164.

34. Naylor, A.M.; Goddard, W.A., III; Kiefer, G.E.; Tomalia, D.A. *J. Am. Chem. Soc.* **1989**, 111, 2339.

35. Moreno-Bundi, M.C.; Orellana, G.; Turro, N.J.; Tomalia, D.A. *Macromolecules* **1990**, 23, 910.

36. Newkome, G.R.; Moorefield, C.N.; Baker, G.R. *Aldrichimicia Acta* **1992**, 25, 31-38.

37. Newkome, G.R.; Arai, S.; Gupta, V.K.; Griffin, R.W. *J. Org. Chem.* **1987**, 52, 5480.

38. Newkome, G.R.; Arai, S.; Fronczek, F.R.; Moorefield, C.N.; Lin, X.; Weis, C.D. submitted to *J. Org. Chem.* **1992**.

39. Newkome, G.R.; Arai, S. Presented at the 193rd National Meeting of the American Chemical Society, Denver, CO; April 5-10, 1987; ORGN 66.

40. Newkome, G.R.; Yao, Z.; Baker, G.R.; Gupta, V.K. *J. Org. Chem.* **1985**, 50, 2003.

41. Newkome, G.R.; Yao, Z.; Baker, G.R.; Gupta, V.K.; Russo, P.S.; Saunders, M.J.*J. Am. Chem. Soc.* **1986**, 108, 849.

42. Newkome, G.R.; Baker, G.R.; Saunders, M.J.; Russo, P.S.; Gupta, V.K.; Yao, Z.; Miller, J.E.; Bouillion, K. *J. Chem. Soc., Chem. Commun.* **1986**, 752.

43. Newkome, G.R.; Moorefield, C.N.; Baker, G.R.; Behera, R.K.; Johnson, A.L. *Angew. Chem., Int. Ed. Engl.* **1991**, 30, 1176.

44. Newkome, G.R.; Moorefield, C.N.; Baker, G.R.; Saunders, M.J.; Grossman, S.H. *Angew. Chem., Int. Ed. Engl.* **1991**, 30, 1178.

45. Newkome, G.R.; Moorefield, C.N.; Theriot, K.J. *J. Org. Chem.* **1988**, 53, 5552.

46. Newkome, G.R.; Behera, R.K.; Moorefield, C.N.; Baker, G.R. *J. Org. Chem.* **1991**, 56, 7162.

47. Newkome, G.R.; Lin, X. *Macromolecules* **1991**, 24, 1443.

48. Newkome, G.R.; Nayak, A.; Behera, R.K.; Moorefield, C.N.; Baker, G.R. *J. Org. Chem.* **1992**, 57, 358.

49. Kwock, E.W.; Neenan, T.X.; Miller, T.M. *Chem. Mater.* **1991**, 3(5), 775-7.

50. Miller, T.M.; Neenan, T.X.; Zayas, R.; Bair, H.E. *J. Am. Chem. Soc.* **1992**, 114(3), 1018-25.

51. Miller, T.M.; Kwock, E.W.; Neenan, T.X. *Macromolecules* **1992**, 25(12), 3143-8.

52. Miller, T.M.; Neenan, T.X. *Chem. Mater.* **1990**, 2(4), 346-9.

53. Uchida, H.; Kabe, Y.; Yoshino, K.; Kawamata, A.; Tsumuraya, T.; Masamune, S. *J. Am. Chem. Soc.* **1990**, 112, 7077-7079.

54. Mathias, L.J.; Carothers, T.W.; Bozen, R.M. *Polym. Prepr., Am. Chem. Soc., Div. Polym. Chem.* **1991**, 32(1), 82-3.

55. Mathias, L.J.; Bozen, R.M. *Gov. Rep. Announce. Index (U.S.)* **1992**, 92(20), Abstr. No. 256,108, Order No. AD-A255195, 3 pp.

56. Mathias, L.J.; Reichert, V.R.; Carothers, T.W.; Bozen, R.M. *Polym. Prepr., Am. Chem. Soc., Div. Polym. Chem.* **1993**, 34(1), 77-8.

57. Carothers, T.W.; Mathias, L.J. submitted to *Macromolecules* **1994**.

58. Carothers, T.W.; Mathias, L.J. *Polym. Prepr., Am. Chem. Soc., Div. Polym. Chem.* **1993**, 34(1), 503-4.

59. Mathias, L.J.; Carothers, T.W. *J. Am. Chem. Soc.* **1991**, 113, 4043.

60. Morikawa, A.; Kakimoto, M.; Imai, Y. *Macromolecules* **1991**, 24(12), 3469-74.

61. Morikawa, A.; Kakimoto, M.; Imai, Y. *Macromolecules* **1992**, 25(12), 3247-53.

62. Van der Made, A.W.; Van Leeuwen, P.W.N.M. *J. Chem. Soc., Chem. Commun.* **1992**, 19, 1400-1.

63. Roovers, J.; Toporowski, P.M.; Zhou, L.L. *Polym. Prepr., Am. Chem. Soc., Div. Polym. Chem.* **1992**, 33(1), 182.

64. Meschke, D.; Hoy, K. European Patent 0,116,978; August 29, 1984.

65. Storey, R.F.; George, S.E. US Patent 5,039,752; August 13, 1991.

66. Storey, R.F.; George, S.E.; Nelson, M.E. *Macromolecules* **1991**, 24(10), 2920-30.

67. Zhou, L; Toporowski, P.M.; Roovers, J. US Patent 5,276,110; January 4, 1994.

68. Roovers, J.; Zhou, L.L.; Toporowski, P.M.; van der Zwan, M.; Iatrou, H.; Hadjichristidi, N. *Macromolecules* **1993**, 26(16), 4324-31.

69. Zhou, L.L.; Hadjichristidi, N.; Toporowski, P.M.; Roovers, J. *Rubber Chem. Technol.* **1992**, 65(2), 303-14.

70. Kansai Shin-Gijyutsu Kenkyo-Sho KK, Japanese Patent 04,285,081; March 11, 1991.

71. Singh, P.; Moll, III, F.; Lin, S.L.; Ferzli, C.; Yu, K.S.; Koski, R.K.; Saul, R.G.; Cronin, P. *Clinical Chemistry* **1994**, 40(9), 1845-1849.

72. O'Sullivan, D.A. *Chemical & Engineering News* **1993**, 71(33), 20-23.

73. Dendritech, Inc. is a subdidiary of Michigan Molecular Institute, located in Midland, Michigan.

74. Sayed-Sweet, Y.; Hedstrand, D.M.; Tomalia, D.A.; Spindler, R. presented at SAMPE Tri-City Michigan Chapter Seminar, Midland, MI, September 10, 1994.

75. Voronkov, M.G.; Lavrent'yet, V.I. *Top. Curr. Chem.* **1982**, 102, 199-236.

76. Wagner, G.H.; Pines, A.N. *Ind. and Eng. Chem.* **1952**, 44(2), 321.

77. Müller, R. *Chem. Techn.* **1950**, 2 (7-13), 41-9.

78. Slinyakova, I.B.; Budkevich, G.B.; Neimark, I.E. *Dokl. Akad. Nauk SSSR* **1964**, 154 (3), 692.

79. Slinyakova, I.B.; Budkevich, G.B.; Neimark, I.E. *Kolloidan Zh.* **1965**, 27 (5), 758.

80. Wiberg, E.; Simmler, W. Z. *Anorg. U. Allgem. Chem.* **1956**, 283, 401.

81. Müller, R.; Köhne, R.; Sliwinski, *S. J. Prakt. Chem.* **1959**, 9 (4), 71.

82. Larson, K. *Arkiv. Kemi.* **1960**, 16, 215.

83. Fyre, C.L.; Collins, W.T. *J. Am. Chem. Soc.* **1970**, 92, 5586.

84. Collins, W.T.; Fyre, C.L. U.S. Patent No. 3,615,272.

85. Haluska, L.A.; Michael, K.W.; Tarhay, L. U.S. Patent 4,756,977.

86. Chandra, G.; Martin (Gentle), T.E. U.S. Patent 5,059,448.

87. Carpenter, L.E.; Gentle, T.E.; Tarhay, L. Dow Corning Patent Application DC 3562.

88. Haluska, L.A.; Michael, K.W.; Tarhay, L. U.S. Patent 4,847,162.

89. Bilgrien, C.J.; Chandra, C.; Haluska, L.A.; Michael, K.W. U.S. Patent 5,262,201.

90. Baney, R.H.; Bilgrien, C.J.; Broderick, D.W.; Carpenter, L.E. U.S. Patent 5,116,637.

91. Ballance, D.S.; Camilletti, R.C.; Gentle, T.E. U.S. Patent 5,145,723.

92. Bank, H.M.; Cifuentes, M.E.; Martin (Gentle), T.E. U.S. Patent 5,010,159.

93. Gentle, T.E.; Hanneman, L.F.; Sharp, K.G. U.S. Patent 5,063,267.

94. Gentle, T.E.; Hanneman, L.F.; Sharp, K.G. U.S. Patent 5,118,530.

95. Gentle, T.E. U.S. Patent 5,165,955.

96. Gentle, T.E. U.S. Patent 5,279,661.

97. Nyman, M.D.; Desu, S.B.; Peng, C.H. *Chem. Mater.* **1993**, 5, 1636.

98. Day, V.W.; Klemperer, W.G.; Mainz, V.V.; Millar, D.M. *J. Am. Chem. Soc.* **1985**, 107(26), 8562-8264.

99. Feher, F.J.; Newman, D.A.; Walzer, J.F. *J. Am. Chem. Soc.* **1989**, 111, 1741-1748.

100. Feher, R.J.; Budzichowski, T.A.; Rahimian, K.; and Ziller, J.W. *J. Am. Chem. Soc.* **1992**, 114(10), 3859-3866.

101. Feher, F.J.; Gonzales, S.L.; Ziller, J.W. *Inorg. Chem.* **1988**, 27, 3440.

102. Feher, F.J.; Blanski, R.L. *J. Chem. Soc., Chem. Commun.* **1990**, 1614.

103. Feher, F.J.; Walzar, J.F. *Inorg. Chem.* **1991**, 30, 1689.

104 Feher, F.J.; Budzichowski, T.A. *Organometallics* **1990**, 10, 812.

105. Feher, F.J.; Walzar, J.F.; Blanski, R.L. *J. Am. Chem. Soc.* **1991**, 113, 3618.

106. Liu, J.-C.; Wilson, S.R.; Shapley, J.R.; Feher, F.J. *Inorg. Chem.* **1990**, 29, 5138.

107. Budzichowski, T.A.; Chacon, S.T.; Chisholm, M.H.; Feher, F.J.; Streib, W. *J. Am. Chem. Soc.* **1991**, 113, 680.

108. Feher, F.J.; Walzer, J. F. *Inorg. Chem.* **1990**, 29, 1604.

109. Feher, F.J.; Newman, D.A. *J. Am. Chem. Soc.* **1990**, 112, 1931.

110. Feher, F.J.; Budzichowski, T.A.; Blanski, R.L.; Weller, K.J.; Ziller, J.W. *Organometallics* **1991**, 10, 2526.

111. Agaskar, P.A. *Inorg. Chem.* **1990**, 29, 1603.

112. Klemperer, W.G.; Mainz, V.V.; Millar, D.M. in Better Ceramics through Chemistry II (*Mat. Res. Soc. Symp. Proc.*, Vol 73, **1986**, 3-13), Ed. Brinker, Clark, Ulrich, Materials Research Society.

113. Agaskar, P.A.; Day, V.W.; Klemperer, W.G. J. *Am. Chem. Soc.* **1987**, 109, 5554-5556.

114. Agaskar, P.A. *Synth. React. Inorg. Met.-Org. Chem.* **1990**, 20(4), 483.

115. Groennen, EJ.; Kortbeck, A.G.T.G.; Mackay, J.; Sudmeijer, O. *Zeolites* 1986, 6, 403.

116. Tamas, F.D.; Sarkar, A.K.; Roy, D.M. *Hung. J. Ind. Chem.* **1977**, 5, 115.

117. Agaskar, P.A. *J. Am. Chem. Soc.* **1989**, 111, 6859-6859.

118. Bürgy, H.; Calzaferri, G.; Herren, D.; Zhdanov, A. *Chimia* **1991**, 45, 3.

119. Feher, F.J.; Budzichowski, T.A. *J. Organomet. Chem.* **1989**, 379, 33.

120. Feher, F.J.; Budzichowski, T.A.; Weller, K.J. *J. Am. Chem. Soc.* **1989**, 111, 7288

121. Feher, F.J. *J. Am. Chem. Soc.* **1986**, 108, 3850.

122. Brown, J.F.; Vogt, L.H. *J. Am. Chem. Soc.* **1965**, 87, 4313.

123. Feher, F.J.; Weller, K.J. *Organometallics* **1990**, 9, 2638.

124. Feher, F.J.; Weller, K.J. *Inorg. Chem.* **1991**, 30, 880.

125. Herren, D.; Burgy, H.; Calzaferri, G. *Helv. Chim. Acta* **1991**, 74, 24-26.

126. Calzaferri, G.; Imhof, R. J. *Chem. Soc., Dalton Trans.* **1992**, 23, 3391-2.

127. Agaskar, P.A. *Inorg. Chem.* **1991**, 30, 2707-2708.

128. Burgy, H.; Calzaferri, G. *J. of Chromatography* **1990**, 507, 481-486.

Chapter Two

Hydrocarbon and Siloxane Octopus Molecules via Hydrosilylation

2.0 Introduction

The aim of this initial work was to investigate the feasibility of putting eight pendant groups onto the T_8 sphere to make octopus molecules. Examples of the proposed types of target pendant groups included, among others, hydrocarbons, siloxanes, polyethers, and acrylate chains. In addition, once successful in synthesizing these monodispersed molecules of defined shape and size, with molecular weights that could go well into the thousands, the characterization of such molecules presented a formidable challenge. The high symmetry of these molecules could make NMR spectroscopy particularly diagnostic and solution NMR was our first method of choice for characterization. In addition, because the molecular weights and volatility of these macromonomers gets very high when eight pendant groups are placed on a core, Gas Chromatography (GC) would not be useful for characterization, but Gel Permeation Chromatography (GPC), sometimes called Size Exclusion Chromatography (SEC), appeared to be appropriate.

The reaction we used to add the pendant groups to T_8 in our initial work was hydrosilylation as shown in the reaction in scheme 2.1.

$$R_3SiH + CH_2{=}CHXR'_3 \rightarrow R_3SiCH_2CH_2XR'_3 \qquad (2.1)$$

2.1 Hydrocarbon Octopus Molecules

At the time of the first experiments in these studies, Herren *et al* reported that T_8 hydrogen silsesquioxane was efficient in hydrosilylations[1]. They reported on the hydrosilylation of 1-hexene by T_8 and showed that hydrosilylation proceeds with retention of the cage structure[1] although ^{29}Si NMR chemical shifts were not reported.

For initial feasibility and a check on the extent of hydrosilylation by T_8, a series of 1-alkenes were used in the reaction with T_8. By these reactions, we hoped to obtain a series of octopus molecules with hydrocarbon arms of various lengths. A model for the product of such a reaction (T_8 + 1-hexene) is shown in Figure 2.1, and the restricted conformational freedom within the molecule is quite apparent. The restrictions imposed by attachment to the core are obvious, but there may be further limitations on conformational mobility owing to the close proximity of the chains, and the limited arc or 'cone angle' for chains rotation that this induces. Dramatic conformational restrictions have already been observed in the ^1H NMR spectra of octopus molecules based on benzene cores[2].

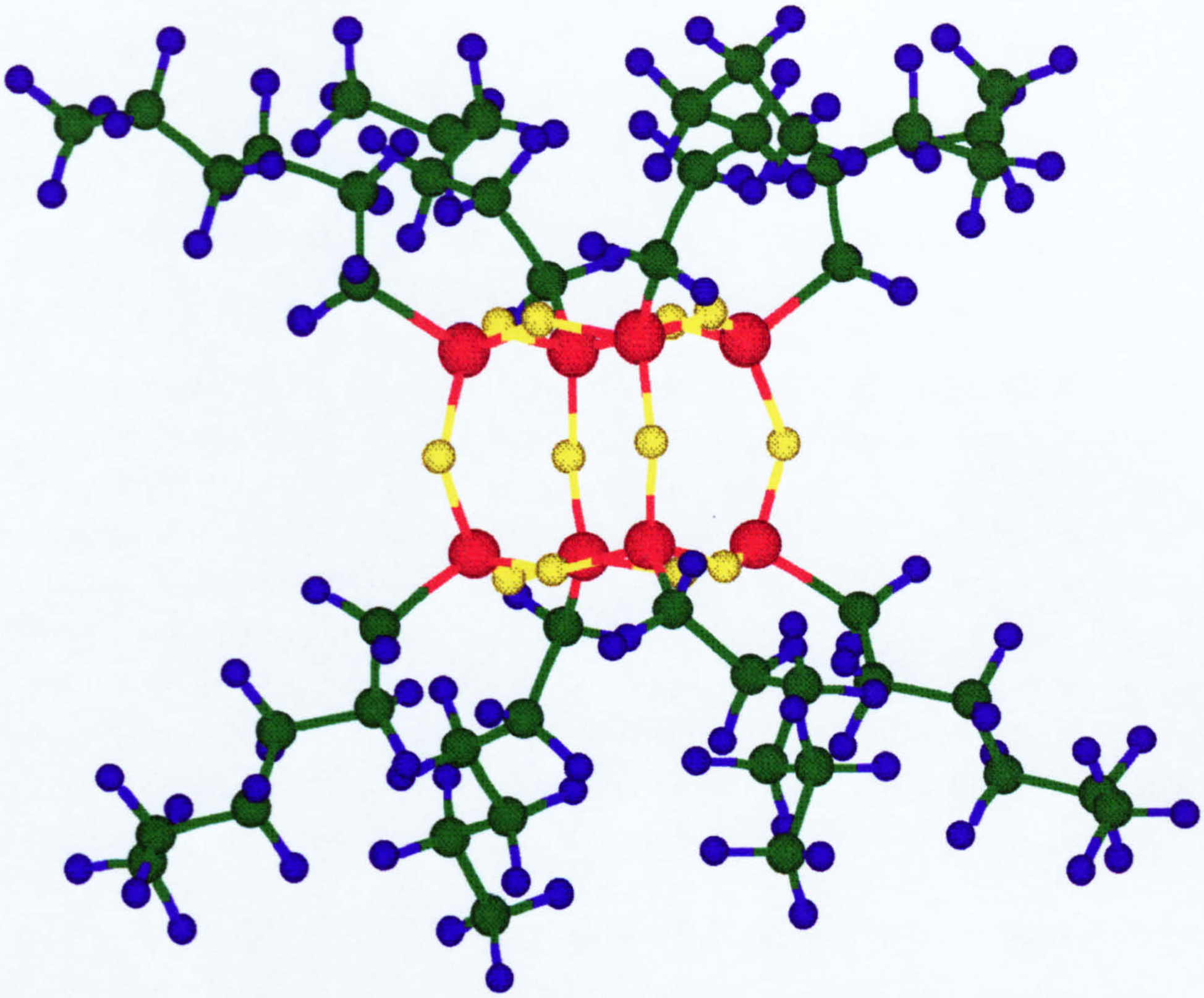

Figure 2.1 Model of the product of the hydrosilylation of 1-hexene by T_8 hydrogen silsesquioxane. Green=Carbon, Yellow=Oxygen, Red=Silicon, Blue=Hydrogen.

2.1.1 NMR Data for Hydrocarbon Octopus Molecules

Hydrocarbon octopus molecules were synthesized by mixing solid T_8 hydrogen silsesquioxane with the appropriate 1-alkene in a T_8:alkene molar ratio of 1:8 and heating the reaction mixtures in the presence of H_2PtCl_6 catalyst at approximately 60 °C. It was found that the hydrosilylations by T_8 of 1-hexene, 1-decene, 1-tetradecene, and 1-octadecene were very efficient and progressed essentially to completion in each case. The disappearance of SiH was followed using FTIR spectroscopy. The ^{29}Si NMR spectra of the products of the reactions of T_8 with 1-hexene (Figure 2.2), with 1-decene (Figure 2.3), with tetradecene (Figure 2.4), and with octadecene (Figure 2.5) confirmed that in all these cases the T_8 cage structure is retained and single products are obtained in the first three reactions. In the case of the reaction of T_8 and 1-octadecene, the 1-octadecene was only 90% pure and resulted in a mixture of products as indicated by the presence of several peaks in the T Si region of the spectrum.

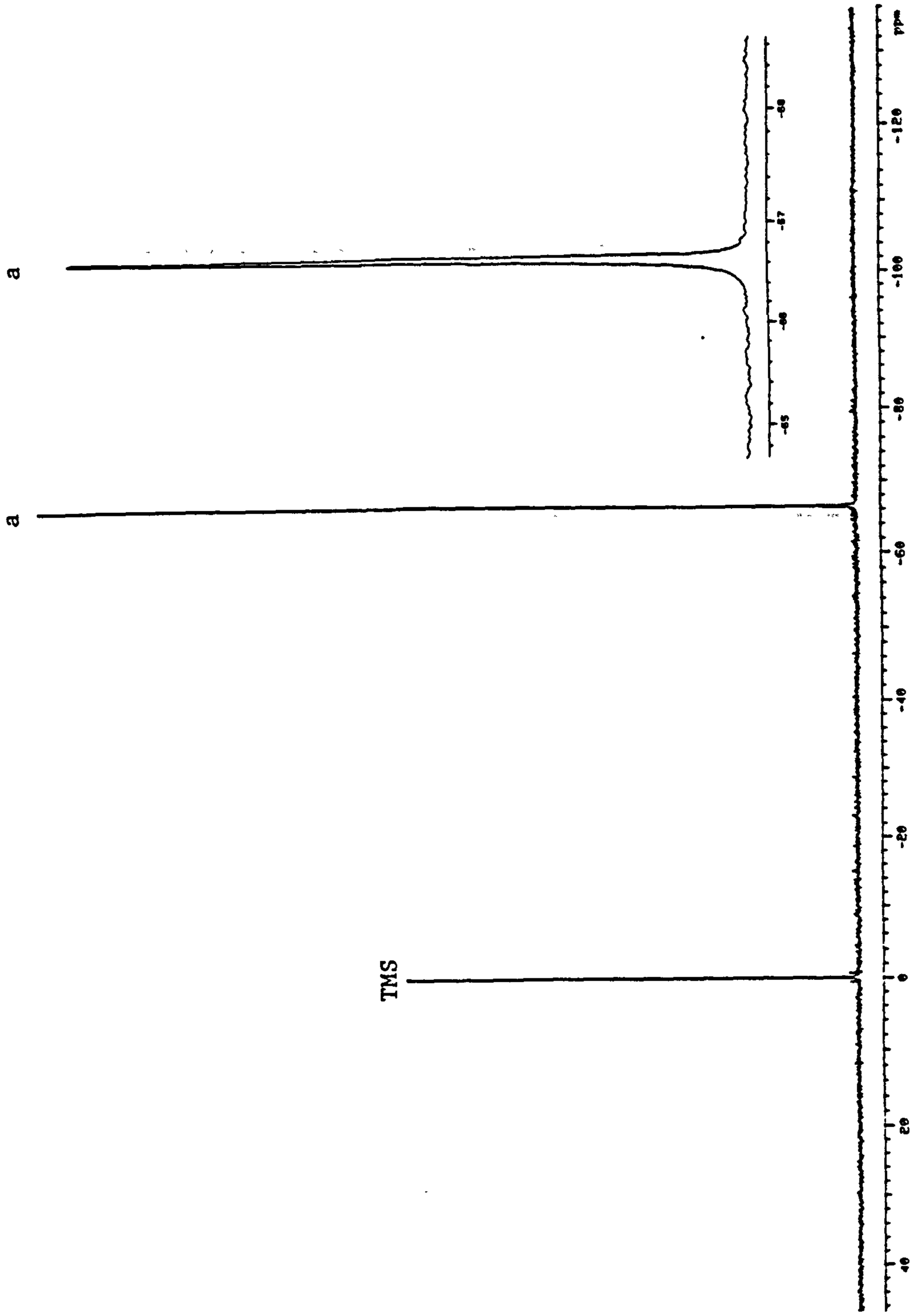

Figure 2.2 ^{29}NMR spectrum of the product of T_8 + 1-hexene reaction.

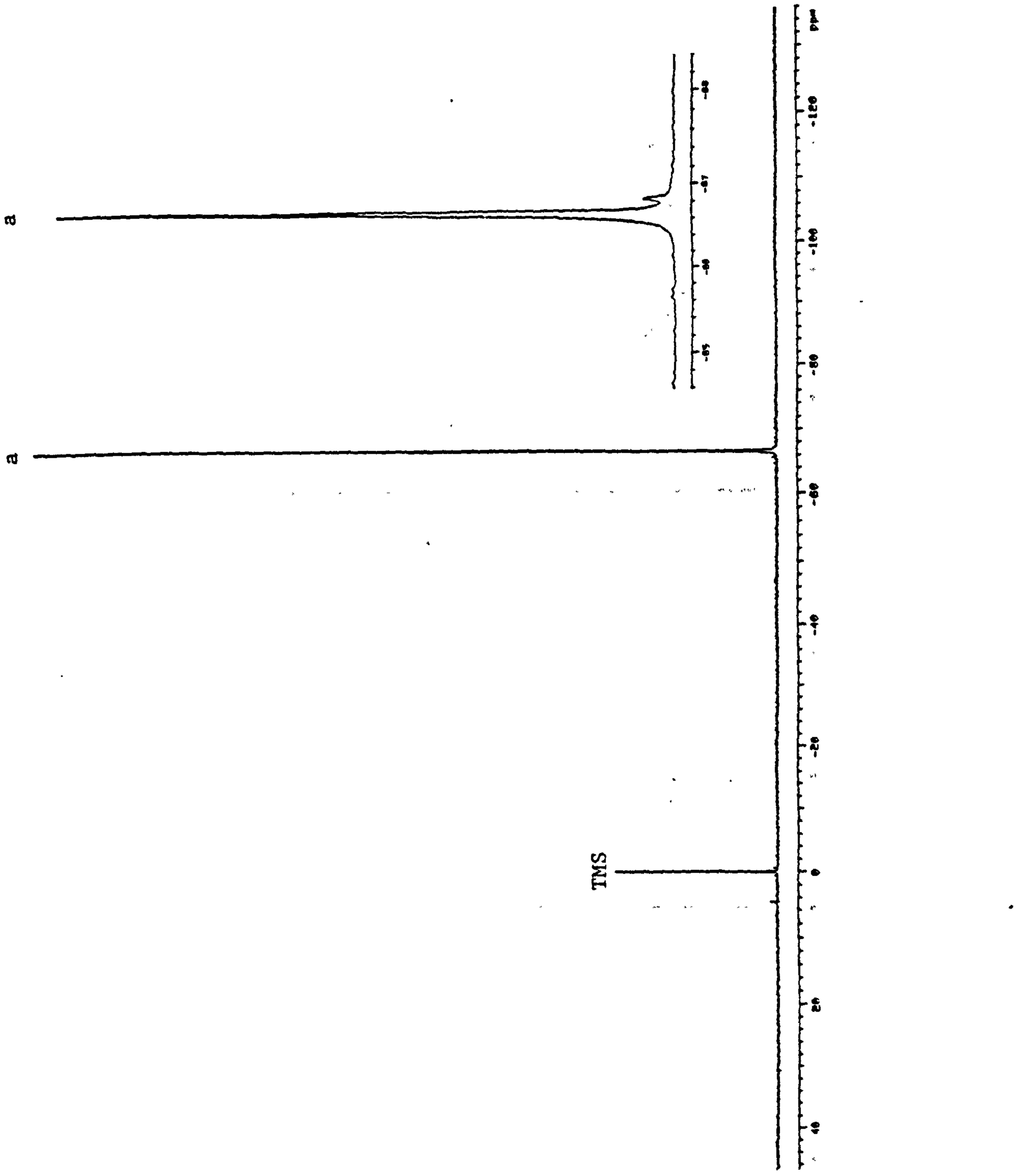

Figure 2.3 ^{29}NMR spectrum of the product of T_8 + 1-decene reaction.

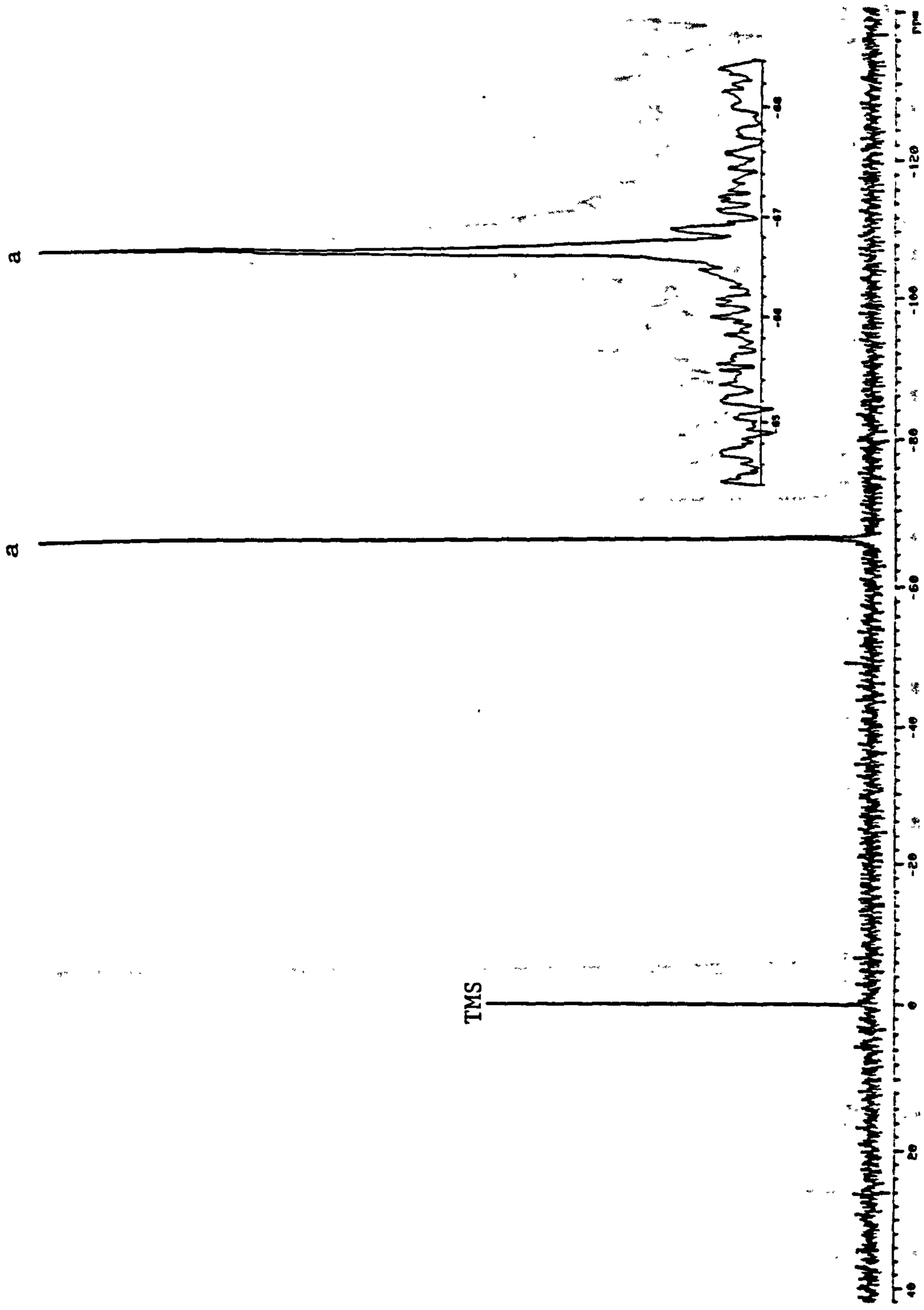

Figure 2.4 ^{29}NMR spectrum of the product of T_8 + 1-tetradecene reaction.

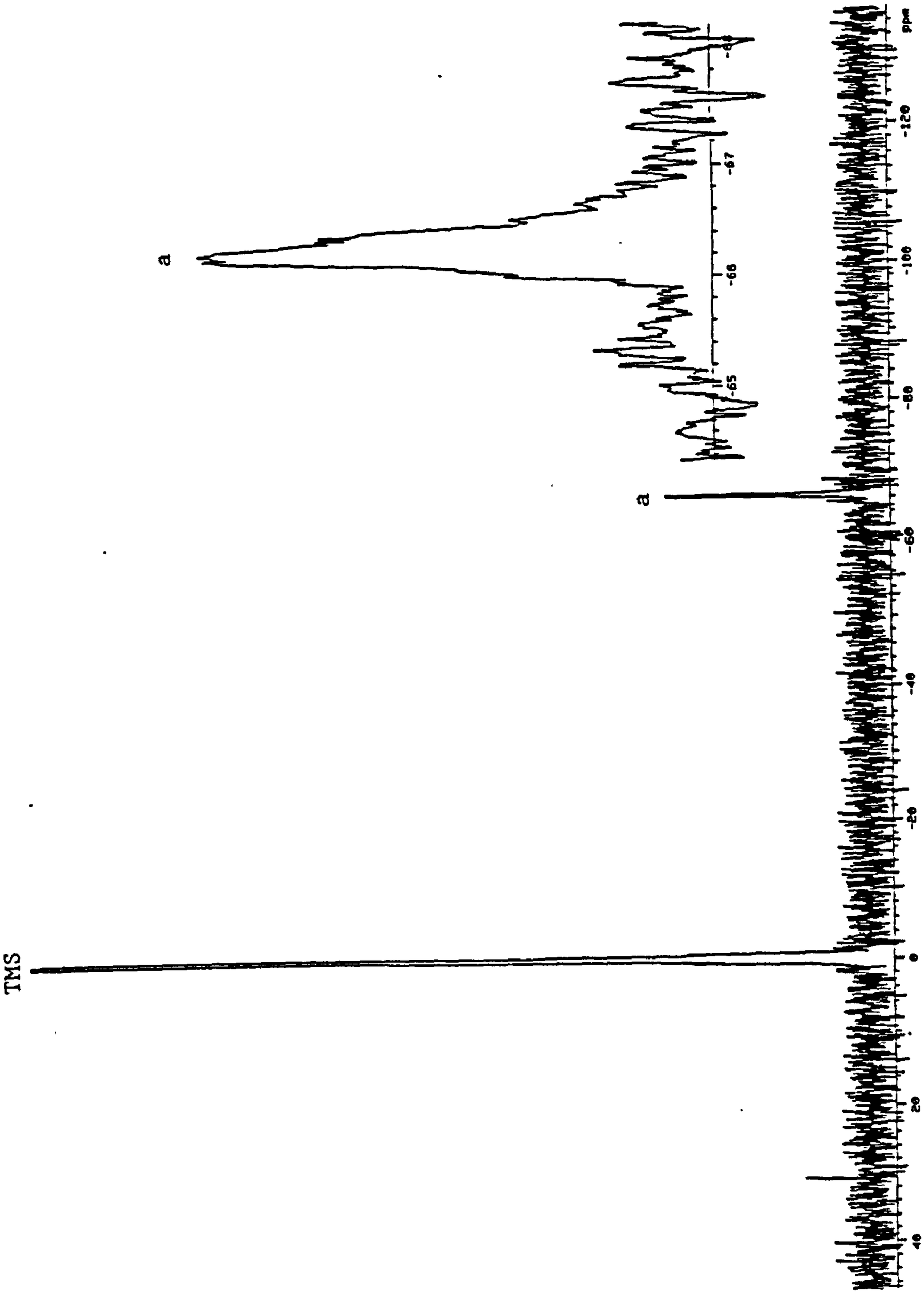

Figure 2.5 ^{29}NMR spectrum of the product of T_8 + 1-octadecene reaction.

2.1.2 GPC Data for Hydrocarbon Octopus Molecules

The overlay of the gel permeation chromatography (GPC) chromatograms from this series of reactions (Figure 2.6) shows the monodispersity of each of the reaction products with the exception of a slight broadening of the peak for the T_8 + 1-octadecene for the same reason as discussed above. The increase in molecular weight with the increase in the size of the pendant group is also apparent from the chromatograms. As these chromatograms are for the unpurified reaction mixtures the remarkable efficiency of these hydrosilylation reactions is demonstrated. Because of the unusual geometry of these novel materials, standards of similar molecular structure are not available. Linear polydimethylsiloxane (PDMS) standards were used in the GPC analysis. Table 2.1 shows that in the case of the alkene adducts to the T_8 core, the molecular weight obtained by GPC are remarkably close to the expected molecular weights and the monodispersed nature of the products is confirmed. As will be shown later, this close relationship between the calculated and observed GPC molecular weights was not generally observed owing to the unavailability of appropriate GPC standards.

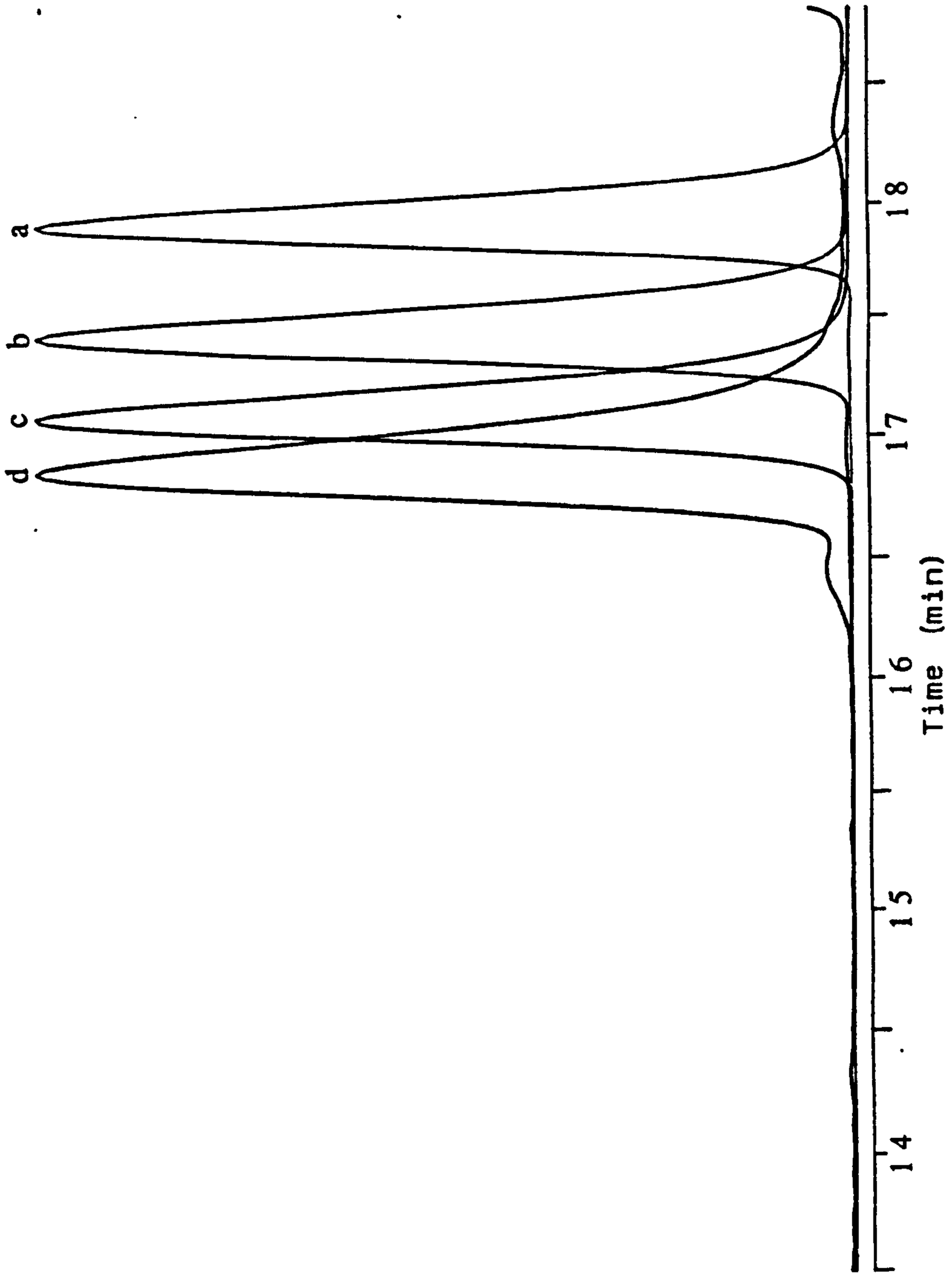

Figure 2.6 The overlay of GPC chromatograms from the series of T_8 + 1-alkene reactions. a= 1-hexene; b= 1-decene; c= 1-tetradecene; d= 1-octadecene.

Table 2.1.

Expected molecular weights of T_8 + 1-alkenes compared to molecular weights determined by GPC

GPC Ret. Time (Min)	Product	M_n	M_w	Dispersity	Expected MW
17.92	T_8+1-hexene	948	958	1.010	1096
17.43	T_8+1-decene	1524	1542	1.012	1544
17.10	T_8+1-tetradecene	2139	2167	1.013	1992
16.87	T_8+1-octadecene	2633	2680	1.018	2440

2.2 Siloxane Octopus Molecules

Having shown the efficiency of hydrosilylation by T_8, we were interested in making an octopus molecule with siloxane "arms" of a particular length. In order to make such a molecule, siloxane chains of a fixed length that were vinyl terminated on just one end were desired for hydrosilylation by the T_8. A synthesis to obtain siloxane chains of this kind has been described by several researchers[3-6], involving the anionic ring-opening polymerization of hexamethylcyclotrisiloxane (D_3) using butyl lithium as an initiator, followed by end-capping with a suitably substituted chlorosilane. By this method, $BuSi(CH_3)_2[OSi(CH_3)_2]_3CH=CH_2$, which has a siloxane chain that is vinyl terminated at one end was obtained. As the GPC in Figure 2.7 shows, a pure, monodispersed portion was obtained after distillation. This vinyl-terminated siloxane chain was used in the reaction with T_8 to form a siloxane octopus.

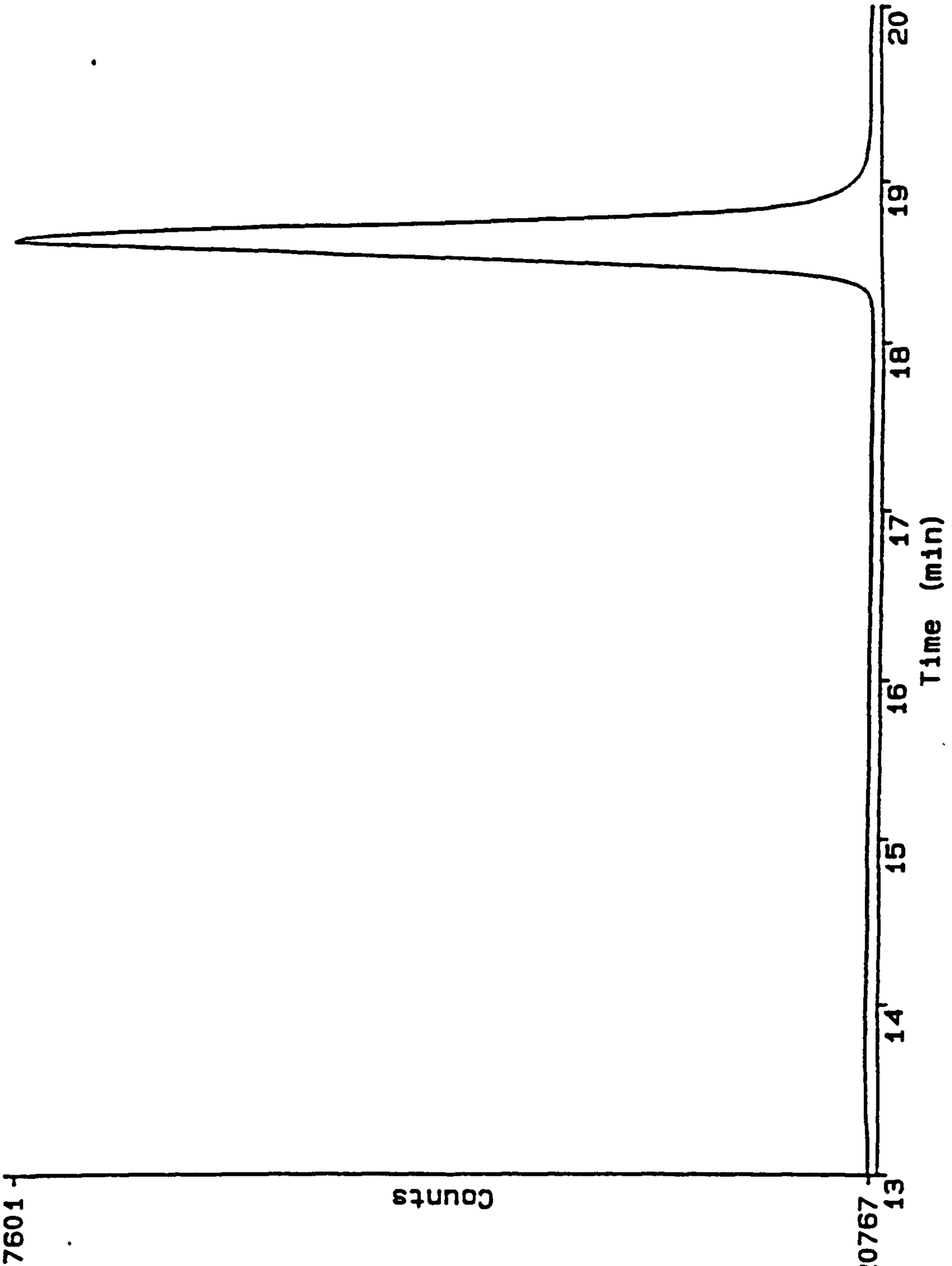

Figure 2.7 GPC chromatogram of purified $BuSi(CH_3)_2[OSi(CH_3)_2]_3CH{=}CH_2$.

2.2.1 NMR Data for Vinyl Siloxane Reaction

Silicon being a good directing group[7], it was expected that the ^{29}Si NMR would be very similar to that of the hydrocarbon octopus molecules. However, as the T-Si region of the ^{29}Si NMR of the siloxane octopus molecule shown in Figure 2.8 indicates, there appears to be several T-Si environments between δ -65.5 and -67.2 ppm referenced to TMS at 0.0 ppm.

Several possible explanations for the multiple resonances in the T Si region were explored initially, including incomplete reaction, conformational differences, impure starting materials, rearrangement of the T_8 cage to higher T structures, and non-regioselective addition.

Impurities in the starting materials was not a likely cause of the multiple resonances. The T_8 appeared to be quite pure as was shown by the ^{29}Si NMR (Figure 2.9) and the vinyl-siloxane was found to be pure by ^{29}Si NMR (Figure 2.10), GC (Figure 2.11), GC/MS (Figure 2.12), and previously shown GPC (Figure 2.7).

Incomplete reaction was considered to be a likely cause of the multiple resonances in the ^{29}Si NMR as there are four different silicon environments in a hepta-substituted T_8 derivative, and many more different silicon environments if hexa- and penta-substituted derivatives are also considered. This cannot, however, be a contributor to the signal multiplicity, in this case, as the FTIR spectrum in Figure 2.13 shows that there was no measurable amount of SiH remaining in the sample.

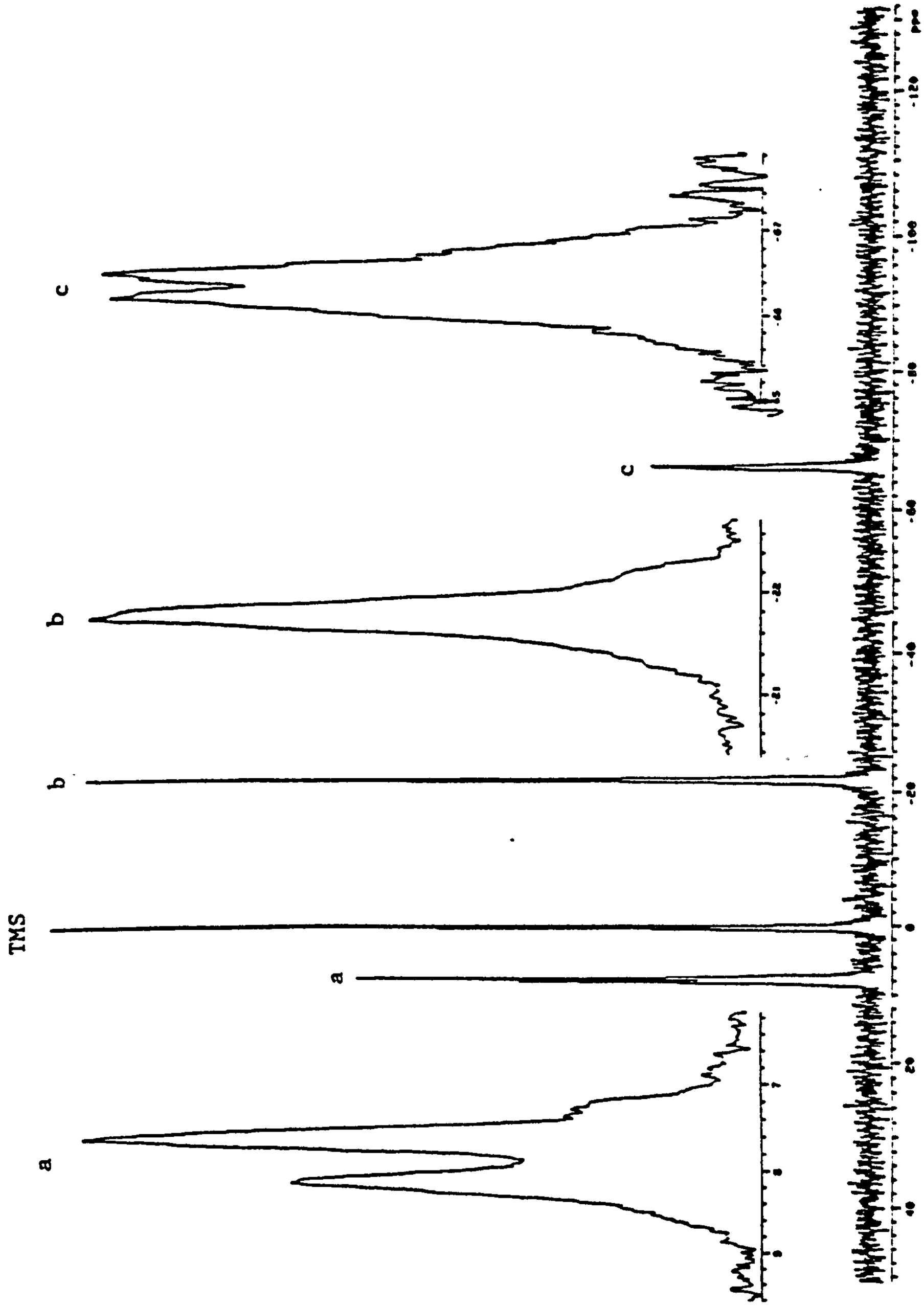

Figure 2.8 ^{29}Si NMR spectrum for the reaction of T_8 + $BuSi(CH_3)_2[OSi(CH_3)_2]_3CH{=}CH_2$.

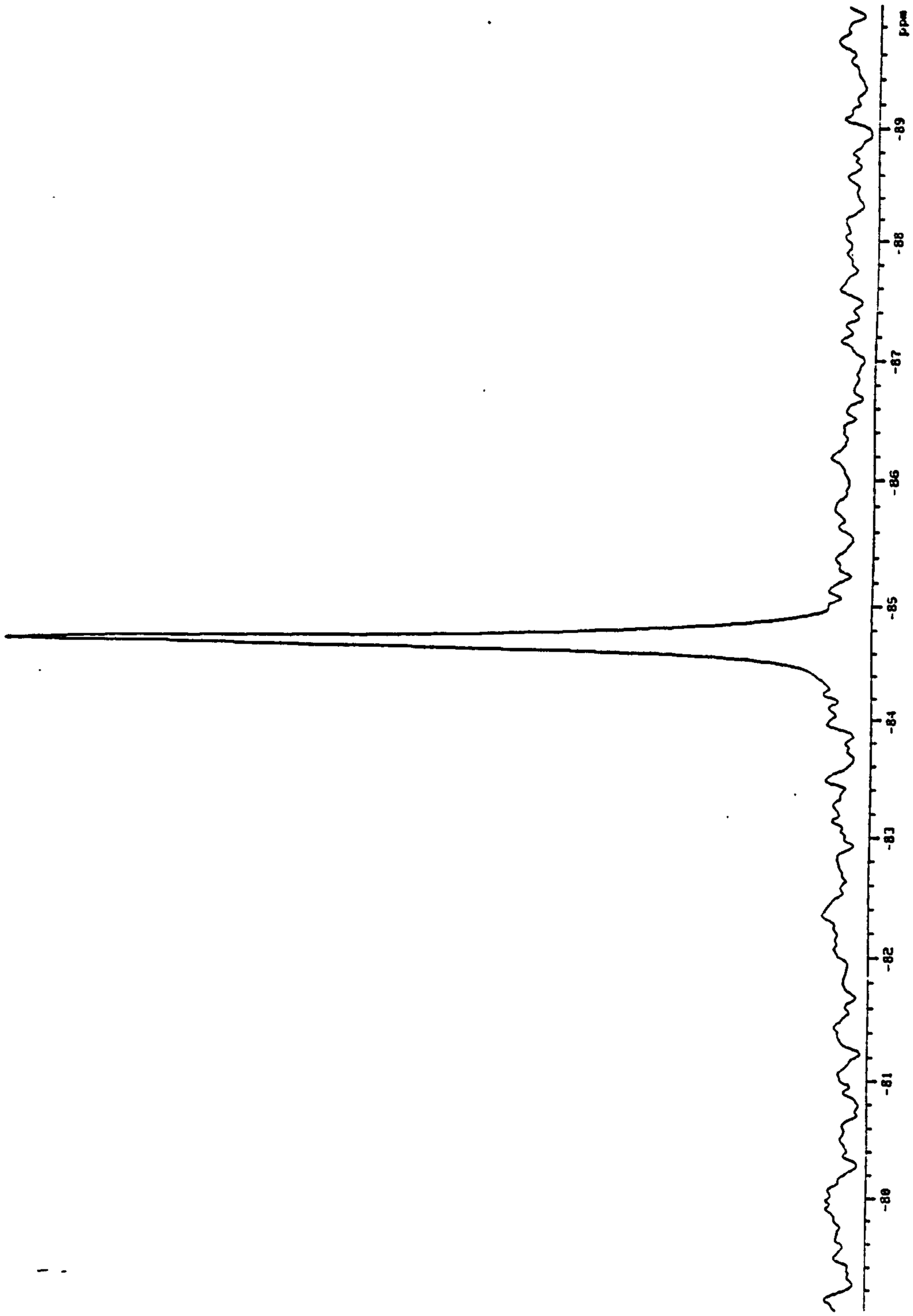

Figure 2.9 ^{29}Si NMR spectrum of $(HSiO_{3/2})_8$.

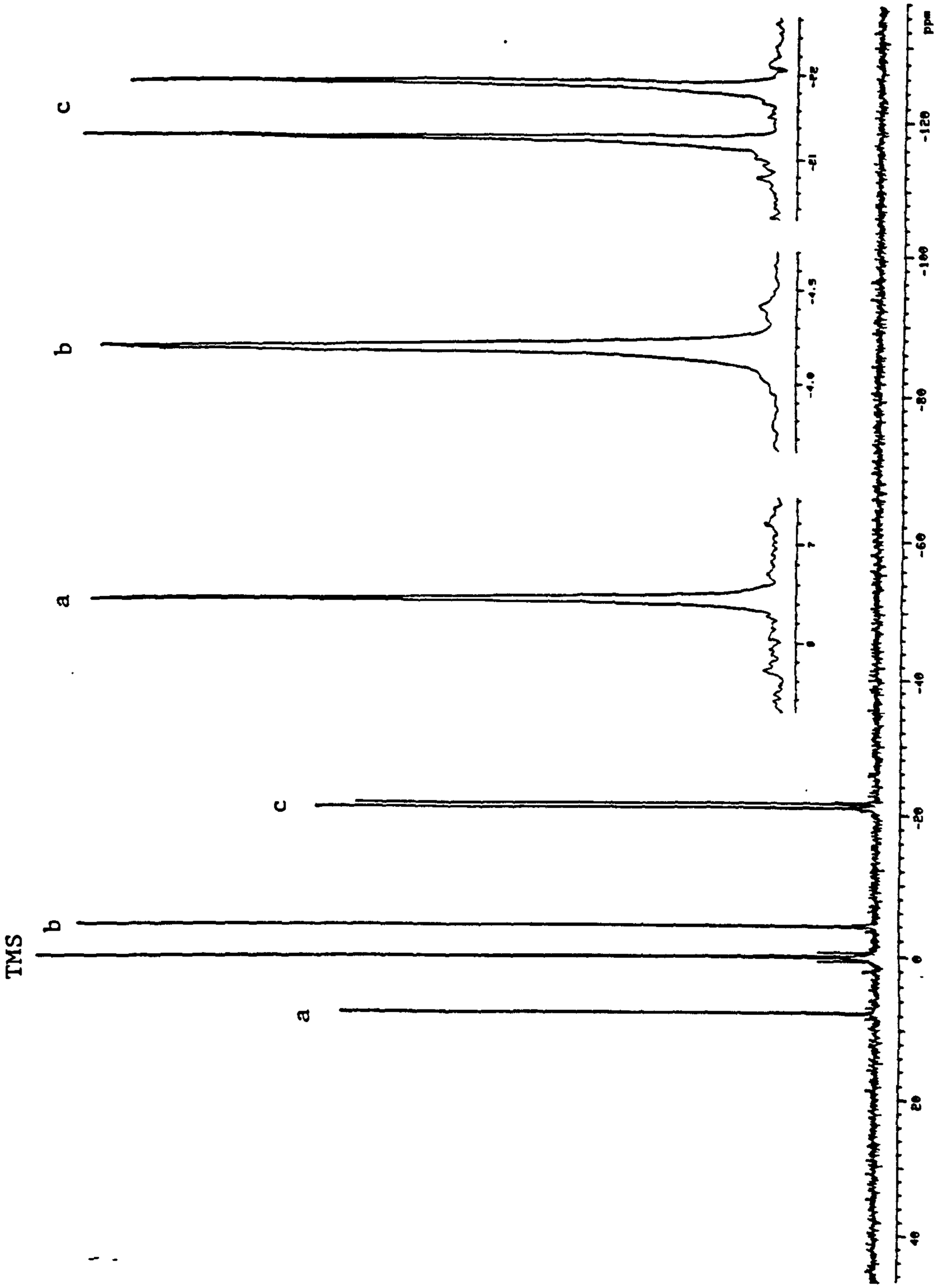

Figure 2.10 ^{29}Si NMR spectrum of $BuSi(CH_3)_2[OSi(CH_3)_2]_3CH{=}CH_2$.

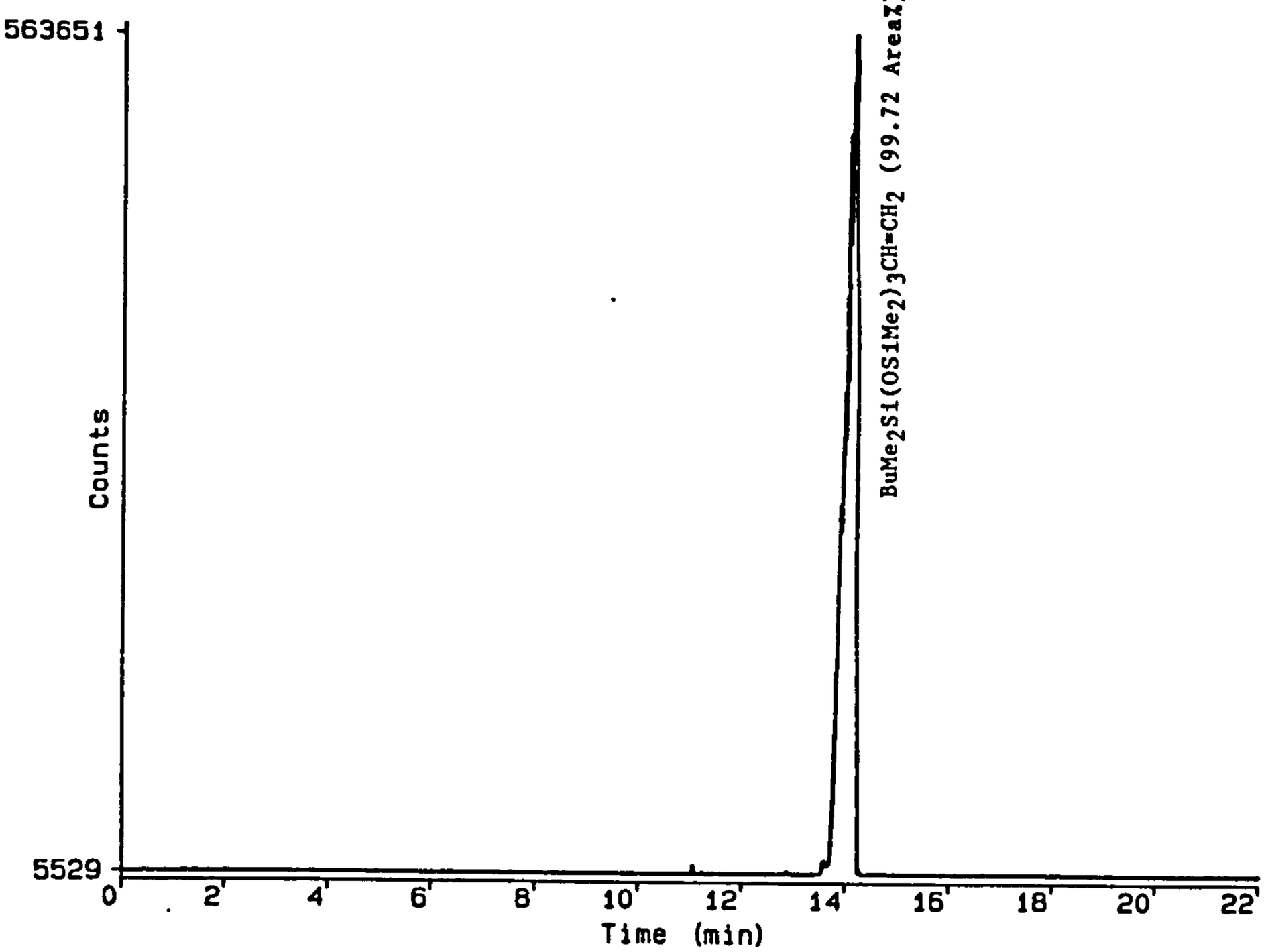

Figure 2.11 GC of $BuSi(CH_3)_2[OSi(CH_3)_2]_3CH{=}CH_2$.

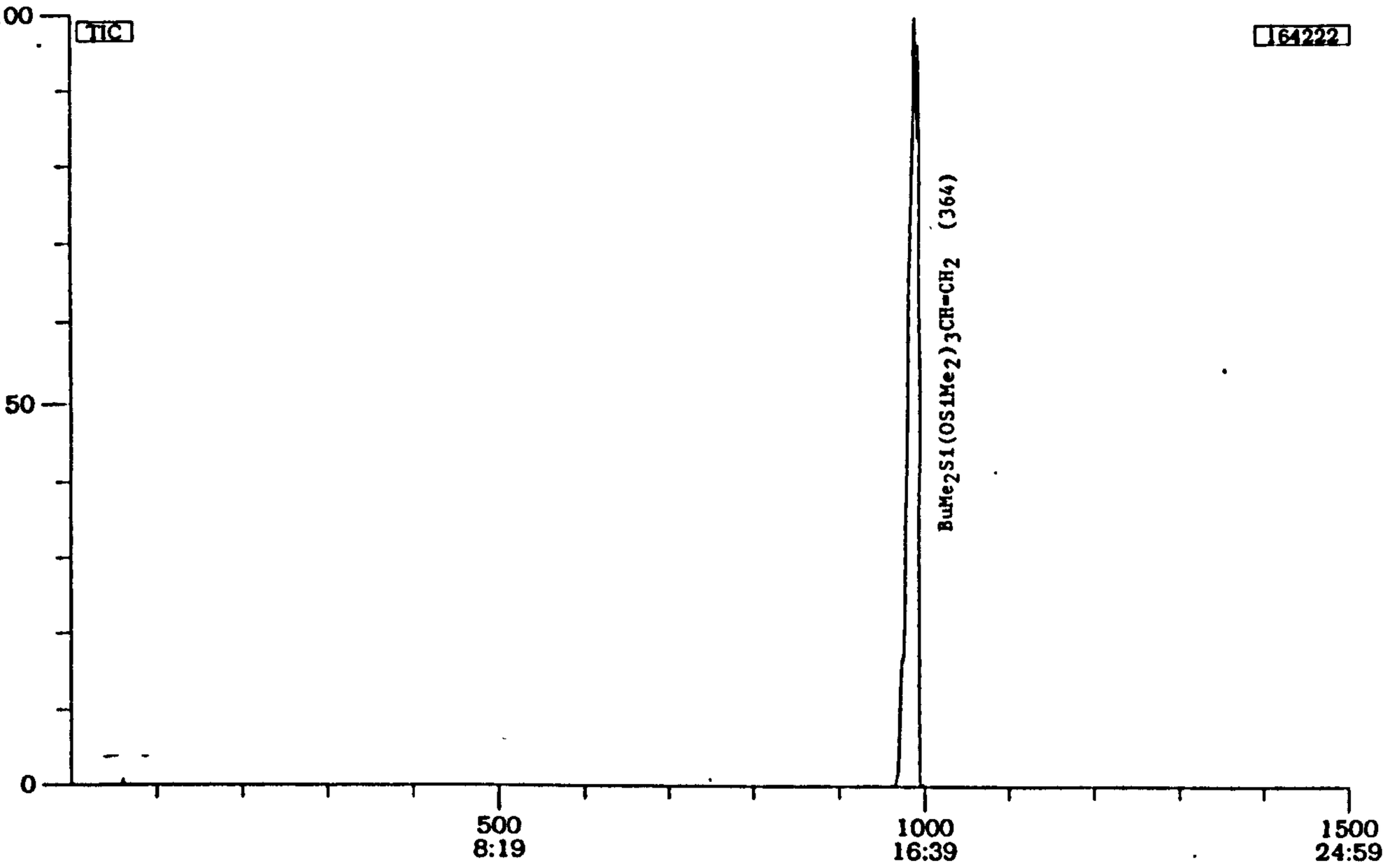

Figure 2.12 GC/MS of $BuSi(CH_3)_2[OSi(CH_3)_2]_3CH{=}CH_2$.

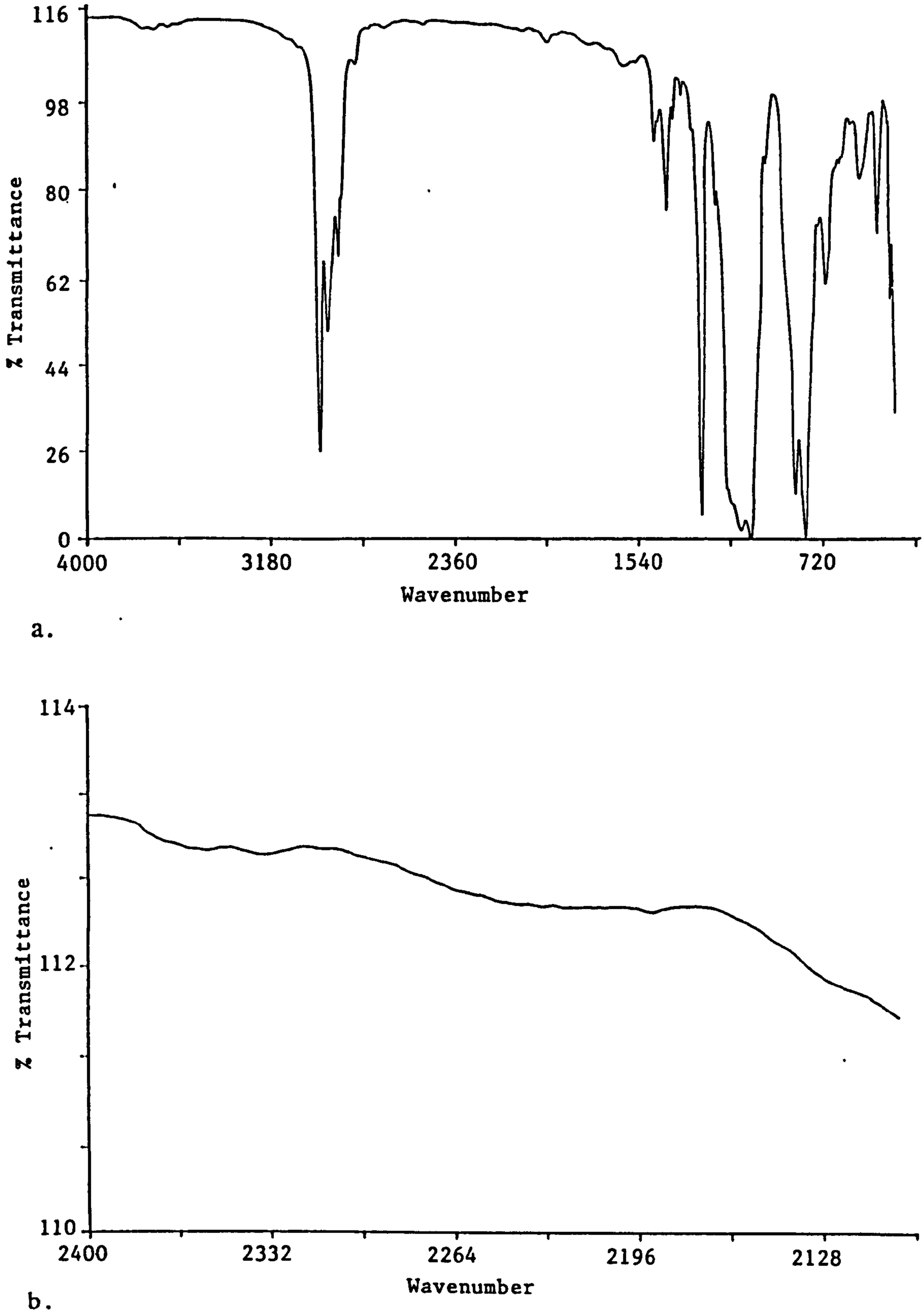

Figure 2.13 FTIR of T_8 + vinyl-siloxane reaction (a. full spectrum, b. enlargement of area of interest) showing no measurable amount of SiH at 2260 cm^{-1}.

It is improbable that conformational effects in the simple cage plus arms structure could produce such a large number of peaks in the ^{29}Si NMR spectrum but if conformational effects were responsible for the multiple peaks, one would expect that with increasing temperature the multiple peaks would become one as the time scale of the conformational changes became greater than that of the NMR experiment with increasing temperature. The ^{29}Si NMR spectrum was measured over a wide range of temperatures and was effectively unchanged between 0° and 120 °C. The temperature invariance of the ^{29}Si NMR spectrum supports the conclusion that conformational effects are not responsible for the multiple peaks.

Similarly, it was not very likely that the T_8 cage had undergone rearrangement to higher T structures such as T_{10} during hydrosilylation. However, to confirm this, an experiment in which a mixture of T_8 and T_{10} was used in the hydrosilylation was conducted and the ^{29}Si NMR of the product was examined to see if the T_8 and T_{10} products were distinct. Figure 2.14 shows the ^{29}Si NMR spectrum of the mixture of T_8 and T_{10} and as the spectrum shows the peak for the T_8 and the peak for T_{10} are well resolved. The T-Si region of the spectrum for the products of the reaction of the mixture of T_8 and T_{10} with the vinyl-siloxane is shown in Figure 2.15 and as can be seen the products are indeed distinct and in each case, the T-Si peak is actually a grouping of unresolved peaks.

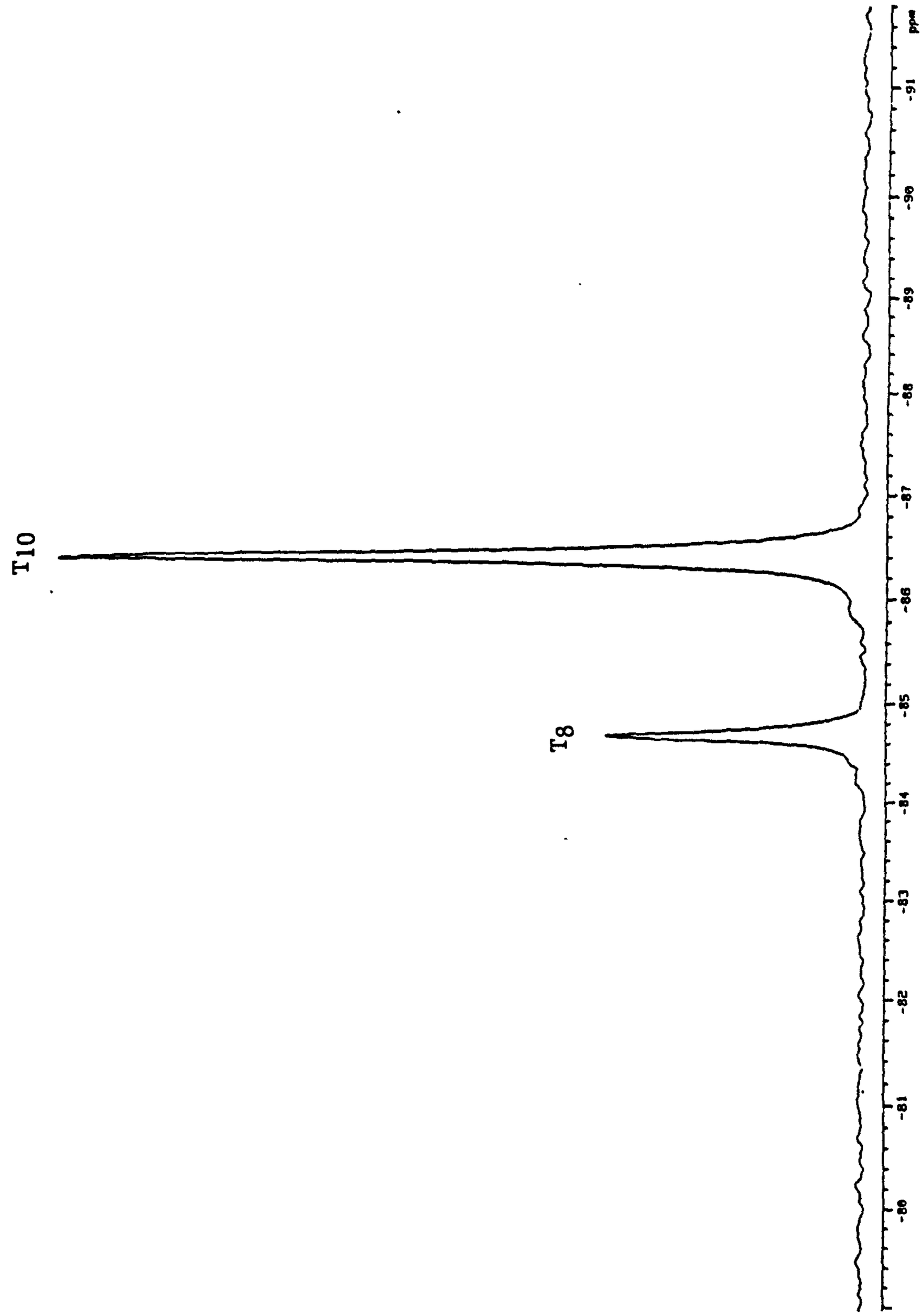

Figure 2.14 ^{29}Si NMR spectrum of a mix of T_8 and T_{10} hydrogen silsesquioxane.

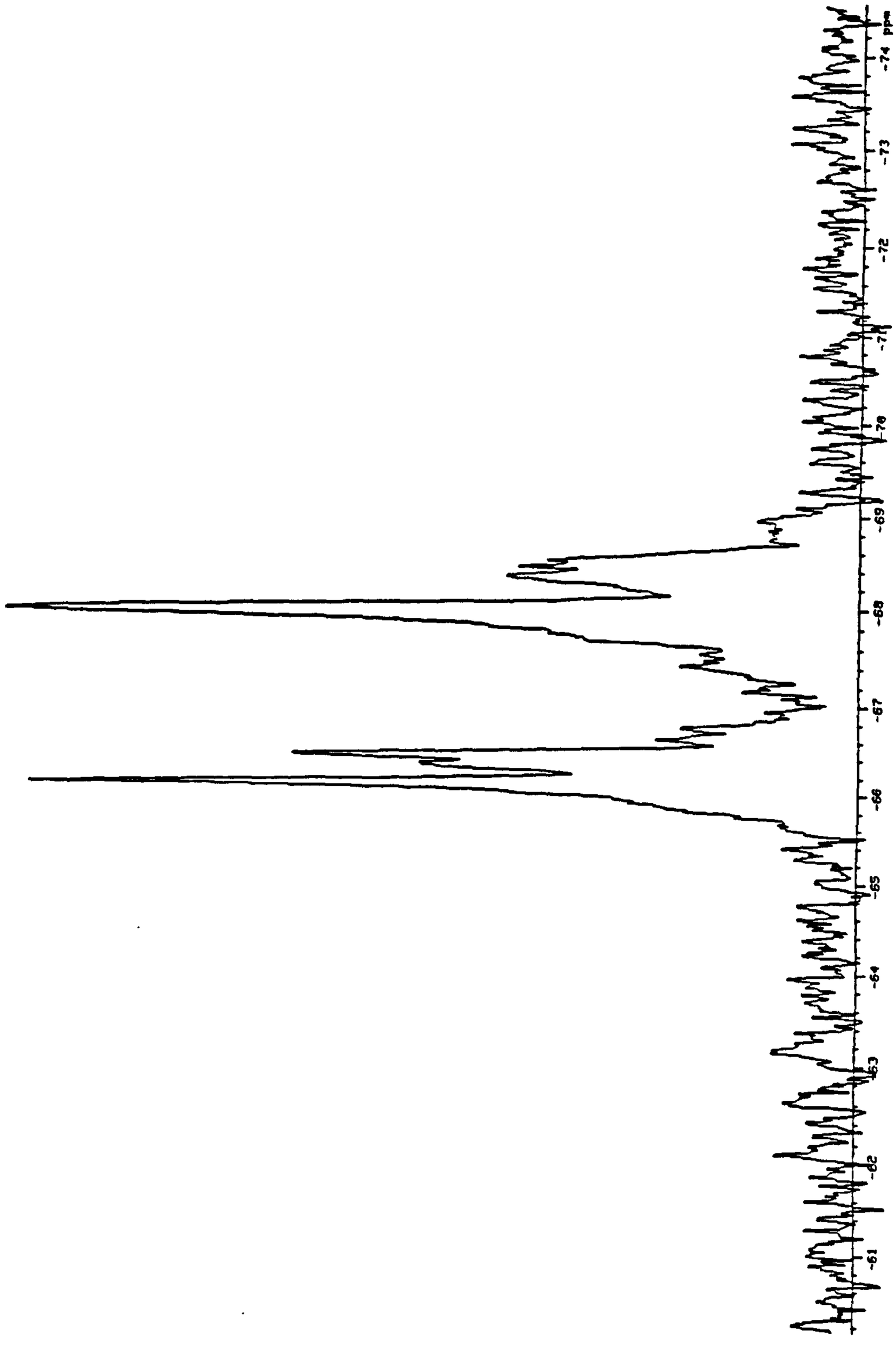

Figure 2.15 The T-Si region of the ^{29}Si NMR spectrum of the products of the reaction of the mix of T_8 and T_{10} hydrogen silsesquioxane and vinyl-siloxane.

The addition of the 1-alkenes to T_8 was regioprecise with only α-addition being observed. There are, however, two possible modes of addition, α and β, as shown in scheme 2.2.

$CH_2=CH\text{-}Si(CH_3)_2O\ldots + HSiO_{3/2} \rightarrow$

$\ldots OSi(CH_3)_2CH_2CH_2SiO_{3/2}$ α-addition

and (2.2)

$\ldots OSi(CH_3)_2CHSiO_{3/2}$ β-addition

CH_3

As silicon has a very strong directing effect, vinylsilanes usually undergo stereoselective addition reactions[7]. It was not therefore expected that the multiplicity of the ^{29}Si NMR signals would arise from products in which the T_8 cores carried some arms from α-addition and some from β-addition.

Although it appeared unlikely initially, both α- and β-addition do occur in the hydrosilylation of the vinyl-siloxane with T_8. The ^{13}C NMR spectrum, and the DEPT spectra in particular revealed that there are peaks that can be positively assigned to the CH and the CH_3 groups (Figure 2.16) that arose from the β-addition. By measuring the area of the ^{13}C NMR peaks assigned to the CH and CH_3 resulting from the beta addition relative to the area of the two CH_2 peaks resulting from the alpha addition, it was estimated that approximately 21% of the additions occurred beta to the vinyl group in this reaction.

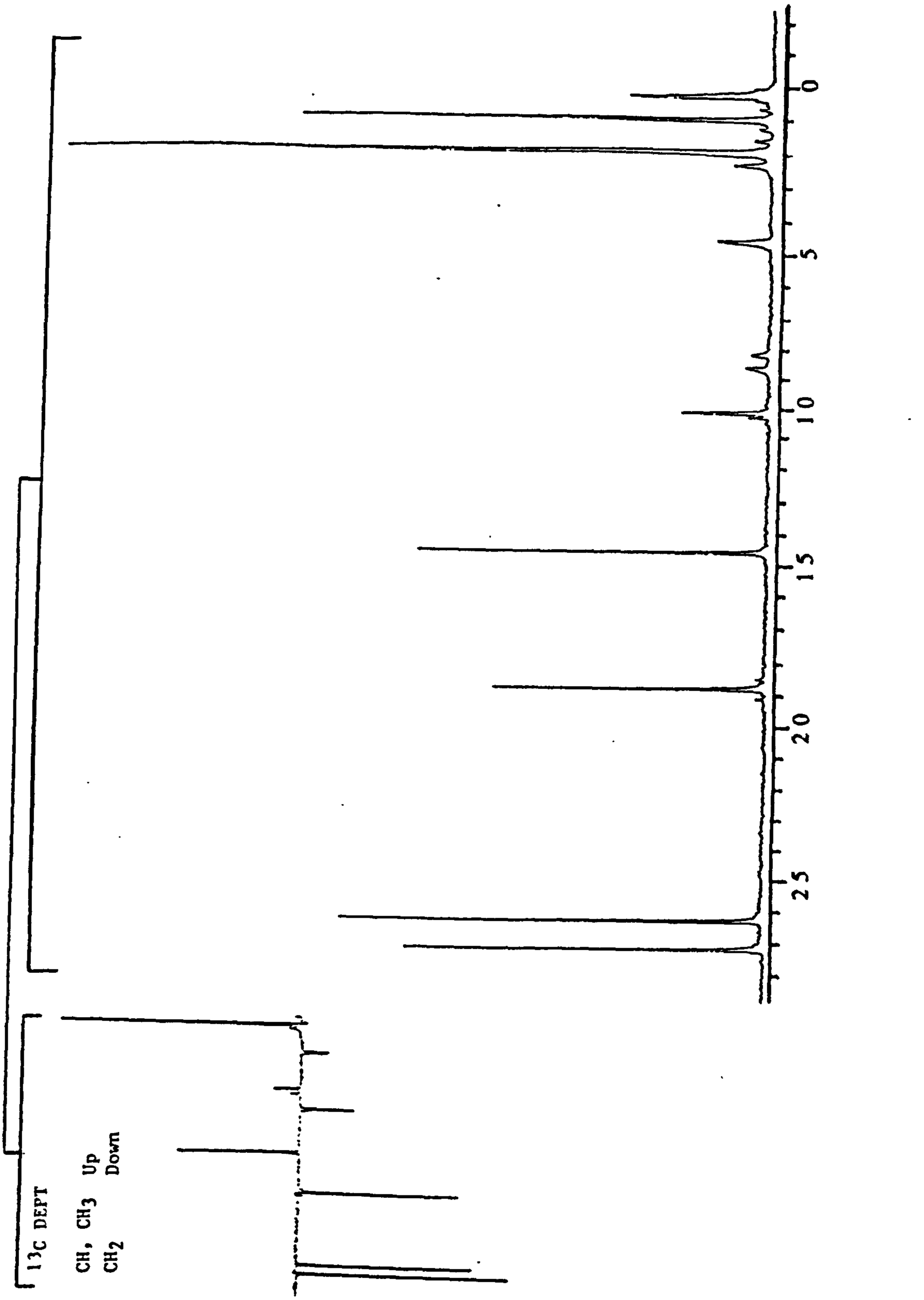

Figure 2.16 ^{13}C NMR spectrum of the products of the reaction of T_8 and vinyl-siloxane.

Janes and Oldfield[8] have used a group electronegativity approach to predict ^{29}Si NMR chemical shifts in silicate structures. They have found that small variations in bridging-oxygen bond angles can have a large effect on the ^{29}Si chemical shift. In the present study, the difference in regiochemistry of addition may cause differences in the bridging-oxygen bond angle by removing the octahedral symmetry and this would result in differences in the T Si chemical shift which are manifested as multiple peaks.

2.2.2 GPC Data for Vinyl Siloxane Reaction

Unlike the reaction between T_8 and the 1-alkenes, the reaction of T_8 with the vinyl-siloxane does not give the monodispersed product or even a mixture of products all with the same molecular weight. The GPC, as illustrated in Figure 2.17, shows a shoulder on the higher molecular weight (larger molecular size) side of the main peak. The major peak in the GPC corresponds to a substance of molecular weight 2520 according to GPC, whereas the actual molecular weight of the octopus molecule is 3343. The higher molecular weight species has an apparent molecular weight of 4467 by GPC. One would not expect a significant difference in molecular size (and no difference in molecular weight) of molecules in which some β-addition occurred relative to the molecules in which all α-addition occurred, so another explanation for the shoulder in the GPC was sought.

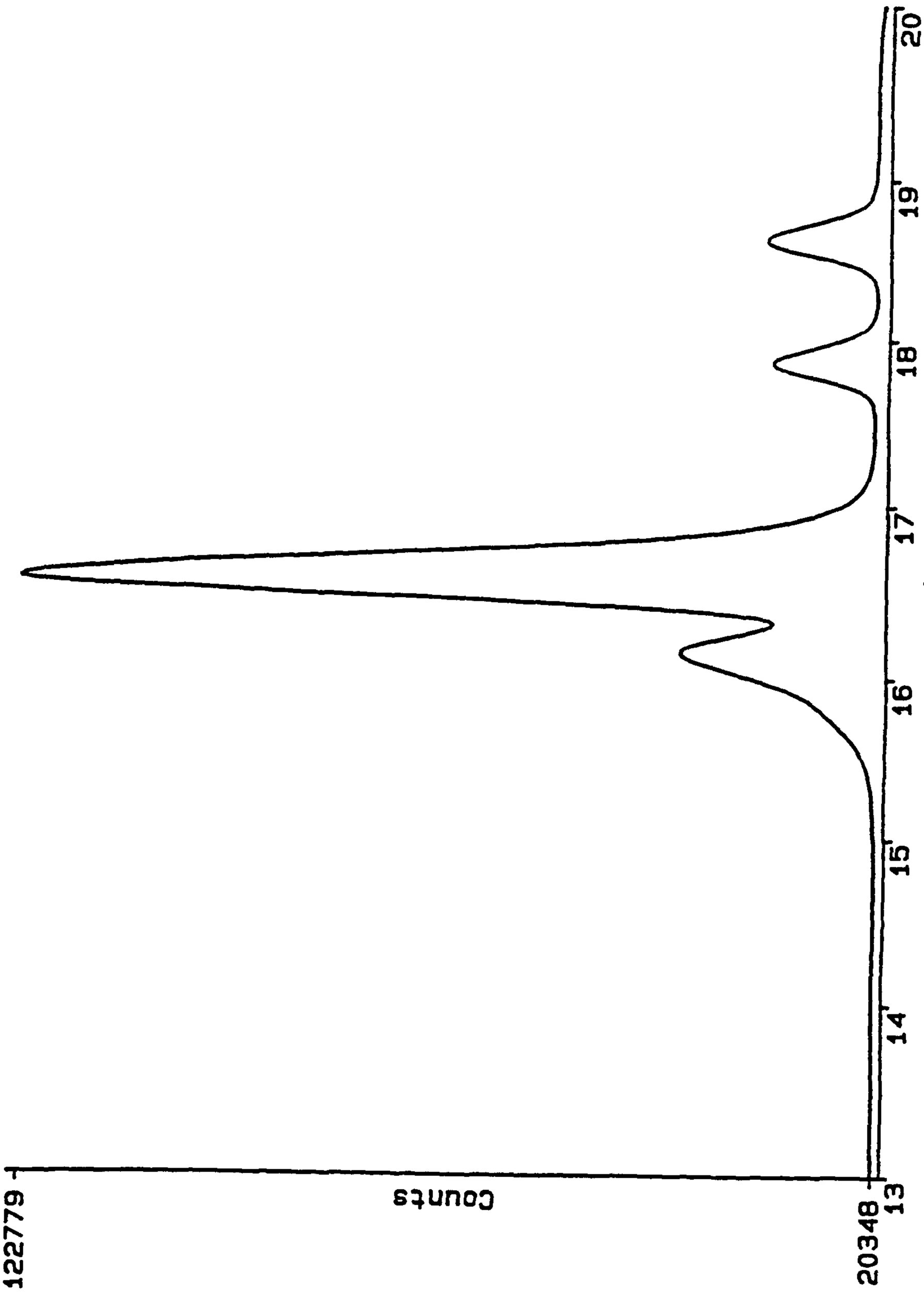

Figure 2.17 GPC chromatogram of the products of the reaction of T_8 and vinyl-siloxane.

There is evidence that during hydrosilylation reactions a vinyl/H exchange on silicon can occur[9-10] as shown in reaction scheme 2.3.

$$R_3SiH + CH_2{=}CHSi^*R'_3 \rightarrow R_3SiCH{=}CH_2 + HSi^*R'_3 \qquad (2.3)$$

If in the case of the hydrosilylation of the vinyl-functional siloxane by $(HSiO_{3/2})_8$, this H/vinyl exchange occurs, then an additional product would be an octopus "dimer" in which two silsesquioxane cores, each with seven siloxane arms, are joined by an ethylene linkage at the eighth reactive site as shown in reaction schemes 2.4 through 2.6.

$$(H_8Si_8O_{12}) + CH_2{=}CHSiMe_2(OSiMe_2)_3Bu \rightarrow [(CH_2{=}CH)H_7Si_8O_{12}] + HSiMe_2(OSiMe_2)_3Bu \qquad (2.4)$$

$$(H_8Si_8O_{12}) + [(CH_2{=}CH)H_7Si_8O_{12}] \rightarrow (O_{12}Si_8H_7\text{-}CH_2CH_2\text{-}H_7Si_8O_{12}) \qquad (2.5)$$

$$(O_{12}Si_8H_7\text{-}CH_2CH_2\text{-}H_7Si_8O_{12}) + CH_2{=}CHSiMe_2(OSiMe_2)_3Bu \rightarrow [CH_2\text{-}(Si_8O_{12})(CH_2CH_2SiMe_2(OSiMe_2)_3Bu)_7]_2 \qquad (2.6)$$

$$CH_2{=}CHSiMe_2(OSiMe_2)_3Bu + HSiMe_2(OSiMe_2)_3Bu \rightarrow BuSi(CH_3)_2[OSi(CH_3)_2]_3CH_2CH_2[Si(CH_3)_2O]_3Si(CH_3)_2Bu \qquad (2.7)$$

It is possible that the octopus dimer is the species making up the shoulder of the main product in the GPC. The calculated molecular weight for such a species is 5982. Although the GPC does no give absolute values for the molecular weights of these

siloxane octopus molecules due to the unavailability of appropriate calibration standards, the ratio of the expected molecular weights of octopus to octopus dimer is 0.564 and the ratio of the values obtained by GPC is 0.559. There is therefore good reason to believe that there is vinyl/H exchange occurring leading to the octopus dimer.

Another consequence of such an exchange would be the formation of $BuSi(CH_3)_2[OSi(CH_3)_2]_3CH_2CH_2[Si(CH_3)_2O]_3Si(CH_3)_2Bu$, the "dimer" of the vinyl-functional fluid as shown in reaction scheme 2.7 above. The GPC of the T_8 + vinyl-siloxane reaction product shows two small, lower molecular weight, peaks. The peak at 18.64 minutes (molecular weight 372 by GPC) was shown to originate from excess vinyl-siloxane (actual molecular weight 369). The peak at 17.87 minutes (molecular weight 756 by GPC) was subsequently shown definitely to arise from the vinyl-siloxane dimer resulting from H/vinyl exchange (actual molecular weight 712). The vinyl-siloxane dimer was synthesized from the hydrosilylation of $BuSi(CH_3)_2[OSi(CH_3)_2]_3CH{=}CH_2$ by $BuSi(CH_3)_2[OSi(CH_3)_2]_3H$. GPC analysis of the $BuSi(CH_3)_2[OSi(CH_3)_2]_3CH_2$-$CH_2[Si(CH_3)_2O]_3Si(CH_3)_2Bu$ resulting from this reaction showed the dimer at a retention time of 17.88 minutes (Figure 2.18), indicating that indeed the unknown peak in the T_8 + vinyl-siloxane was from the siloxane-dimer following the H/vinyl exchange.

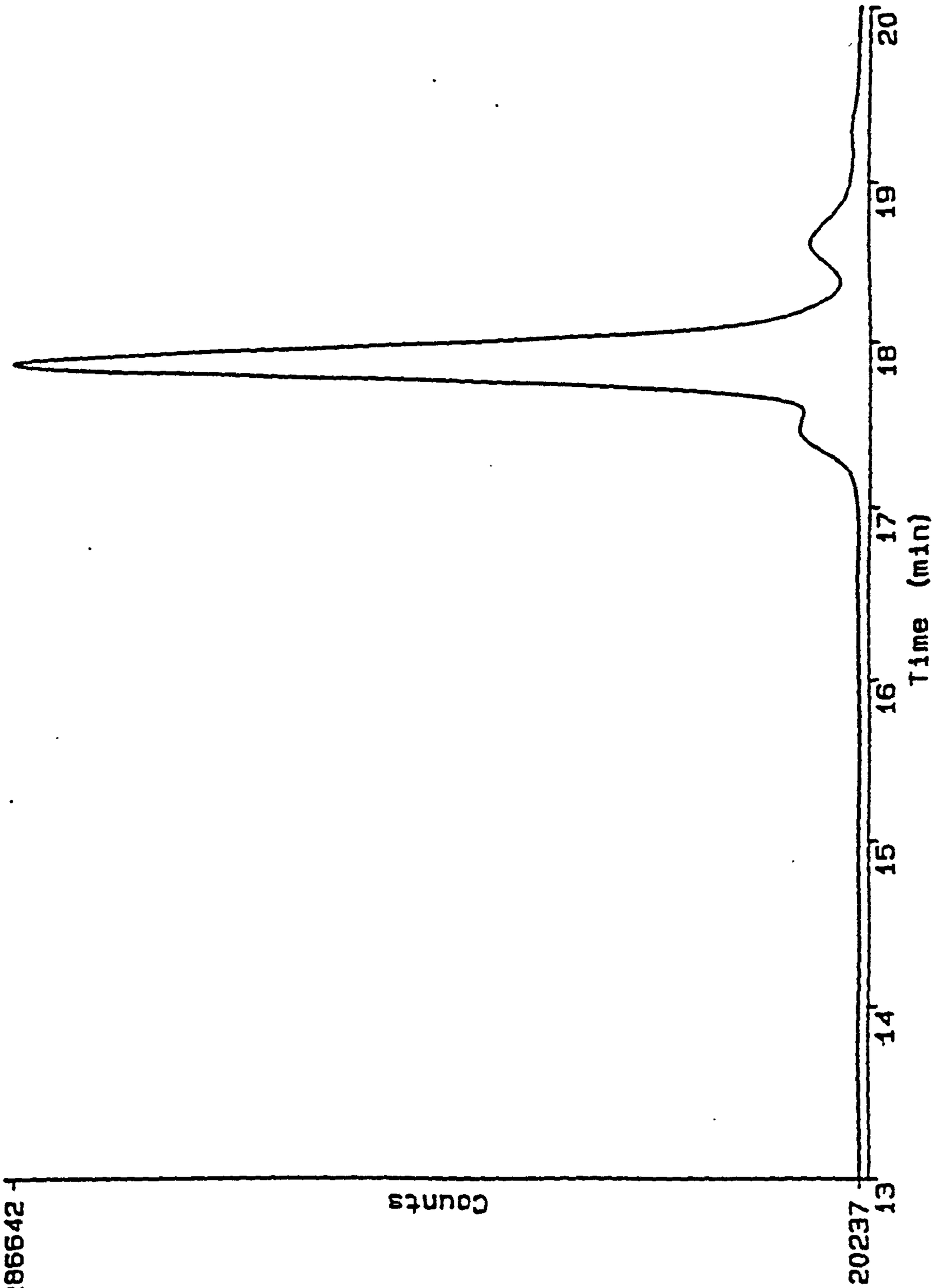

Figure 2.18 GPC chromatogram of $BuSi(CH_3)_2[OSi(CH_3)_2]_3CH_2CH_2[Si(CH_3)_2O]_3Si(CH_3)_2Bu$.

2.2.3 Allyl Siloxane Reaction

The aim of this initial work was to demonstrate the synthesis of molecules of well-defined shape and size. While the addition of vinylsilanes to T_8 had been successful, the occurrence of both α- and β-addition made interpretation of the NMR spectra difficult, and the T_8 dimer molecule also introduced an unwanted impurity. The use of allyl-siloxanes rather then the vinyl-siloxanes seemed to be an attractive option as the regiochemistry of hydrosilylation should show greater selectivity and to our knowledge allyl/H exchanged has not been reported in hydrosilylations. The allyl analogue of the T_8 siloxane octopus was synthesized by the hydrosilylation of $CH_2=CHCH_2[Si(CH_3)_2O]_3Si(CH_3)_2Bu$ by T_8. As Figure 2.19 indicates, the ^{29}Si NMR spectrum is much simpler than the spectrum of the vinyl product. Based on the presence of the single sharp peak at δ -67.4 ppm (referenced to TMS at 0.0), it does not appear that the β-addition occurred in this case. However, there are some smaller peaks between δ -66.5 and -68 ppm. The presence of these smaller resolved peaks in the ^{29}Si NMR may indicate that the H/allyl exchange occurred in this reaction.

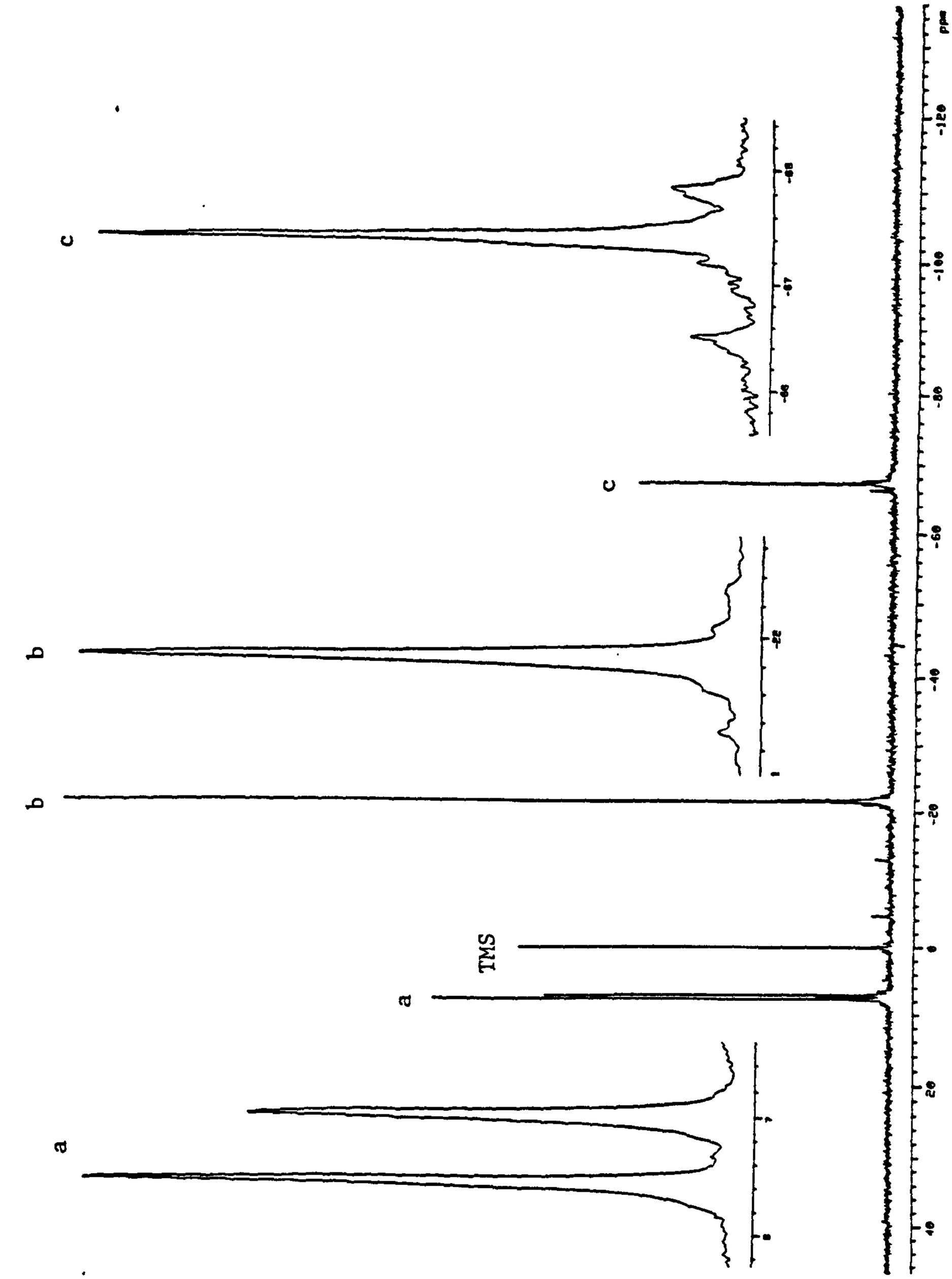

Figure 2.19 ^{29}Si NMR spectrum of the product of T_8 + $CH_2=CHCH_2[Si(CH_3)_2O]_3Si(CH_3)_2Bu$ reaction.

The GPC of the T_8 + allyl-siloxane product would also support this explanation (Figure 2.20). As in the T_8 + vinyl-siloxane reaction, the GPC of the allyl-siloxane product has a shoulder on the main peak that is most likely the octopus dimer (two hepta-substituted T_8 cores linked by a $CH_2CH_2CH_2$ bridge) and also a similar additional lower molecular peak that was shown in the vinyl-siloxane product to be the siloxane dimer. Molecular weights obtained by GPC using linear siloxane standards are compared to the actual molecular weights of the postulated products in Table 2.2.

Table 2.2

Molecular weights obtained by GPC compared to actual molecular weights for T_8 + allyl-siloxane.

Species	M_n by GPC	Actual Molecular Weights
excess allyl-siloxane	373	388
allyl-siloxane dimer	766	716
T_8 octopus	2547	3455
octopus dimer	4467	5982

The allyl-siloxane reaction with T_8 was more successful than the vinyl-siloxane reaction as the regioselectivity was excellent, although the high molecular weight dimer was still formed from allyl/H exchange. This is the first reported instance of allyl/H exchange in a hydrosilylation reaction.

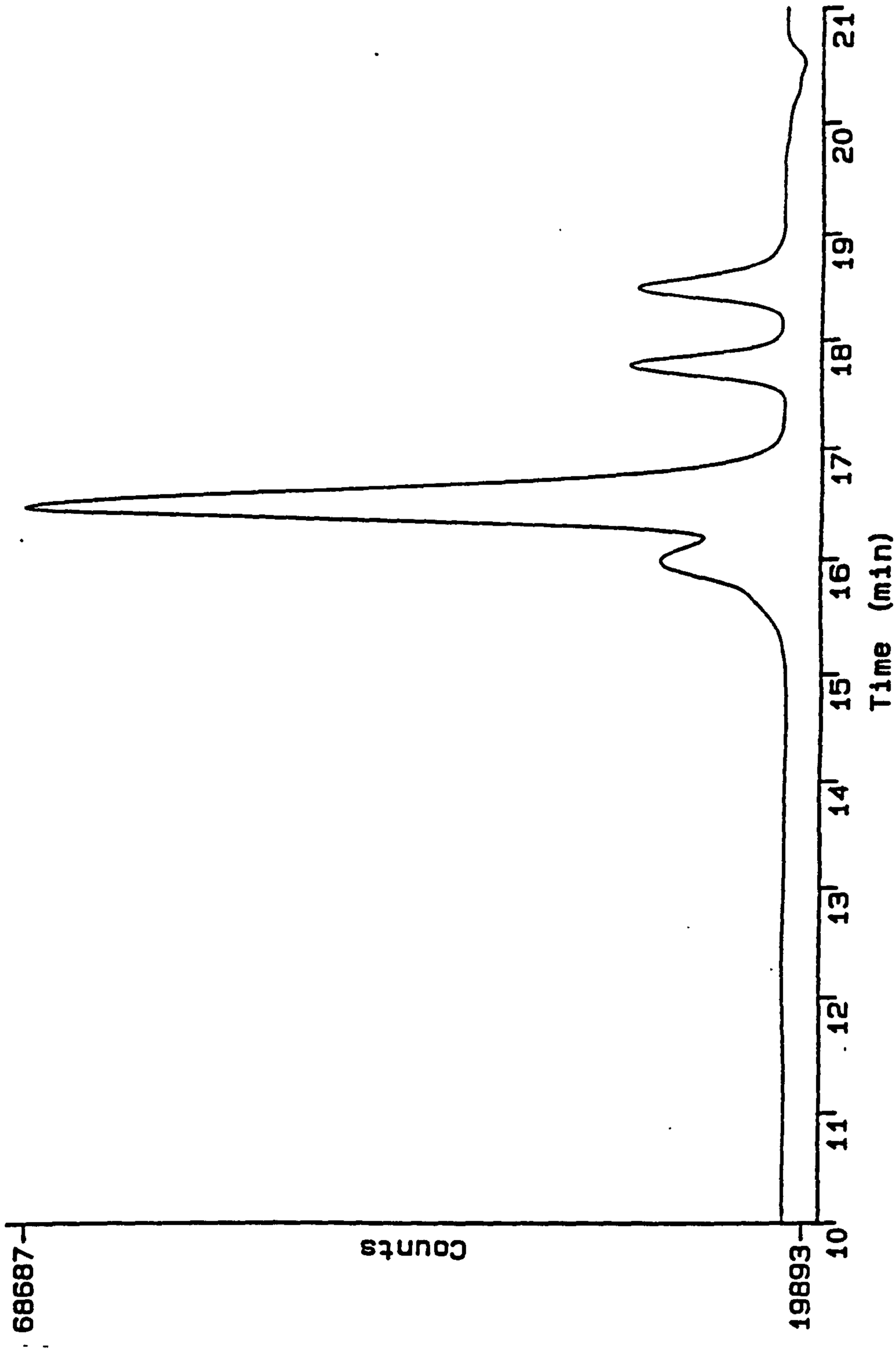

Figure 2.20 GPC chromatogram of the product of T_8 + $CH_2=CHCH_2[Si(CH_3)_2O]_3Si(CH_3)_2Bu$ reaction.

2.3 Conclusions from Hydrocarbon and Siloxane Octopus Molecules

In conclusion, in this initial work on siloxane functional octopus molecules, a facile, one-step route to hydrocarbon and siloxane functional octopus molecules via H_2PtCl_6 catalyzed hydrosilylation of 1-alkenes and vinyl-functional siloxanes by T_8 hydrogen silsesquioxane, $(HSiO_{3/2})_8$ was demonstrated. The chemistry of addition was studied, and it was found that while the addition of the 1-alkenes to T_8 was regioprecise with only α-addition being observed, both α- and β-addition occurred with vinyl-siloxane. In addition, H/vinyl exchange on silicon was observed to occur with addition of vinyl- and allyl-siloxanes to T_8. These addition reactions of silyl-substituted alkenes were found to present more problems than those of simple alkenes because of the unwanted exchange reactions. We believed that these effects could possibly be minimized by the choice of other hydrosilylation catalysts. The studies reported in Chapter Two were limited to use of chloroplatinic acid as the catalyst.

2.4 Experimental

2.4.1 General

All solvents were dried and used immediately after distilling from Na metal and benzophenone as an indicator.

IR spectra were obtained on a Perkin-Elmer 1710 FTIR spectrometer using a thin film of the neat liquid samples between KBr plates.

A Varian VRX200s NMR spectrometer fitted with a 5 mm probe and operating at 39 MHz was used to obtain ^{29}Si NMR spectra of solutions composed of approximately 10 wt% solute in $CDCl_3$ solvent and containing $Cr(acac)_3$ at a concentration of approximately 0.02M. For ^{13}C distortionless enhancements by polarisation transfer (DEPT) and insensitive nuclei enhanced by polarisation transfer (INEPT) NMR spectra, on the same solutions, a JOEL EX400 NMR spectrometer fitted with a 10 mm probe and operating at 100 MHz was used. Standard software as supplied with the spectrometer was used to generate the pulse sequences. Throughout this thesis, proton NMRs were not obtained and ^{13}C NMR spectrum were only obtained where indicated due to the finding that the information to be gained could not justify additional time when instrument time was very limited.

GPC measurements were carried out using a Waters chromatograph fitted with a Waters 410 Differential Refractometer detector and attached to a microvax 3400

computer, using the software PE Nelson Access-Chrom. Version 1.8. The instrument was fitted with three Polymer Laboratories columns in series: two PLgel 5 µm Mixed-C and one PLgel 5µm guard. The mobile phase was toluene and the flow rate was 1 $c\,m^3\ min^{-1}$ at a temperature of 45 °C. For each run, 50-100 µl of a 1 wt% solution in toluene that had been filtered through a 0.45 µm PTFE filter was injected. Narrow molecular weight polydimethylsiloxane standards supplied by Dow Corning Corporation were used as calibration standards.

GC/MS analyses were carried out using a Finnegan 4610 mass spectrometer with electron impact at 70 eV as the ionization mode and scan rate of 1 scan per second. The mass range was 15-650u. The GC column was a DB-1 30m x 0.25mm with a 0.1 µm film. The temperature program was from 50 °C initial temperature (held for 2 minutes) to a final temperature of 250 °C (held for 5 minutes) and ramp at 10 °C per minute. An injection volume of 1.0 µl with split ratio of approximately 20:1 was used.

GC analyses were performed using a Varian 3700 gas chromatograph with a DB-1 column whose dimensions were 30m x 0.25mm with a 0.25 µm film. The detector was a FID at 350 °C and injection port was at 250 °C. The temperature program used was 50 °C (held for 2 minutes) to 250 °C (held for 5 minutes) at 10 °C per minute. An injection volume of 1.0 µl with split ratio of approximately 50:1 was used. GC results were given as normalized area percents. Peak identifications were based on GC/MS results.

2.4.2 Synthesis of $(HSiO_{3/2})_8$

The general procedure for obtaining pure $(HSiO_{3/2})_8$ has been described by Agaskar[11]. In this work, the process was scaled up (6X scale) with some additional modifications. A description of one typical synthesis follows. In a 5-litre, 3-neck Morton flask with a bottom drain were placed, $FeCl_3$ (309 grams), MeOH (198 grams), 37% HCl (149 grams), $C_6H_5CH_3$ (272 grams) and C_6H_{14} (mixture of isomers, 1411 grams). The mixture was stirred using a stir rod and paddle turned by an air motor. To the biphasic mixture, a solution of $HSiCl_3$ (166 grams, 1.23 mol) in C_6H_{14} (602 grams) was added over a 6.5 hour period using a peristalic pump (through Viton tubing). A dry ice condenser and an N_2 blanket were used during the reaction. After an additional 30 minutes stirring, the biphasic mixture was allowed to separate and the lower $FeCl_3$/HCl/MeOH layer (691 grams) was drained from the reactor through the bottom drain. K_2CO_3 (151 grams) and $CaCl_2$ (64 grams) were added to the flask. The mixture was stirred overnight and then filtered through a layer of celite (filter aid) in a fritted filter funnel. Hexane was then distilled from the filtrate until a volume of ~200 ml remained. Upon cooling, needle-shaped crystals precipitated and were filtered and washed with hexane. The air-dried crystals weighed 10.73 grams (16.5% yield of T_8 based on $HSiCl_3$). A single peak in the ^{29}Si NMR at δ -84.7 ppm (T-Si region) referenced to tetramethylsilane (TMS) at δ 0.0 ppm indicated that this first set of crystals was essentially pure T_8. The GPC chromatogram of the pure T_8 shown in Figure 2.21 shows a single monodispersed peak at retention time 19.00 minutes.

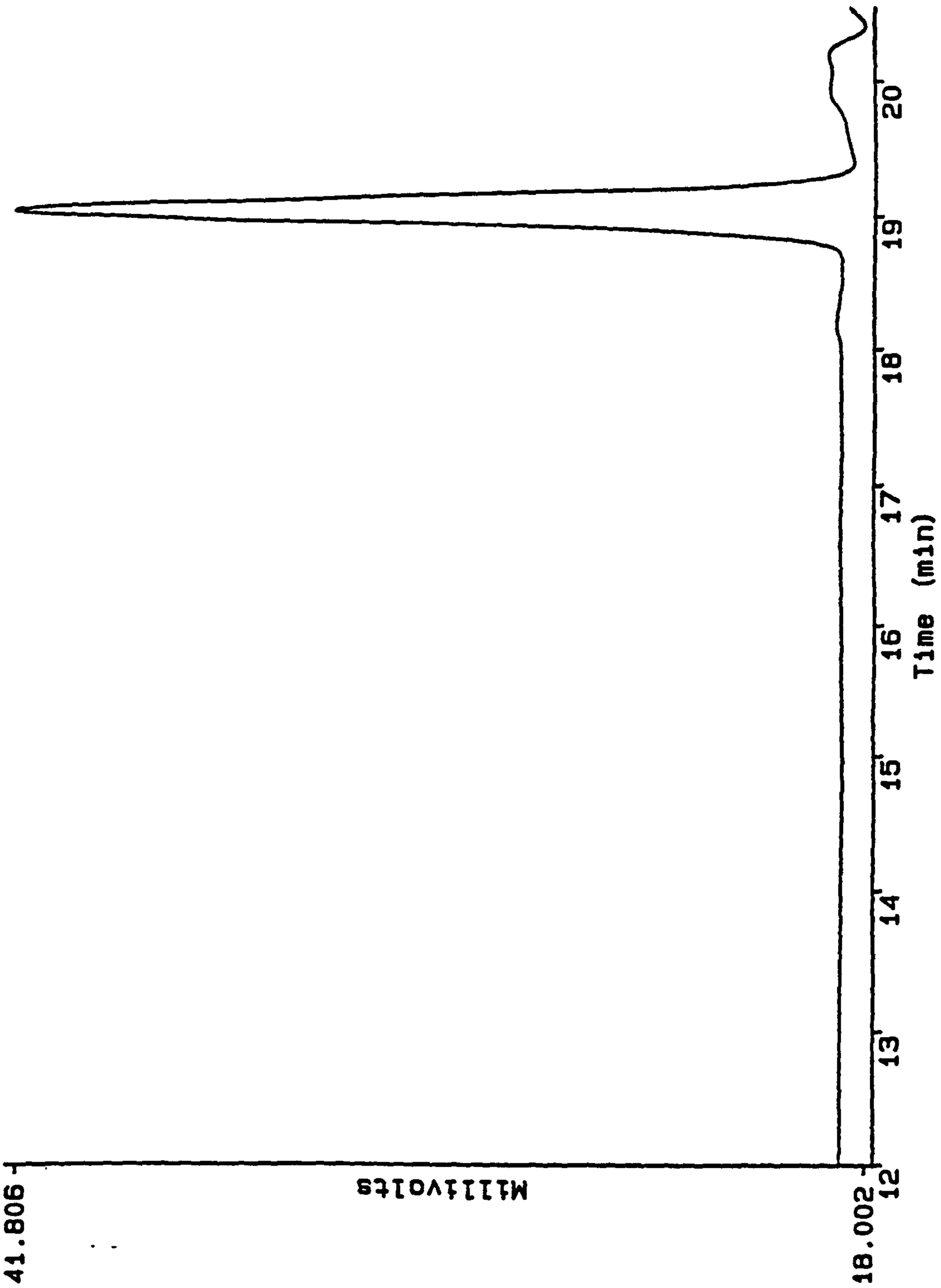

Figure 2.21 GPC chromatogram of T_8 hydrogen silsesquioxane.

The filtrate and the hexane washings from the first set of crystals were combined and the volume reduced further to approximately 125 ml. The precipitate (4.07 grams) obtained by filtration following this second solvent reduction was a white powder that in the in the ^{29}Si NMR showed two resolved peaks at δ -84.7 ppm (T-Si region, T_8) and δ -86.4 (T-Si region, T_{10}) relative to (TMS) at δ 0.0 ppm. A third precipitation of crystals from the second filtrate yielded 1.04 grams of powder.

2.4.3 Synthesis of $[CH_3(CH_2)_n]_8[SiO_{3/2}]_8$ series

T_8 was used to hydrosilylate a series of 1-alkenes, C_6H_{12}, $C_{10}H_{20}$, $C_{14}C_{28}$, and $C_{18}H_{36}$. For the reaction of hexene with T_8, T_8 (0.20 grams, 0.47 mmol), 1-hexene (0.35 grams, 4.16 mmol, 99+% pure), and 5 μl of 0.02M solution of H_2PtCl_6 in isopropyl alcohol were placed in a small vial. For the reaction of decene and T_8, T_8 (0.20 grams, 0.47 mmol), 1-decene (0.58 grams, 4.13 mmol, 94% pure), and 5 μl of 0.02M solution of H_2PtCl_6 in isopropyl alcohol were placed in a small vial. For the reaction of tetradecene and T_8, T_8 (0.20 grams, 0.47 mmol), 1-tetradecene (0.83 grams, 4.23 mmol, 92% pure), and 5 μl of 0.02M solution of H_2PtCl_6 in isopropyl alcohol were placed in a small vial. Finally, for the reaction of octadecene with T_8, T_8 (0.20 grams, 0.47 mmol), 1-octadecene (1.08 grams, 4.28 mmol, 90% pure), and 5 μl of 0.02M solution of H_2PtCl_6 in isopropyl alcohol were placed in a small vial. The four small vials were capped and placed in a 60 °C oven for 24 hours. An FTIR spectrum was obtained of each of the above reaction mixtures and the reactions all appeared to have gone to completion, as indicated by the lack of an SiH

absorbance peak at 2260 cm^{-1} in the spectra. The product of the reaction of T_8 with 1-hexene was a slightly yellow, opaque, viscous liquid. Similarly, the reaction product of T_8 and 1-decene was also an opaque, slightly yellow, very viscous liquid. The reaction products of T_8 and the higher 1-alkenes were opaque, off-white, waxy solids.

A single peak at δ-66.63 ppm (T-Si region) referenced to TMS was observed in the ^{29}Si NMR spectrum for the reaction of T_8 with 1-hexene. The ^{29}Si NMR of the product of the T_8 and 1-decene also showed a single peak at δ-66.63 ppm (T-Si region) referenced to TMS. The ^{29}Si NMR of the product of the T_8 and 1-tetradecene reaction showed a single peak at δ-66.65 ppm (T-Si region) referenced to TMS. A broader set of unresolved peaks between δ-65.9 and -66.8 ppm (T-Si region) referenced to TMS was observed in the ^{29}Si NMR spectrum for the reaction of T_8 with 1-octadecene. The ^{29}Si NMR spectrum were shown in Section 2.2.1 (Figures 2.2 through 2.5). GPC of the reaction products of the four 1-alkenes and T_8 are displayed and are discussed in Section 2.1.2 (Figure 2.6 and Table 2.1).

2.4.4 Synthesis of $Bu[Si(CH_3)_2O]_3Si(CH_3)_2CH=CH_2$

A siloxane chain of fixed length and with vinyl functionality on one end only was synthesized using an established method involving anionic ring-opening polymerization of hexamethylcyclotrisiloxane (D_3) using butyl lithium, followed by end-capping with a chlorosilane having the desired functional group[3-6]. In this case, the use of a mole ratio of D_3/butyl lithium

of 1/1 and CH_2=$CHSi(CH_3)_2Cl$ as the capping agent followed by purification produced $Bu[Si(CH_3)_2O]_3Si(CH_3)_2CH$=$CH_2$. Although made via a different route, this compound was previously reported in a German patent application[12]. D_3 (100.0 grams, 0.45 moles), and tetrahydrofuran (203.0 grams, distilled from Na) were placed in a 1-litre, 3-neck round bottom flask equipped with a stirring bar and cooled by an ice/H_2O bath. To the stirring D_3 solution, 2.5M butyllithium in hexanes (182.5 ml, 0.46 moles) was added dropwise over an approximately 1 hour period. After addition of the butyllithium was complete, the ice/H_2O bath was removed and the reaction mixture came to room temperature and was kept stirring for an additional 2.5 hours at which time the capping agent, CH_2=$CHSi(CH_3)_2Cl$ (Hüls, 62.5 grams, 0.52 moles) was added in excess. The reaction mixture was stirred overnight. THF was removed using a rotary evaporator. Pure (98.2% by GC) $Bu[Si(CH_3)_2O]_3Si(CH_3)_2CH$=$CH_2$ (56.9 grams, 0.16 moles, 35% yield based on D_3) was obtained by distillation on a spinning band column at a temperature of 69-70 °C and vacuum between 1.2 and 1.7 mm Hg. The ^{29}Si NMR of the distilled $Bu[Si(CH_3)_2O]_3Si(CH_3)_2CH$=$CH_2$ was shown in Figure 2.10 in Section 2.1.2. The spectrum showed a single peak at δ 7.55 ppm [M-Si region, $BuSi(Me)_2$-], a single peak at δ -4.21 ppm (M-Si region, CH_2=$CHSi(Me)_2$-] and 2 well resolved peaks at δ -21.23 (D-Si closest to vinyl end) and δ -21.87 ppm (D-Si closest to butyl end). The ratio of the integrated areas of the four peaks was approximately 1:1:1:1. The integrated area of the GC peak for the distilled product was 99.7%. A molecular peak of mass 364 by GC/MS confirmed the identification of the product as $Bu[Si(CH_3)_2O]_3Si(CH_3)_2CH$=$CH_2$.

2.4.5 Synthesis of $Bu[Si(CH_3)_2O]_3Si(CH_3)_2CH_2CH=CH_2$

The previously unreported compound, $Bu[Si(CH_3)_2O]_3Si(CH_3)_2CH_2CH=CH_2$, was synthesized using the method described above except the capping agent used was $CH_2=CHCH_2Si(CH_3)_2Cl$. The pure product was obtained by distilling at 98 °C and approximately 0.5 mm Hg. The ^{29}Si NMR spectrum of the distilled product is shown in Figure 2.22. The ^{29}Si NMR spectrum shows four well resolved peaks at δ 7.60 ppm [M-Si, $BuSi(Me)_2$-], 4.31 ppm [M-Si, $CH_2=CHCH_2Si(Me)_2$-], -21.49 ppm (D-Si closest to allyl end), and -21.86 ppm (D-Si closest to butyl end). The ratio of the integrated areas of the four peaks was approximately 1:1:1:1. The integrated area of the GC peak for the distilled $Bu[Si(CH_3)_2O]_3Si(CH_3)_2CH_2CH=CH_2$ was 96.7%. A molecular ion of mass 378 confirmed the product was $Bu[Si(CH_3)_2O]_3Si(CH_3)_2CH_2CH=CH_2$. The GPC chromatogram (Figure 2.23) indicated the presence of a single peak at retention time 18.52 minutes.

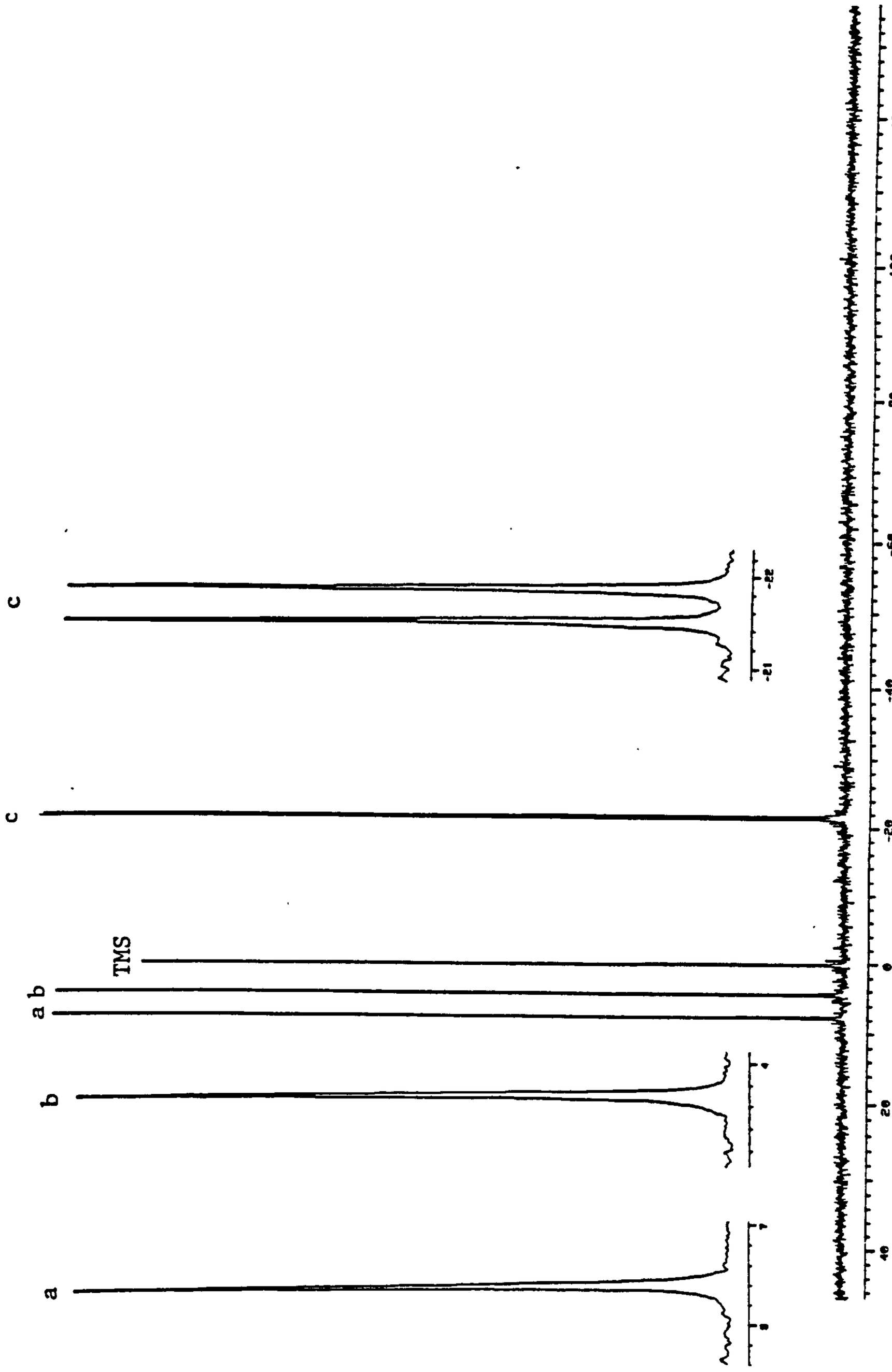

Figure 2.22 ^{29}Si NMR spectrum of $Bu[Si(CH_3)_2O]_3Si(CH_3)_2CH_2CH{=}CH_2$.

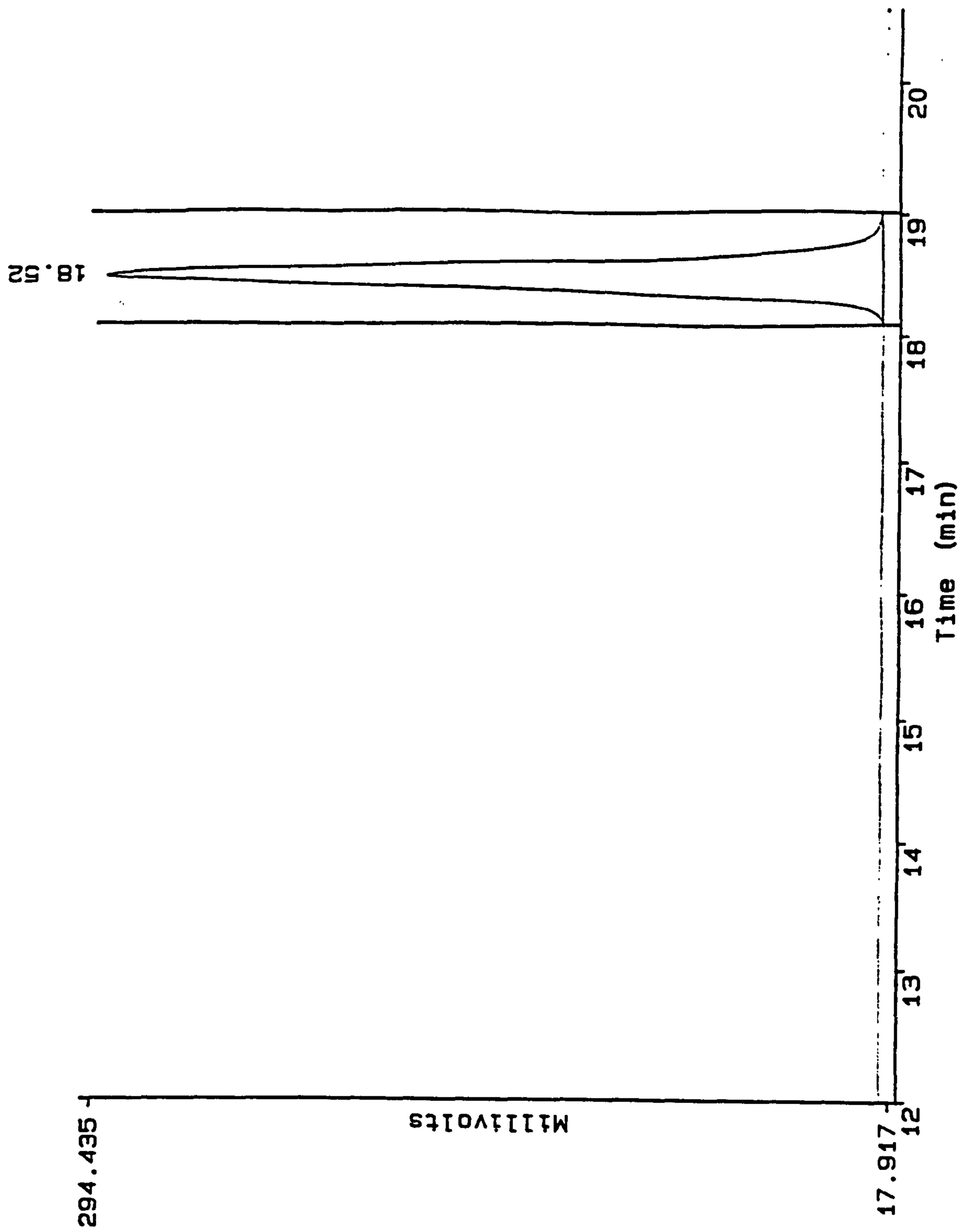

Figure 2.23 GPC chromatogram for $Bu[Si(CH_3)_2O]_3Si(CH_3)_2CH_2CH{=}CH_2$.

2.4.6 Synthesis of $Bu[Si(CH_3)_2O]_3Si(CH_3)_2H$

The previously reported[12] compound, $Bu[Si(CH_3)_2O]_3Si(CH_3)_2H$, was synthesized using the method described for $Bu[Si(CH_3)_2O]_3Si(CH_3)_2CH=CH_2$ (section 2.4.4) except the capping agent used was $HSi(CH_3)_2Cl$. The pure product (~95%) was obtained by distilling at 100 °C and approximately 5-15 mm Hg. The ^{29}Si NMR is shown in Figure 2.24. There is a single M-Si peak at 7.67 ppm assigned to the $BuSiMe_2$ of the chain end, another M-Si peak at -7.02 ppm assigned to the $HSiMe_2$ chain end, and 2 D-Si peaks at -20.16 and -21.65 ppm assigned to the D-Si adjacent to the SiBu end and the D-Si adjacent to the SiH end of the chain. Each of these peaks has very small peaks around them due to impurities in the product as identified by GC and GC/MS results. The GC shown in Figure 2.25 has the main product peak and the impurities labeled based on identifications made by GC/MS. The main product peak had a molecular ion peak of mass 338 which confirmed the product was $Bu[Si(CH_3)_2O]_3Si(CH_3)_2H$. The GPC (Figure 2.26) indicates the presence of the product at retention time 18.71 minutes, a higher molecular weight peak at retention time 18.17 minutes, and two lower molecular weight peaks at retention times 19.33 and 19.85 minutes.

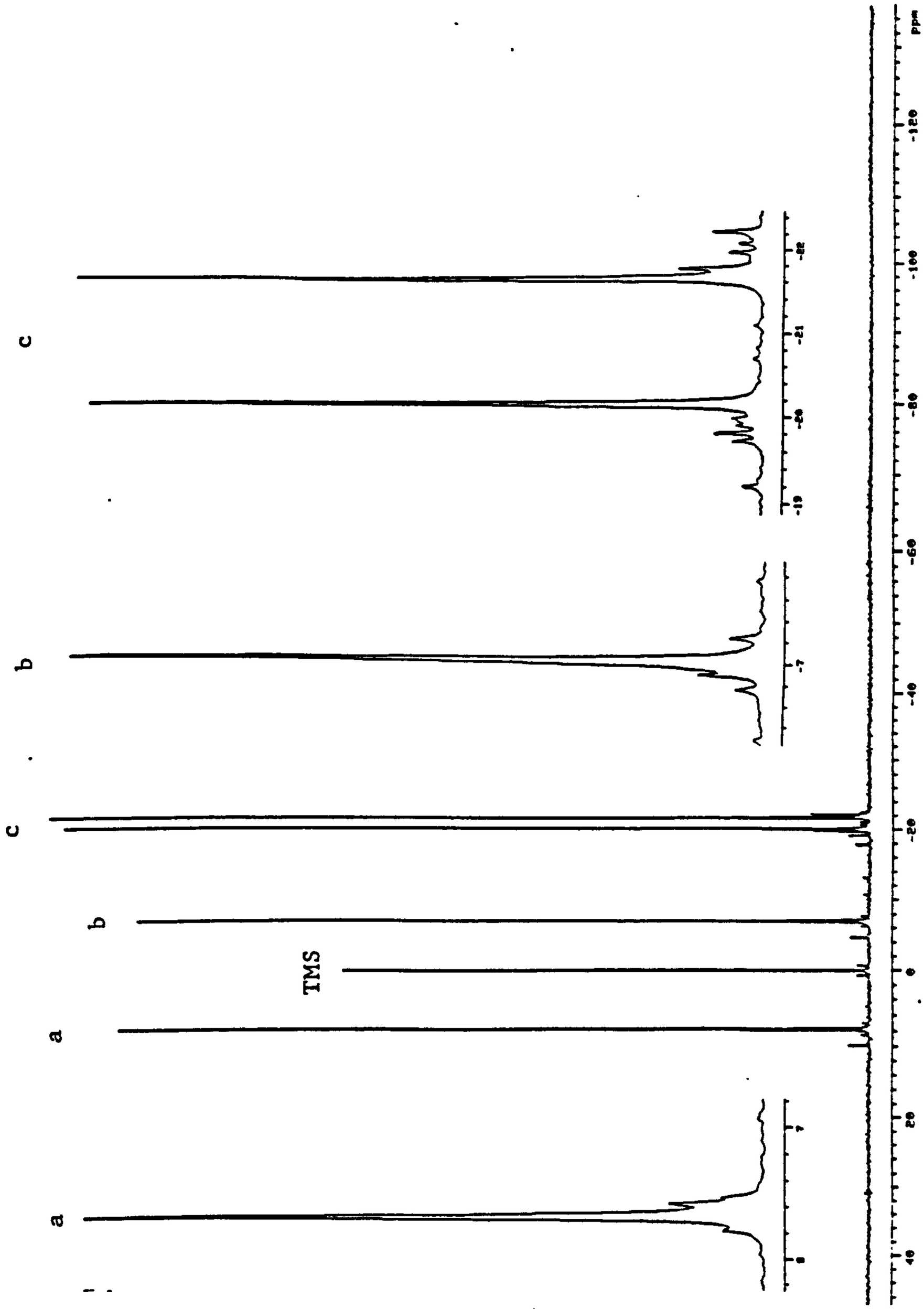

Figure 2.24 ^{29}Si NMR spectrum of $Bu[Si(CH_3)_2O]_3Si(CH_3)_2H$.

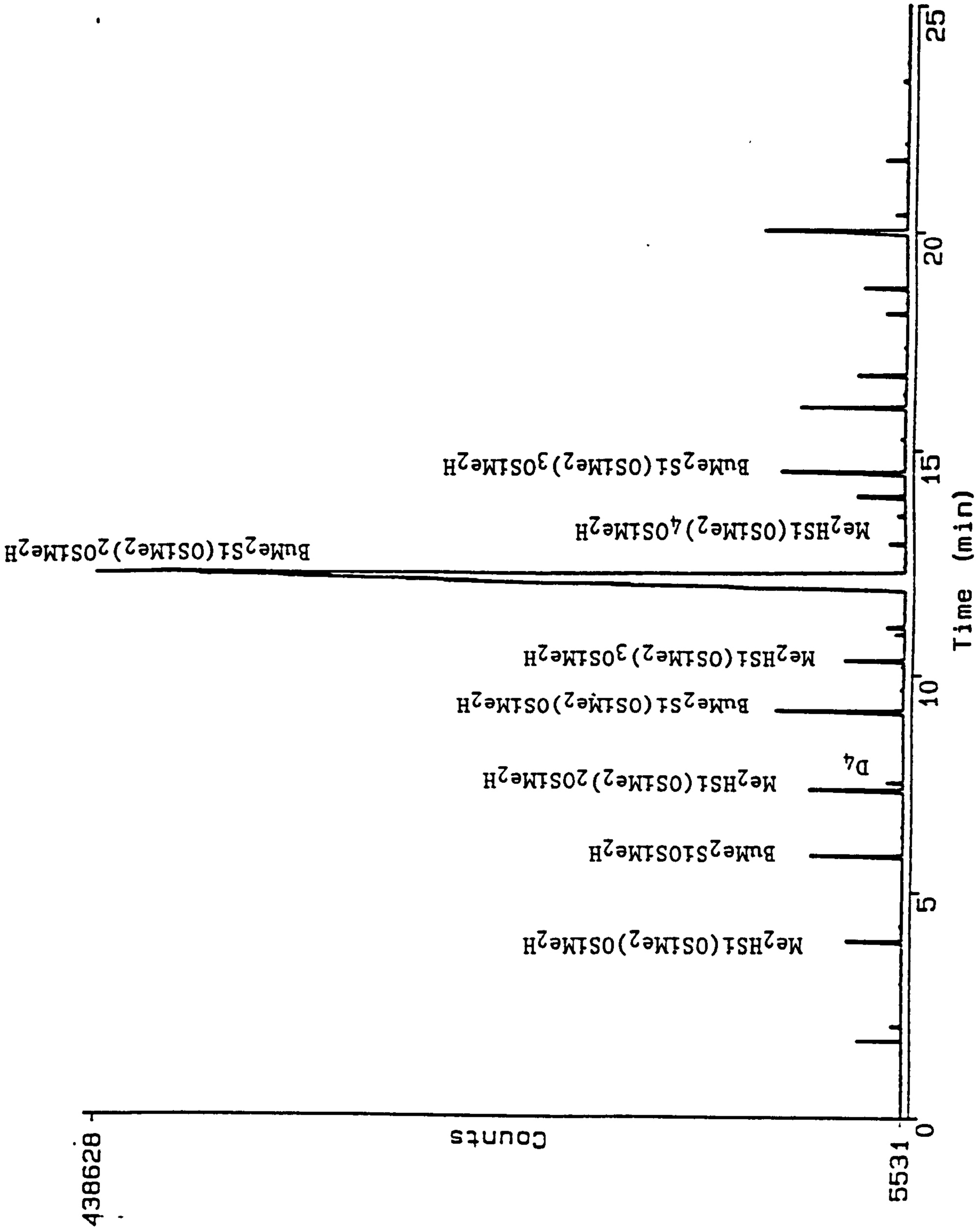

Figure 2.25 GC chromatogram of $Bu[Si(CH_3)_2O]_3Si(CH_3)_2H$.

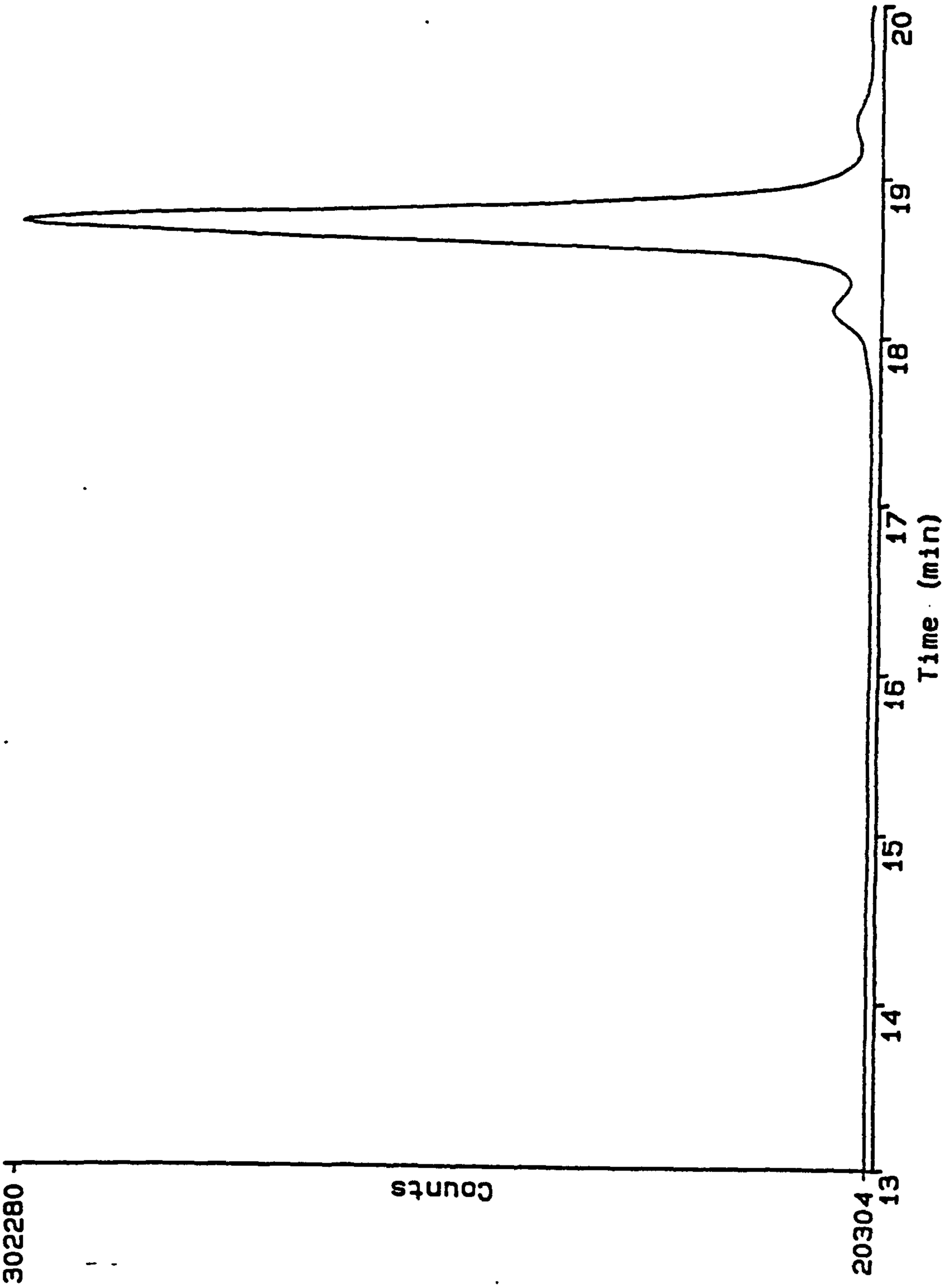

Figure 2.26 GPC chromatogram of $Bu[Si(CH_3)_2O]_3Si(CH_3)_2H$.

2.4.7 Synthesis of $\{Bu[Si(CH_3)_2O]_3Si(CH_3)_2CH_2CH_2\}_8[SiO_{3/2}]_8$

A slight excess of the vinyl-functional siloxane, $Bu[Si(CH_3)_2O]_3Si(CH_3)_2CH{=}CH_2$ (10.59 grams, 29.09 mmol, 99.7% pure by GC) was added to the $(HSiO_{3/2})_8$ crystals (1.45 grams, 3.42 mmol) in a small vial. The capped vial containing the T_8 and the siloxane fluid was heated to 70 °C in a water bath. A platinum catalyst solution (45 µl of 0.02M H_2PtCl_6 in isopropyl alcohol) was added to the mixture. The mixture of solid T_8 in the siloxane fluid was swirled several times while being heated to 82 °C. The solid T_8 in the mixture disappeared as the reaction progressed. The absence of the SiH absorbance in the FTIR (originally at ~2260 cm^{-1}) was used to indicate completion of the reaction. NMR and GPC analyses of this compound were discussed in detail in Sections 2.2.1 and 2.2.2. The ^{29}Si NMR spectrum had a grouping of at least seven unresolved peaks between δ -65.5 and -67.2 ppm (T-Si region, the $O_{3/2}\underline{Si}C$ of the T_8 cage linked to the appendages).

2.4.8 Synthesis of $\{Bu[Si(CH_3)_2O]_3Si(CH_3)_2CH_2CH_2CH_2\}_8[SiO_{3/2}]_8$

To a small vial, allyl-functional siloxane fluid, $Bu[Si(CH_3)_2O]_3Si(CH_3)_2CH_2CH{=}CH_2$ (1.48 grams, 3.92 mmol, 96.7% pure by GC), 0.20 grams of T_8 (0.47 mmol), and 1 drop of 0.02M solution of H_2PtCl_6 in isopropyl alcohol was added. The vial was capped and placed in an 84 °C oven for two hours. ^{29}Si NMR indicated that SiH was still remaining after 2 hours so the vial

was returned to the oven and was left for approximately 16 hours. After this period of time the reaction appeared complete as indicated by the absence of an absorbance for SiH in the FTIR The ^{29}Si NMR spectrum was shown in Figure 2.19. The spectrum indicated the presence of a peak at δ -67.4 ppm with some smaller less resolved peaks at approximately -66.5 ppm and -67.8 ppm (T-Si region). Three other peaks were present in the ^{29}Si NMR at δ 7.57 and 7.01 ppm [M-Si region, $(CH_2)_3Si(Me_2)O$ and $OSi(Me_2)(Bu)$] and at δ -21.86 ppm (D-Si region). The ratio of the integrated ^{29}Si T:M(propyl) + M(Bu):D peaks was 1:2:2.

2.4.9 Reaction of T_8/ T_{10} + Vinyl-Siloxane

A T_8 and T_{10} mixture (0.4 grams, the ^{29}Si NMR spectrum of which was shown in Figure 2.14), $Bu[Si(CH_3)_2O]_3Si(CH_3)_2CH=CH_2$ (3.02 grams, 97.8% pure by GC), and 60 µl of 0.02M H_2PtCl_6 in isopropyl alcohol were placed in a small vial with cap. The vial was placed in an 81 °C oven for approximately 16 hours after which time the SiH was essentially gone by FTIR analysis. ^{29}Si NMR was done and is shown in Figure 2.15 in the discussion. The spectrum for the products of the reaction of the mixture of T_8 and T_{10} with the vinyl-siloxane had four not entirely resolved M-Si peaks at δ 8.29, 8.07, 7.99, and 7.54 ppm; two not entirely resolved D-Si peaks at d -21.76 and -21.85 ppm; and two main groupings of peaks T-Si peaks, one in the region of -65.5 to -67.0 ppm (product with T_8) and the other in the region of -67.0 to -69.0 ppm (product of vinyl-siloxane with T_{10}). The integrated areas of the groupings of M:D:T silicon peaks were 1:1:1.

2.4.10 Synthesis of $BuSi(CH_3)_2[OSi(CH_3)_2]_3CH_2$-$CH_2[Si(CH_3)_2O]_3Si(CH_3)_2Bu$

The previously unreported compound, $BuSi(CH_3)_2[OSi(CH_3)_2]_3CH_2CH_2[Si(CH_3)_2O]_3Si(CH_3)_2Bu$, was made as follows. $Bu[Si(CH_3)_2O]_3Si(CH_3)_2CH{=}CH_2$ (99.7%, 0.14 grams), $Bu[Si(CH_3)_2O]_3Si(CH_3)_2H$ (~95%, 0.13 grams) and approximately 1 µl of 0.02M H_2PtCl_6 in isopropyl alcohol were placed in a small vial with cap. The mixture was placed in a 73 °C oven for 65 hours. After removal from the oven, FTIR analysis indicated no SiH was present. GPC of the previously unreported reaction product (see Figure 2.18) indicated that the product was monodispersed and had a retention time of 17.88 minutes.

2.5 References

1. Herren, D.; Bürgy, H.; Calzaferri, G. *Helv. Chim. Acta*, 1991, 74, 24-26.

2. Vogtle, F.; Weber, E. *Angew. Chem., Int. Ed.*, 1974, 13, 814.

3. Saam, J.; Gordon, D.; and Lindsey, S. *Macromolecules* 1970, 3, 1.

4. Cameron, G. and Chisholm, S. *Polymer* 1985, 26, 437.

5. Kawakami, Y. and Yamashita, Y. *ACS Symp. Ser.* 1985, 286, 245.

6. Tezuka, Y.; Fukushima, A.; and Imai, K. *Macromol. Chem.* 1985, 186, 685.

7. Bassindale, A R.; and Taylor, P G ; Activating and Directive Effects of Organosilicon Compounds, chapter 14 in *The Chemistry of Organosilicon Compounds*, Wiley 1988, Ed. S Patai and Z Rappoport.

8. Janes, N. and Oldfield, E. *J. Am. Chem. Soc.* 1985, 107, 6769-6775.

9. Speier, J.L. in: *Advances in Organometallic Chemistry*, Vol. 17, Academic Press, Inc., New York, 1979, 407-447.

10. Pitt, C. and Skillern, K. *J. Organometal. Chem.* 1967, 7, 525-528.

11. Agaskar, P.A. *Inorg. Chem.* 1991, 30, 2707-2708.

12. Fleischmann, G.; Eck, H.; Wenzeler, P. German Patent Application 3726028, May 8, 1987.

Chapter Three

Effect of Catalyst on Hydrosilylation of Vinyl Siloxane by T8

3.0 Introduction and Background

The feasibility of synthesizing octopus molecules of defined shape and size with molecular weights well into the thousands was demonstrated in the last chapter. These octopus molecules were made by placing eight pendant groups symmetrically about a central silsesquioxane core via the H_2PtCl_6 catalyzed hydrosilylation of 1-alkenes as well as vinyl- and allyl-siloxanes by T_8 hydrogen silsesquioxane, $(HSiO_{3/2})_8$. The chemistry of addition was studied and it was found that while the addition of the 1-alkenes to T_8 was regioprecise with only α-addition being observed, both α- and β-addition occurred with vinyl-siloxane. In addition, H/vinyl exchange on silicon was observed to occur with addition of vinyl-siloxane to T_8.

While there is not a tremendous amount of literature available on the regioselectivity of addition and extent of exchange on silicon during hydrosilylation, there are a few reports of hydrosilylation of vinyltrichlorosilane by trichlorosilane catalyzed by H_2PtCl_6 in isopropanol[1] and H_2PtCl_6 in cyclohexanone[2] yielding the α-adduct only. There are also references indicating that the same hydrosilylation reaction catalyzed by $RhCl(PPh_3)_3$ (Wilkinson catalyst)[2] and a heterogeneous Pt catalyst[3] resulted also in the α-adduct. However, it was found that complexes of nickel[2, 4] resulted in the mixture of both adducts. In another study on the use of a chloroplatinic acid catalyst[5], both adducts were observed, which appears to be in conflict with the earlier reported results from H_2PtCl_6[1-2]. Marciniec *et al* have reported on the use of

tetrakis(triphenylphosphine)palladium(0) for the hydrosilylation of vinyltri(chloromethyl)silane by tri(chloromethyl) silanes[6]. They found that the palladium phosphine complexes resulted in the selective formation of the α-adducts, except in the reaction in which all substituents on both silicons of the reactants were chloro. This latter reaction was previously reported to give selectively the β-adduct[2]. Possible explanations for the differences in the modes of addition in the above mentioned reactions include substituent effects, catalyst effects, and/or process conditions.

Since there appeared to be a precedent in the literature for the catalyst to affect especially the regioselectivity of addition, we were interested in the effect of the hydrosilylation catalyst, homogeneous and heterogeneous, on the mode of addition during the hydrosilylation of $Bu[Si(CH_3)_2O]_3Si(CH_3)_2CH=CH_2$ by T_8 hydrogen silsesquioxane. At the same time, the effect of the catalyst on the extent of vinyl/H exchange on silicon was also evaluated.

3.1 Results

3.1.1 Effect of Catalyst on Regioselectivity and H/Vinyl Exchange on Si

The siloxane-functional octopus synthesis discussed in the previous chapter was accomplished using H_2PtCl_6 as the catalyst for the hydrosilylation of $Bu(Si(CH_3)_2O)_3Si(CH_3)_2CH{=}CH_2$ by T_8 hydrogen silsesquioxane. Subsequent to those results the effect of the catalyst on the mode of addition was studied. It was thought that perhaps a supported catalyst would limit the addition to the terminal carbon of the vinyl group (α-addition) due to steric constraints. Supported catalysts, 1 and 5% Pt/C, 5% sulfided Pt/C, 5% Pd/C, 5% unreduced Pd/C, 5% Pd/Alumina, and 5% Rh/C, were evaluated in the vinyl-siloxane addition to T_8 for this reason. Another homogeneous Pt catalyst, the tetramethyldivinyldisiloxane complex of Pt, was also evaluated to see if the type of Pt complex had an effect on the mode of addition.

All the reactions were done by first heating the mixture of T_8, vinyl-siloxane, and catalyst to approximately 80 °C for 2 hours and then increasing the temperature if necessary to get complete reaction as monitored by the disappearance of SiH in the FTIR. The reactions using the homogeneous catalysts were essentially complete after the initial 2 hours at 80 °C. The reactions catalyzed by the supported catalysts required significantly higher temperature (120 °C and above) and longer time (4-8 hours) before complete disappearance of the SiH was observed.

This higher temperature and time requirement for the supported catalysts was despite the supported catalysts being present at a significantly higher concentration of metal species than the homogeneous catalysts, i.e., 400 ppm Pt from 5% Pt/C vs. 50 ppm Pt from H_2PtCl_6. The hydrosilylations catalyzed by any of the Pd supported catalysts did not occur to any measurable extent as indicated by effectively no product formation even after extended periods of time at elevated temperatures.

All reaction mixtures were characterized by ^{13}C NMR to determine the extent of regioselectivity of addition and by GPC to observe if vinyl/H exchange on Si occurred. A quantification of the proportion of α- and β-addition for each reaction was calculated using the integration of the ^{13}C NMR peaks assigned to the CH and CH_3 resulting from the beta addition relative to the integration of the two CH_2 peaks resulting from the alpha addition as assigned using DEPT NMR experiments and as indicated in the spectrum shown in Figure 3.1.

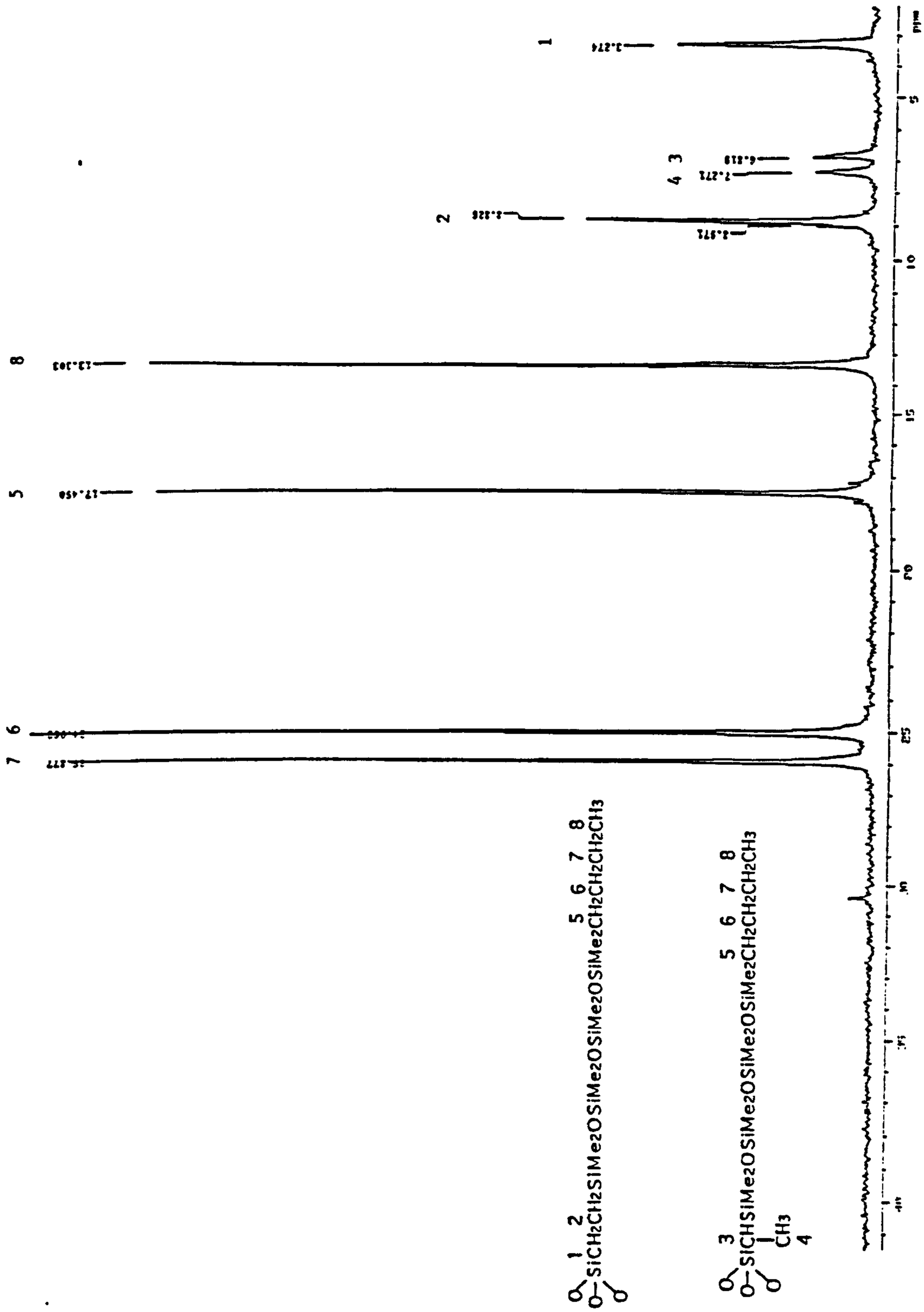

Figure -3.1 ^{13}C NMR spectrum indicating peaks assigned to the CH and CH_3 resulting from the β-addition and the two CH_2 peaks resulting from the α-addition in the reaction of T_8 + vinyl-siloxane.

As a relative measure of the amount of vinyl/H exchange on Si occurring in each reaction, the area of the shoulder (octopus dimer resulting from exchange) as a per cent of shoulder and the main product peak (siloxane octopus) in the GPC was calculated. Since the two peaks are not entirely resolved, area was simply approximated by dropping a line straight down from the valley between the two peaks and taking the area on both sides of the lines as shown in Figure 3.2. Since the area of the GPC peaks may not be directly related to number of molecules, especially in this case when comparing a sphere (octopus) to a dumbell-shaped (octopus dimer), the calculated percentages are only meant to give an indication of more or less exchange occurring relative to the other reactions and not an actual per cent of the vinyls and hydrogens exchanging on Si. It is impossible to calibrate for these molecules as the pure compounds are not available. Figures 3.2 through 3.7 show the GPC chromatograms for the T_8 + vinyl-siloxane reactions employing the different catalysts as labelled in the figure. As can be seen in the series of figures, the amount of H/vinyl exchange on silicon varied with the different catalysts.

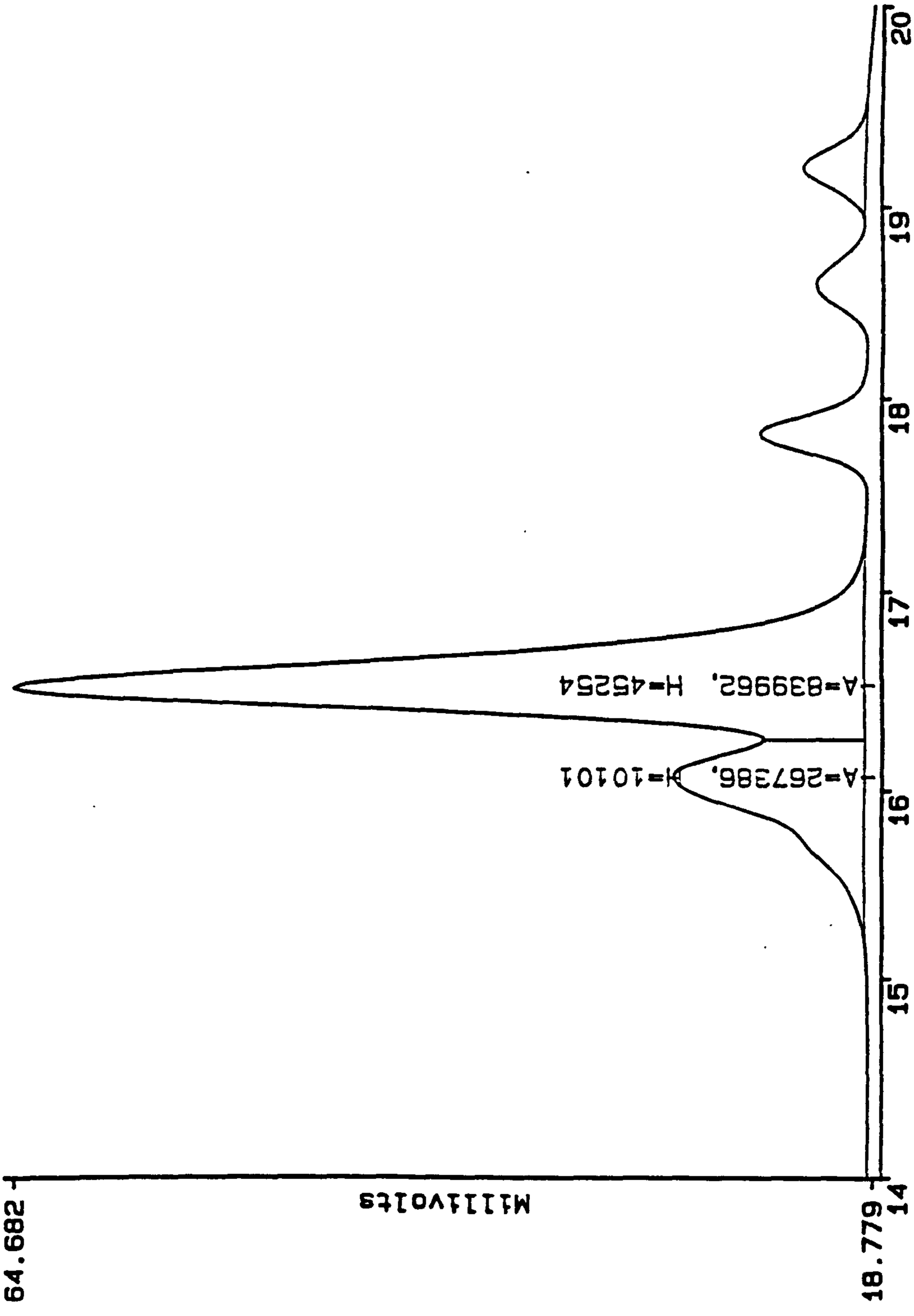

Figure 3.2 GPC chromatogram of a T_8 + vinyl-siloxane reaction product catalyzed by H_2PtCl_6. The area of the shoulder and the main product peak were calculated as the shading indicates.

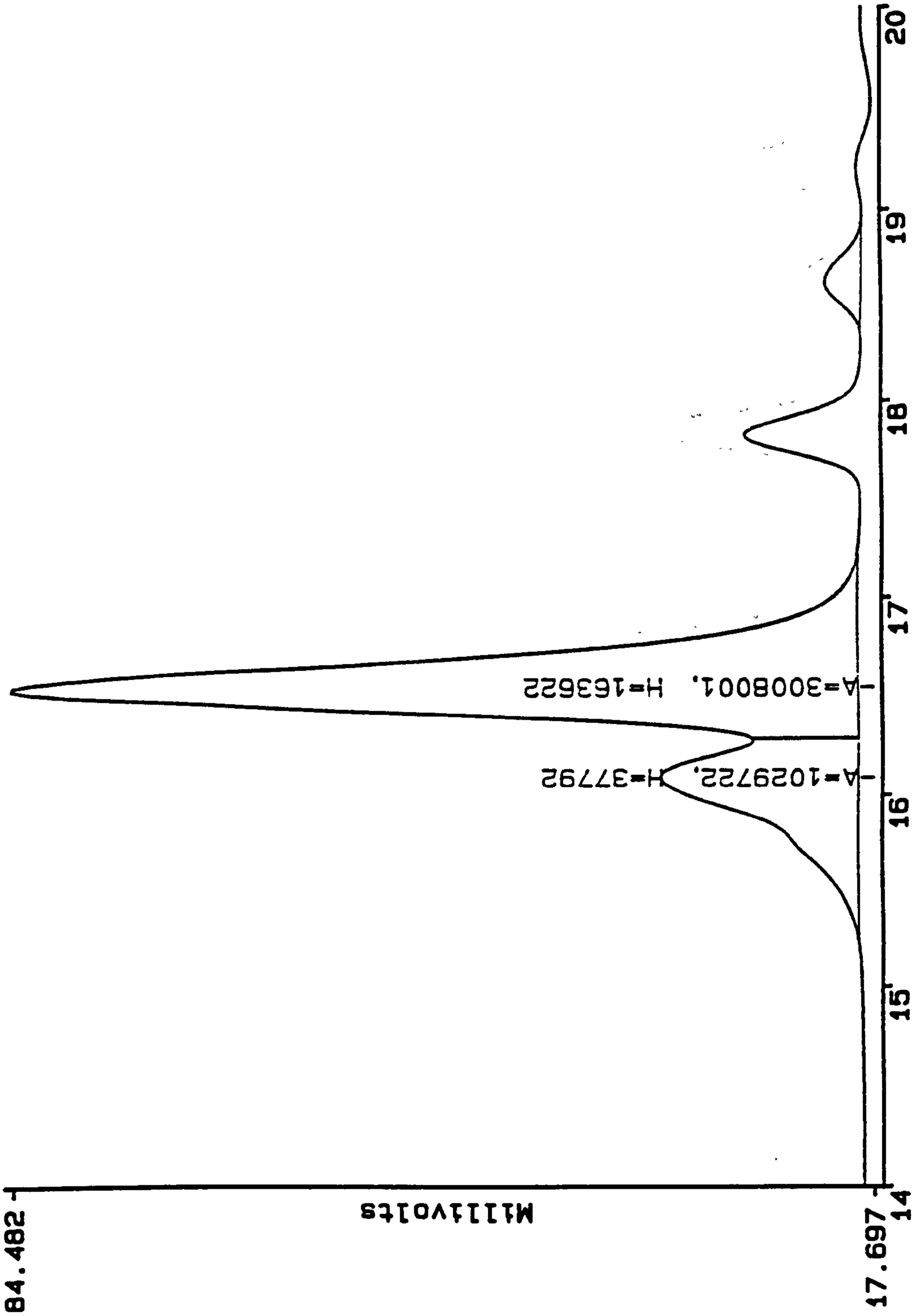

Figure 3.3 GPC chromatogram of a T_8 + vinyl-siloxane reaction product catalyzed by the tetramethyldivinyldisiloxane complex of Pt.

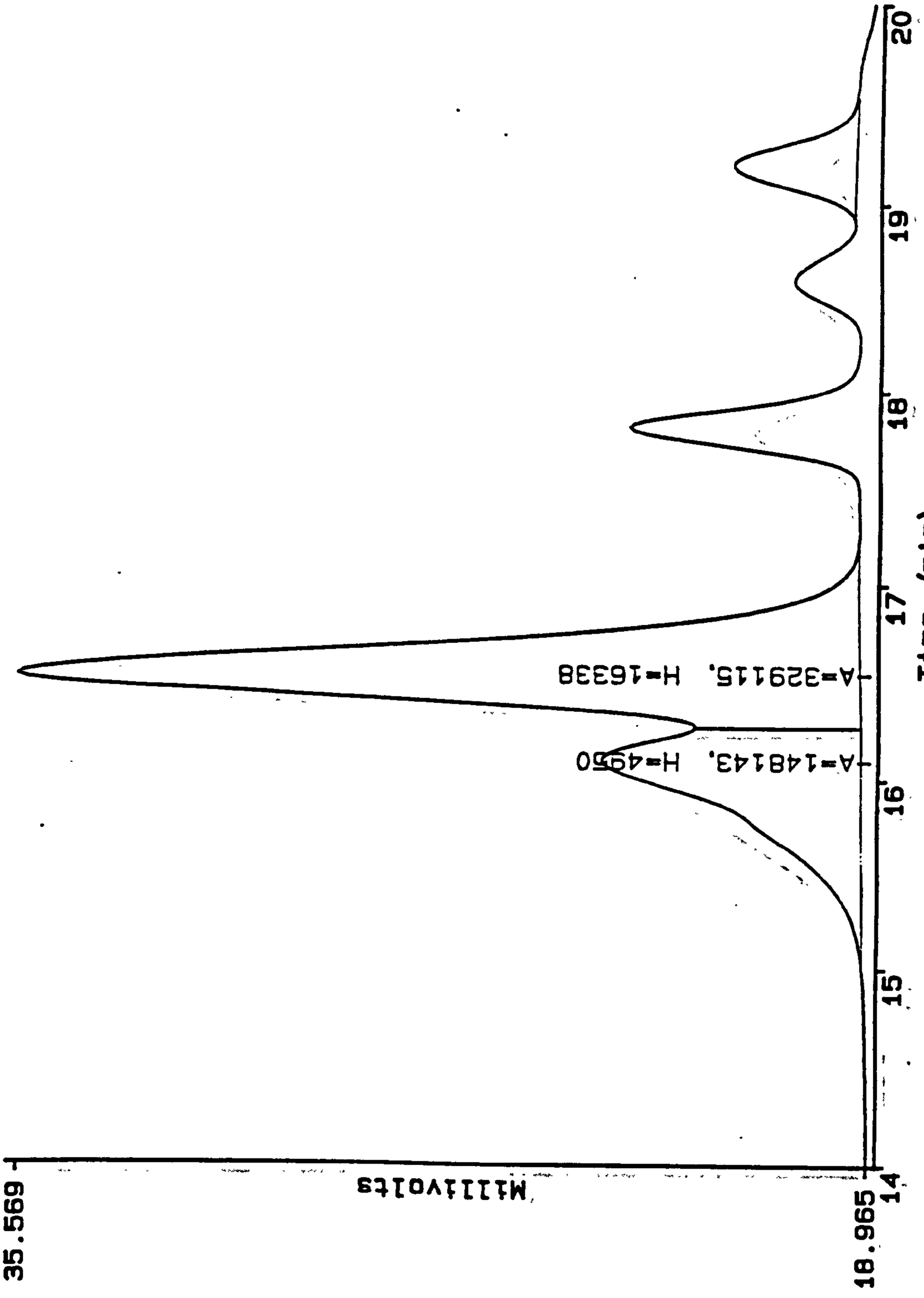

Figure 3.4 GPC chromatogram of a T_8 + vinyl-siloxane reaction product catalyzed by 5% Pt/C.

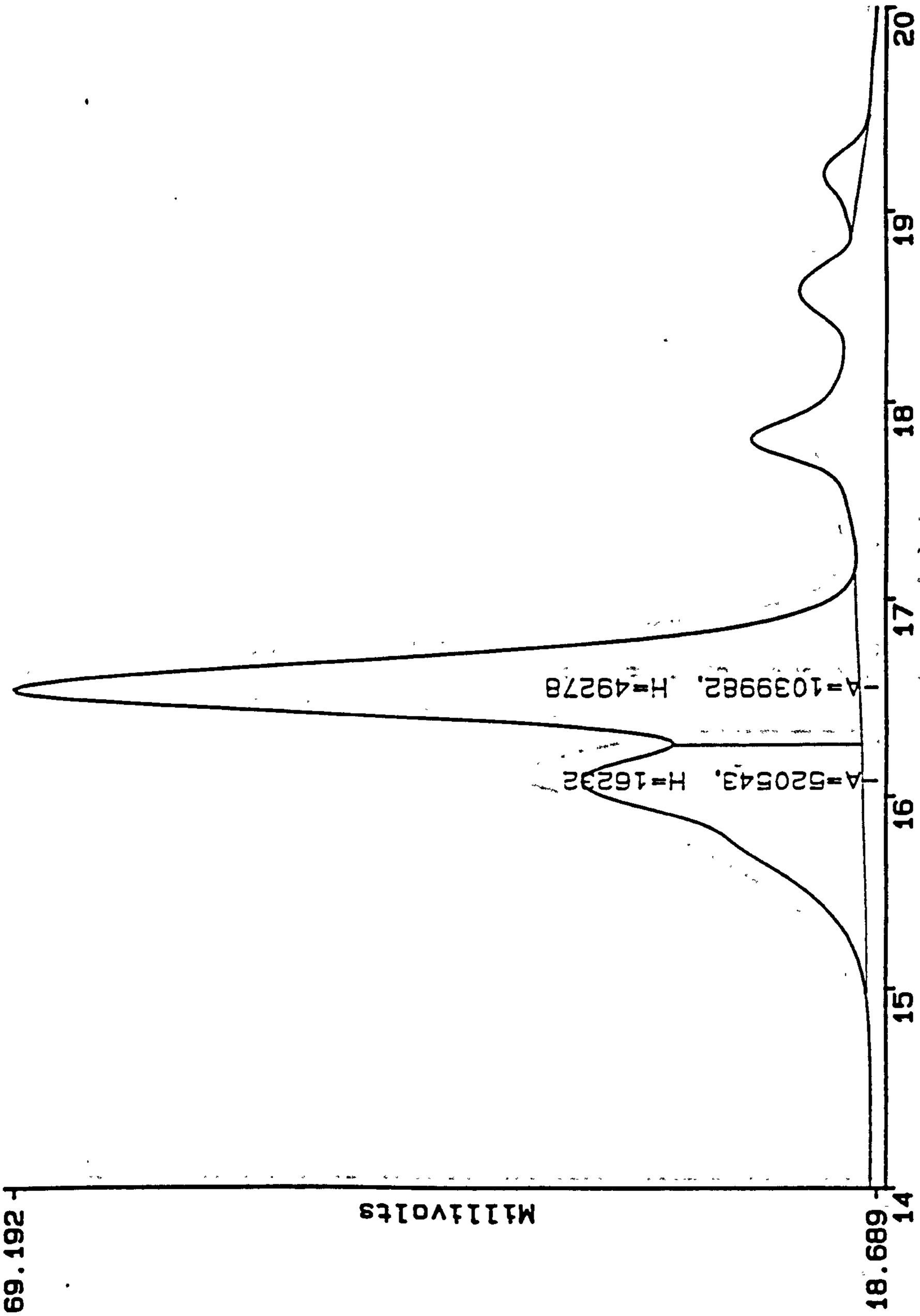

Figure 3.5 GPC chromatogram of a T_8 + vinyl-siloxane reaction product catalyzed by 1% Pt/C.

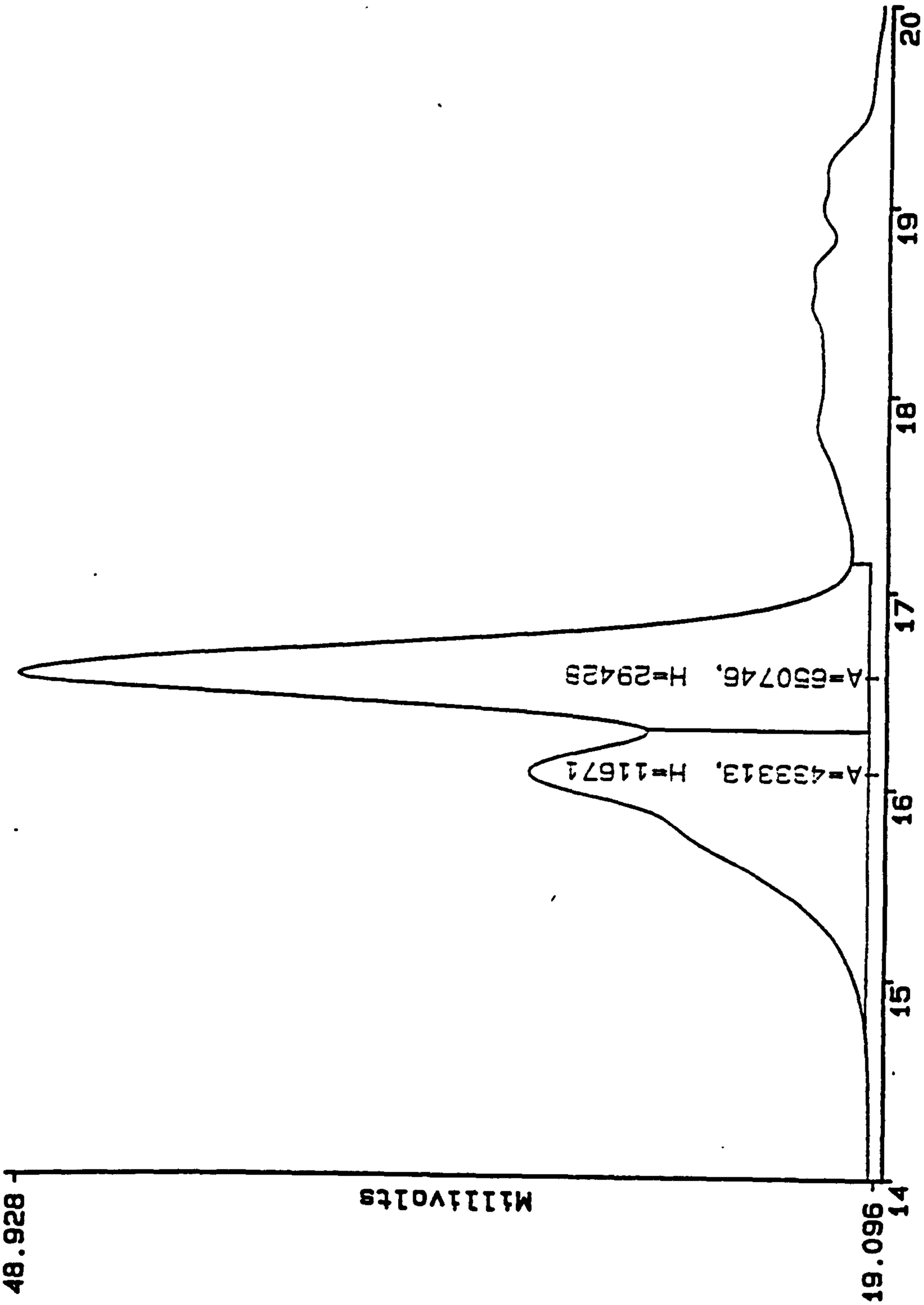

Figure 3.6 GPC chromatogram of a T_8 + vinyl-siloxane reaction product catalyzed by 5% sulfided Pt/C.

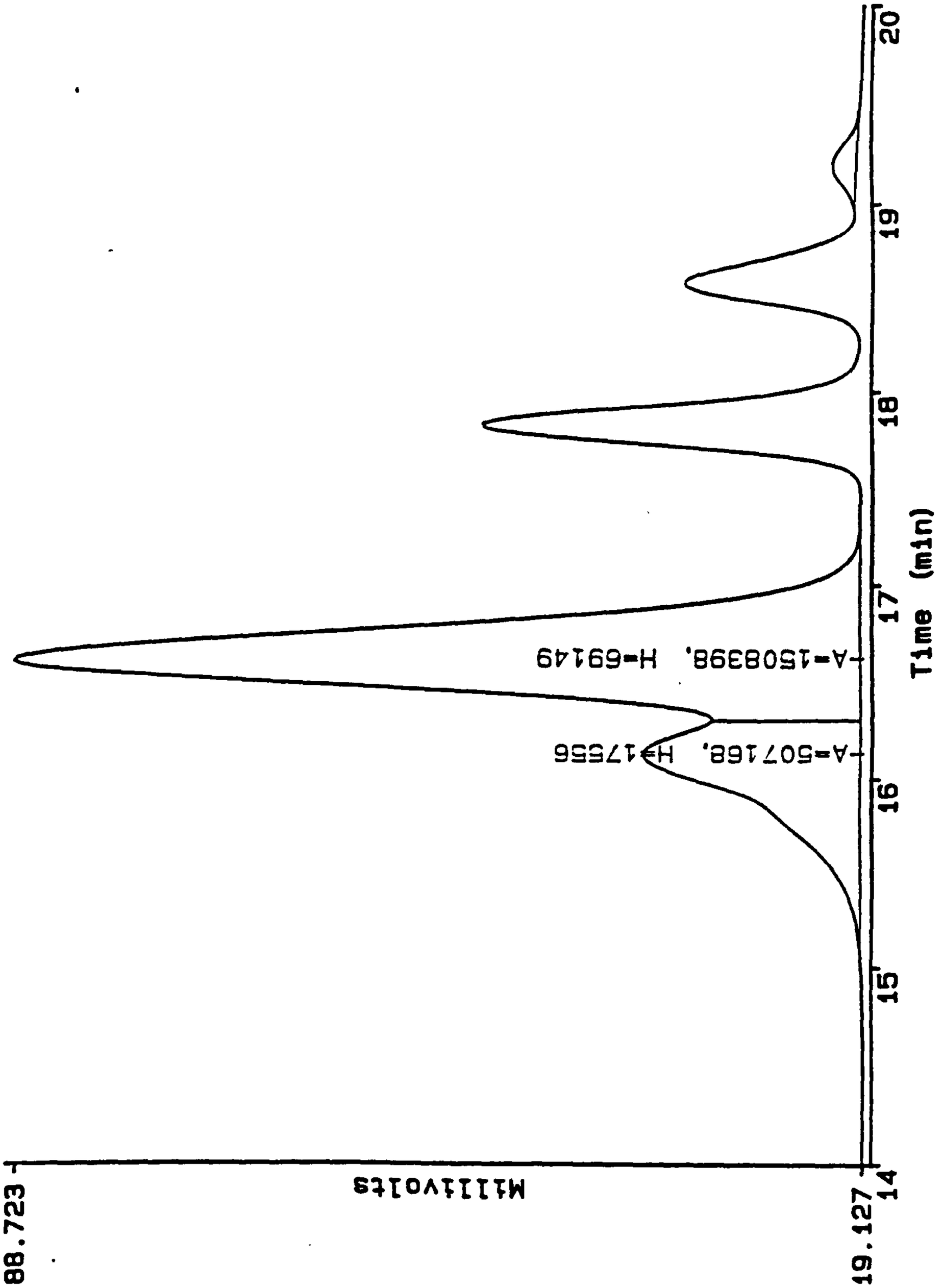

Figure 3.7 GPC chromatogram of a T_8 + vinyl-siloxane reaction product catalyzed by 5% Rh/C.

Table 3.1 summarizes the calculated % beta and %alpha addition from the ^{13}C NMR analysis and the per cent area of the shoulder resulting from vinyl/H exchange on Si relative to the total of the shoulder and the main product peak from GPC analysis for each of the hydrosilylation reactions.

The data indicate that unlike the reduction in the amount of β-addition that was hoped for using the heterogeneous catalysts, the products of the reactions catalyzed by the heterogeneous catalysts contained a higher proportion of product resulting from β-addition. This may be related to the higher temperatures required to get complete reaction with the heterogeneous reactions. The data also indicates that the extent of exchange on silicon is less for the reactions catalyzed by the homogeneous catalysts, H_2PtCl_6 and the tetramethyldivinyldisiloxane complex of Pt, than for the reactions catalyzed by the heterogeneous catalysts. One exception to this is the 5% Rh/C catalyzed reaction. Although this reaction required significantly higher temperature to get complete reaction, the extent of vinyl/H exchange on Si appears by GPC to be similar to the reactions catalyzed by the homogeneous catalysts.

Table 3.1

Reaction conditions and results from $(HSiO_{3/2})_8$ + $Bu[Si(CH_3)_2O]_3Si(CH_3)_2CH=CH_2$ hydrosilylation using different catalysts.

Catalyst	Temp.	Time	alpha (by ^{13}C NMR)	beta (by ^{13}C NMR)	shoulder (by GPC)	main (by GPC)
H_2PtCl_6	80 °C	2 hrs.	80.6%	19.4%	24%	76%
Pt complex*	80 °C	2 hrs	75.5%	24.5%	25%	75%
5% Pt/C	80 °C 120-130	2 hrs., 7 hrs.	74.3%	25.7%	31%	69%
1% Pt/C	80 °C 120-150	2 hrs. 8 hrs.	70.6%	29.4%	34%	66%
5% sulf. Pt/C	80 °C 120-143	2 hrs., 8 hrs.	71.3%	28.7%	40%	60%
5% Rh/C	80 °C 120-155	2 hrs., 8 hrs.	71.8%	28.2%	25%	75%
5% Pd/C	80 °C 120-160	2 hrs., 8 hrs.	No reaction			
5% unred Pd/C	80 °C 120-148	2 hrs., 8 hrs.	No reaction			
5% Pd/ alumina	80 °C 120-134	2 hrs., 8 hrs.	No reaction			

*the tetramethyldivinyldisiloxane complex of Pt

3.2 Conclusion

In conclusion of the studies of the effect of the hydrosilylation catalyst on the regioselectivity and vinyl/H exchange on silicon, it was found that the heterogeneous catalysts Pt/C, sulfided Pt/C, and Rh/C required higher reaction temperatures and longer times to get complete reaction than the homogeneous catalysts, H_2PtCl_6 and the tetramethyldivinyldisiloxane complex of Pt. Pd supported catalysts were not effective catalysts for this hydrosilylation as indicated by effectively no product formation even after extended periods of time at elevated temperatures. The extent of exchange on silicon and the degree of the second mode of addition occurring were higher with the heterogenous catalysts and may be a result of the higher reaction temperatures required to get complete reaction.

3.3 Experimental

3.3.1 General

Solutions of approximately 10 wt% solute in $CDCl_3$ with a final concentration of ~0.02M $Cr(acac)_3$ were made for NMR. A Varian VRX200s NMR spectrometer fitted with a 5 mm probe and operating at 39 MHz was used to obtain ^{29}Si NMR spectra. A Varian VRX400 NMR fitted with a 5 mm probe and operating at 100 MHz was used to obtain ^{13}C spectra. GPC and FTIR analyses were accomplishes using the techniques described in Chapter Two, Section 2.4.1.

3.3.2 Synthesis of $(HSiO_{3/2})_8$

The procedure for obtaining T_8 hydrogen silsesquioxane outlined in Chapter Two, Section 2.4.2, was used.

3.3.3 Synthesis of $Bu[Si(CH_3)_2O]_3Si(CH_3)_2CH=CH_2$

The procedure outlined in Chapter Two, Section 2.4.4, was used to obtain $Bu[Si(CH_3)_2O]_3Si(CH_3)_2CH=CH_2$.

3.3.4 Reactions of T_8 + $Bu(Si(CH_3)_2O)_3Si(CH_3)_2CH=CH_2$

Nine reactions of T_8 + $Bu(Si(CH_3)_2O)_3Si(CH_3)_2CH=CH_2$ using a different catalyst for each were done on a scale of 0.60 grams of T_8 (1.4 mmol) and 4.31 grams of $Bu(Si(CH_3)_2O)_3Si(CH_3)_2CH=CH_2$ (11.8 mmol, 98.2% pure by GC). Each reaction was done in a 50-ml, 1-neck round bottom flask equipped with a stir bar. Before use, the heterogeneous catalysts were dried at 105 °C for 16 hours followed by 130 °C for 1 week. Table 3.2 below lists the catalysts used, their amounts, and calculated concentration of the metal species in the reaction.

Table 3.2

Hydrosilylation Catalysts for T_8 + $Bu(Si(CH_3)_2O)_3Si(CH_3)_2CH=CH_2$

Catalyst	Amount	ppm of metal
H_2PtCl_6	60 µl of 0.02M in isopropanol	48
Pt complex	30 µl of 1.0 wt% Pt in toluene	53
Pt/C	0.04 grams 5 wt% Pt	407
Pt/C	0.21 grams 1 wt% Pt	428
sulfided Pt/C	0.04 grams 5 wt% Pt	407
Rh/C	0.04 grams 5 wt% Rh	407
Pd/C	0.04 grams 5 wt% Pd	407
unreduced Pd/C	0.04 grams 5 wt% Pd	407
Pd/alumina	0.04 grams 5 wt% Pd	407

In each reaction, the mixture of T_8, vinyl-siloxane, and catalyst was first heated to approximately 80 °C for 2 hours and then if needed the reaction temperature was increased to get complete reaction as monitored by the disappearance of SiH in the FTIR. The reactions using the homogeneous catalysts were essentially complete after the initial 2 hours at 80 °C. The reactions catalyzed by the supported catalysts required significantly higher temperature (120 °C and above) and longer time (4-8 hours) before complete disappearance of the SiH was observed. The times and temperatures used for each reaction are listed in Table 3.1 of the results section. The reaction products were separated from the heterogeneous catalysts by filtration through

a glass-fritted funnel containing a layer of filter aid (celite) to remove the catalyst.

The products were characterized by GPC and ^{13}C NMR. The ^{13}C NMR from each reaction was discussed in the results section (3.1) and summarized in Table 3.1 of the results section. An example ^{13}C NMR spectrum was shown in Figure 3.1 along with peak assignments. In all the ^{13}C NMR spectra excluding those in which the hydrosilylation did not occur to any extent (Pd catalyzed reactions), five peaks between 0.95 and -0.79 ppm relative to the central peak at 77.0 ppm of the $CDCl_3$ triplet were observed and assigned to the $\underline{C}H_3$ groups on the silicons of the siloxane chains on the octopus. Eight other main peaks were observed in the region between 140 and -1 ppm. These eight carbons in the major α-addition product and the minor β-addition by-product were numbered as follows:

$[O_{3/2}Si]_8[C^1H_2C^2H_2(SiMe_2O)_3SiMe_2C^5H_2C^6H_2C^7H_2C^8H_3]_8$ and

$[O_{3/2}Si]_8[C^3H(C^4H_3)(SiMe_2O)_3SiMe_2C^5H_2C^6H_2C^7H_2C^8H_3]_8$.

Table 3.3 lists the peak assignments for these 8 carbons.

Table 3.3

^{13}C NMR peak assignments for the products of the T_8 + vinyl-siloxane hydrosilylation reactions

Carbon#	δ (ppm)
CH_3 on Si	0.95, 0.82, -0.06, -0.74, -0.79
1	3.27
2	8.97 (small shoulder), 8.83
3	6.82
4	7.27
5	17.45
6	24.96
7	25.88
8	13.30

GPC chromatograms of each reaction product were shown in Figures 3.2 through 3.7. Each reaction product had a main product peak at a retention time of approximately16.6 minutes and a shoulder on the main peak at a retention time of approximately 16.1 minutes. The shoulder was assigned to the octopus dimer that results from H/Vinyl exchange on silicon during the hydrosilylation. The area of the shoulder and main product peak varied for each reaction. These areas were given as a percent of the total area in Table 3.1 of the results section.

3.4 References

1. Vdovin, V.M.; Petrov, A.D. *Zh. Obshch. Khim.* **1960**, 30, 838.

2. Marciniec, B.; Bulinski, J.; Urbaniak, W. *Synth. React. Inorg. Met.-Org. Chem.* **1982**, 12, 139.

3. Ceskuslovenska, Akademie V., German Patent 2,245,187; March 15, **1973**.

4. Nozakura, S. *Bull. Chem. Soc. Jpn.* **1956**, 29, 660.

5. Sheludyakov, V.D.; Zhun, V.I.; Vlaskenko, S.D.; Bochkarev, V.N.; Slyusarenko, T.F.; Kisin, A.V.; Nosova, V.M.; Turkel'Taub, G.N.; Chernyshev, E.A. *Zh. Obshch. Khim.* **1981**, 51, 2022.

6. Marciniec, B.; Mackowska, E.; Gulinski, J.; Urbaniak, W. Z. *Anorg. Allg. Chem.* **1985**, 529, 222.

Chapter Four

Variety of Octopus Molecules Possible via Hydrosilylation Route

4.0 Introduction

To further show the general utility and demonstrate the almost limitless types of functional octopus molecules possible, it was of interest to look at placement of a number of additional moieties on the silsesquioxane core. Since the initial work demonstrating the feasibility of using hydrosilylation of the SiH functional silsesquioxane to make octopus molecules, hydrosilylation of a number of other unsaturated substrates to make a variety of octopus molecules was further demonstrated and is the topic of this chapter.

4.1 Results

The reaction chosen to add the pendant groups to T_8 to make octopus molecules in the initial work was hydrosilylation as discussed in Chapters 2 and 3 and as shown in reaction scheme 4.1.

$$R_3SiH + CH_2{=}CHXR'_3 \rightarrow R_3SiCH_2CH_2XR'_3 \qquad (4.1)$$

4.1.1 Acrylate Functional Octopus Molecule

One molecule obtained via hydrosilylation was an acrylate functional octopus. This molecule was synthesized via hydrosilylation of allyl methacrylate by T_8 hydrogen silsesquioxane as shown in reaction scheme 4.2.

$$(HSiO_{3/2})_8 + 8\ CH_2{=}CHCH_2OC(O)C(CH_3){=}CH_2 \rightarrow$$
$$[SiO_{3/2}]_8[(CH_2)_3OC(O)C(CH_3){=}CH_2]_8 \qquad (4.2)$$

In the above reaction, polymerization of the methacrylate functionality during hydrosilylation was avoided by use of the inhibitor, phenothiazine.

As the ^{29}Si NMR in Figure 4.1 indicates, there is a grouping of not entirely resolved peaks between δ -64 and -67 ppm referenced to TMS at 0.0 ppm indicating several T-Si environments. There also appears to be a small amount of Q-Si as evidenced by the group of peaks between δ -105.5 and -106.5 ppm referenced to TMS at 0.0 ppm. This Q-Si environment could be from the condensation of SiH on the T_8 with the -C(O) on the allylmethacrylate. This condensation side reaction could also be the cause of the multiple T-Si environments since the occurrence of condensation of one SiH of the cube would create three different Si environments for the remaining silicons of the T_8 cube. The extent of the condensation reaction was roughly estimated from the integration of the peaks between δ -105.5 and -106.5 ppm relative to all the peaks and was found to be approximately 9%. The product was of relatively low viscosity so this amount of condensation did not cause gellation products. The product is still quite fluid two years after the original synthesis.

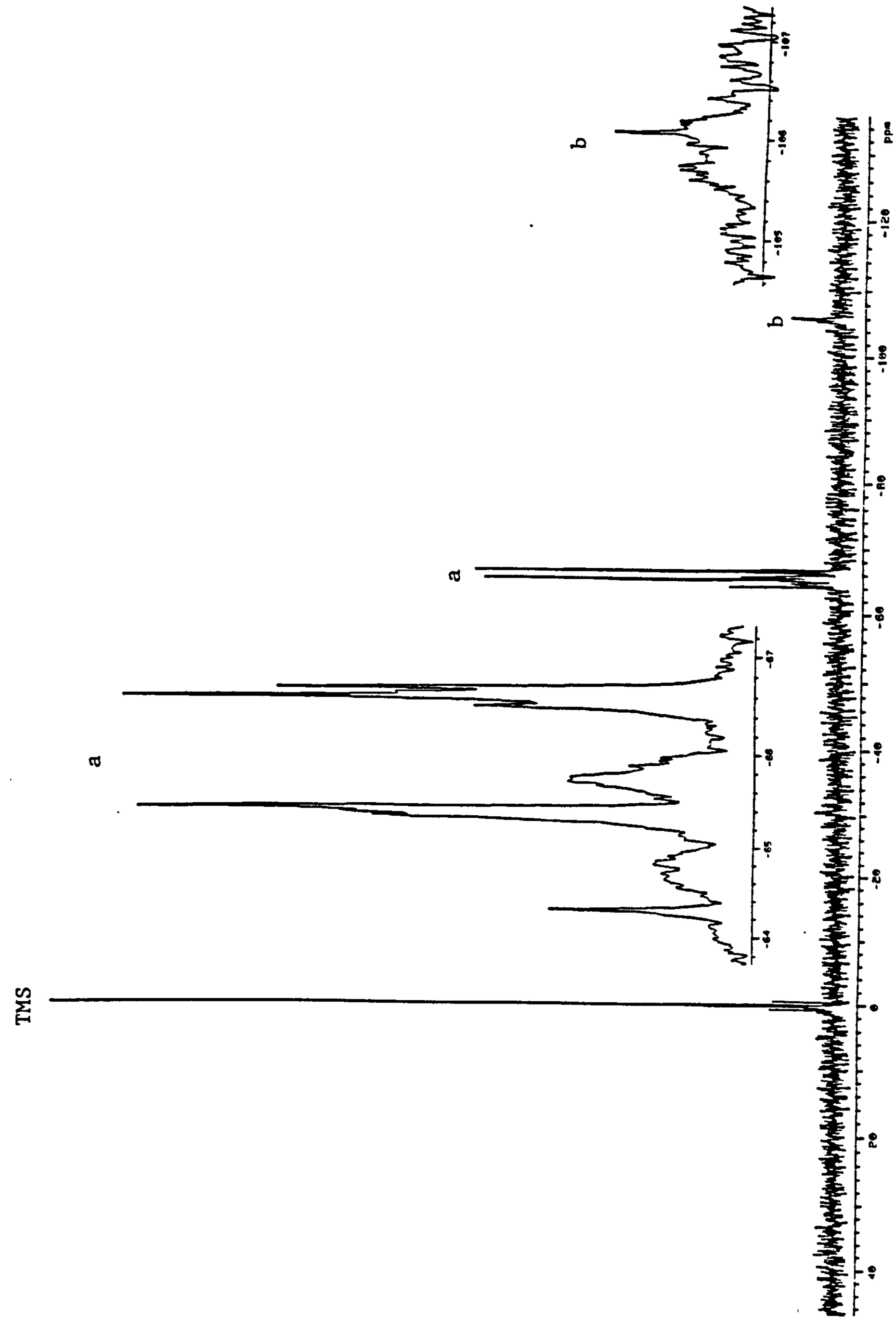

Figure 4.1 ^{29}Si NMR spectrum of the product of the reaction $T_8 + CH_2=CHCH_2OC(O)C(CH_3)=CH_2$.

Three formulations containing the reaction product (Table 4.1) were coated on polycarbonate.

Table 4.1

Coating formulations containing acrylate functional octopus molecules

Components	Formulation# 1	2	3
Acrylate Octopus (parts)	1.0	1.0	1.0
TMPTA (parts)	--	--	0.2
HDDA (parts)	--	0.2	--
Irgacure 500 (parts) (photo initiator)	0.05	0.05	0.05

where Irgacure 500 is a 50/50 (wt/wt) mixture of 1-hydroxycylcohexylphenylketone and benzophenone; TMPTA is trimethyolpropanetriacrylate; and HDDA is hexanedioldiacrylate.

The coatings were found to be curable using ultraviolet radiation. The scratch resistant properties of the cured coatings were evaluated using a Taber Abrasion Test which involves determining the change in light transmission and haze of the coated transparent plastics after a predetermined number of cycles of surface abrasion (typically 100 and 500 cycles). Haze is defined as the percentage of transmitted light which in passing through the abraded track deviates from the incident beam by forward scattering. Table 4.2 shows the results of the surface

abrasion testing and for comparison the properties typically sought in a scratch resistant coating are also listed.

Table 4.2

Surface abrasion test results for UV-cured coatings containing acrylate functional octopus

Property	Formulation# 1	2	3	Ideal/Required
Adhesion (%)	0	100	100	100
Light Transmission (%)	86.6	87.2	86.0	>86
Yellow Index	5.3	3.7	4.5	<2
Haze	0.7	1.4	0.7	<2
Taber 100 (D %)	9.5	13.4	7.0	<5
Taber 500 (D %)	----	----	20.5	<10

As the data indicates, the coating containing only octopus molecule and photo initiator in the formulation has poor adhesion. Upon addition of the difunctional or trifunctional acrylate monomers, adhesion is greatly improved suggesting that some linear segments between octopus molecules allows for better adhesion than the perhaps too high crosslinked coating that results from using only the octopus molecule. The initial light transmittance of the coatings in all cases are above the typical. The yellow index for all three coatings is higher than ideal due to the great excess of phenothiazine inhibitor that was used in the synthesis of the acrylate functional octopus. The

yellow index could easily be brought into the desired range but reducing the amount of inhibitor. The haze values are all very good. The Taber abrasion results after 100 cycles are somewhat above the desired level and actually close to the level allowed after 500 cycles. For this reason only coating #3 was continued to 500 cycles and as the results indicate the value is above the desired level of abrasion.

The results were considered to be very encouraging in that the coatings were UV-curable, the properties were within or close to the range of typical, and finally this was a first attempt without any optimization of the formulations[1]. This acrylate octopus approach is very different from the typical silane/acrylate/silica filler approach currently being used and shows promise for potential commercial interest[2].

4.1.2 Bromoalkyl Functional Octopus Molecule

As another example of the variety of octopus molecules with silsesquioxane cores that can be made via hydrosilylation, a bromoalkene, 5-bromo-1-pentene, was hydrosilylated by T_8 to make a bromoalkyl functional octopus molecule as shown in reaction scheme 4.3.

$$(HSiO_{3/2})_8 + CH_2{=}CHCH_2CH_2CH_2Br \rightarrow [SiO_{3/2}]_8[(CH_2)_5Br]_8 \qquad (4.3)$$

The ^{29}Si NMR spectrum shown in Figure 4.2 indicates the presence of a group of peaks between δ -65.8 and -67.0 ppm with the primary product peak at δ -66.86 ppm relative to TMS. This primary product peak makes up greater than 84% of the T-Si peak area. The ^{29}Si NMR spectrum taken shortly after synthesis of the bromoalkyl functional octopus molecule contained no Q-Si peaks. When the analysis was repeated 18 months later, some small peaks between -100 and -111 ppm were then found to be present in the sample after aging. These peaks make up a very small portion of the total sample and are probably due to hydrolysis and condensation of any residual SiH that may have remained in the original product.

The above bromoalkyl functional octopus molecule has the bromine available for further functionalization, for instance, possibly for subsequent branching of each arm of the octopus to make a dendrimer.

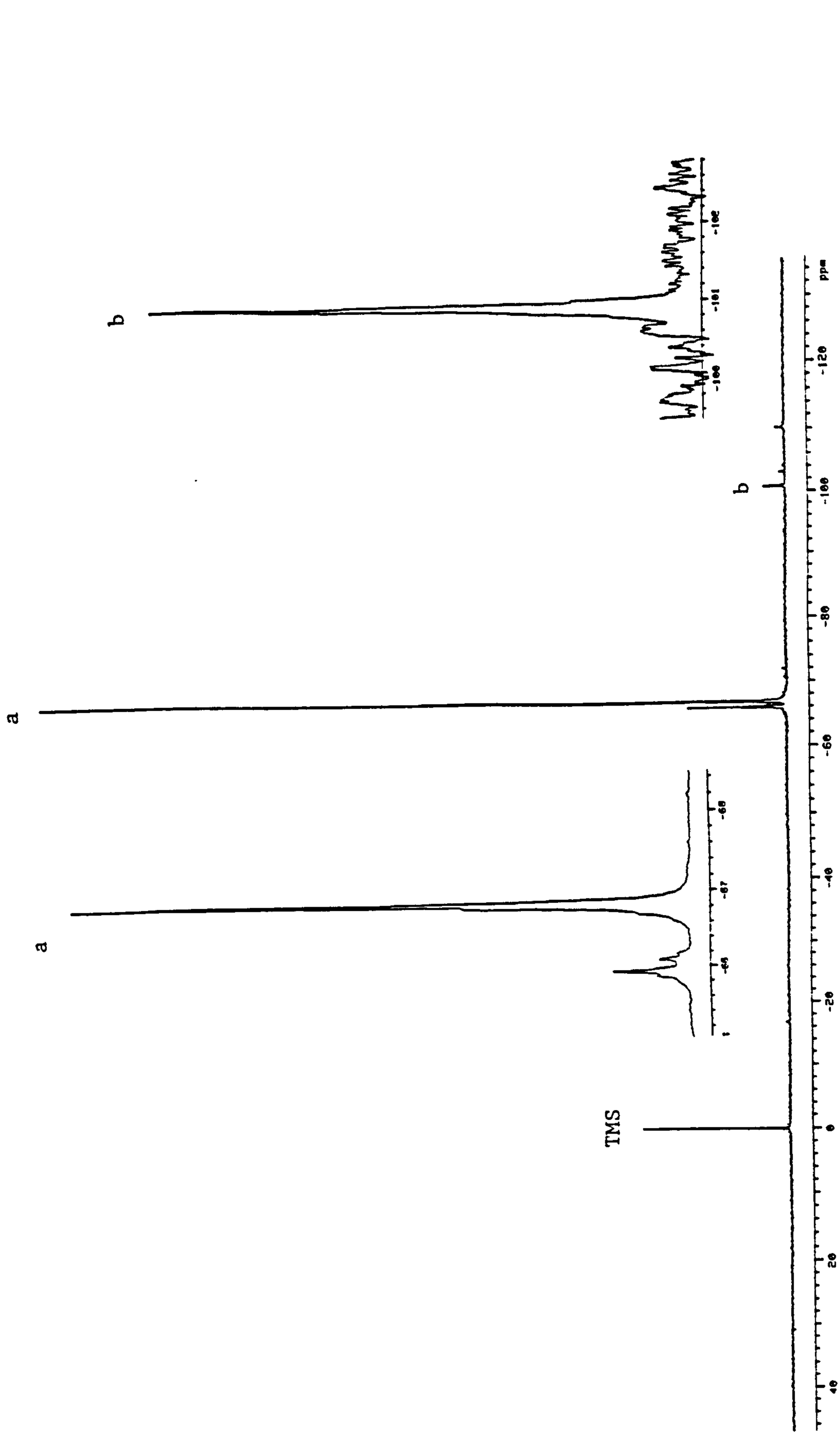

Figure 4.2 ^{29}Si NMR spectrum of the product of the reaction $T_8 + CH_2=CHCH_2CH_2CH_2Br$.

4.1.3 Trimethylsilyloxy-capped Hydrocarbon Octopus Molecules

It was found that trimethylsilyloxy-capped hydrocarbon octopus molecules could be obtained using $CH_2=CH(CH_2)_xOSiMe_3$ made via silylating unsaturated alcohols. These trimethylsilyloxy-capped alkenes were then hydrosilylated by T_8 hydrogen silsesquioxane to form the trimethylsilyloxy-capped hydrocarbon octopus molecules as shown in reaction scheme 4.4.

$$(HSiO_{3/2})_8 + CH_2=CH(CH_2)_xOSiMe_3 \rightarrow [SiO_{3/2}]_8[(CH_2)_{x+2}OSiMe_3]_8 \quad (4.4)$$

Two molecules were made to illustrate the range of hydrocarbon chain length possible. One of these molecules was based on the use of $CH_2=CHCH_2OSiMe_3$ (x=1 in scheme 4.4) made from silylating allyl alcohol. The use of this molecule in the hydrosilylation results in a molecule with short appendages. The reaction product was a liquid that readily dissolved in toluene and chloroform. Analysis of the reaction product by ^{29}Si NMR (Figure 4.3) indicated that the hydrosilylation was regioprecise like those of the 1-alkenes as demonstrated by the single T-Si peak at δ -66.45 ppm for the Si of the cage and the single M-Si peak at δ 17.01 ppm for the trimethyl silicons of the arms off the core. The GPC chromatogram shown in Figure 4.4 indicates that the reaction product was monodispersed.

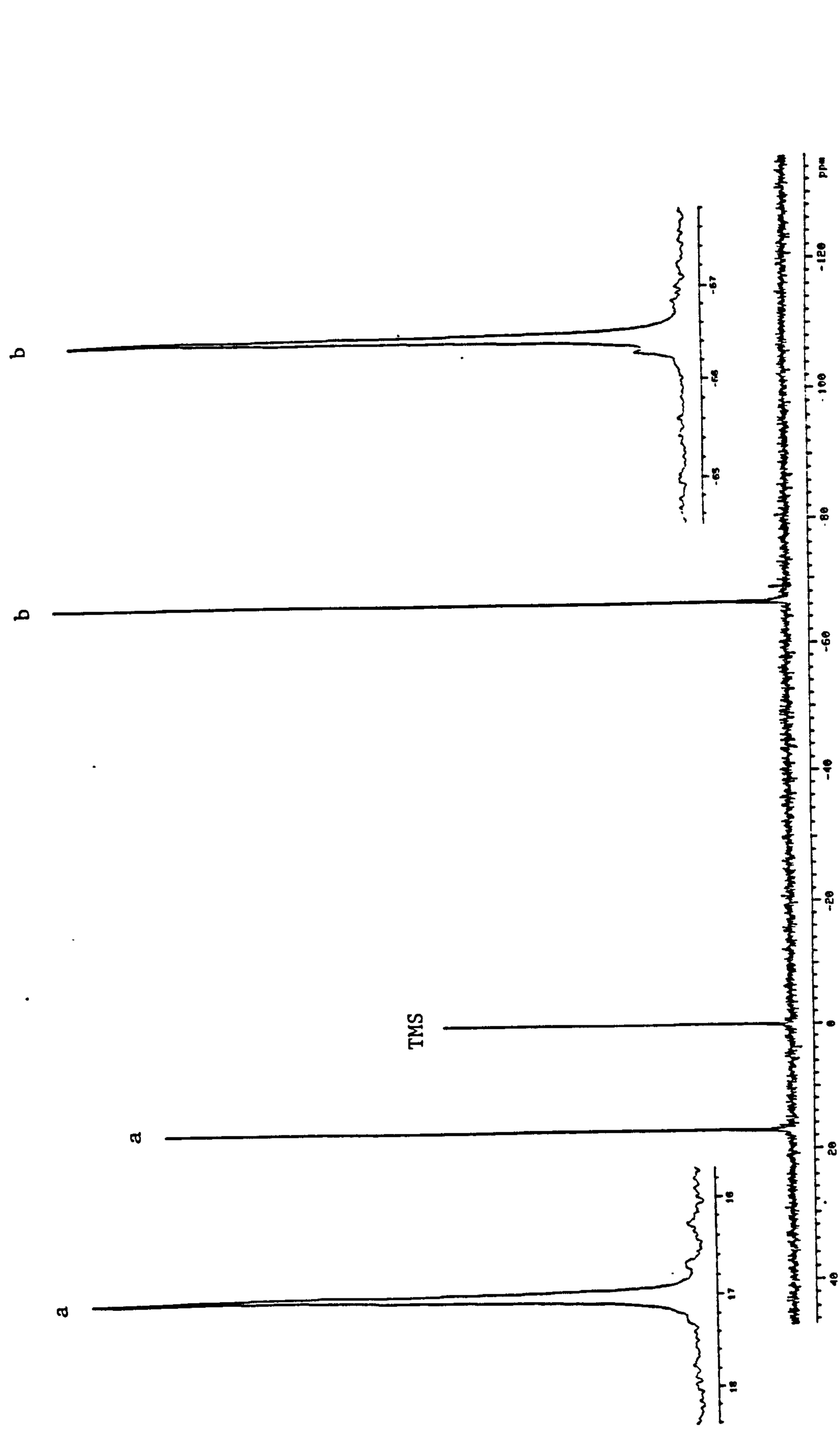

Figure 4.3 ^{29}Si NMR spectrum of the product of the reaction $T_8 + CH_2=CHCH_2OSiMe_3$.

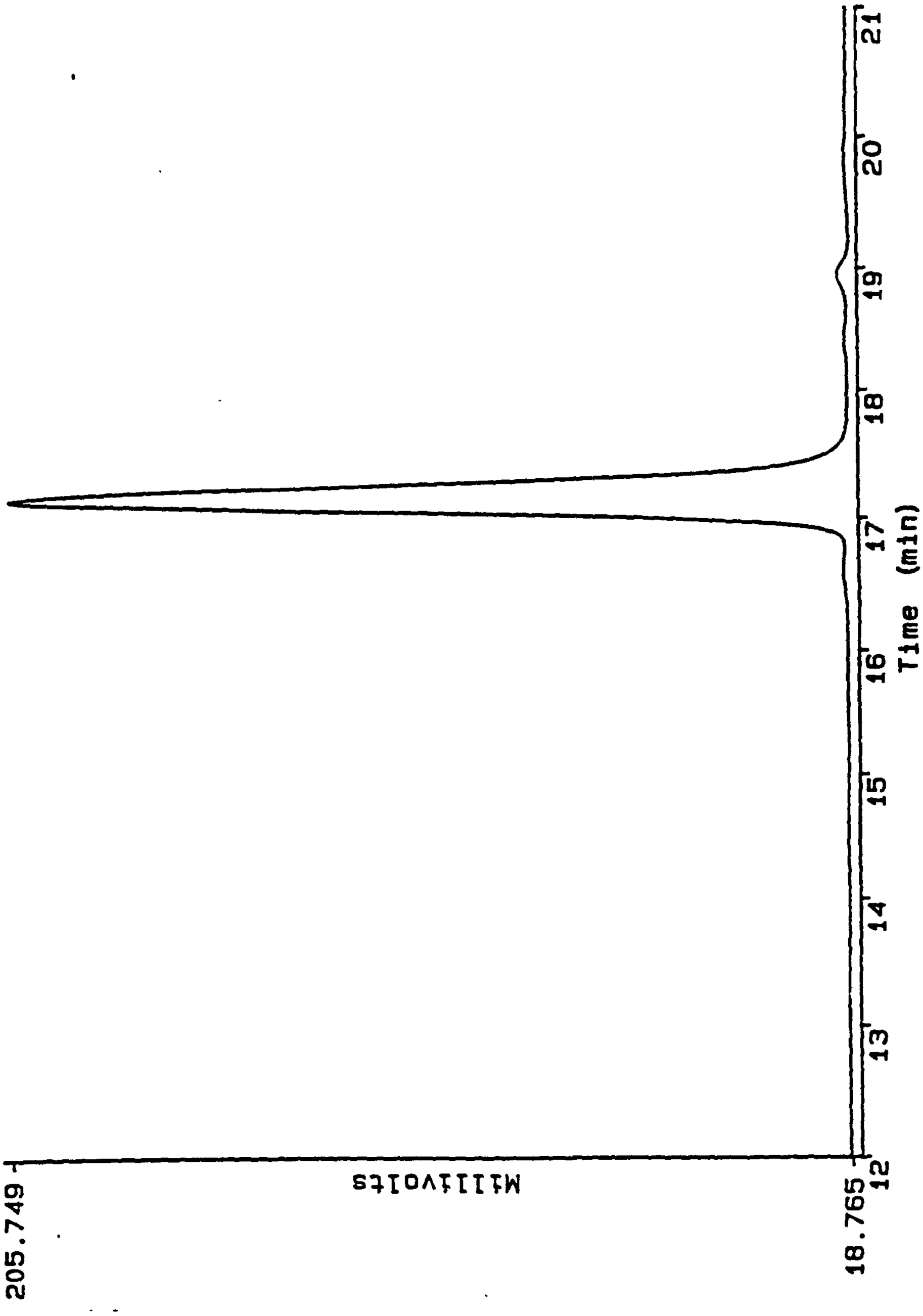

Figure 4.4 GPC chromatogram of the product of the reaction $T_8 + CH_2{=}CHCH_2OSiMe_3$.

To illustrate how this same approach can lead to a molecule with longer appendages, $CH_2=CH(CH_2)_9OSiMe_3$ (x = 9 in scheme 4.4), was hydrosilylated by T_8 to form $[SiO_{3/2}]_8[(CH_2)_{11}OSiMe_3]_8$. The product was a viscous liquid that was soluble in toluene and chloroform. The ^{29}Si NMR spectrum shown in Figure 4.5 indicates that several T-Si peaks are present between δ -65 and -67 with a single well resolved peak at δ -66.63 ppm assigned to the silicon of the cage, $O_{3/2}\underline{Si}CH_2$-. The spectrum also shows two peaks at δ 17.01 and 16.05 ppm for the trimethyl silicon. There are also some smaller peaks in the Q-Si region at δ -102.88, -102.96 and -108.78 ppm.

It was also later discovered that the starting material, $CH_2=CH(CH_2)_9OSiMe_3$, that when first made and distilled was very pure (>98%) had decreased in purity (to ~94%) by the time it was used for the reaction with T_8. Hydrolysis of the trimethylsilyl group apparently had occurred resulting in the reformation of some of the unsaturated alcohol. The reaction of the alcohol with the SiH of T_8 would explain the Q-Si peaks seen in the ^{29}Si NMR. This reaction occurring at even just one corner of the T_8 cube while the remaining seven participated in hydrosilylation would create a multitude of T-Si environments as is seen in the ^{29}Si NMR of Figure 4.5. This condensation reaction would also leave the other end of the chain available for hydrosilylation and thus the formation of dimers and higher adducts could take place. GPC of the reaction product (Figure 4.6) indicates that was the case as it is apparent that dimer and higher species are present to a great extent. This reaction provides an example of the importance of the purity of the

starting materials especially when dual functional impurities such as the unsaturated alcohol are present. The previous reaction that only differed by the length of the pendent chains went very cleanly and resulted in a single product because the silylated alcohol starting material was very pure and used immediately after being made. The longer chain $CH_2=CH(CH_2)_9OSiMe_3$ was made some time before its use in the reaction with T_8 and resulted in a multitude of reaction products due to the reversibility of the silylating reaction.

Although applications of these trimethylsilyloxy-capped hydrocarbon octopus molecules have not yet been pursued, it is envisioned that having a molecule that is essentially a sphere coated with trimethylsilyl groups could lead to some interesting properties and applications in the area of lubricants, additives for water repellancy, viscosity modifiers, compatibilizers, and a number of other applications. It would also be expected that by varying the length of the appendages on the trimethylsilyloxy-capped octopus molecules, the properties of these types of molecules could be varied significantly leading to a way of "tuning" physical properties depending on the application of interest.

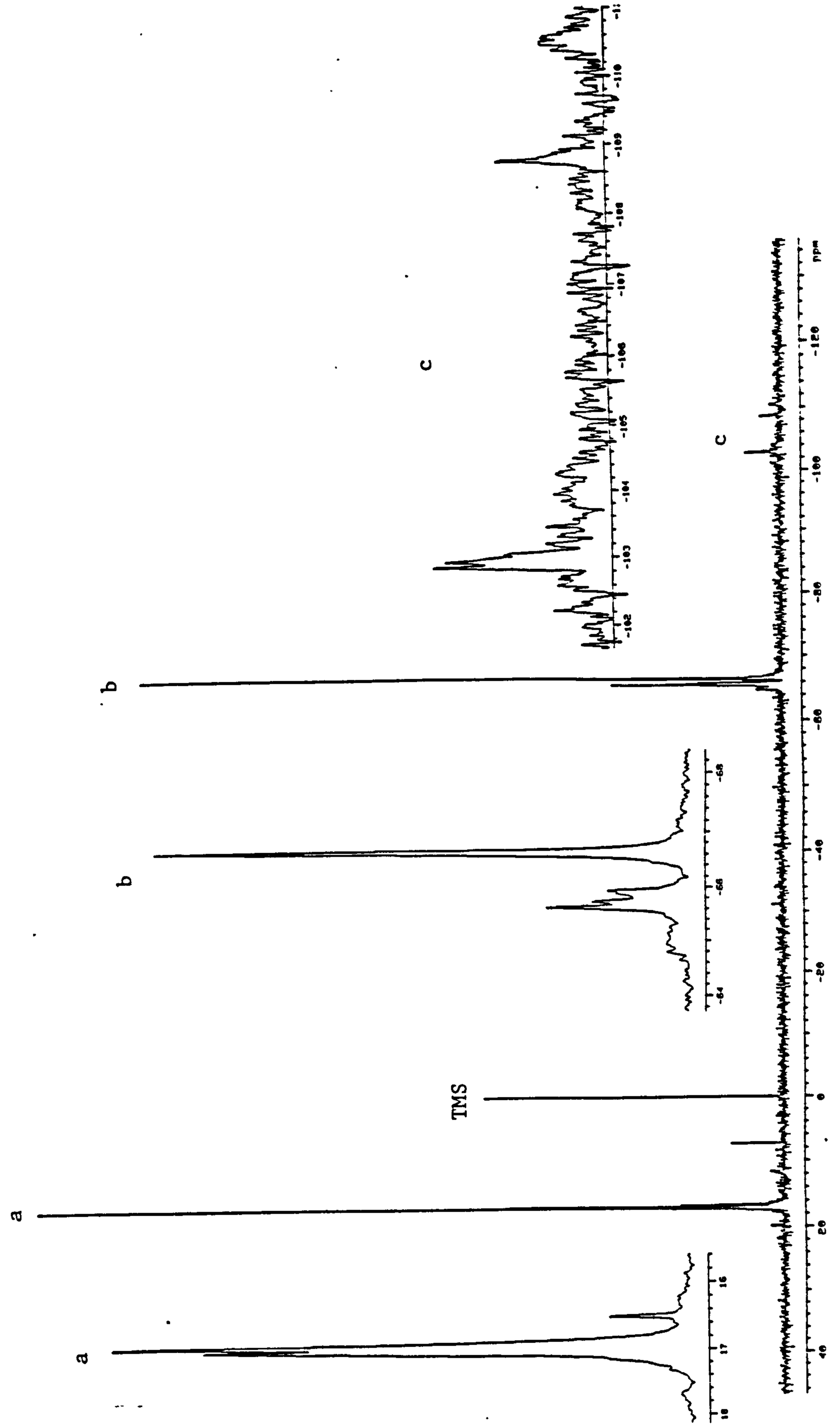

Figure 4.5 ^{29}Si NMR spectrum of the product of the reaction $T_8 + CH_2=CH(CH_2)_9OSiMe_3$.

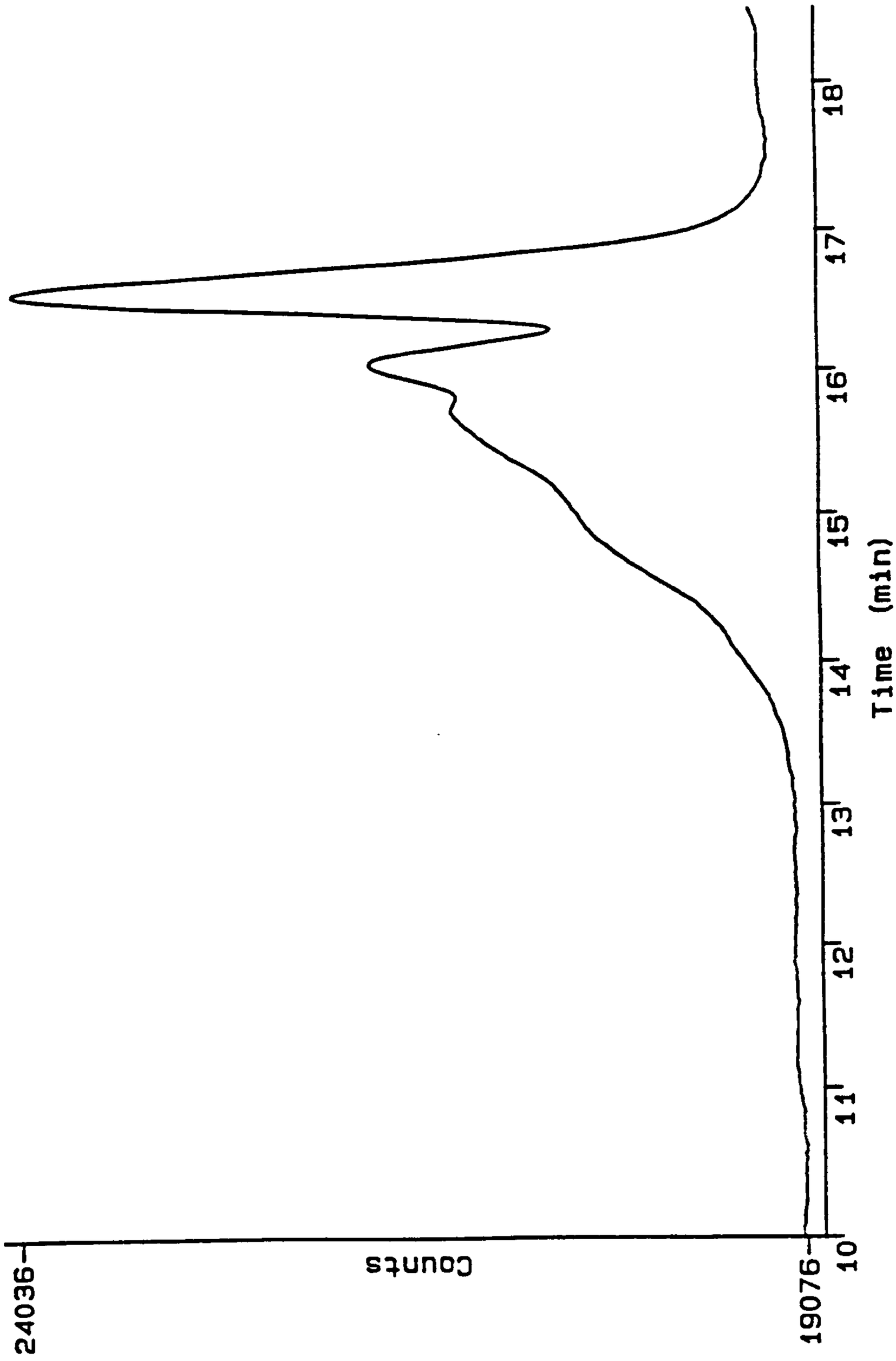

Figure 4.6 GPC chromatogram of the product of the reaction $T_8 + CH_2=CH(CH_2)_9OSiMe_3$.

4.1.4 Hydroxy Functional Octopus Molecules

To test whether the unsaturated terminus of a dual functional molecule such as an unsaturated alcohol, could be selectively reacted resulting in an octopus with hydroxyl functionality at the end of each appendage, the hydrosilylation of unsaturated alcohols by T_8 hydrogen silsesquioxane was done as shown in reaction scheme 4.5.

$$(HSiO_{3/2})_8 + CH_2{=}CH(CH_2)_xOH \rightarrow [SiO_{3/2}]_8[(CH_2)_{x+2}OH]_8 \qquad (4.5)$$

The reaction of 4-penten-1-ol (x=3 in reaction scheme 4.5) with T_8 resulted in the formation of a white solid. The ^{29}Si NMR spectrum of this reaction product shown in Figure 4.7 indicated a major peak in the T-Si at δ -66.45 ppm region although there appears to be some additional minor peaks in the T-Si region at δ -66.36 and -65.46 ppm making up 13.5% of the total integrated peak area. There appears that there may also be a very small peak in the Q-Si region around δ -103 ppm possibly due to some of the OH functionality undergoing condensation with the SiH of the cage. This occurrence would explain the multiple T-Si environments seen. The product, $[SiO_{3/2}]_8[CH_2)_5OH]_8$, was insoluble in all solvents tested (toluene, chloroform, THF) with the exception of alcohols (i.e., methanol).

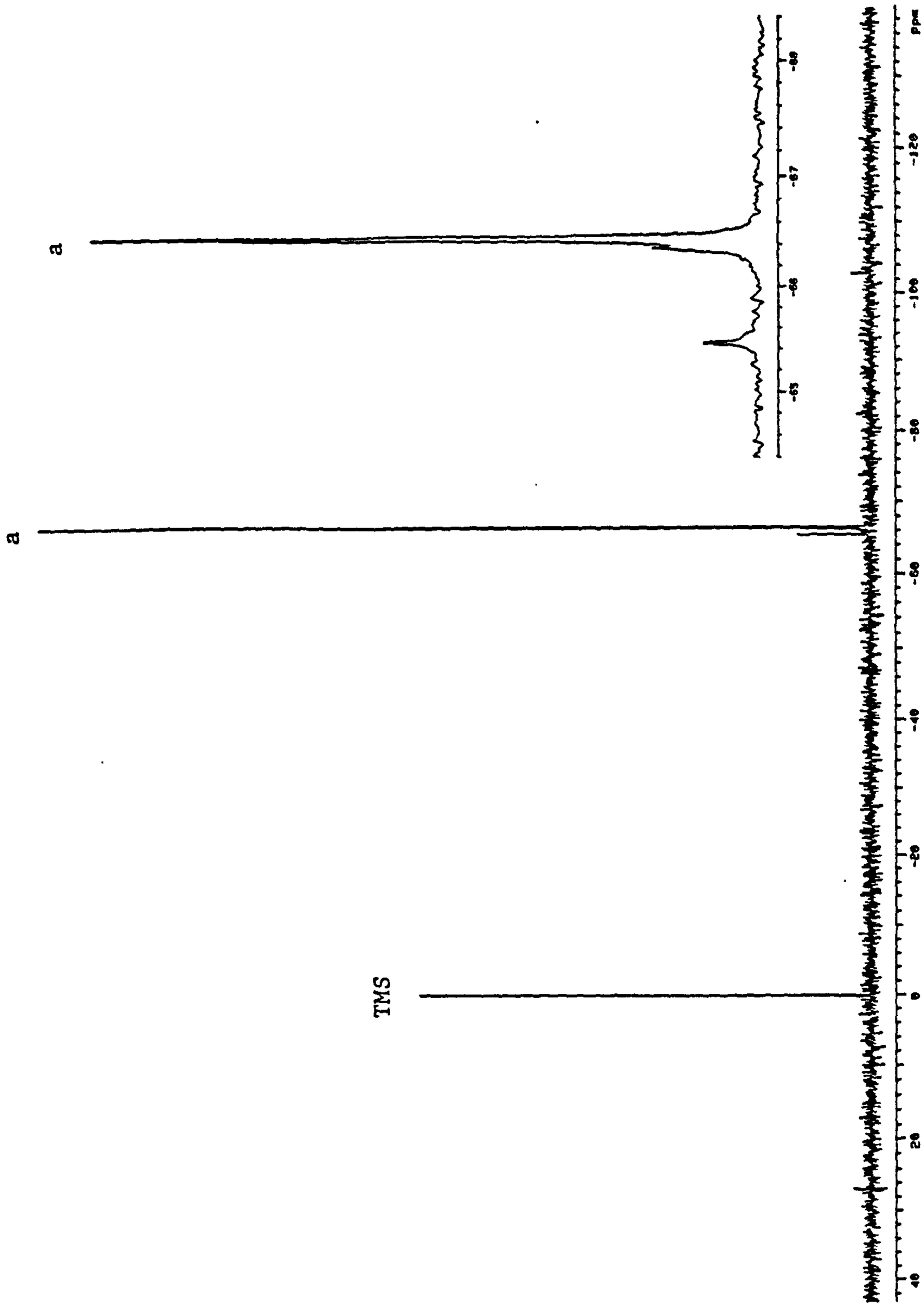

Figure 4.7 ^{29}Si NMR spectrum of the product of the reaction $T_8 + CH_2=CH(CH_2)_3OH$.

GPC was difficult to perform on the $[SiO_{3/2}]_8[CH_2)_5OH]_8$ since the product was insoluble in the mobile phases of all the GPC units available (toluene, chloroform, and THF) but was attempted using a mix of toluene and methanol. The GPC chromatogram is shown in Figure 4.8. As can be seen, the chromatogram is inverted because the refractive index of the product was greater than that of toluene and the detection is based on the difference in refractive indices. The chromatogram shows a peak at a retention time of approximately 20.3 minutes which is most likely the product peak. There also appears to be a second, higher molecular weight peak at a retention time of approximately 19.9 minutes which could be attributed to an octopus "dimer" resulting from OH to SiH condensation suggested above in the discussion of the ^{29}Si NMR spectrum.

This class of molecules, hydroxy functional octopus molecules are an important class since they can be used as precursors to dendrimers with silsesquioxane cores as will be discussed in Chapter Six. The OH end of each appendage is available for further functionalization. These molecules also serve as an example of how drastically the polarity and solubility characteristics can be change by choice of functional group on the end of the appendages. Silylation of these molecules would lead to the trimethylsilyloxy-capped octopus molecules discussed in Section 4.1.3.

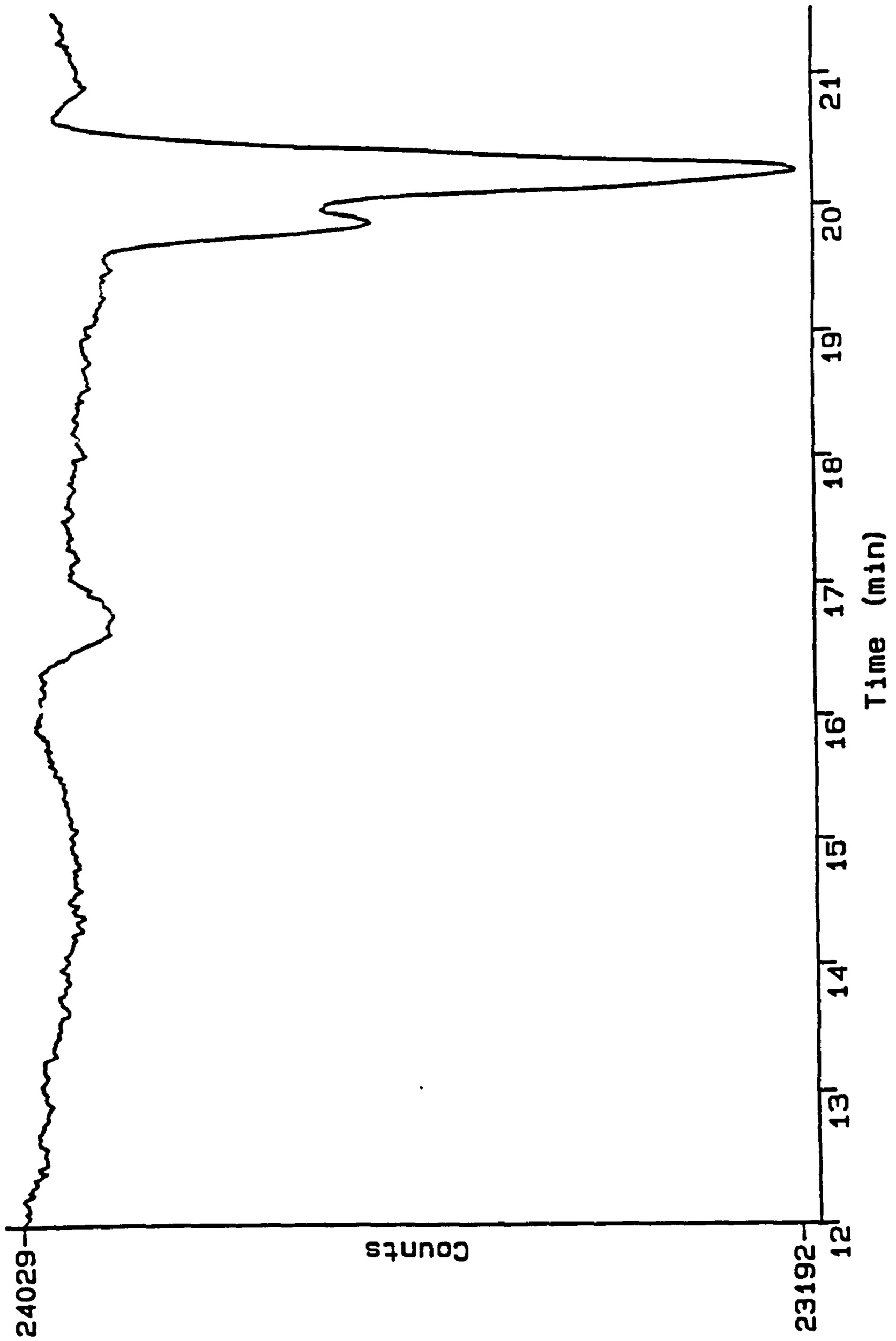

Figure 4.8 GPC chromatogram of the product of the reaction $T_8 + CH_2=CH(CH_2)_3OH$.

4.1.5 Trimethoxysilyl Functional Octopus Molecules

The synthesis of $[SiO_{3/2}]_8[(CH_2)_2Si(OMe)_3]_8$ was accomplished via hydrosilylation of vinyltrimethoxysilane by T_8 hydrogen silsesquioxane as shown in reaction scheme 4.6.

$$(HSiO_{3/2})_8 + CH_2{=}CHSi(OMe)_3 \rightarrow [SiO_{3/2}]_8[(CH_2)_2Si(OMe)_3]_8 \qquad (4.6)$$

The ^{29}Si NMR spectrum shown in Figure 4.9 indicates the presence of a group of T-Si peaks between δ -66 and -68 ppm. These multiple peaks indicate that the hydrosilylation of vinyltrimethoxysilane is not regioprecise like the previously discussed hydrosilylation of vinyl-siloxanes. If the hydrosilylation is not regioprecise, one would also expect multiple Si environments for the trimethoxy silicon and this appears to be the case as evidenced by the grouping of peaks between δ -41.4 and -44.3 ppm. These results are not surprising considering the previously discussed T_8 + vinyl-siloxane reaction in chapters 2 and 3.

The GPC of the product of the reaction of T_8 with vinyltrimethoxysilane (Figure 4.10) contains a primary peak at retention time 17.72 minutes that is most likely the expected reaction product. Again, considering the previous T_8 + vinyl-siloxane reaction, it is not surprising to find that the GPC of the T_8 + vinyltrimethoxysilane reaction also contains a minor peak on the higher molecular weight side product (retention time 7.15 minutes) that is probably octopus dimer that results from H/Vinyl exchange on silicon. A low molecular weight peak at

approximately 20.5 minutes is also seen and is most likely the other by-product of H/Vinyl exchange on silicon, $(MeO)_3SiCH_2CH_2Si(OMe)_3$.

These trimethoxysilyl functional octopus molecules could have several potential applications. In the area of adhesion, many adhesion promoters are trialkoxysilyl functional for reaction with the hydroxy functionality on metal and inorganic substrates that helps adhere the material of interest to the substrate. These molecules have a very high concentration of trimethoxysilyl functionality and could prove to be very effective adhesion promoters. Having each appendage terminated with three functional groups could also prove to be very useful as branch points for obtaining dendrimers as will be discussed in Chapter Six. Finally, most sol gel processing involves the hydrolysis and condensation of alkoxy silanes, typically tetraethoxysilane. These octopus molecules with 24 alkoxy groups per silsesquioxane could serve as highly functional precursor in sol gel processing or as crosslinking agents in alkoxy functional silicone rubbers and sealants.

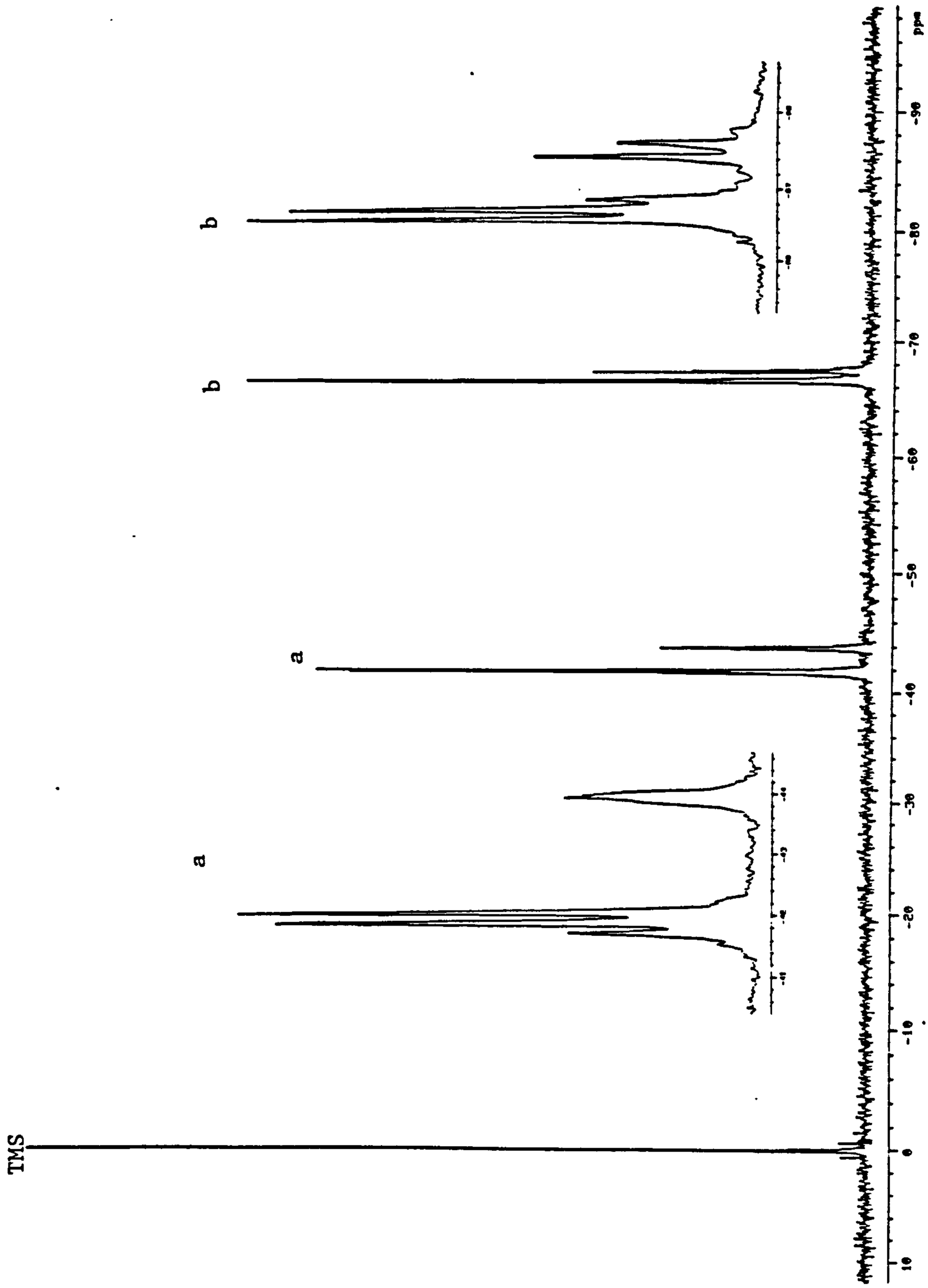

Figure 4.9 ^{29}Si NMR spectrum of the product of the reaction $T_8 + CH_2=CHSi(OMe)_3$.

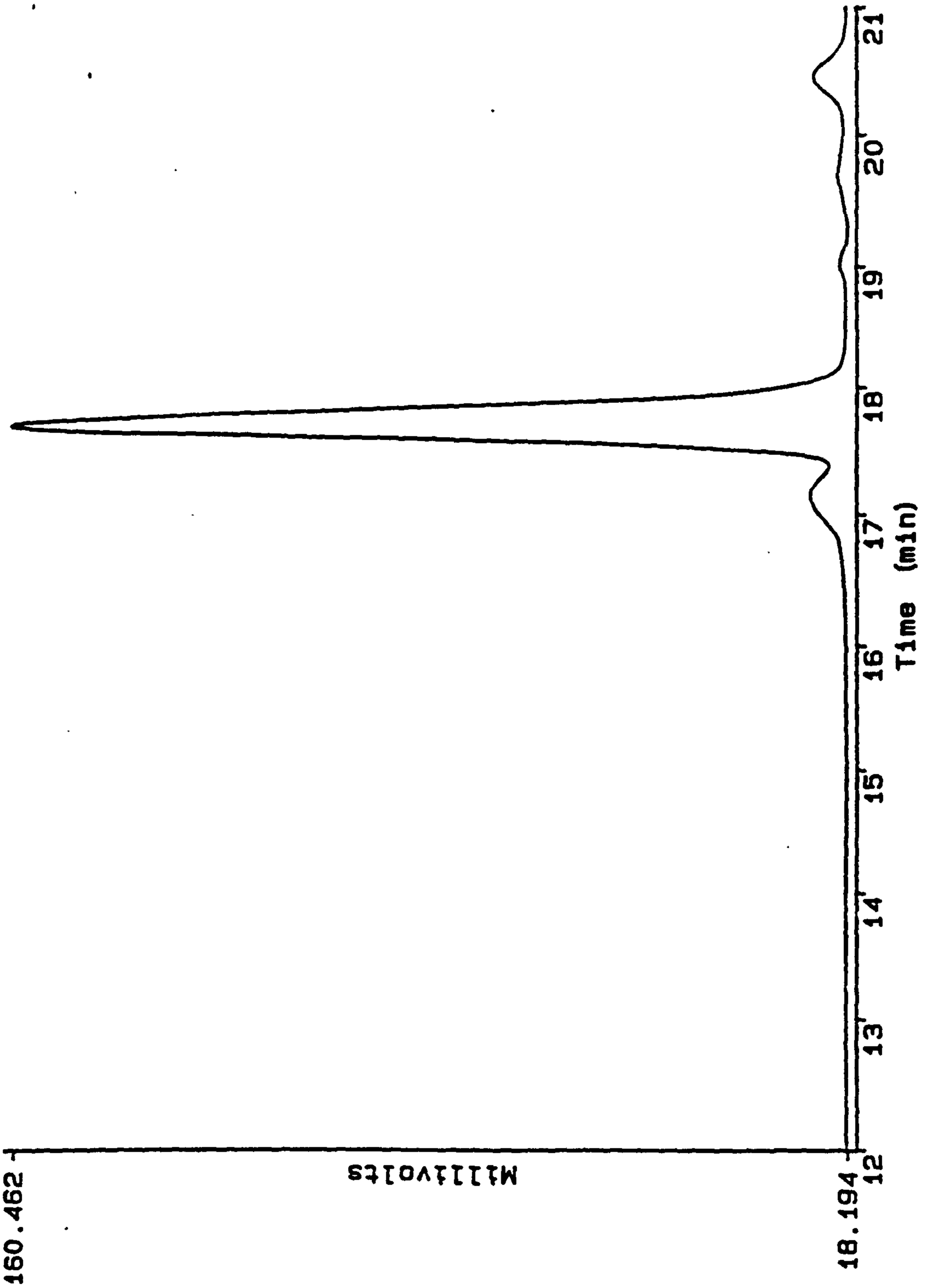

Figure 4.10 GPC chromatogram of the product of the reaction $T_8 + CH_2{=}CHSi(OMe)_3$.

4.1.6 Polyether and Mixed Polyether/Siloxane Functional Octopus Molecules

4.1.6.1 Synthesis and Characterization

A polyether functional octopus molecule was made via the hydrosilylation of allyl-functional polyethers by T_8 hydrogen silsesquioxane as shown in reaction scheme 4.7.

$$(HSiO_{3/2})_8 + 8\ CH_2{=}CHCH_2(OCH_2CH_2)_4OH \rightarrow [SiO_{3/2}]_8[(CH_2)_3(OCH_2CH_2)_4OH]_8 \quad (4.7)$$

In addition to the all polyether functional octopus molecule, molecules were made in which both polyether and siloxane chains were placed on the T_8 core. By varying the ratio of allyl-functional polyether to vinyl-functional siloxane starting materials, a number of mixed polyether/siloxane octopus systems were made as the general reaction scheme 4.8 shows. Materials were made in which, on average, x in reaction scheme 4.8 was 1, 2, 4, 6, and 8 (the all polyether functional molecule in scheme 4.7). It should be noted that in the discussion of these materials, each reaction product is actually a distribution of molecules in which on average the x in reaction scheme 4.8 is as indicated.

$$(HSiO_{3/2})_8 + x\ CH_2{=}CHCH_2(OCH_2CH_2)_4OH + (8\text{-}x)\ CH_2{=}CH[SiMe_2O]_3SiMe_2Bu \rightarrow [SiO_{3/2}]_8[(CH_2)_3(OCH_2CH_2)_4OH]_x[(CH_2)_2\{SiMe_2O\}_3SiMe_2Bu]_{8-x} \quad (4.8)$$

^{29}Si NMR analysis was done on each reaction mixture. Figures 4.11 through 4.15 show the T-Si region of each of the spectra. It would be impossible to make specific peak assignments due to the products being distributions of molecules and not pure species. In addition, as determined earlier, both α-addition and β-addition occur with the hydrosilylation of vinyl-siloxane by T_8 and therefore multiple peaks in the T-Si region would be expected. Also, since the placement of the differing chains on the core would vary (adjacent, at opposite corners, etc.) from molecule to molecule in the reaction mixtures, the spectra are further complicated. Despite these difficulties in interpreting the ^{29}Si NMR data, it is interesting to note the changes that occur in the T-Si region of the spectra with the change in the ratio of polyether/siloxane on the silsesquioxane cage.

Figure 4.11 is the ^{29}Si NMR spectrum for the reaction mixture in which on average there are 1 polyether and 7 siloxane chains on the silsesquioxane core. The spectrum shows a grouping of unresolved peaks between δ -65 and -67 ppm with the peaks between δ-65 and -66 ppm being much smaller than those between δ-66 and -67 ppm. At first glance, one might assign the smaller group of peaks to polyether chains on the core and the larger group to the siloxane chains. However, reexamining the ^{29}Si NMR for the all siloxane octopus (Figure 2.8) indicates that the T-Si peaks for the siloxane chains fall between δ -65.5 and -67.2 ppm so there appears to be some overlap of these peaks in the T-Si region from the siloxane appendages on the core with those peaks from the polyether appendages on the core. In addition, in examining the spectrum for the all

polyether octopus (Figure 4.15), it can be seen that there is a grouping of T-Si peaks between δ -64.4 and -66.5 ppm so there appears to be a definite overlap between the peaks for the silicons of the core attached to polyether chains and those attached to siloxane chains. Because of this overlap integration of the two groupings of peaks can not be used to quantitate the average number of polyether versus siloxane chains on the molecules. Despite this, there is still an interesting change in the grouping of peaks in the T-Si region.

Figure 4.12 is the ^{29}Si NMR spectrum for the reaction mixture in which on average there are 2 polyether and 6 siloxane chains on the silsesquioxane core. It is interesting to note that the grouping of unresolved peaks covers the same region of δ -65 to -67 ppm as the 1 polyether/7 siloxane octopus discussed above, but in this spectrum the peaks between δ-65 and -66 ppm, although still much smaller than those between δ-66 and -67 ppm, have increased in relative size.

The increase in the relative size of the peaks between δ-65 and -66 ppm seen in the spectrum for the reaction mixture in which on average there are 4 polyether and 4 siloxane chains on the silsesquioxane core (Figure 4.13) is further exaggerated as would be expected with the change in the mix of the two differing appendages.

The trend continues for the reaction mixture in which on average there are 6 polyether and 2 siloxane chains on the silsesquioxane

core as indicated by the ^{29}Si NMR spectrum shown in Figure 4.14.

The products of the above reactions were found to be water soluble to varying degrees and the aqueous solutions foamed somewhat upon shaking indicating possible surface activity. Siloxane containing surfactants are well known[1-21] and it was therefore of interest to test the surface activity of these molecules.

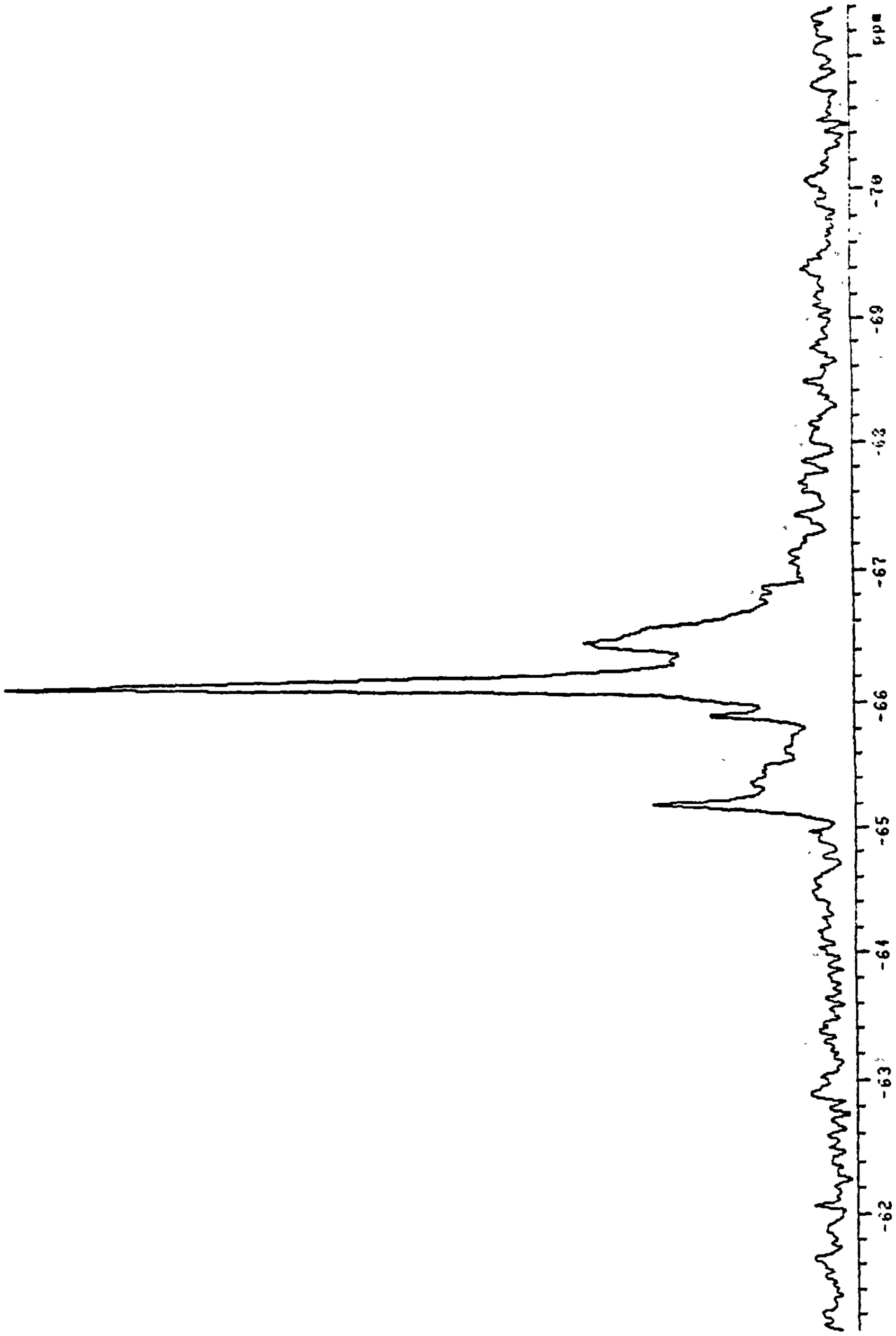

Figure 4.11 ^{29}Si NMR spectrum of the product of the reaction T_8 + x CH_2=$CHCH_2(OCH_2CH_2)_4OH$ + (8-x) CH_2=$CH[SiMe_2O]_3SiMe_2Bu$, where x=1.

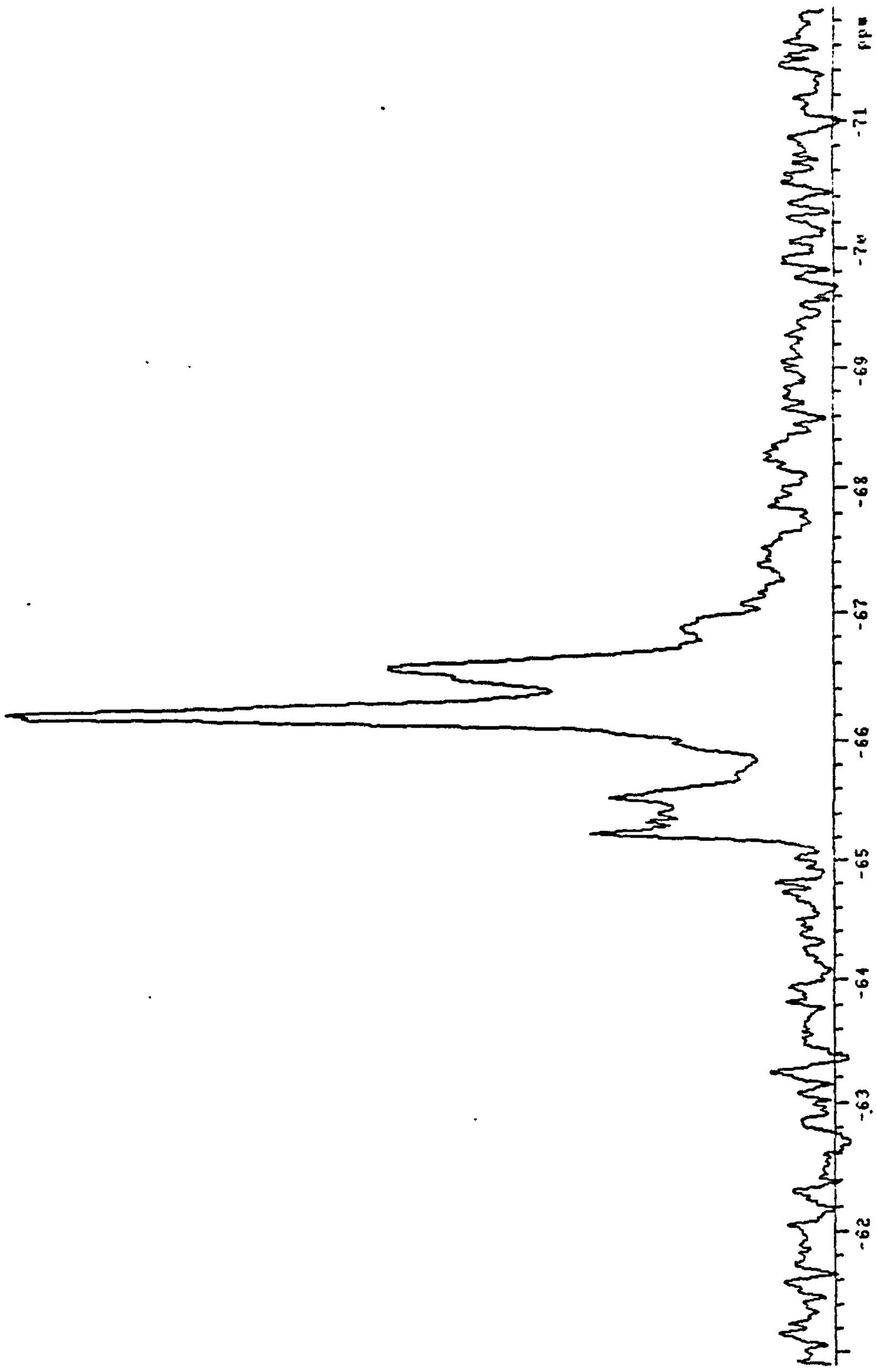

Figure 4.12 ^{29}Si NMR spectrum of the product of the reaction T_8 + x CH_2=$CHCH_2(OCH_2CH_2)_4OH$ + (8-x) CH_2=$CH[SiMe_2O]_3SiMe_2Bu$, where x=2.

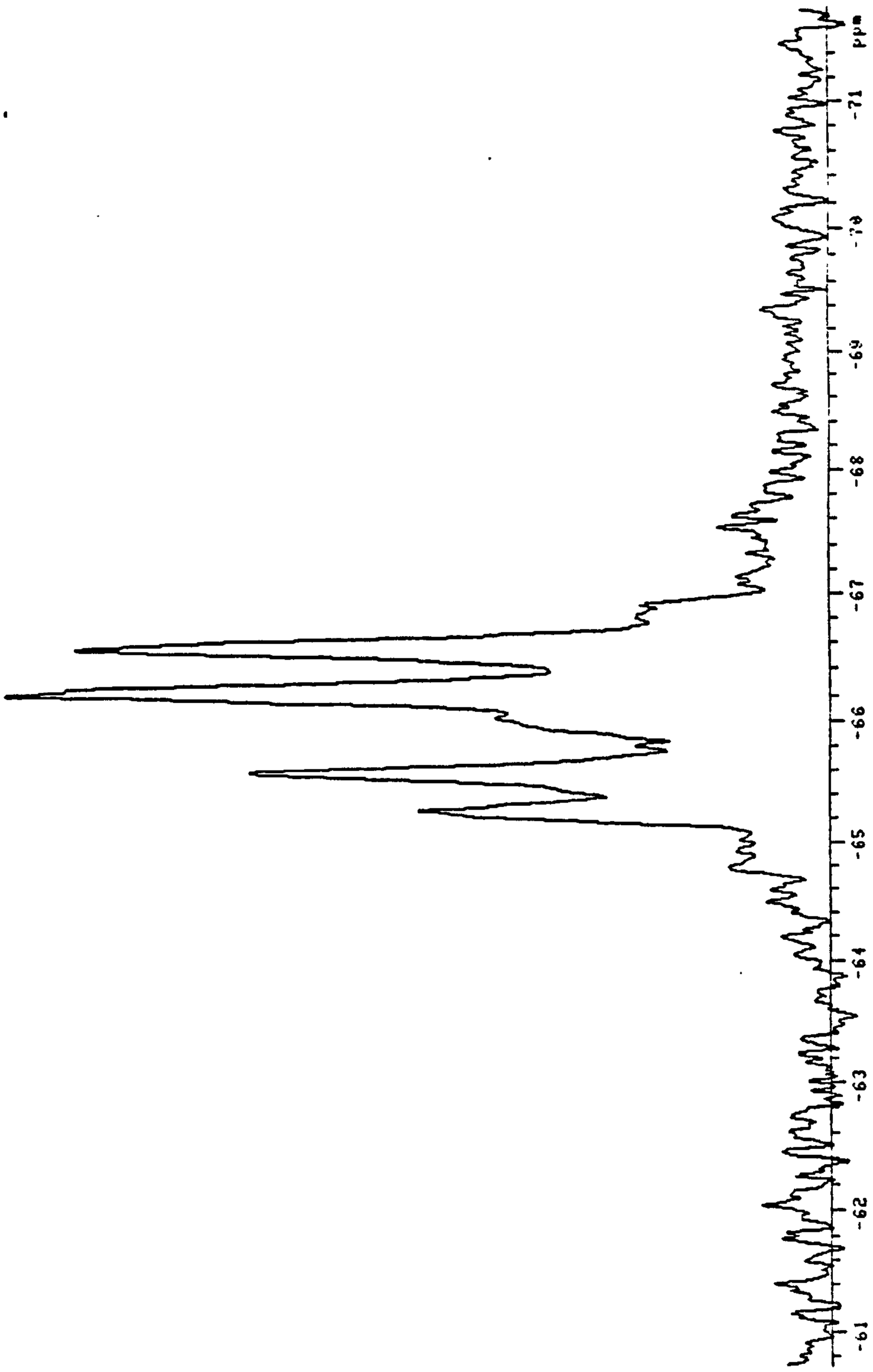

Figure 4.13 ^{29}Si NMR spectrum of the product of the reaction T_8 + x $CH_2=CHCH_2(OCH_2CH_2)_4OH$ + (8-x) $CH_2=CH[SiMe_2O]_3SiMe_2Bu$, where x=4.

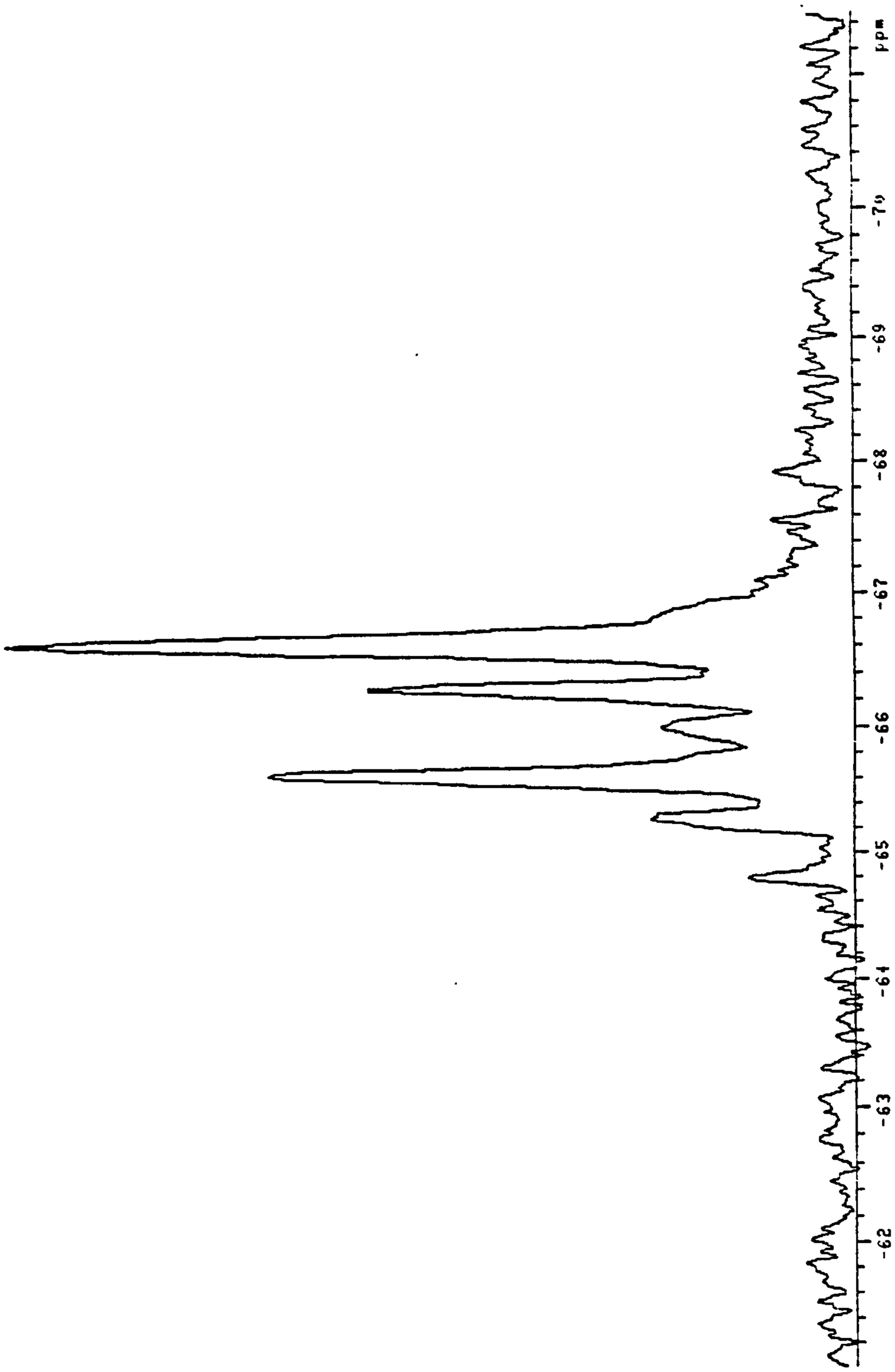

Figure 4.14 ^{29}Si NMR spectrum of the product of the reaction T_8 + x CH_2=$CHCH_2(OCH_2CH_2)_4OH$ + (8-x) CH_2=$CH[SiMe_2O]_3SiMe_2Bu$, where x=6.

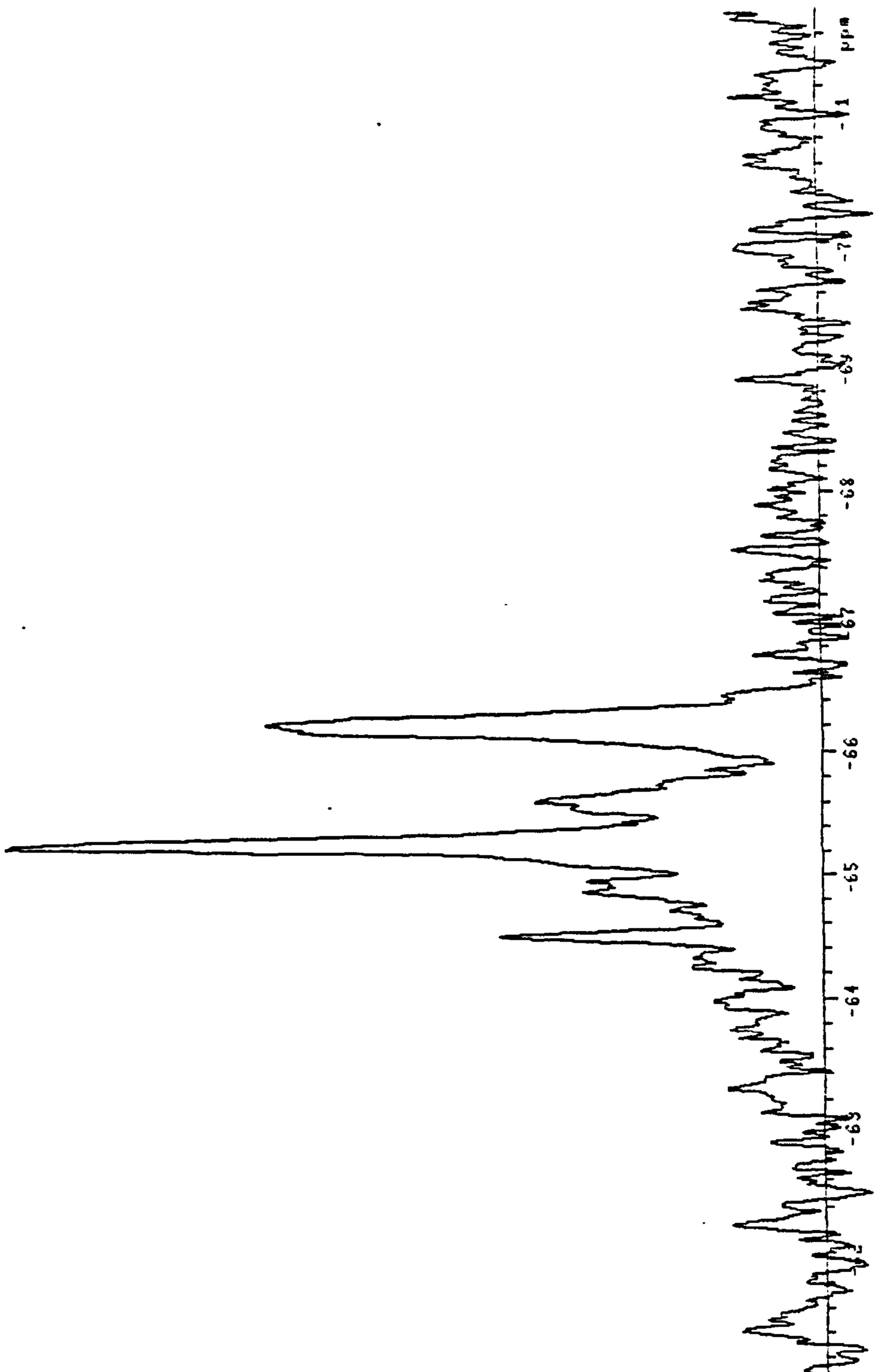

Figure 4.15 ^{29}Si NMR spectrum of the product of the reaction T_8 + x CH_2=$CHCH_2(OCH_2CH_2)_4OH$ + (8-x) CH_2=$CH[SiMe_2O]_3SiMe_2Bu$, where x=8.

4.1.6.2 Surface Activity Background

In the last twenty years, there has been a significant amount of research and development activity involving low molecular weight siloxane polyether copolymers. In an early paper by Kanner[3], the preparation, surface activity, and wetting properties of these materials were reported. They were prepared by the hydrosilylation of olefinic-terminated polyethers [polyoxyethylene(EO) and polyoxypropylene(PO)] by the appropriate Si-H functional siloxane compound. One of their outstanding features was their ability to reduce the surface tension of water down to the low value of 20-25 mN/m[3-10]. By comparison, typical organic surfactants reduce the surface tension of water down to 30-45 mN/m. Aqueous solutions of some of these materials demonstrated both rapid and extensive wetting of polyethylene.

These initial studies stimulated a number of application-oriented investigation[11]. These include their application in pharmaceutical and cosmetic formulations[12], particularly as emulsifiers[13], as foam control agents and lubricants, as ingredients in textile surface treatments for penetration and levelling agents in fibre finishing[14], as agents for coal and mineral dewetting, and as paint additives[15]. A significant amount of research has been carried out investigating their activity as adjuvants (additives that improve performance) for sprayed-on herbicides and fungicides. This topic has been comprehensively reviewed[16-18] and commercial products, such as Dow Corning's Sylgard® 309 and Union Carbide's Silwet® L-77

are available. Both of these products have the structure $(Me_3SiO)_2Si(Me)(R)$, where R is a polyoxyethylene (EO) moiety.

The successes at finding technological applications for these materials has spawned a number of recent fundamental studies. The phenomena of rapid and extensive wetting of low energy surfaces ("superwetting") by aqueous solutions of these materials has been investigated by Ananthapadmanabhan[4], Zhu[19], Tiberg[20], Hill[21], and He[22]. This phenomenon has been linked to the presence of specific surfactant aggregates in solution, and the structures of these aggregates have been extensively studied recently[19-23].

In this work, the interest was in preparing octopus silicon and polyether containing macromonomers with a configuration never before considered. An octopus with a silsesquioxane core and polyether appendages could be viewed as a 'permanent' micelle of sorts with the hydrophilic groups permanently radiating from a $(SiO_{3/2})_8$ spherical core. Mathias and Carothers mention very briefly a hyperbranched poly(siloxysilane) dendrimer with terminal SiH functional branches end-capped via a reaction of the SiH with an allyl-terminated oligomer of oxyethylene to give a material with a hydrophobic core and hydrophilic exterior. They did not test properties of such a material though.

To demonstrate the above concept of a 'permanent' micelle structure and to test the properties of such a molecule, the allyl functional polyether $[CH_2{=}CHCH_2(OCH_2CH_2)_4OH]$ was hydrosilylated by T_8 to form a polyether functional octopus

molecule with a silsesquioxane core. The reaction product was found to be water soluble, unlike any of the previously made octopus molecules. An aqueous solution of product also appeared to foam when shaken and therefore was suspected to be surface active. The surface tensions of aqueous solutions of varying concentration were then obtained by the du Noüy ring method using a Krüss surface tensiometer as illustrated in Figure 4.16. In this technique, the force necessary to withdraw a fine wire ring from the aqueous surfactant solution is measured. Typically measurements of surface tension are taken at several concentrations of the surfactant in water. A plot is then made of surface tension versus log[surfactant molar concentration] from which various quantifications of surface activity of the surfactant can be derived. These plots are often referred to as Gibbs plots due to the derivation of quantities from these plots originating from the Gibbs equation as will become apparent in the discussion.

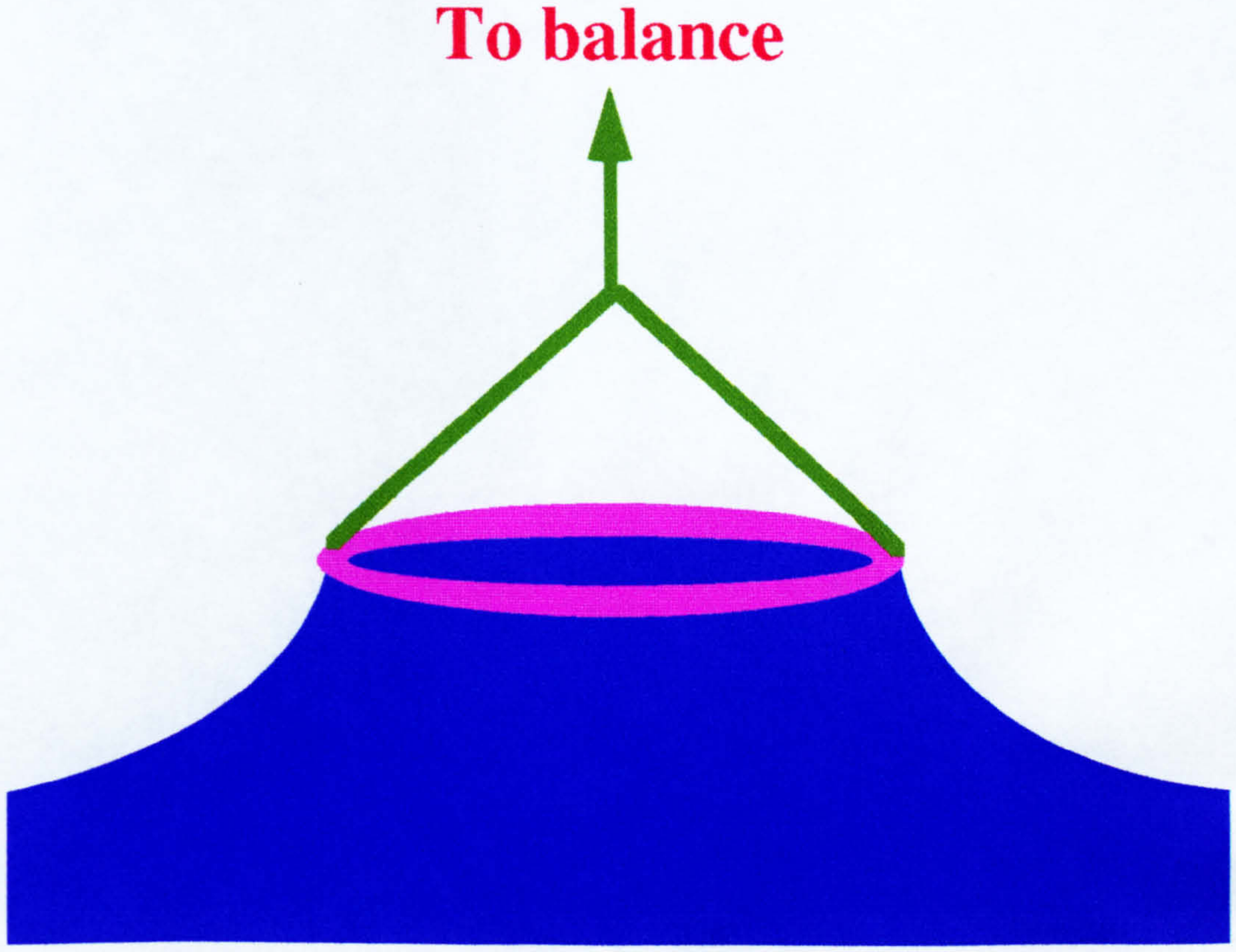

Figure 4.16 Schematic of surface tension measurement technique.

Before discussing the data obtained from these plots, it is useful to go through a description of the phenomena underlying the various regions of the Gibbs plots and the assumptions used to obtain information from these plots.

A schematic of the bulk and surface behaviour of a 'typical' or linear surfactant in aqueous solution is shown in Figure 4.17. This schematic depicts a physical model of the surfactant aggregation, both at the air/water surface and in bulk solution. The soluble surfactant monomer is in equilibrium with both states of aggregation. Aggregation at the surface is commonly referred to as adsorption. The molecular structure of the surfactant, consisting of a hydrophobic portion (hydrocarbon or silicone) and a hydrophilic portion (such as polyethylene oxide), favours these aggregation processes. However, the octopus configuration with a silsesquioxane core with hydrophobic -$CH_2CH_2CH_2$- linkages to the hydrophilic polyether appendages may adsorb very differently at the surface and aggregate differently in the bulk.

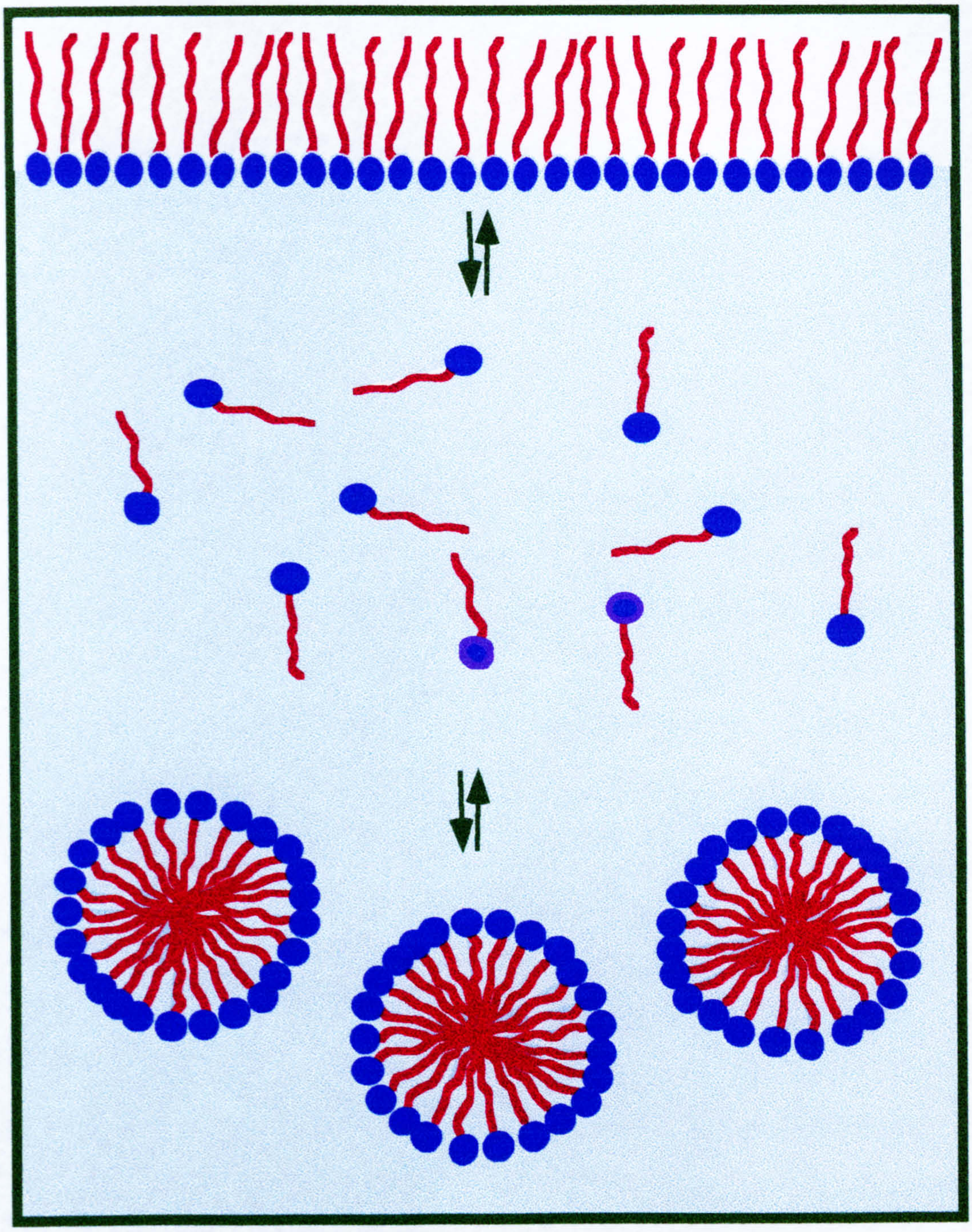

Figure 4.17 A schematic of the bulk and surface behaviour of a 'typical' or linear surfactant in aqueous solution.

An "idealized" plot of surface tension versus surfactant concentration is shown in Figure 4.18 along with the behaviour of the surfactant proposed to occur in each of the regions of the plot (regions A through F). Using log [surfactant] as the scale for the X-axis conveniently gives a linear relationship between points B and C. The following description of the phenomena occurring in each region of these types of plots is based on information in a number of sources[24-27].

Point A is the surface tension of water, uncontaminated by surfactant, approximately 72 mN/m. Addition of surfactant causes some proportion of the surfactant molecules to adsorb at the air/water surface. Once the surfactant molecule adsorbs at the surface it orients itself relative to the air/water surface. The hydrophobic group is on the "air" side and the hydrophilic group is on the "water" side. More subtly, either the hydrophobic or hydrophilic group might be perpendicular (normal) to the surface, or tilted, with the extreme being parallel to the surface. The number of surfactant molecules at the surface and their individual orientations affect the surface area per molecule. The more molecules at the surface, the smaller the area/molecule. The surface area/molecule also decreases as the orientation tends to more perpendicular to the surface.

Between A and B the concentration of surface adsorbed surfactant is constantly increasing. At point B, the change in slope (more rapid decrease in surface tension with increasing surfactant concentration) indicates that the molecules at the surface can now interact with each other and aggregate to form a

monolayer of surfactant at the air/water surface. The surface beyond point B is almost saturated with surfactant molecules. Beyond point B and up to point C, a small number of molecules can penetrate the surface layer, possibly changing the orientation or packing of the surface absorbed molecules. Through this region, the concentration of surfactant in bulk solution increases.

Point D, extrapolated as the intersection of the linear B-C region and the plateau region E-F, corresponds to the minimum bulk surfactant concentration where bulk aggregation phenomena, such as micellization, occurs. Often, it is reported as the critical micelle concentration (CMC). In these studies, it will be referred to as the critical aggregation concentration (CAC), since the structure of aggregates that occurs is uncertain.

Beyond point E (region E-F), the surface tension does not vary significantly with increasing surfactant concentration. The surface is saturated with surfactant and the excess surfactant forms aggregates, whose amount and shape changes as the surfactant concentration increases. With linear siloxane surfactants there is often a progression from micelles (liquid phase) to liquid crystalline, to solid phases[28].

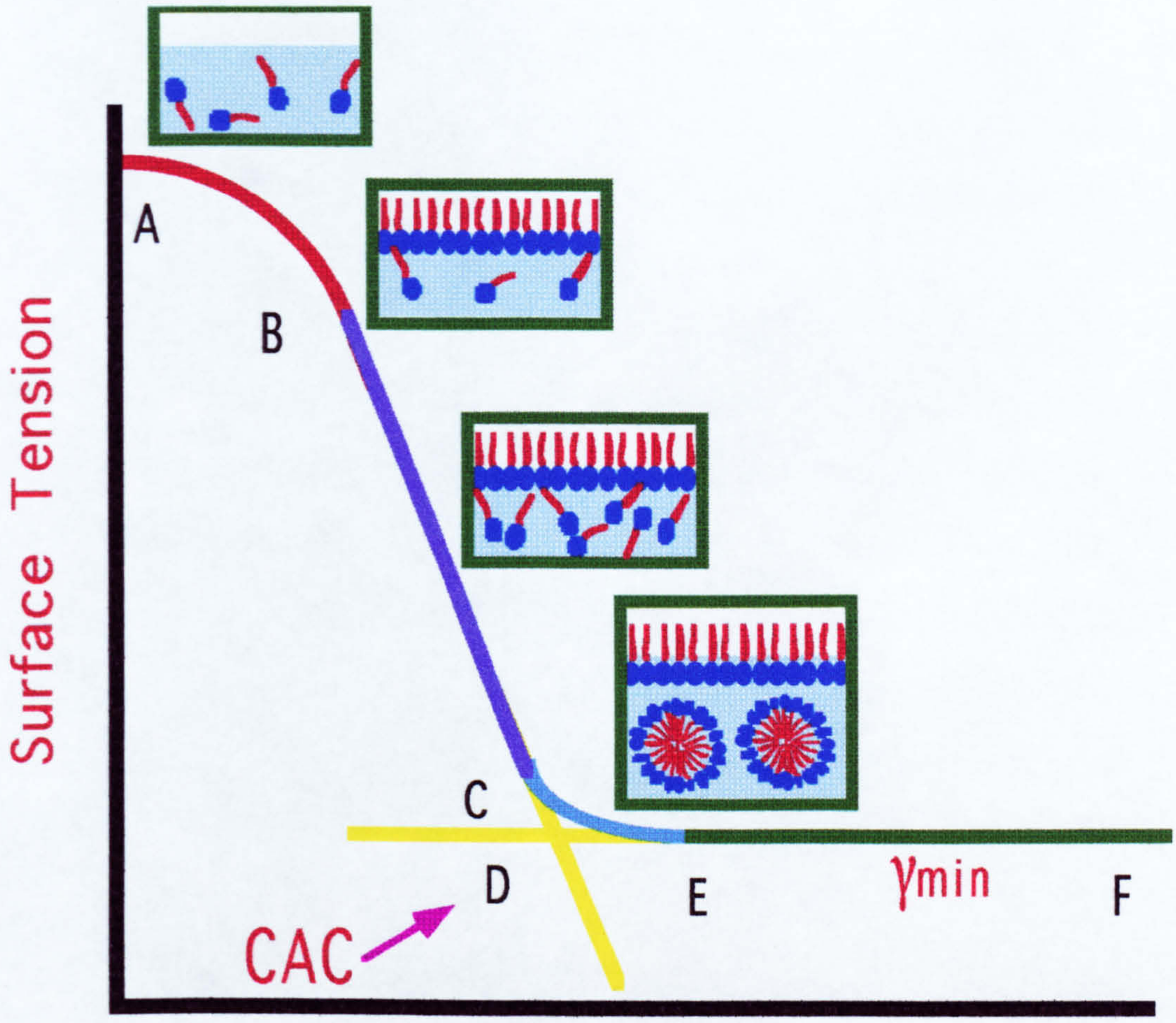

Figure 4.18 An "idealized" plot of surface tension versus surfactant concentration showing the proposed behaviour of a linear surfactant in each region.

It is apparent how the CAC and minimum surface tensions are obtainable directly from the plot of surface tension versus log surfactant concentration. However, as mentioned earlier, the area/molecule at the surface cannot be directly evaluated by inspection of the plot. In order to calculate this quantity, fundamental thermodynamic principles must be applied to quantify and understand the relationship between surfactant concentration and surface tension[29-30] as described below.

From thermodynamic principles, the relationship between surfactant concentration and solution surface tension is expressed by the Gibbs equation, first introduced in 1928, in its most general form, as shown in Equation 1. This equation is fundamental to adsorption processes, and states that a change in total surface free energy ($d\gamma$) is equal to the sum of the concentration of surface-adsorbed molecules (Γ) multiplied by their individual changes in chemical potential (μ).

$$d\gamma = -\Sigma_i \Gamma_i d\mu_i \qquad (1)$$

Equation 2 expresses the the Gibbs equation for a two component system, specifically a solvent and solute.

For a 2 component system (1= solvent, 2= solute),

$$d\gamma = -\Gamma_1 d\mu_1 - \Gamma_2 d\mu_2 \qquad (2)$$

From equation 2, one might think that the adsorption of each component could be determined from variation of surface tension

with composition, i.e., $\Gamma_1 = -(d\gamma/ d\mu_1)$ holding Γ_2 and μ_2 constant. However, this is not possible because μ_1 and μ_2 cannot be varied independently. To deal with this problem, Gibbs introduced the idea of relative adsorptions. By making adsorption of all components at the surface relative to that of component 1, Γ_1 can be set to zero, and equation 2 can be simplified as shown in equation 3, where the term $\Gamma_{2,1}$ refers to Gibbs relative adsorption isotherm (adsorption of component 2 relative to component 1, sometimes shown as just Γ_2).

$$d\gamma = -\Gamma_{2,1}d\mu_2 \qquad (3)$$

For a dilute (ideal) solution, chemical potential is defined as shown in equation 4, where μ_2^o is chemical potential in reference state (constant) and c_2 is the molar concentration of solute[31].

$$\mu_2 = \mu_2^o + RTlnc_2 \qquad (4)$$

And so, $$d\mu_2 = RTdlnc_2 \qquad (5)$$

Making this substitution in equation 3, leads to equation 6.

$$d\gamma = -RT\Gamma_{2,1}dlnc_2 \qquad (6)$$

This is the typical form of the Gibbs equation applied to dilute solutions of non-ionic surfactants. Equation 7 and 8 are simply the result of converting natural to base-10 logarithms and rearranging.

$$d\gamma = -2.303RT\Gamma_{2,1}d\log c_2 \qquad (7)$$

$$d\gamma/d\log c_2 = -2.303RT\Gamma_{2,1} \qquad (8)$$

Further rearranging of Equation 8 yields Equation 9. Equation 9 contains the slope of the linear portion of the surface tension versus log [surfactant] plot, $d\gamma/d\log c_2$, and is a particularly useful form of the Gibbs equation. The surface excess concentration can be directly calculated from analysis of the linear portion of the plot in Figure 4.18, as it is constant in this range. From Equation 9, the surface area/molecule can be directly calculated using Avogadro's number (N) (Equation 10). Thus, a method to calculate the sought-after quantity, the area per molecule (A) is available.

$$\Gamma_{2,1} = (d\gamma/d\log c_2)/-2.303RT \qquad (9)$$

$$\Gamma_{2,1} = \frac{(\text{slope in mNewtons/metre})\ (\text{m}/100\ \text{cm})^2}{-2.303(8.314\ \text{Newton}\cdot\text{metre/K}\cdot\text{mole})(^\circ\ \text{K})}$$

units: $\Gamma_{2,1} = \text{mol/cm}^2$

$$\text{Area/molecule} = 1/N(\Gamma_{2,1}) \qquad (10)$$

$$\text{Area/molecule} = [\text{cm}^2(10^8\text{Å/cm})^2]/(\text{mol})(6.023\text{x}10^{23}\text{molecules/mol})$$

units: $\text{Area/molecule} = \text{Å}^2$

The Gibbs adsorption equation has been tested using several experimental methods. One method reported some time ago (1940) by McBain[31] involved calculation of $\Gamma_{2,1}$ from samples of the air/water surface obtained using a microtome to slice off the top layer of a solution. Good agreement between adsorptions calculated from analysis and those obtained using the Gibbs equation were found. Several other techniques have been used to measure directly the surface excess concentration of a number of surfactants, and reasonable agreement with the Gibbs equation has been obtained in many cases as well[32]. The most common experimental method used is the detection of radio-labelled compounds[33-34].

It would appear then that a reasonable estimate of the surface excess concentration (Γ) can be made by applying the Gibbs equation to plots of surface tension versus log of molar concentration of solute. From this value, an area/molecule at the surface can be directly calculated, and the effect of composition of the octopus (varying functional groups off the core) on area/molecule can be assessed to obtain Γ and area/molecule (A).

4.1.6.3 Surface Tension Measurements

Surface tension as a function of concentration in aqueous solution were measured on the polyether functional octopus molecule as well as the mixed polyether/siloxane octopus molecules.

Figures 4.19 through 4.23 show the plots of surface tension versus log concentration of each of the polyether/siloxane functional octopus molecules with the data used to obtain each plot given below each figure. A best fit line has been drawn in the linear portion of the plot and another line in the plateau region (from which the minimum surface tension value was determined). A third line has been drawn from the intersection point of the first two lines and the x-axis to obtain the log CAC value.

From the plots of surface tension versus molar concentrations of the various octopus molecules, the area per molecule (A) and the adsorption (Γ) were calculated using the slope of the linear portion of the plot ($d\gamma/d\log c_2$) as previously described. The log CAC and minimum surface tension (γ_{min}) were obtained directly from inspection of the plots. These values are given in Table 4.8.

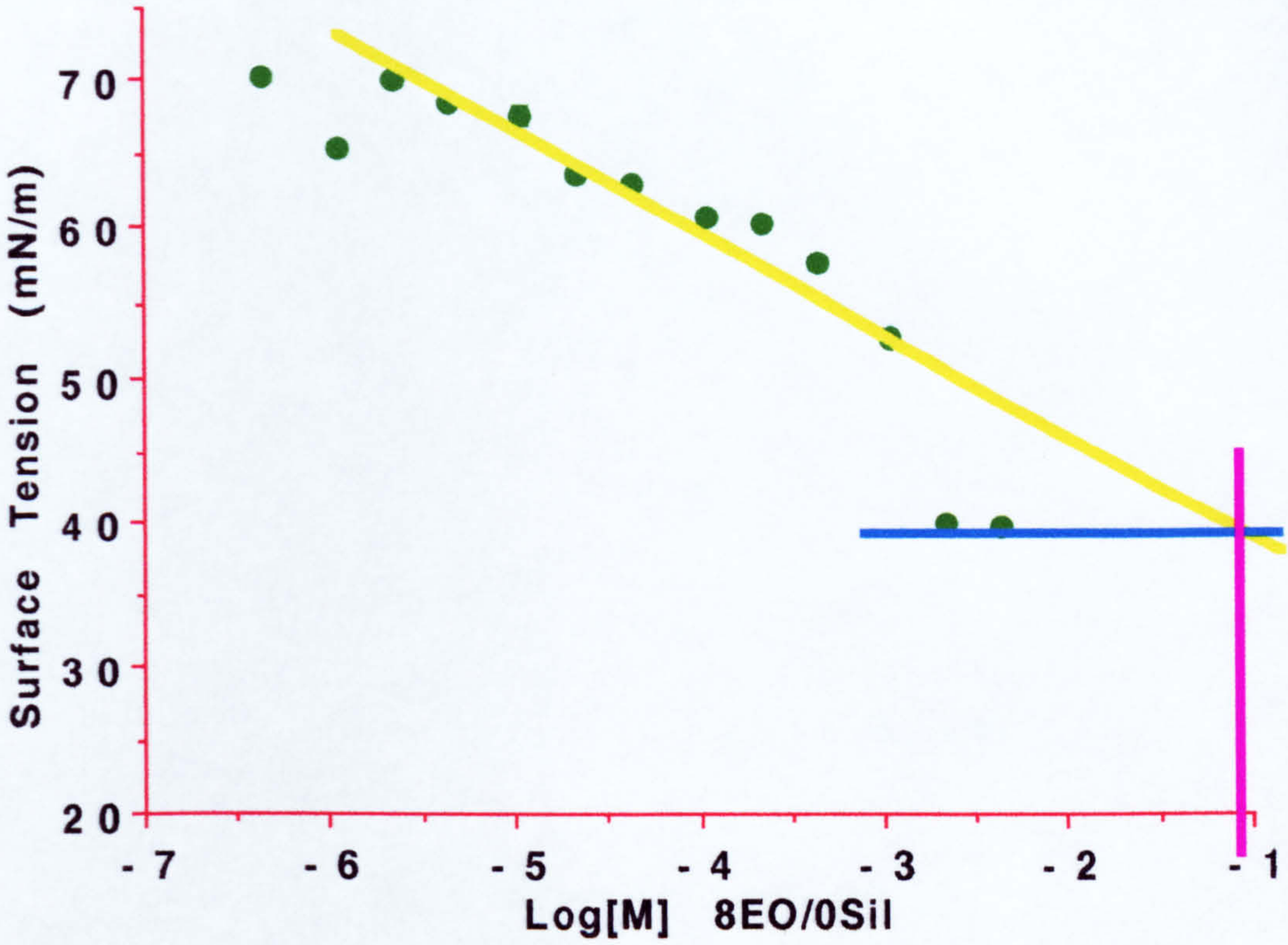

Figure 4.19 Plot of the surface tension of aqueous solutions of an octopus with polyether/siloxane ratio of 8/0 as a function of concentration.

Table 4.3
Surface tension data for octopus with polyether/siloxane ratio of 8/0

Log Concentration (Molar)	Surface Tension (mN/m) (Av. of 3 values)	Standard Deviation
-2.36	39.9	0.2
-2.66	40.0	0.1
-2.96	52.8	0.3
-3.36	57.7	0.3
-3.66	60.2	0.3
-3.96	60.8	0.1
-4.36	62.9	0.1
-4.66	63.7	0.2
-4.96	67.7	0.7
-5.36	68.6	0.5
-5.66	70.2	0.2
-5.96	65.4	0.2
-6.36	70.4	0.5

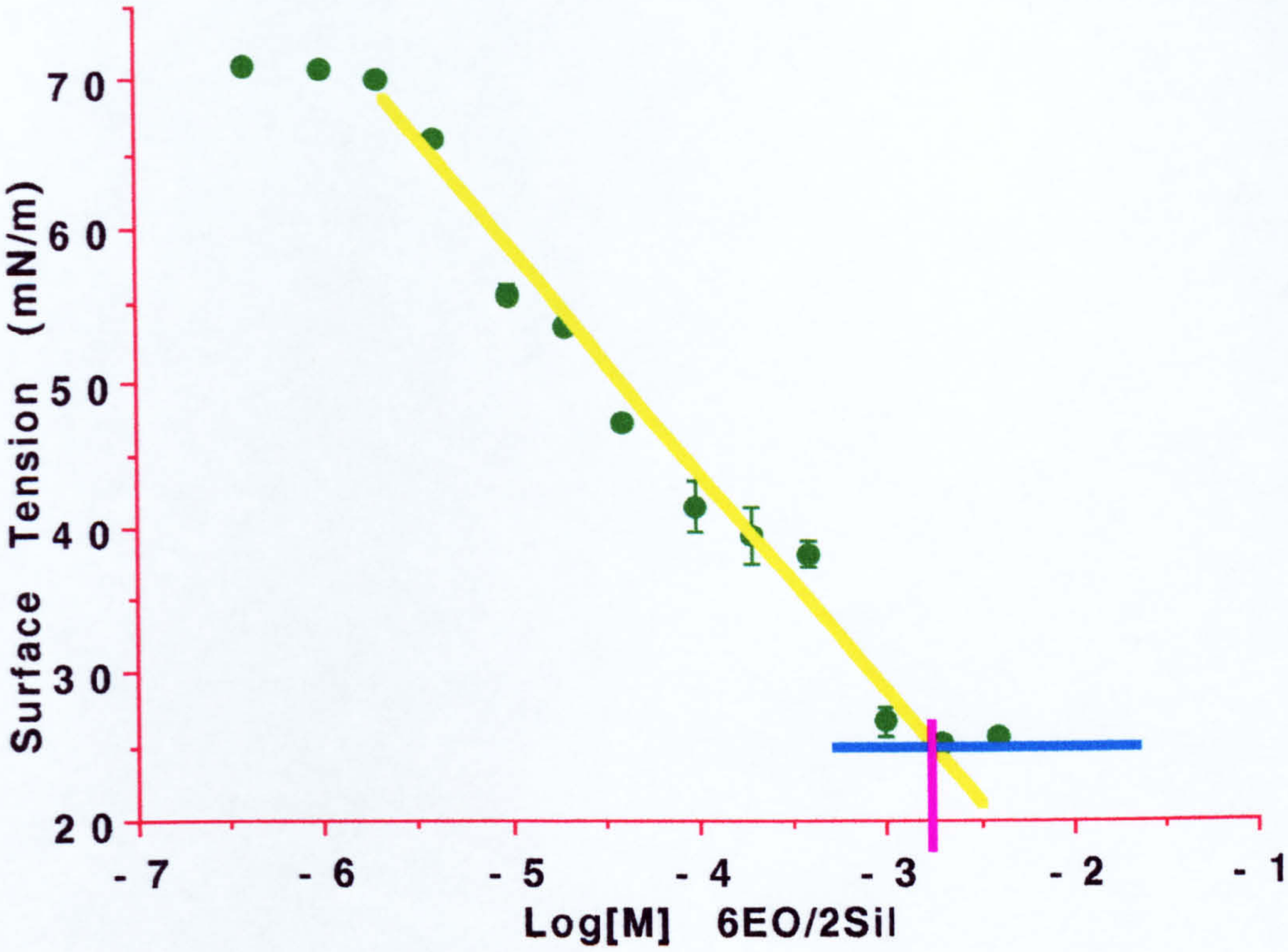

Figure 4.20 Plot of the surface tension of aqueous solutions of an octopus with polyether/siloxane ratio of 6/2 as a function of concentration.

Table 4.4
Surface tension data for octopus with polyether/siloxane ratio of 6/2

Log Concentration (Molar)	Surface Tension (mN/m) (Av. of 3 values)	Standard Deviation
-2.41	25.7	0.3
-2.71	25.1	0.2
-3.01	26.6	0.9
-3.41	38.1	0.9
-3.71	39.5	2.0
-4.01	41.4	1.8
-4.41	47.3	0.5
-4.71	53.6	0.4
-5.01	55.6	0.5
-5.41	66.0	0.3
-5.71	70.1	0.2
-6.01	70.7	0.2
-6.41	71.9	0.1

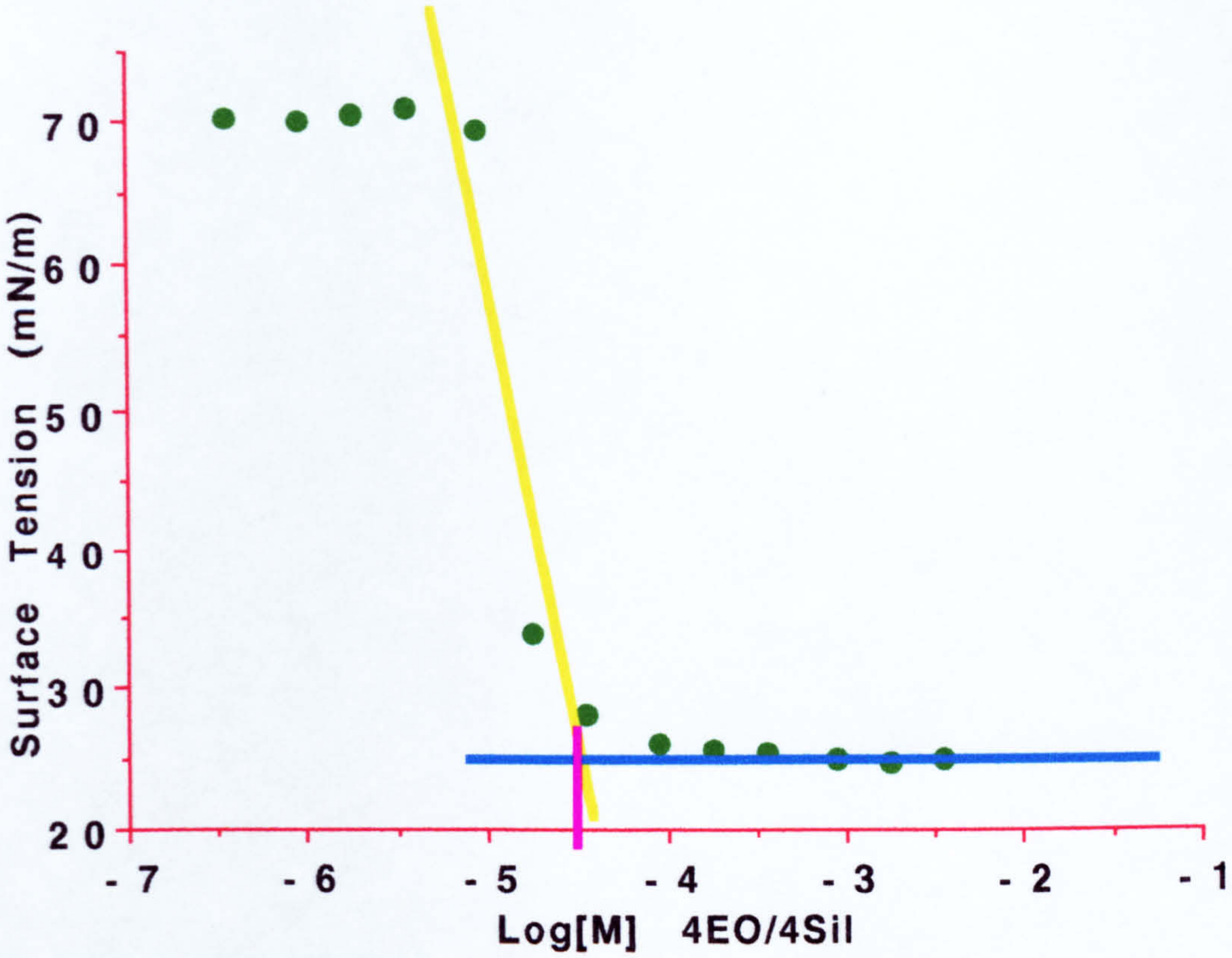

Figure 4.21 Plot of the surface tension of aqueous solutions of an octopus with polyether/siloxane ratio of 4/4 as a function of concentration.

Table 4.5
Surface tension data for octopus with polyether/siloxane ratio of 4/4

Log Concentration (Molar)	Surface Tension (mN/m) (Av. of 3 values)	Standard Deviation
-2.45	25.0	0.1
-2.75	24.8	0.1
-3.05	25.0	0.1
-3.45	25.4	0.3
-3.75	25.7	0.1
-4.05	26.1	0.2
-4.45	28.1	0.5
-4.75	33.8	0.8
-5.05	69.4	0.6
-5.45	70.9	0.1
-5.75	70.6	0.4
-6.05	70.1	0.2
-6.45	70.2	0.2

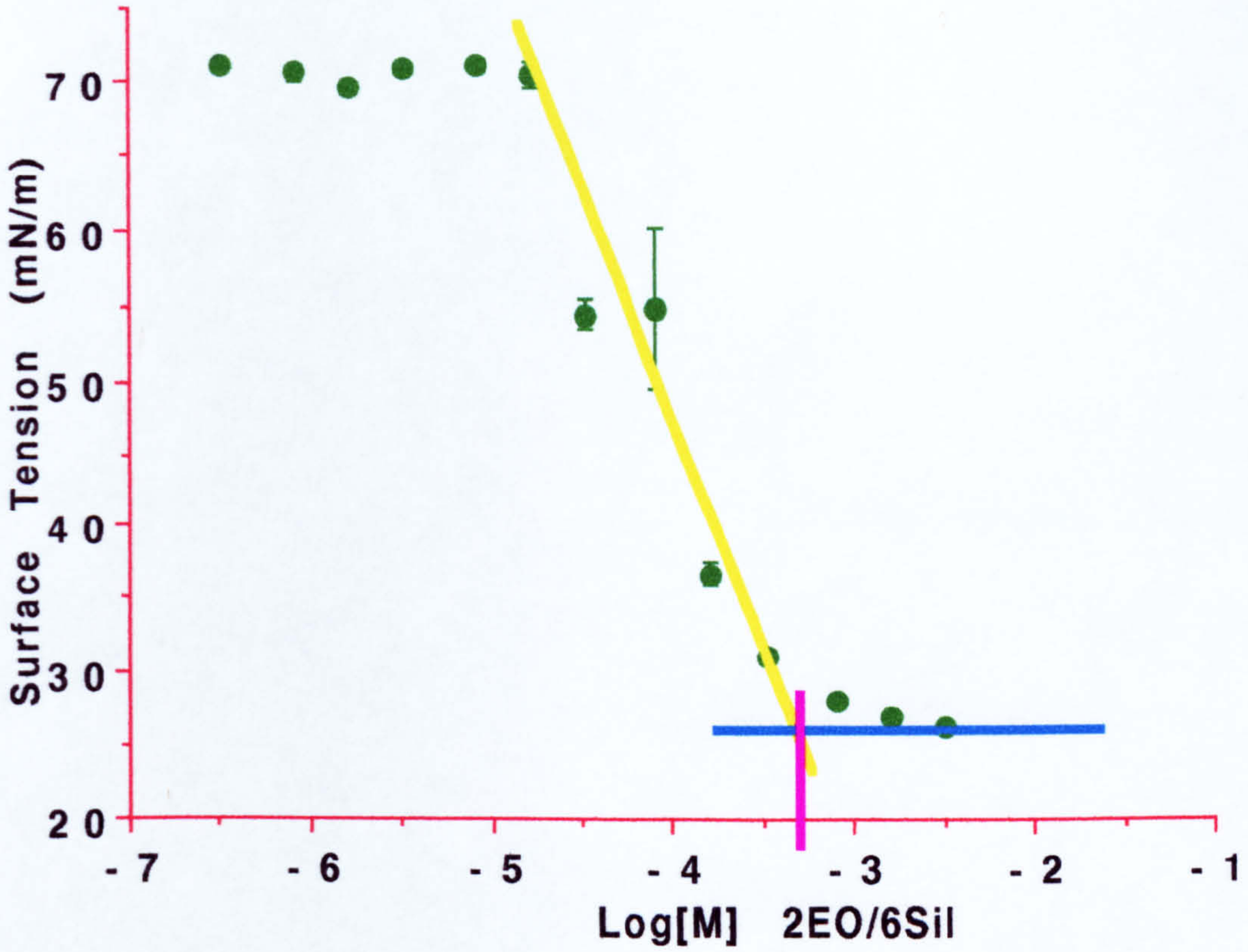

Figure 4.22 Plot of the surface tension of aqueous solutions of an octopus with polyether/siloxane ratio of 2/6 as a function of concentration.

Table 4.6
Surface tension data for octopus with polyether/siloxane ratio of 2/6

Log Concentration (Molar)	Surface Tension (mN/m) (Av. of 3 values)	Standard Deviation
-2.49	26.3	0.2
-2.79	26.9	0.1
-3.09	27.9	0.2
-3.49	30.9	0.2
-3.79	36.7	0.7
-4.09	54.8	5.3
-4.49	54.4	0.9
-4.79	70.5	0.9
-5.09	71.1	0.2
-5.49	70.9	0.1
-5.79	69.7	0.4
-6.09	70.6	0.5
-6.49	71.1	0.2

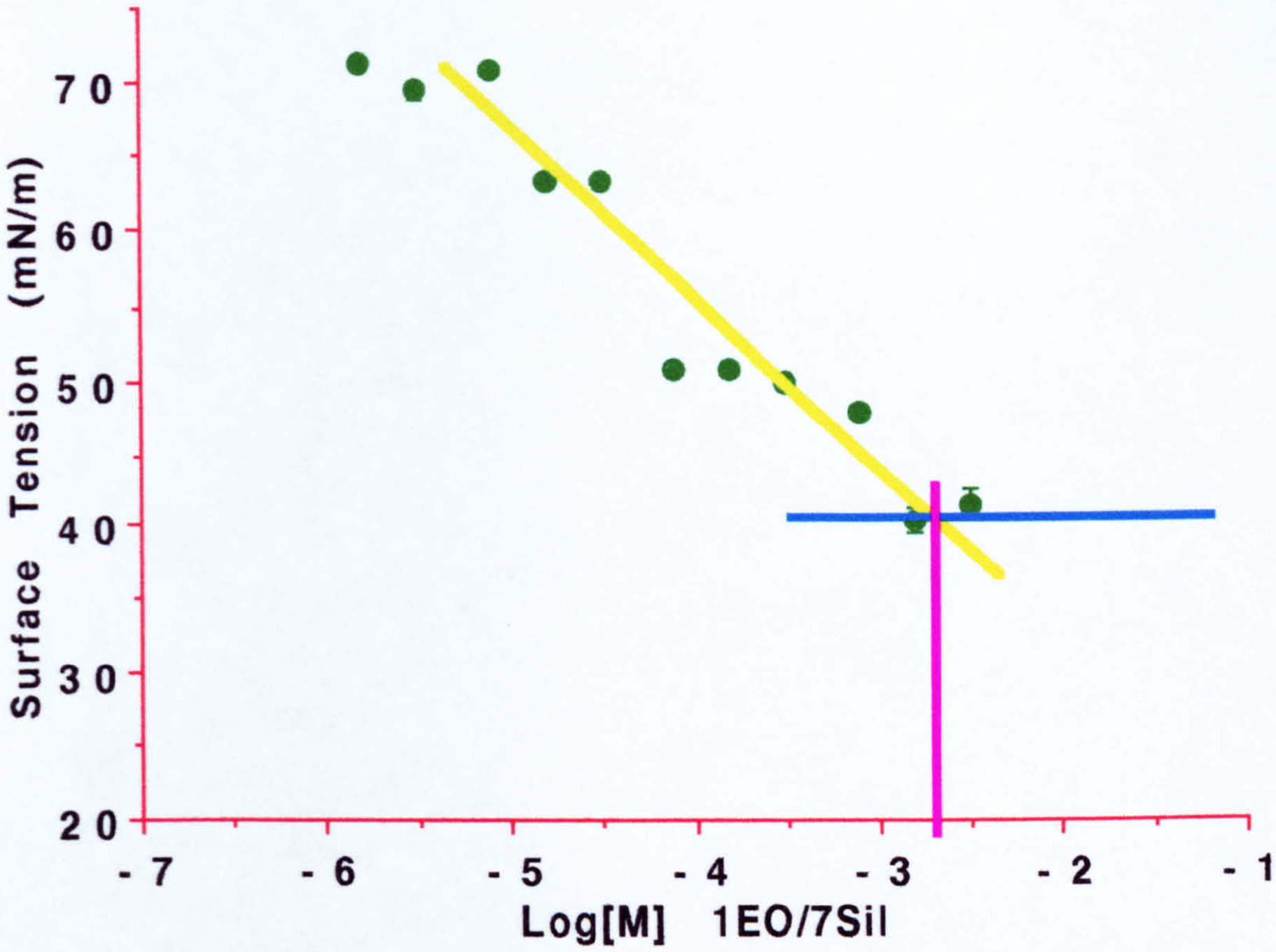

Figure 4.23 Plot of the surface tension of aqueous solutions of an octopus with polyether/siloxane ratio of 1/7 as a function of concentration.

Table 4.7
Surface tension data for octopus with polyether/siloxane ratio of 1/7

Log Concentration (Molar)	Surface Tension (mN/m) (Av. of 3 values)	Standard Deviation
-2.51	41.7	1.0
-2.81	40.6	0.9
-3.11	48.0	0.3
-3.51	50.1	0.5
-3.81	51.0	0.1
-4.11	50.9	0.3
-4.51	63.3	0.3
-4.81	63.2	0.3
-5.11	70.9	0.2
-5.51	69.4	0.6
-5.81	71.2	0.3

Table 4.8

γ_{min}, CAC, A, and Γ for polyether/siloxane octopus molecules

Octopus Comp. (EO_4)/Siloxane	γ_{min} (mN/m)	Log CAC	Γ (moles/cm^2 x 10^{-10})	Area/Molec. (Å^2)
8/0	40.2	-1.1	1.0	159
6/2	26.0	-2.8	2.6	63
4/4	25.8	-4.5	8.5	19
2/6	26.8	-3.3	5.1	33
1/7	41.0	-2.7	1.8	90.4

Examination of the plots in Figures 4.19 through 4.23 and the data obtained from them in Table 4.8 indicates some interesting trends in the various measures of surface activity with changing octopus composition.

Although the effect of all-polyether functional octopus is not as dramatic as some of the other molecules, it does reduce the solution surface tension somewhat as compared to the surface tension of distilled water, ~72 mN/m. Some of the mixed polyether/siloxane functional octopus molecules reduce the

solution surface tension quite significantly. The large reduction in the solution surface tension caused by the presence of some of these molecules at low concentrations indicates that these molecules adsorb strongly at the air/water interface.

The values for minimum surface tension (γ_{min}) range from 41.0 down to 25.8 mN/m. A plot of minimum surface tension versus the composition of the chains on the core of the octopus molecules (number of EO chains) as shown in Figure 4.24 indicates that the lowest γ_{min} was obtained when there were 4 polyether and 4 siloxane chains on the silsesquioxane core with the values for the octopus molecules with 2 and 6 polyether chains (6 and 2 siloxane chains respectively) are also very low. The γ_{min} values for the octopus molecules with 2, 4, and 6 polyether chains are significantly lower than those reported for organic ethoxylates[33, 35-40]. These three octopus molecules have γ_{min} values comparable to low molecular weight silicone surfactants, for instance those containing a polyether segment off of a trisiloxane backbone[3-23, 41-44].

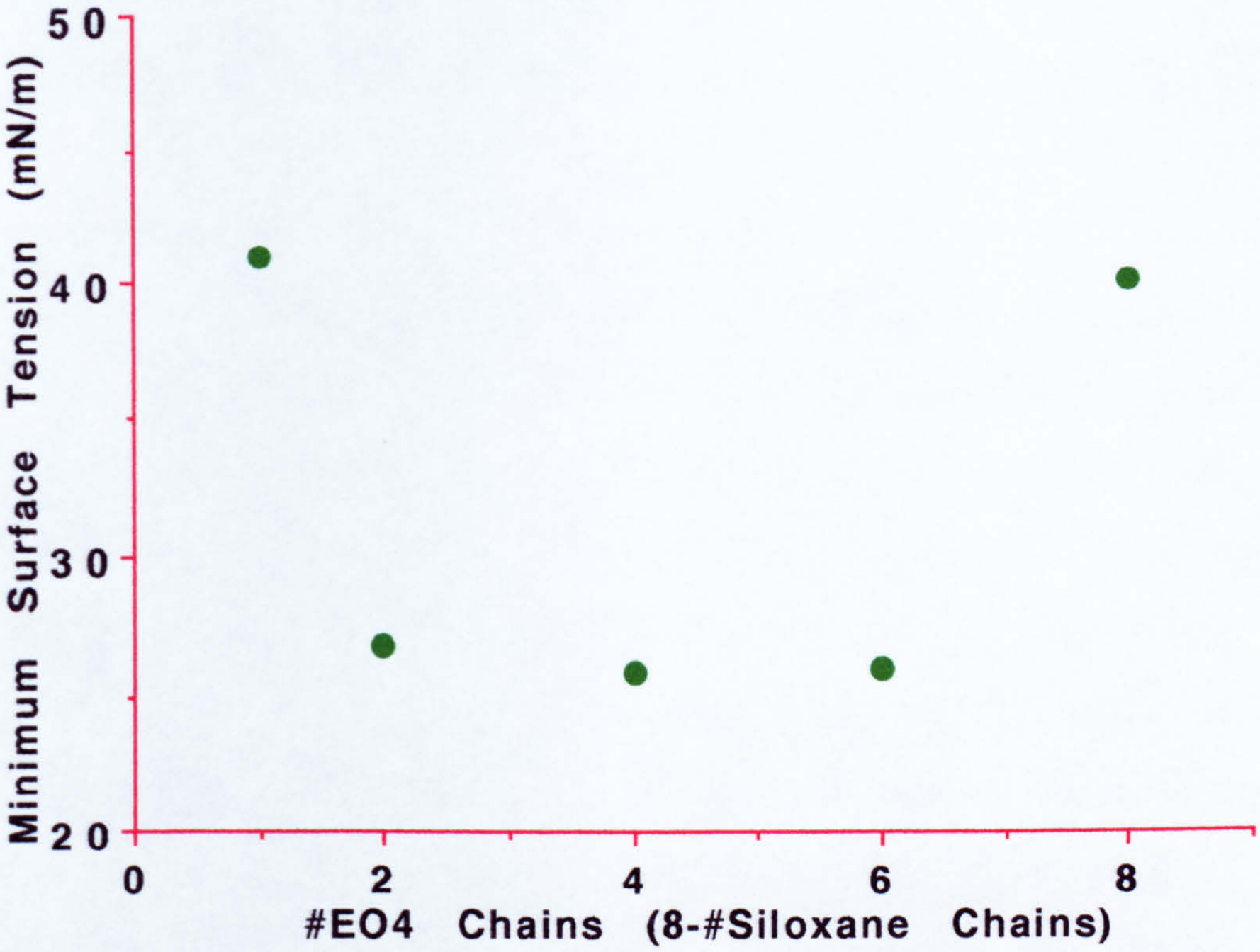

Figure 4.24 Minimum surface tension vs. #EO_4 chains.

The significant surface tension reduction by the octopus molecules with 2, 4, and 6 polyether chains might suggest some type of orientation of the molecules such that the siloxane portions become closely packed at the air/water interface exposing the low energy methyl groups. The molecule with 4 polyether and 4 siloxane chains may have just the right balance of hydrophilicity and hydrophobicity to allow for this type of orientation.

In looking at the plots in Figures 4.19 through 4.23, it can be seen that the point at which the downward sloping linear portion of the plot goes into the plateau region varies greatly for the different octopus compositions. This large change of slope has been shown for many surfactants to indicate that aggregation in bulk solution is occurring[40]. And as described previously, this break point is determined by extrapolation of the intersection of the downward sloping linear portion and the linear plateau region from which γ_{min} was taken. This extrapolated break point is used to estimate log critical aggregation concentrations (log CAC).

The plot of the CAC versus the average composition of the octopus molecules is shown in Figure 4.25. Again, the system with on average 4 polyether and 4 siloxane chains has the lowest log CAC and again may be tied to having the right balance of hydrophilicity and hydrophobicity. Increasing the polyether content increases the hydrophilicity, or solubility of the molecule, and may therefore suppress aggregation until a higher concentration of the molecule is present. Having less polyether

on the octopus may take the solubility too far in the other direction, such that its bulk solubility is so limited that aggregation is curtailed. At this time, all of this is very speculative and in depth studies of surface and bulk aggregation such as those done on low molecular weight siloxane surfactants[19-22] is necessary before anything definitive can be said.

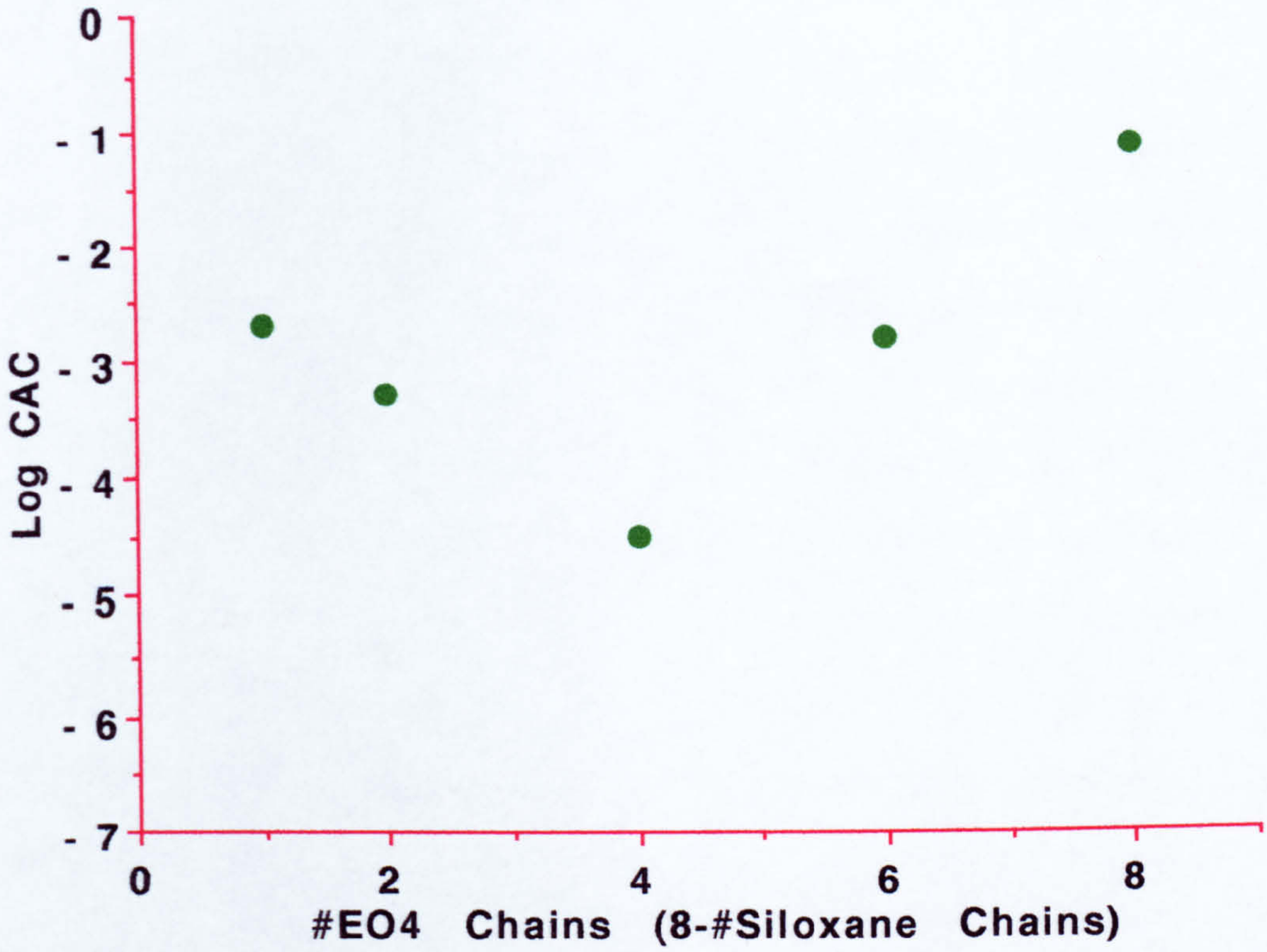

Figure 4.25. Log CAC vs. #EO_4 chains.

Plots of the effect of the number of polyether chains on the octopus molecule on the adsorption and the area/molecule are shown in Figures 4.26 and 4.27. As expected these two plots are similar due to the fact that adsorption (molecules per surface area) is used to derive area per molecule [Area/molecule = 1/(adsorption x Avogadro's number)] as described earlier. It appears that adsorption and area per molecule are greatly affected by the composition of the octopus indicating that packing of the molecules at the air/water interface is highly dependent on the composition of the octopus molecule. It is interesting to find that again the system with on average 4 polyether chains and 4 siloxane chains is the one with the highest average adsorption and smallest average area per molecule. Again, at this time very little can be said about the packing and orientation of these molecules since these studies are not straightforward and require very sophisticated instruments, but these studies could prove to be very interesting.

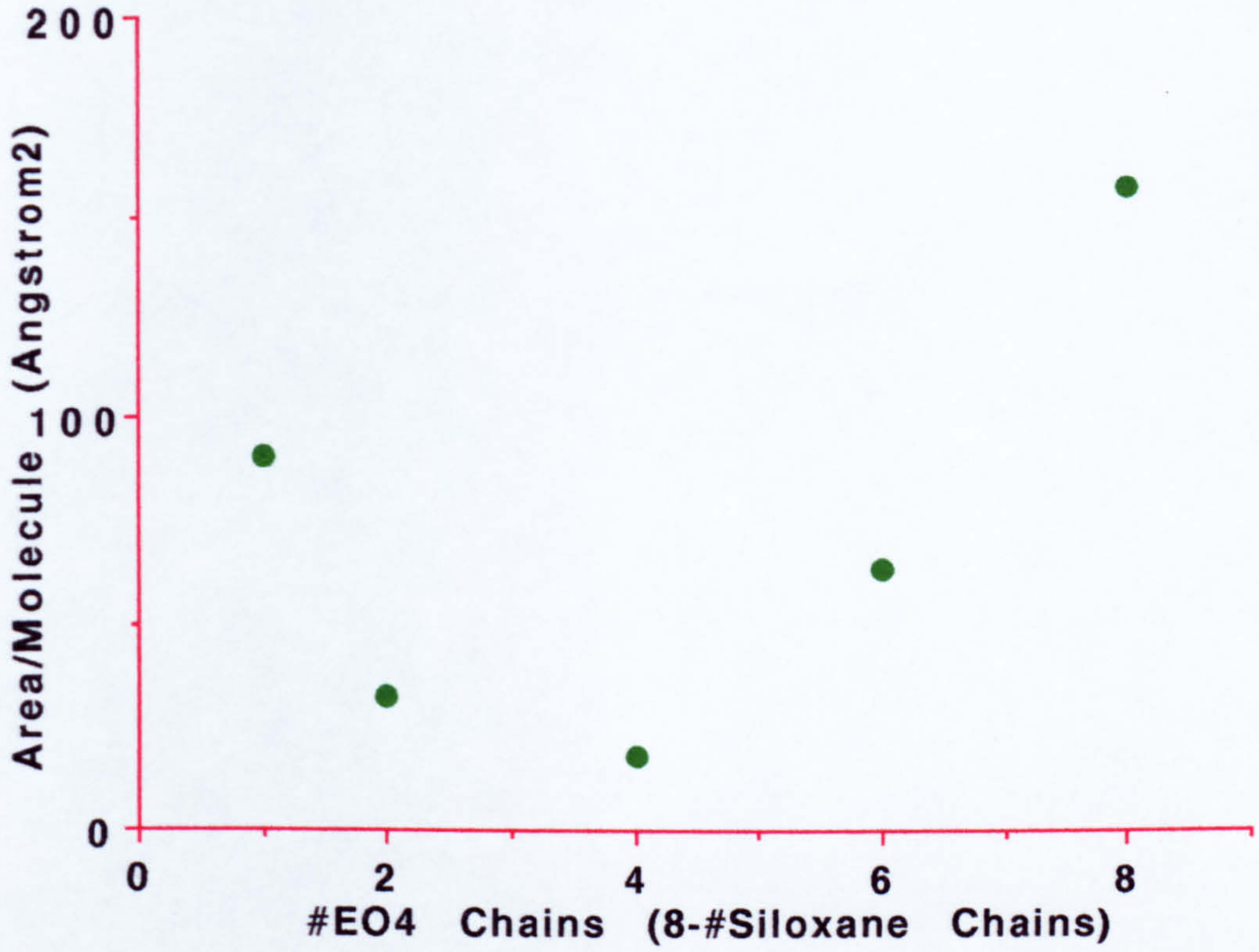

Figure 4.26. Area/molecule vs. #EO_4 chains.

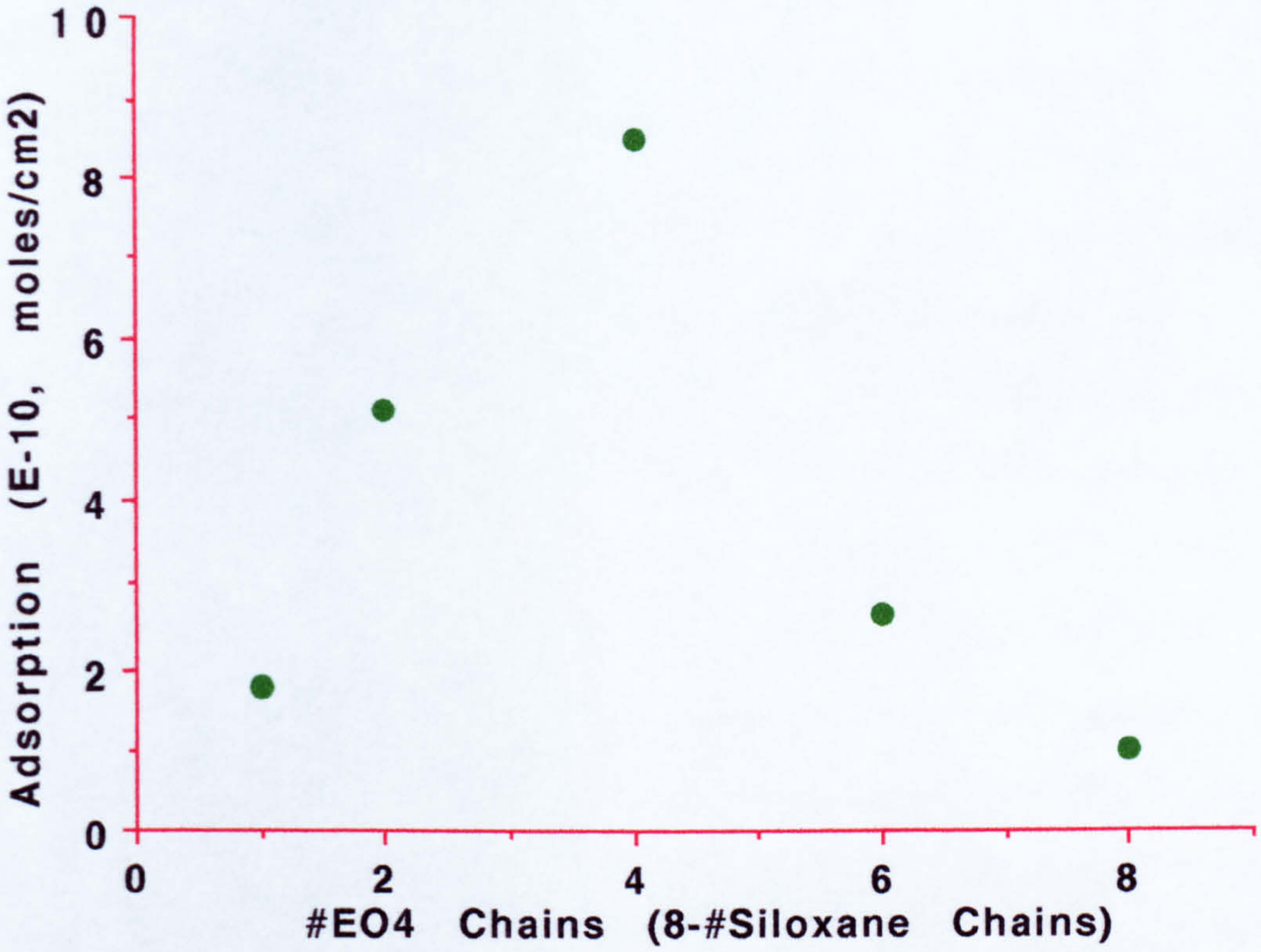

Figure 4.27. Adsorption vs. #EO_4 chains.

It is interesting to compare these results of the studies of the effect of the composition of the polyether/siloxane octopus molecules on the surface activity to those recently obtained for more traditional low molecular weight siloxane surfactants[45]. Gentle and Snow[45] studied the effect of surfactant structure, specifically the polyether [ethylene oxide (EO)] chain length of a series of $(Me_3SiO)_2Si(Me)$-$(CH_2)_3(EO)_xOH$ (or Bis-$(EO)_xOH$) molecules (depicted in Figure 4.28). The surface adsorption and area/molecule of these species did not vary significantly with EO lengths x = 4 to 16, but surface absorption decreased and area/molecule increased when x >16. These findings are shown in Figures 4.29 and 4.30. The authors believed the results for x = 4 to 16 were consistent with a tightly packed surface monolayer whose area/molecule is determined by the dimensions and conformation of the trisiloxane group, and the close packing of the siloxane methyl groups was responsible for the low surface tension. For x >16, the authors believed that the polyether chain penetrated the surface and disrupted the close packing[45]. These results are in contrast to the findings for the octopus molecules in which a change in adsorption and area/molecule was found with changes in polyether content. This difference in findings is not surprising considering the vastly different structure of the octopus and the trisiloxane surfactants. The area/molecule values for the trisiloxane based surfactants were also significantly smaller for the most part than for the values for the octopus molecules which is not surprising considering the octopus molecules are macromonomers. The one exception to this is the area/molecule for the octopus with 4 polyether and 4 siloxane chains.

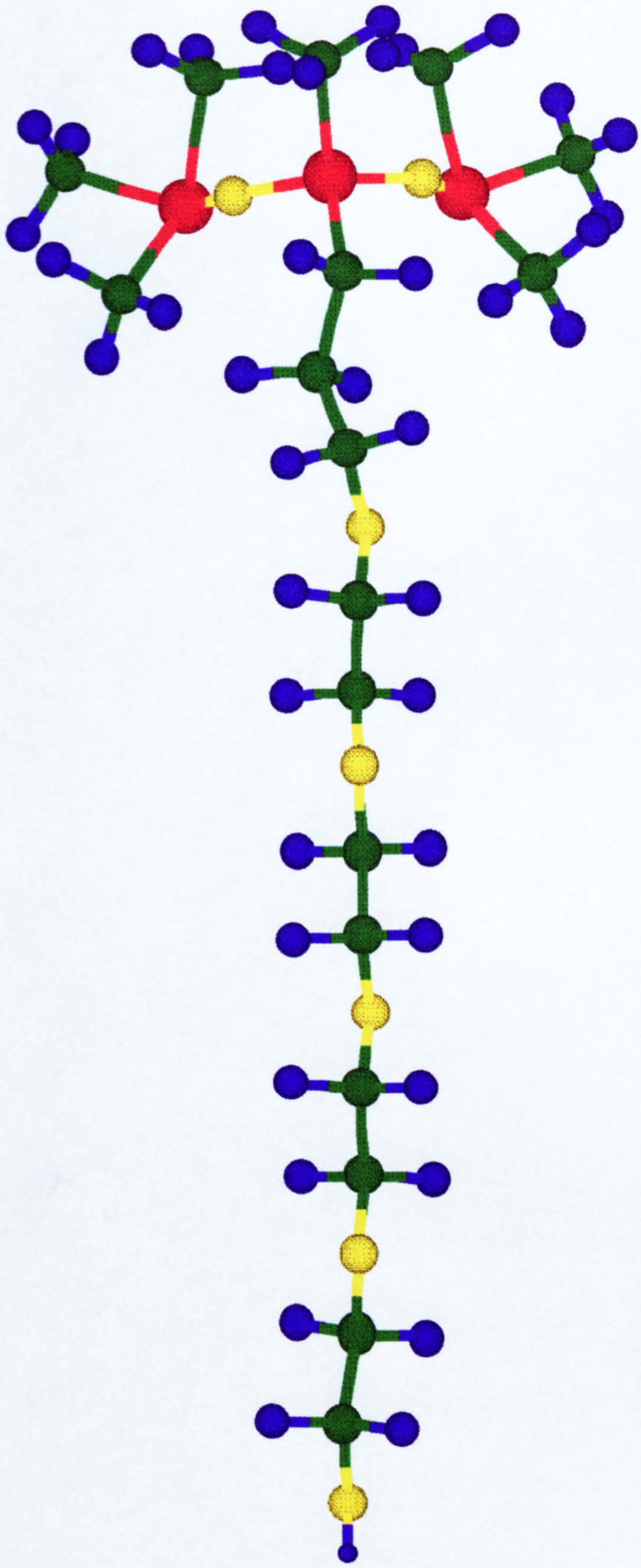

Figure 4.28. Umbrella model of Bis-$(EO)_4OH$ molecule. Green=Carbon, Yellow=Oxygen, Red=Silicon, Blue=Hydrogen.

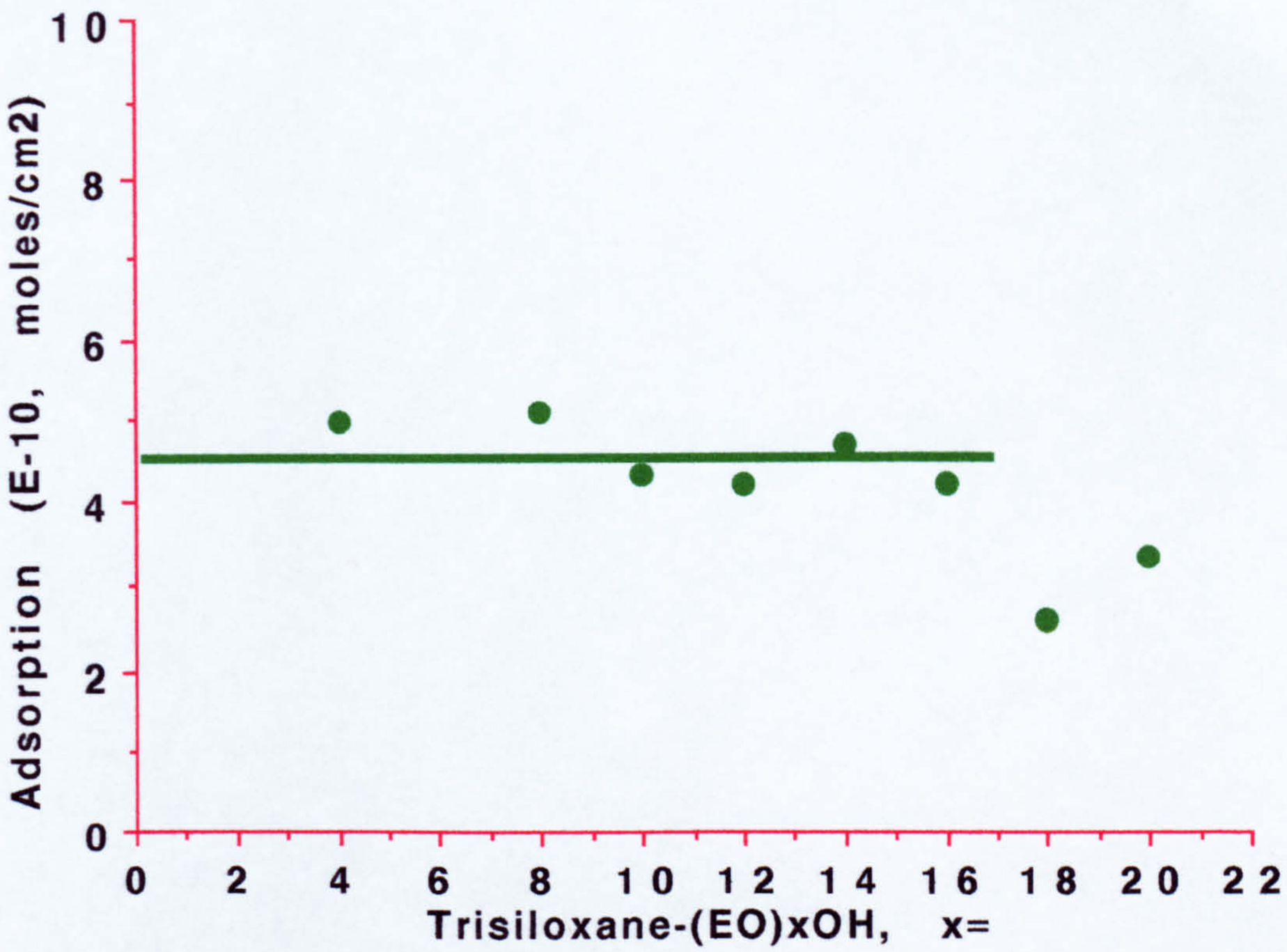

Figure 4.29 Adsorption of $(Me_3SiO)_2Si(Me)(CH_2)_3(EO)_xOH$ surfactant molecules as a function of the polyether chain length.

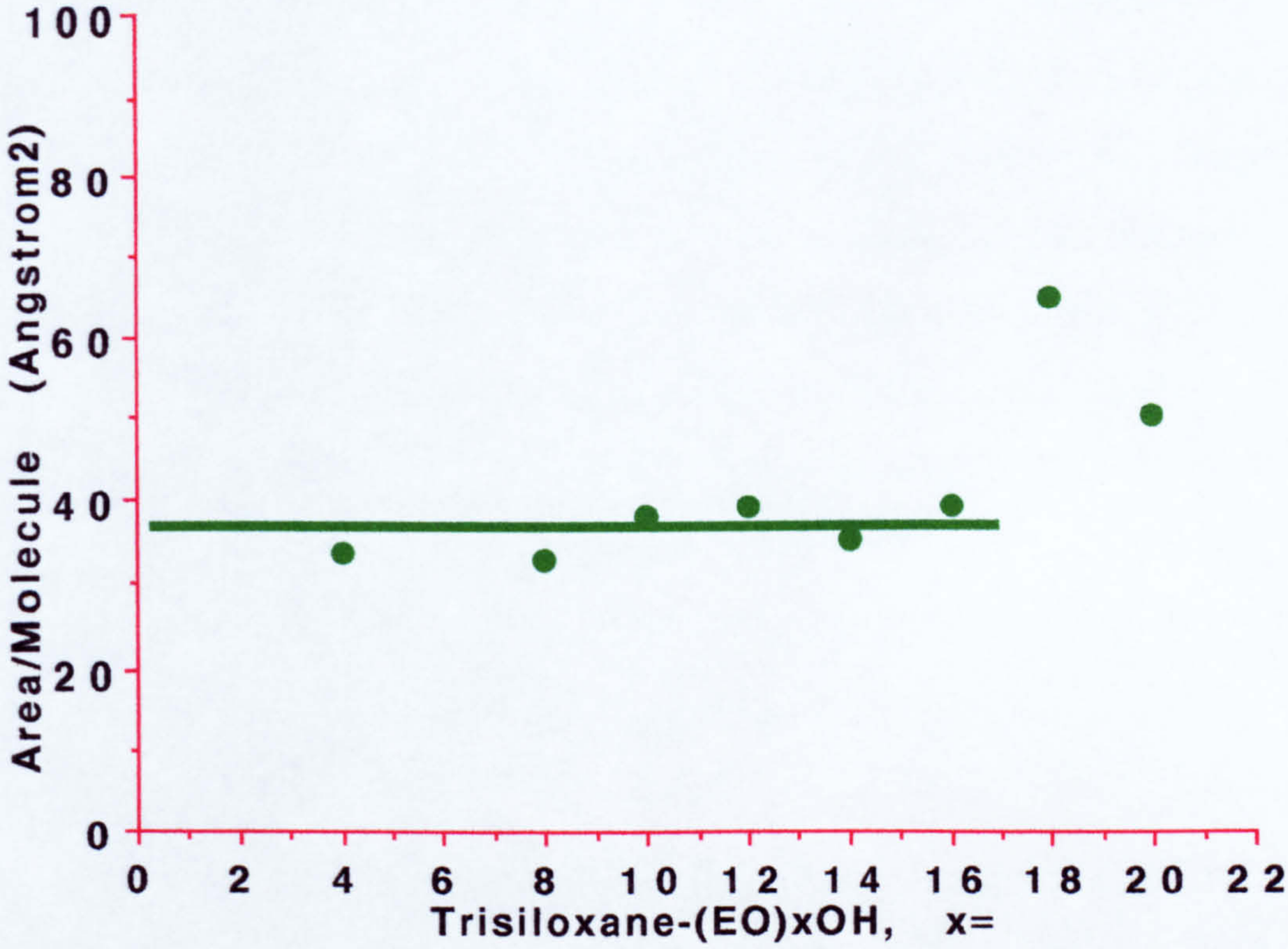

Figure 4.30 Area/molecule of $(Me_3SiO)_2Si(Me)(CH_2)_3(EO)_xOH$ surfactant molecules as a function of the polyether chain length.

In the same study of the series of $(Me_3SiO)_2Si(Me)$-$(CH_2)_3(EO)_xOH$ surfactants, it was found that the γ_{min} values varied over a much narrower range than those of the octopus molecules (22.6 to 27.8 mN/m for the trisiloxane surfactants versus 25.8 to 41.0 mN/m). The γ_{min} values for the $(Me_3SiO)_2Si(Me)$-$(CH_2)_3(EO)_xOH$ surfactants also increased in a linear fashion as x increased as shown in Figure 4.31. The authors attributed this to a systematic disordering of the packed methyl groups as the EO chain length increased. Again these findings are in contrast to the findings for the octopus molecule in which the lowest γ_{min} was for the octopus with 4 polyether and 4 siloxane chains, and increasing or decreasing the polyether content (and conversely the siloxane content) resulted in a higher γ_{min}. However, another look at the data for the trisiloxane molecules indicates the lowest γ_{min} is for the molecule with the most "balanced" polyether/siloxane content as was found with the octopus molecules. No structures were studied in which the siloxane content was increased rather than the polyether content, the results of which might look similar to the findings from the octopus molecules.

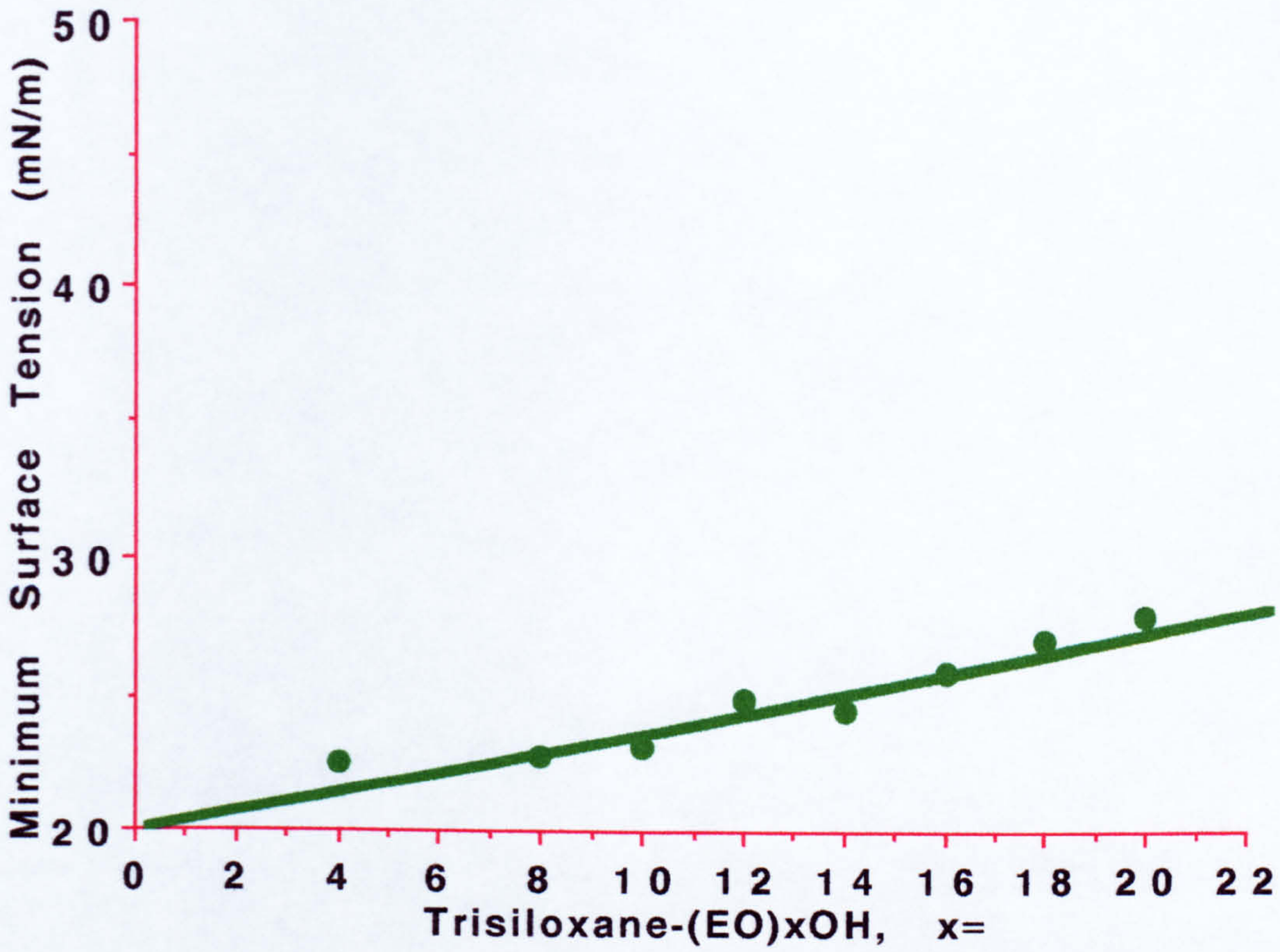

Figure 4.31. Minimum surface tension of $(Me_3SiO)_2Si(Me)(CH_2)_3(EO)_xOH$ surfactant molecules as a function of the polyether chain length.

In the study of the series of $(Me_3SiO)_2Si(Me)$-$(CH_2)_3(EO)_xOH$ surfactants[45], log CAC ranged from -2.5 to -4.1. The values for the octopus molecules in a similar range except for the all polyether functional molecule that had a log CAC of -1.1 indicating that a relatively high concentration of that particular molecule was necessary before aggregation took place. The log CAC value for the 4 polyether and 4 siloxane chain octopus was lower than any of the $(Me_3SiO)_2Si(Me)$-$(CH_2)_3(EO)_xOH$ surfactants indicating that it aggregates at a very low concentration. The log CAC values for the $(Me_3SiO)_2Si(Me)$-$(CH_2)_3(EO)_xOH$ surfactants increased linearly as x increased (Figure 4.32) which was attributed to the increase in hydrophilicity of the surfactant as the EO content of the copolymer increased. Again these findings are in contrast to the findings for the octopus molecules in which the lowest log CAC was for the octopus with 4 polyether and 4 siloxane chains, the molecule with the most "balanced" polyether/siloxane content. Increasing or decreasing the polyether content (and conversely the siloxane content) resulted in a higher log CAC.

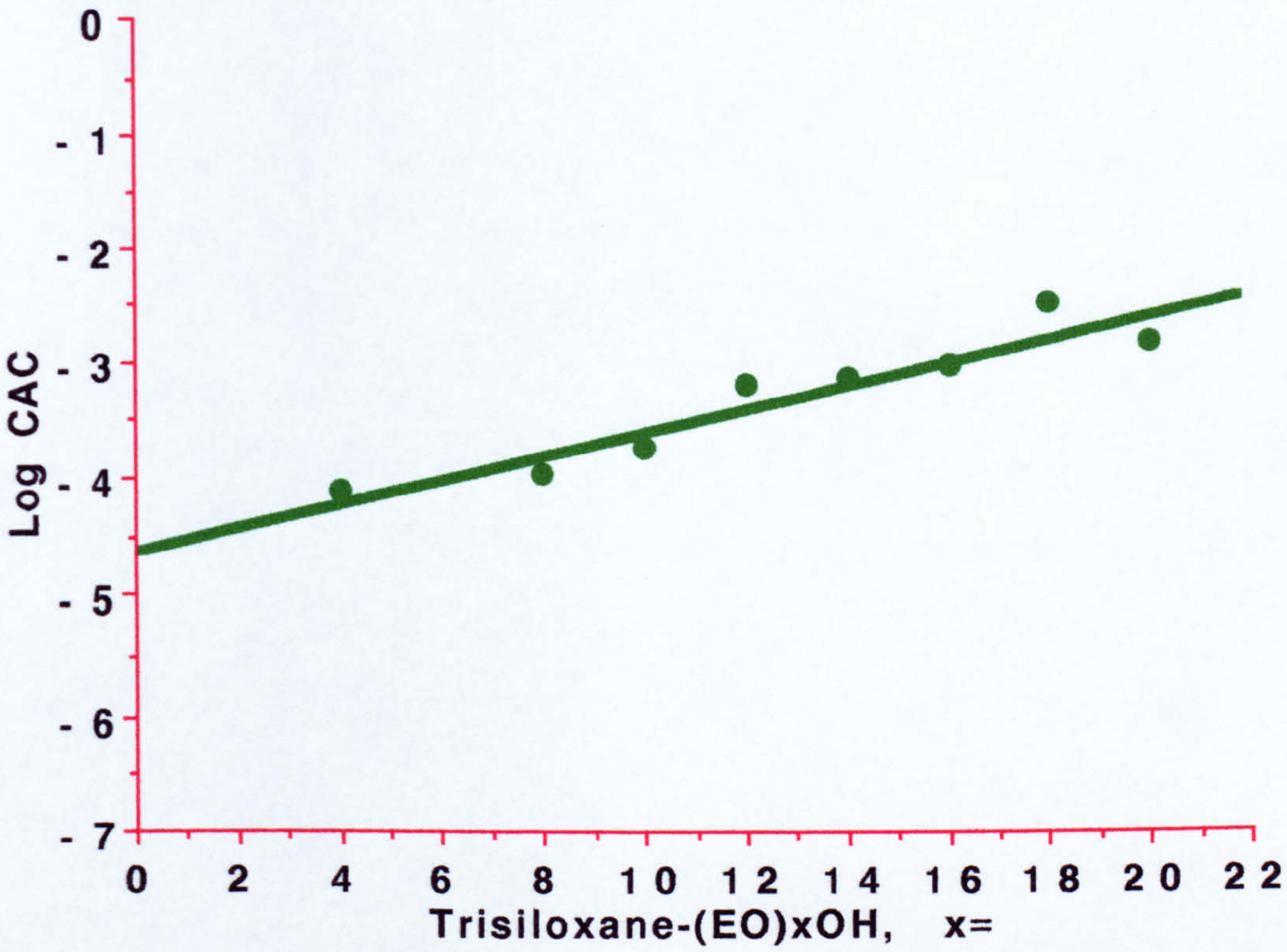

Figure 4.32 Log CAC for $(Me_3SiO)_2Si(Me)(CH_2)_3(EO)_xOH$ surfactant molecules as a function of the polyether chain length.

4.2 Conclusions

In conclusion, the work described in this chapter demonstrated expansion from the hydrocarbon and siloxane functional octopus molecules originally reported to octopuses with other functionalities on the silsesquioxane core. Polyether chains were placed on the T_8 core to make a water soluble octopus molecule. Octopus molecules with a mix of siloxane and polyether chains were also synthesized and found to be surface active. The synthesis of an acrylate functional octopus molecule was also found to be possible and shown to have potential as a UV-curable coating material. A bromoalkene was hydrosilylated by T_8 to make a bromoalkyl functional octopus molecule for the purpose of having the bromine available for further functionalization. The example reactions serve to show the variety of octopus molecules that can be made via hydrosilylation of unsaturated substrates and the numerous applications possibly depending on the functionality placed on the core. Any number of additional reactions involving hydrosilylation can be imagined to produce many other types of octopus molecules.

4.3 Experimental

4.3.1 General

FTIR, NMR, and GPC analyses were done using methods previously described in Chapter Two (Section 2.4.1).

4.3.2 Synthesis of $(HSiO_{3/2})_8$

The procedure for obtaining T_8 hydrogen silsesquioxane outlined in Chapter Two, Section 2.4.2, was used.

4.3.3 Synthesis of $Bu[Si(CH_3)_2O]_3Si(CH_3)_2CH=CH_2$

The procedure outlined in Chapter Two, Section 2.4.4, was used to obtain $Bu[Si(CH_3)_2O]_3Si(CH_3)_2CH=CH_2$.

4.3.4 Synthesis of Acrylate Functional Octopus

T_8 (1.02 grams, 2.4 mmol), excess allyl methacrylate (7.69 grams, 61.5 mmol of Aldrich 98% pure with 50-185 ppm hydroquinone monomethyl ether), 0.11 g phenothiazine, and 30 µl of 0.02M solution of H_2PtCl_6 in isopropyl alcohol were placed in a 50 ml, 3 neck round bottom flask equipped with a stir bar, H_2O condenser, and thermometer. The reaction mixture was stirred and a 4% O_2/96% N_2 blanket was maintained while the mixture was heated to 136 °C over a 4 hour period. No SiH remained by FTIR. The ^{29}Si NMR spectrum (previously shown in Figure 4.1) had a grouping of not entirely resolved peaks between δ -64 and

-67 ppm (T-Si region) referenced to TMS at 0.0 ppm. A group of peaks between δ -105.5 and -106.5 ppm (Q-Si region) referenced to TMS at 0.0 ppm were also present. The ratio of the integrated areas of the T:Q peaks was 10:1.

4.3.5 Synthesis of Bromoalkyl Functional Octopus

T_8 (0.50 grams, 1.2 mmol), 5-bromo-1-pentene (1.55 grams, 10.4 mmol, Aldrich 97% pure), and 15 µl of 0.02M solution of H_2PtCl_6 in isopropyl alcohol were placed in a 50 ml 3-neck flask equipped with a H_2O condenser, thermometer, and stir bar. The reaction mixture was stirred and a 4% O_2/96% N_2 blanket was maintained while the reaction mixture was heated to 140 °C over a 3 hour period after which time no SiH remained by FTIR. The reaction mixture had turned a very dark brown color. The ^{29}Si NMR spectrum previously shown in Figure 4.2 indicates the presence of a group of peaks between δ -65.8 and -67.0 ppm (T-Si region) with the primary product peak at δ -66.86 ppm relative to TMS. This primary product peak makes up greater than 84% of the T-Si peaks integrated area. The ^{29}Si NMR spectrum taken shortly after synthesis of the bromoalkyl functional octopus molecule contained no Q-Si peaks. When the analysis was repeated 18 months later, some small peaks between -100 and -111 ppm (one at δ -100.88 and a second at -110.1 ppm) were then found to be present in the sample after aging. The integrated area of these peaks made up less then 5% of the integrated area of all the peaks in the spectrum.

4.3.6 Synthesis of CH_2=$CHCH_2OSiMe_3$

The compound, CH_2=$CHCH_2OSiMe_3$, is a known compound and is commercially available (Aldrich Chemical Co.). However, for these studies, the CH_2=$CHCH_2OSiMe_3$ was synthesized as follows. In a 250 ml 3-neck, round bottom flask equipped with an H_2O condenser, thermometer, stir bar and blanket of dry N_2, 70.05 grams of hexamethyldisilazane (HMDZ, distilled to >98% purity), 50.08 grams of allyl alcohol (99%, used as supplied by Aldrich Chemical Co.), and 10 µl of trifluoroacetic acid (used as supplied by Aldrich Chemical Co.) were placed. The reaction mixture was heated to reflux conditions (approximately 95 °C) for one hour at which time GC analysis indicated that all the HMDZ had been consumed and approximately 4.2% allyl alcohol remained unreacted. An additional 2.0 grams of HMDZ was added and heating continued for another hour at which time again all HMDZ was consumed and 2.1% (by GC) allyl alcohol remained unreacted. A second 2.0 gram aliquot of HMDZ was added. After heating for an additional 30 minutes, all the HMDZ had been consumed and only 0.2 % (by GC) allyl alcohol remained. A final 0.5 gram sample of HMDZ was added and after heating to 99 °C for 30 minutes, all the allyl alcohol was converted to CH_2=$CHCH_2OSiMe_3$ according to GC analysis. The final product was 98.0% pure by GC. No further characterization was done to confirm the structure.

4.3.7 Synthesis of $[SiO_{3/2}]_8[(CH_2)_3OSiMe_3]_8$

The above reaction product (CH_2=$CHCH_2OSiMe_3$, 1.27 grams, 9.8 mmol), T_8 (0.50 grams, 1.2 mmol), and 15 µl of the tetramethyldivinyldisiloxane complex of Pt diluted in toluene to 1.0 wt% Pt metal were placed in a 15 ml 3-neck round bottom flask equipped with an H_2O condenser, thermometer, stir bar, and an inlet tube for a flow of dry air, and an outlet tube connected to a bubbler. After heating to 65 °C for just 30 minutes with the flow of air, it appeared that much of the CH_2=$CHCH_2OSiMe_3$ had volatilized so an additional 2.30 grams (17.7 mmol) was added and the reaction mixture was heated to 74 °C for 30 minutes at which time a very small SiH peak was detected in the FTIR spectrum at 2260 cm^{-1}. Increasing the temperature to between 95 and 133 °C for one hour resulted in no apparent SiH in the FTIR spectrum. ^{29}Si NMR spectrum (previously shown in Figure 4.3 of the results section) of the reaction product showed a single peak in the T-Si region at δ -66.45 ppm (relative to TMS at 0.0) for the Si of the cage and a single peak in the M-Si region at 17.01 ppm for the trimethyl silicon of the arms. The GPC chromatogram (previously shown, Figure 4.4) indicate a monodispersed product with retention time 17.17 minutes.

4.3.8 Synthesis of CH_2=$CH(CH_2)_9OSiMe_3$

Using a technique similar to the above described method for synthesis of CH_2=$CHCH_2OSiMe_3$, the previously unreported compound, CH_2=$CH(CH_2)_9OSiMe_3$, was made. In a 250 ml 3-neck,

round bottom flask equipped with an H_2O condenser, thermometer, stir bar and blanket of dry N_2, 47.4 grams of hexamethyldisilazane (HMDZ, distilled to >98% purity), 100.0 grams of undecylenyl alcohol (99%, used as supplied by Aldrich Chemical Co.), and 10 µl of trifluoroacetic acid (used as supplied by Aldrich Chemical Co.) were placed. The reaction mixture was heated to reflux (approximately 97 °C) for two hours at which time GC analysis indicated that all the HMDZ had been consumed and approximately 5.8% undecylenyl alcohol remained unreacted. An additional 2.0 grams of HMDZ was added and heating continued for another 30 minutes at which time again all HMDZ was consumed and 4.3% (by GC) undecylenyl alcohol remained unreacted. This process of heating (8.5 hours total time heating), checking by GC every half hour, and adding HMDZ (total amount of HMDZ for reaction was 52.6 grams) continued until all the undecylenyl alcohol was consumed. Final product purity by GC analysis was 98.2%. ^{29}Si NMR spectrum indicated the presence of 1 peak at δ 16.50 ppm relative to TMS as shown in Figure 4.33.

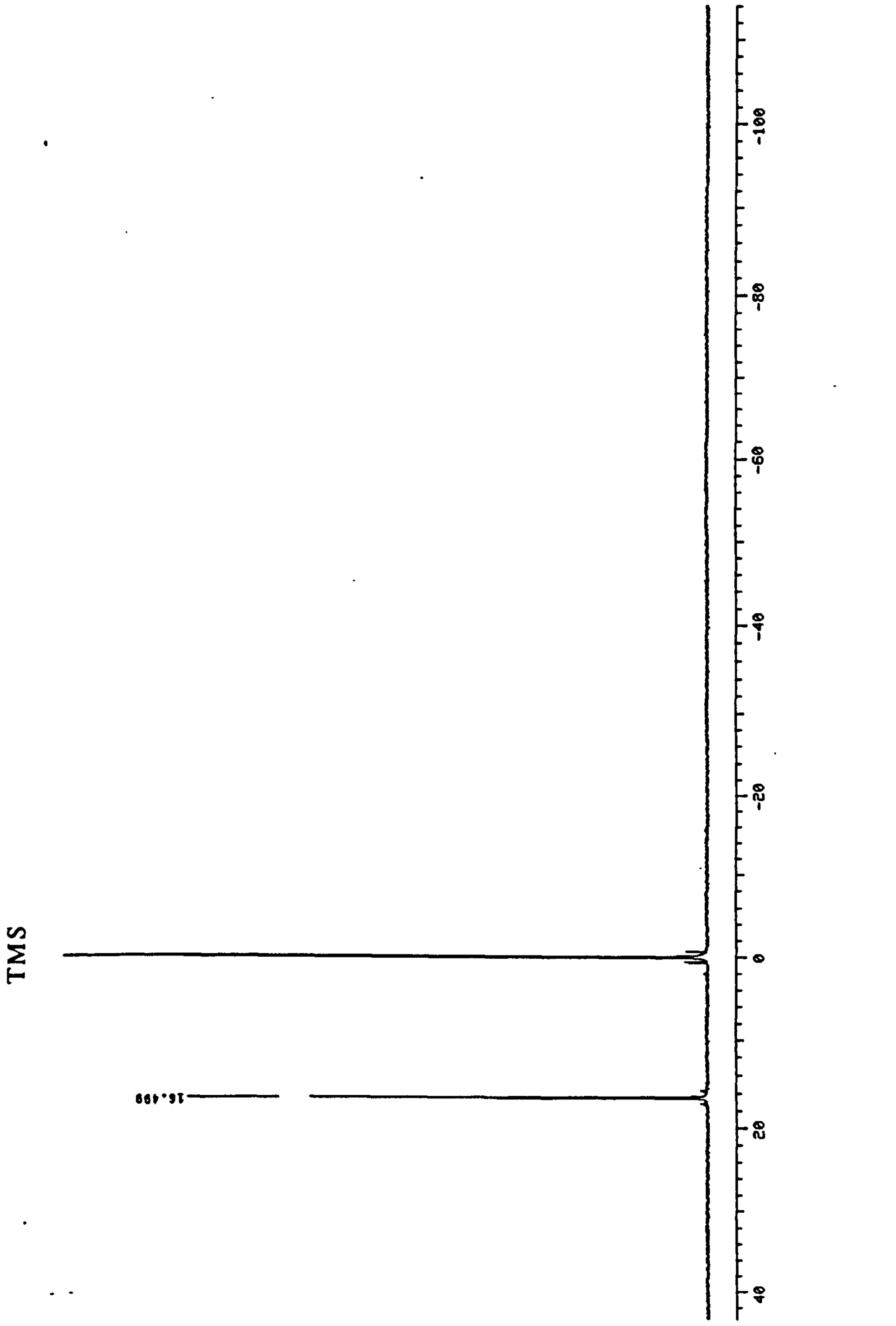

Figure 4.33 ^{29}Si NMR spectrum for $CH_2=CH(CH_2)_9OSiMe_3$.

4.3.9 Synthesis of $[SiO_{3/2}]_8[(CH_2)_{11}OSiMe_3]_8$

Into a 50 ml 3-neck round bottom flask equipped with an H_2O condenser, thermometer, stir bar, and an inlet tube for a flow of dry air, and an outlet tube connected to a bubbler, 0.50 grams of T_8 hydrogen silsesquioxane (1.18 mmol), 2.28 grams of $CH_2=CH(CH_2)_9OSiMe_3$ (obtained as in above reaction, 9.4 mmol, 94.1% pure by GC analysis), and 20 µl of H_2PtCl_6 diluted to 0.02 M in isopropyl alcohol were placed. The reaction was heated to approximately 80 °C for 4 hours at which time a large SiH peak at 2257 cm^{-1} remained in the FTIR spectrum indicating the reaction was incomplete. An additional aliquot of catalyst (20 µl of H_2PtCl_6 diluted to 0.02 M in isopropyl alcohol) was added and the reaction mixture was heated to between 100 and 125 °C for 2.5 hours at which time, the reaction appeared to be completed based on the absence of an SiH peak at 2257 cm^{-1} in the FTIR spectrum. The ^{29}Si NMR spectrum previously shown in Figure 4.5 indicates that several T-Si peaks are present between δ -65 and -67 with the a single well resolved peak at -66.63 ppm assigned to the silicon of the cage, $O_{3/2}\underline{Si}CH_2$-. The spectrum also shows two peaks at δ 17.01 and 16.05 ppm for the trimethyl silicon. There are also some smaller peaks in the Q-Si region at δ -102.88, -102.96 and -108.78 ppm. GPC of the reaction product (Figure 4.6) shows peaks with retention times 16.58 minutes (the octopus), 16.05 minutes (octopus dimer), and a broad shoulder between 13.6 and 15.8 minutes that can be attributed to higher adducts (3 or more octopus molecules linked together).

4.3.10 Synthesis of $[SiO_{3/2}]_8[(CH_2)_5OH]_8$

In a 50 ml 3-neck round bottom flask equipped with an H_2O condenser, thermometer, stir bar, and an inlet tube for a flow of dry air, and an outlet tube connected to a bubbler were placed 0.50 grams of T_8 (1.2 mmol), 0.82 grams 4-penten-1-ol (supplied by Aldrich Chemical Co., stored over molecular sieves), 0.85 grams of toluene distilled from Na, and 20 µl of the tetramethyldivinyldisiloxane complex of Pt diluted in toluene to 1.0 wt% Pt metal. The reaction mixture was heated between 80 and 110 °C over a period of 6 hours at which time all SiH was gone by FTIR analysis (absence of peak at 2260 cm^{-1}). At the elevated temperatures, the product was dissolved or dispersed in the toluene. Upon cooling, a solid precipitated. This solid was insoluble in toluene but dissolved in methanol. ^{29}Si NMR done in d_4-methanol indicated the presence as previously shown in Figure 4.7 of a major peak in the T-Si at δ -66.45 ppm region (Si of the T_8 cage) although there also appeared to be some additional minor peaks in the T-Si region at δ -66.36 and -65.46 ppm making up 13.5% of the total integrated peak area. A very small peak in the Q-Si region around δ -103 ppm relative to TMS was also seen. An assignment of this peak to $O_{3/2}SiOCH_2$- resulting from condensation of the OH of 4-penten-1-ol with SiH of the T_8 was suggested. A mixture of the product, methanol, and toluene was used to obtain the GPC analysis on a toluene unit. The resulting chromatogram was shown in Figure 4.8 previously. A peak at a retention time of approximately 20.3 minutes was seen and was assigned to the hydroxy functional octopus. A second, higher molecular weight peak at a retention

time of approximately 19.9 minutes was also seen and attributed to an octopus "dimer" resulting from OH to SiH condensation.

4.3.11 Synthesis of $[SiO_{3/2}]_8[(CH_2)_2Si(OMe)_3]_8$

In a 100 ml 3-neck round bottom flask equipped with an H_2O condenser, thermometer, stir bar, and an inlet tube for a flow of dry air, and an outlet tube connected to a bubbler, 2.0 grams of T_8 (4.7 mmol), 6.0 grams of vinyltrimethoxysilane (40.5 mmol, 98%, used as supplied by Aldrich Chemical Co.), and 80 µl of the tetramethyldivinyldisiloxane complex of Pt diluted in toluene to 1.0 wt% Pt metal were placed. The reaction exothermed to 140 °C. After cooling by surrounding the reaction flask with a cold water bath, heating of the reaction was started. The reaction mixture was heated at approximately 80 °C for 2 hours during which time FTIR analysis was done to follow the reduction of SiH as the T_8 reacted. During this same 2 hour period, an additional 4.0 grams of vinyltrimethoxysilane was added (in increments of 1.0 gram each) to get the reaction to go to completion. At the end of this 2 hour period, the temperature was increased to 120 °C momentarily and then cooled to room temperature. FTIR analysis then indicated the absence of SiH (no peak at 2260 cm^{-1}). Excess vinyltrimethoxysilane was stripped off using reduced pressure (3.5 mm Hg) and heat (up to 95°C). After stripping excess vinyltrimethoxysilane, ^{29}Si NMR was done. The spectrum was previously shown in Figure 4.9. It shows the presence of a group of not entirely resolved T-Si peaks between δ -66 and -68 ppm assigned to the silicon of the cage. There was also a grouping of peaks between δ -41.4 and -44.3 ppm

assigned to the T-Si of the trimethoxysilyl group. The multiple peaks for both these silicons was thought to be due to both α- and β-addition of the vinyltrimethoxysilane to the cage as explained in the results section. The GPC chromatogram (previously shown as Figure 4.10) indicated that there was a peak at retention time 17.72 minutes that was the reaction product. There appeared to be a minor higher molecular weight side product (retention time 17.15 minutes) that was assigned as octopus dimer resulting from some H/Vinyl exchange on silicon as was seen previously for the reaction of T_8 with vinyl-siloxane. A low molecular weight peak at approximately 20.5 minutes was thought to be the other by-product of H/Vinyl exchange on silicon, $(MeO)_3SiCH_2CH_2Si(OMe)_3$.

4.3.12 Synthesis of $[SiO_{3/2}]_8[(CH_2)_3(OCH_2CH_2)_4OH]_8$

In a 100 ml 3-neck flask equipped with a H_2O condenser, thermometer, and stir bar were placed T_8 (1.50 grams, 3.5 mmol), $CH_2=CHCH_2(OCH_2CH_2)_4OH$ in excess (8.60 grams, 36.8 mmol) and 26 µl of 0.02M solution of H_2PtCl_6 in isopropyl alcohol. While being heated, the contents of the flask were stirred and a 4% O_2/96% N_2 blanket over the reaction was maintained. Solids formed as the reaction progressed so 5.03 grams of toluene was added to the flask along with 20 µl of 0.02M solution of H_2PtCl_6 in isopropyl alcohol. The reaction mixture was heated to toluene reflux temperature (112 °C). After approximately 5.5 hours of heating, the reaction was not quite complete as indicated by residual SiH in the FTIR spectrum. The reaction mixture was transferred to a vial and the toluene

was stripped off before heating the mixture to 139 °C for 21 hours at which time the reaction appeared complete by FTIR. A rubbery solid product was obtained. ^{29}Si NMR was run on a CD_3OD solution of the product. The spectrum previously shown in Figure 4.15 showed the presence of unresolved peaks between δ -64.4 and -66.5 ppm referenced to TMS at 0.0 ppm.

4.3.13 Synthesis of $[SiO_{3/2}]_8[(CH_2)_3(OCH_2CH_2)_4OH]_{8-x}[(CH_2)_2(Si(CH_3)_2O)_3Si(CH_3)_2Bu]_x$

The mixed siloxane/polyether functional octopus molecules were made via hydrosilylation of vinyl-functional siloxane and allyl-functional polyether. The ratio of the unsaturated reactants was used to vary the ratio of polyether to siloxane functionality on the octopus product. A series of materials were made in which the ratio of polyether/siloxane were as follows: 1/7, 2/6, 4/4, 6/2, 8/0 (all polyether, described above). As an example of the typical procedure used to prepare these mixed polyether/siloxane octopus molecules, the procedure used for the 4 siloxane/4 polyether functional material will be described. T_8 (0.40 grams, 0.94 mmol), $Bu[Si(CH_3)_2O]_3Si(CH_3)_2CH=CH_2$ (1.37 grams, 3.76 mmol), and $CH_2=CHCH_2(OCH_2CH_2)_4OH$ (1.10 grams, 4.70 mmol, 1.25x excess), 2.90 grams of isopropanol solvent (optima grade, Fisher), and 30 µl of 0.02M solution of H_2PtCl_6 in isopropyl alcohol were placed in a 50 ml 3-neck flask equipped with a H_2O condenser, thermometer, and stir bar. The reaction mixture was stirred and a 4% O_2/96% N_2 blanket was maintained while the mixture was heated from 67 °C up to 132 °C over an approximately 4 hour period at which time no SiH was

apparent in the FTIR spectrum of the product so the reaction was considered complete. The reaction product was a viscous liquid.

^{29}Si NMR analysis of each of the reaction product mixtures where the ratio of the polyether/siloxane starting materials were 1/7, 2/6, 4/4, and 6/2 was done. The spectrum for the product mixture that had the 1/7 polyether/siloxane ratio had a group of M-Si peaks [$\underline{Si}(CH_3)_2Bu$ and $-CH_2CH_2\underline{Si}(Me_2)$] between δ 8.3 and 7.6 ppm; a group of D-Si peaks (the two D-silicons of the siloxane chain appendages) between δ -21.7 and -21.9 ppm; and a group of T-Si peaks (the $O_{3/2}\underline{Si}$-CH_2 of the cage) between δ -65 and -66.8 ppm. The ratio of integrated area of the groups of M:D:T peaks was found to be approximately 1.8:1.9:1.0. The T-Si region of the spectrum was shown in Figure 4.11.

The spectrum for the product mixture that had the 2/6 polyether/siloxane ratio had a group of M-Si peaks [$\underline{Si}(CH_3)_2Bu$ and $-CH_2CH_2\underline{Si}(Me_2)$] between δ 8.1 and 7.6 ppm; a group of D-Si peaks (the two D-silicons of the siloxane chain appendages) between δ -21.7 and -21.8 ppm; and a group of T-Si peaks (the $O_{3/2}\underline{Si}$-CH_2 of the cage) between δ -65.2 and -67.0 ppm. The ratio of integrated area of the groups of M:D:T peaks was found to be approximately 1.5:1.6:1.0. The T-Si region of the spectrum was shown in Figure 4.12.

The spectrum for the product mixture that had the 4/4 polyether/siloxane ratio had a group of M-Si peaks [$\underline{Si}(CH_3)_2Bu$ and $-CH_2CH_2\underline{Si}(Me_2)$] between δ 8.3 and 7.6 ppm; a group of D-Si peaks (the two D-silicons of the siloxane chain appendages)

between δ -21.6 and -21.9 ppm; and a group of T-Si peaks (the $O_{3/2}\underline{Si}$-CH_2 of the cage) between δ -65.2 and -67.0 ppm. The ratio of integrated area of the groups of M:D:T peaks was found to be approximately 1.1:1.1:1.0. The T-Si region of the spectrum was shown in Figure 4.13.

The spectrum for the product mixture that had the 6/2 polyether/siloxane ratio had a group of M-Si peaks [$\underline{Si}(CH_3)_2Bu$ and -$CH_2CH_2\underline{Si}(Me_2)$] between δ 8.3 and 7.6 ppm; a group of D-Si peaks (the two D-silicons of the siloxane chain appendages) between δ -21.6 and -21.9 ppm; and a group of T-Si peaks (the $O_{3/2}\underline{Si}$-CH_2 of the cage) between δ -64.8 and -66.8 ppm. There was also a group of Q-Si peaks between δ -103.0 and -103.2 ppm probably resulting from condensation of the OH end of the polyether chain with the SiH of the T_8. The ratio of integrated area of the groups of M:D:T:Q peaks was found to be approximately 0.55:0.64:1.0:0.16. The T-Si region of the spectrum was shown in Figure 4.14.

4.3.14 Surface Tension Measurements

Surface tension of aqueous solutions of the polyether functional octopus molecules and the mixed polyether/siloxane functional octopus molecules as well as the polyether starting materials were obtained by the du Noüy ring method using a Krüss surface tensiometer. The siloxane-polyether solutions were prepared from distilled, deionized water. Solutions were prepared and the surface tension measured after aging for approximately 90-100 minutes. The surface tension at each concentration was

calculated using an average of three or more measurements. Variation in the three or more measurements at each concentration is the basis for the error bars in the surface tension vs. log concentration plots.

4.3.15 Coating, Curing, Testing of Acrylate Functional Octopus

Three coating formulations containing the acrylate functional octopus molecule as synthesized in section 4.3.4 were made up as indicated in Table 4.1 previously shown in Section 4.1.1.

Each coating formulation was coated onto polycarbonate panels using a #4 Meyer rod. The coatings were then cured after two passes through an ultraviolet cure chamber at 300 Watts/cm^2, 8 feet/minute (~4000 mJ/cm^2).

The scratch resistant properties of the coatings were evaluated by determining the change in light transmission and haze of the coated transparent plastics after surface abrasion. Haze is defined as the percentage of transmitted light which in passing through the abraded track deviates from the incident beam by forward scattering. The instrument used for the abrading was a Teledyne model 503 Taber Abraser with two 250 gram auxiliary weights (500 gram load) for each wheel. The samples were placed in the sample holder and the instrument was used to abrade the sample for 100 cycles. The haze in four areas on the plastic substrate was determined using Hunter Hazemeter model D55H. The four readings were averaged. The initial haze was

subtracted from the haze after abrading and a Delta Haze was determined for 100 cycles. The sample was then abraded for an additional 400 cycles for a total of 500 cycles and the Delta Haze was determined for 500 cycles.

4.4 References

1. Blizzard, John D. Dow Corning employee who evaluated scratch resistant properties and found results encouraging.

2. Gentle, T.E.; Bassindale, A.R.; Blizzard, J.D. Invention Disclosure 8764 submitted at Dow Corning, August 23, 1993.

3. Kanner, B.; Reid, W.G.; Petersen, I.H.*I&EC Prod. Res. Dev.*, **1967**, 6(2), 88-92.

4. Ananthapadmanabhan, K.P.; Goddard, E.D.; Chandhan, P. *Coll. Surf.*, **1990**, 281-297.

5. Kendrick, T.C.; Owen, M.J. *Chim. Phys. Appl. Prat. Ag. Surf. C.R. 5th Congr. Int. Deterg.*, **1969**, 2 (1) 571-580.

6. Knoche, M.; Tamura, H.; Bulcovac, M.J. *J. Agric. Food Chem.* **1991**, 39, 202-206.

7. Lavygin, I.A.; Leitan, O.V.; Uklonskii, D.A. *Kolloidnyi Zhurnal* **1975**, 37 (4), 790-793.

8. Hamann, H.; Ritter, J. *Plaste und Kautschuk* **1983**, 30 (7), 364-366.

9. Maki, H.; Saeki, S.; Ikeda, I.; Komori, S. *J. Am. Oil Chem. Soc.* **1969**, Dec., 635-637.

10. Maki, H.; Murakami, Y.; Ikeda, I. *Kogyo Kagaku Zasshi* **1968**, 71 (10), 1675-1679.

11. Gruning, B.; Koerner, G. *Tenside Surf. Det.* **1989**, 26(5), 312-317.

12. Schaefer, D. *Tenside Surf. Det.* **1990**, 27(3), 154-158.

13. Smid-Korbar, J.; Kristl, J. *Int. J. Cosmet. Sci.* **1990**, 12, 135-139.

14. Schmidt, G. *Tenside Surf. Det.* **1990**, 27(5), 324-328.

15. Fink, H. *Tenside Surf. Det.* **1991**, 28(5), 306-312.

16. Roggenbuck, R.; Rowe, L.; Penner, D.; Petroff, L.; Burow, R. *Weed Technol.* **1990**, 4, 576.

17. Steven, P. *Pestic. Sci.* **1993**, 38(2-3), 103-122.

18. Koche, M. *Weed Research* **1994**, 34(3), 221-239.

19. Zhu, X. Ph.D. Thesis, University of Minnesota, **1992**.

20. Tiberg, F.; Cazabat, A. *Europhysics Letters* **1994**, 25(3), 205-210.

21. Hill, R.M.; He, M.; Davis, H.T.; Scriven, L.E. *Langmuir* **1994**, 10, 1724-1734.

22. He, M.; Hill, R.M.; Lin, Z.; Scriven, L.E.; Davis, H.T. *J. Phys. Chem.* **1993**, 97, 8820-8834.

23. Gradzielski, M.; Hoffman, H.; Robisch, P.; Ulbricht, W. *Tenside Surf. Det.* **1990**, 27(6), 366-379.

24. Pape, Peter, G. "Commercialization of Silicone Specialty Surfactants-Status Report"; Dow Corning Proprietary Report #1983-I0249-122.

25. Pape, P.G. "Dow Corning Specialty Surfactants-Situation Analysis"; Dow Corning Proprietary Report #1983-I0240-376.

26. Zombeck, A. "Aqueous Silicone Surfactants"; Dow Corning Proprietary Report #1983-I000-5636.

27. Petroff, L.J. "The Development of Dow CorningR X2-5211 and X2-5212 Superwetting Agents"; Dow Corning Proprietary Report #1987-I0240-513.

28. Snow, S.A. "Phase Behavior and Molecular Aggregate Microstructure of the Surface Active Salts $(Me_3SiO)_2Si(Me)-(CH_2)_3{}^+NMe_2(CH_2)_2OH\,X^-$ in Aqueous Solution"; Dow Corning Proprietary Report #1993-I0000-38270.

29. Rosen, Milton J. Surfactants and Interfacial Phenomena; 1978, Wiley-Interscience, Chapters 2,5.

30. Moore, W.J. Physical Chemistry, Fourth Edition, 1972, Prentice-Hall, Inc., Chapter 11.

31. McBain, J.W.; Wood, L.A. *Proc. Roy. Soc. London, Ser. A,* **1940**, 174, 286.

32. Adamson, A.W. Physical Chemistry of Surfaces 1990, Wiley-Interscience, Chapters 1-4.

33. Tajima, K.; Muramatsu, M.; Tsunetaka, S. *Bull. Chem. Soc. Jap.* **1970**, 43, 1991-8 and references therein.

34. Nilsson, G. *J. Phys. Chem.* **1957**, 61, 1135.

35. Schott, H. *J. Pharm. Sci.* **1980**, 69(7), 852-4.

36. Schick, M.J. *J. Coll. Sci.* **1962**, 17, 801-813.

37. Crook, E.H.; Trebbi, G.F.; Fordyce, D.B. *J. Phys. Chem.* **1964**, 68(12), 3592.

38. Elworthy, P.H.; Macfarlane, C. B. *J. Pharm. Pharmacol.* **1962**, December, 100T-102T.

39. Crook, E.H.; Fordyce, D.B.; Trebbi, G.F. *J. Phys. Chem.* **1963**, 67, 1987.

40. Myers, D. Surfactant Science and Technology 1988, VCH Publishers, New York.

41. Snow, S.A. *Langmuir* **1993**, 9, 424 and references therein.

42. Snow, S.A.; Fenton, W.N.; Owen, M.J. *Langmuir* **1990**, 6, 385-391.

43. Snow, S.A.; Fenton, W.N.; Owen, M.J. *Langmuir* **1991**, 7, 868-871.

44. Schmaucks, G.; Sonnek, G.; Wustmeck, R.; Herbst, M.; Ramm, M. *Langmuir* **1992**, 8, 1724-1730.

45. Gentle, T.E.; Snow, S.A. "The Adsorption of Small Silicone Polyether Surfactants at the Air/Water Surface," submitted to Langmuir, October 1994.

Chapter Five

Additional Routes to Octopus Molecules

5.0 Introduction

The route used in chapters 2 through 4 to functionalize T_8 hydrogen silsesquioxane was hydrosilylation. In the interest of expanding on the variety of octopus molecules with silsesquioxane cores and the type of linkage to the core (only Si-C linkage possible with hydrosilylation), the feasibility of using condensation reactions involving the SiH of $(HSiO_{3/2})_8$ with R-OH and Si-OH functional materials was investigated and is the topic of this chapter.

5.1 Results

5.1.1 Siloxane Octopus Molecule via Condensation Reaction

Amines are known to catalyze the condensation reaction of SiH + SiOH[3]. Using the reaction in scheme 5.1 catalyzed by a hydroxyl amine catalyst, a siloxane functional octopus molecule was made.

$$(HSiO_{3/2})_8 + 8\ HOSiMe_2(OSiMe_2)_3CH_3 \rightarrow [SiO_{3/2}]_8[OSiMe_2(OSiMe_2)_3CH_3]_8 + H_2 \qquad (5.1)$$

The above reaction went very efficiently, very fast, and at low temperature using a hydroxyl amine catalyst, Et_2NOH. The resulting product has a SiOSi linkage of the "arms" to the core in contrast to the siloxane octopus molecule made via hydrosilylation that has the $SiCH_2CH_2Si$ linkage.

^{29}Si NMR analysis was done on the reaction product and the spectrum is shown in Figure 5.1. The spectrum for the product of the reaction of T_8 and $HOSiMe_2(OSiMe_2)_3CH_3$ is fairly simple in the Q-Si region with a peak at δ -110.16 ppm referenced to TMS at 0.0 ppm. There are possibly one or two very small peaks that are not very well resolved from the noise around the peak at -110.16 ppm an explanation of which could be the result of any SiH to SiH coupling (hydrolysis and condensation) that is known to occur in the presence of any moisture[1-3] and especially in the presence of an amine catalyst[4-5]. There is a single peak for the M-Si of each appendage terminus at δ 7.24 ppm. The D-Si region of the spectrum is not as simple as would be expected if the reaction went cleanly. One would expect to see 3 D-Si peaks (D-Si closest to the Si of the cage, the next D-Si along the siloxane chain, and the third along the chain nearest the M-Si at the chain terminus) in a ratio of 1:1:1. Instead there are at least 6 D-Si peaks between δ -19 and -22 ppm. These additional D-Si peaks could be the result of some silanol condensation reactions of the $HOSiMe_2(OSiMe_2)_3CH_3$ with itself.

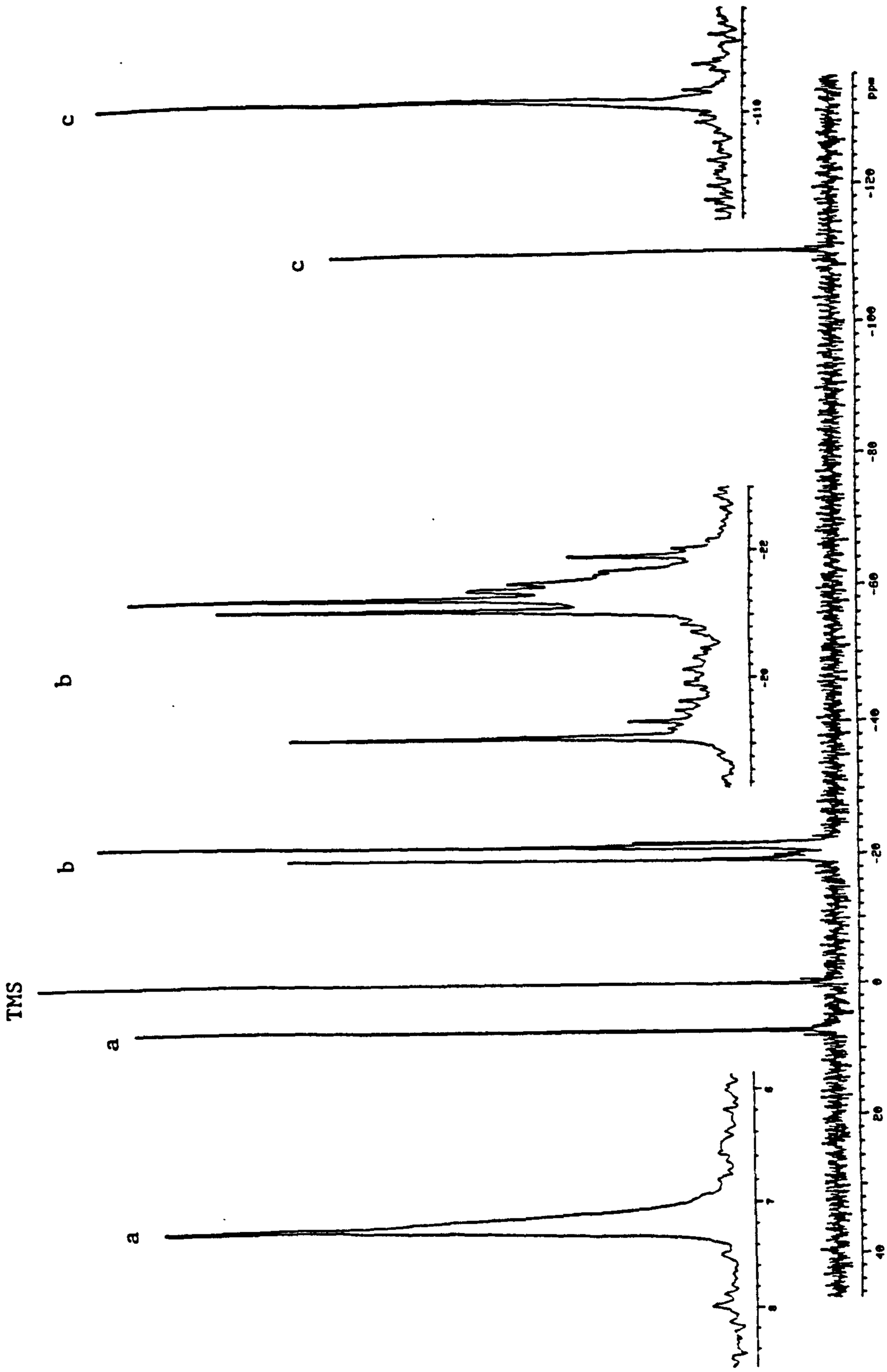

Figure 5.1 ^{29}Si NMR spectrum for the product of the reaction of T_8 + $HOSiMe_2(OSiMe_2)_3CH_3$.

The GPC chromatogram of the reaction product is shown in Figure 5.2. The chromatogram shows a fairly monodispersed product peak at a retention time of 16.50 minutes. However, there does appear to be a slight broadening of the product peak on the high molecular weight side, a slight shoulder on the peak. If any cage to cage condensation had occurred as suggested by the presence of the very small peaks in the ^{29}Si NMR spectrum around the peak at δ -110.16 ppm, this shoulder on the main product peak in the GPC could be due to the resultant octopus dimer. In addition to the product peak in the GPC there appears to be lower molecular weight impurities. The very small peak at 19.11 minutes is residual $HOSiMe_2(OSiMe_2)_3CH_3$ as confirmed by the GPC of the starting material itself (Figure 5.3). There are some additional low molecular weight peaks at 18.27 minutes, 17.79 minutes, and 17.39 minutes. These additional peaks could be the result of silanol condensation reactions of the $HOSiMe_2(OSiMe_2)_3CH_3$ with itself. The peaks at 18.27 minutes, 17.79 minutes are seen in very small quantities in the GPC chromatogram for the starting material, $HOSiMe_2(OSiMe_2)_3CH_3$, but appear to have increased during the synthesis of the octopus molecule.

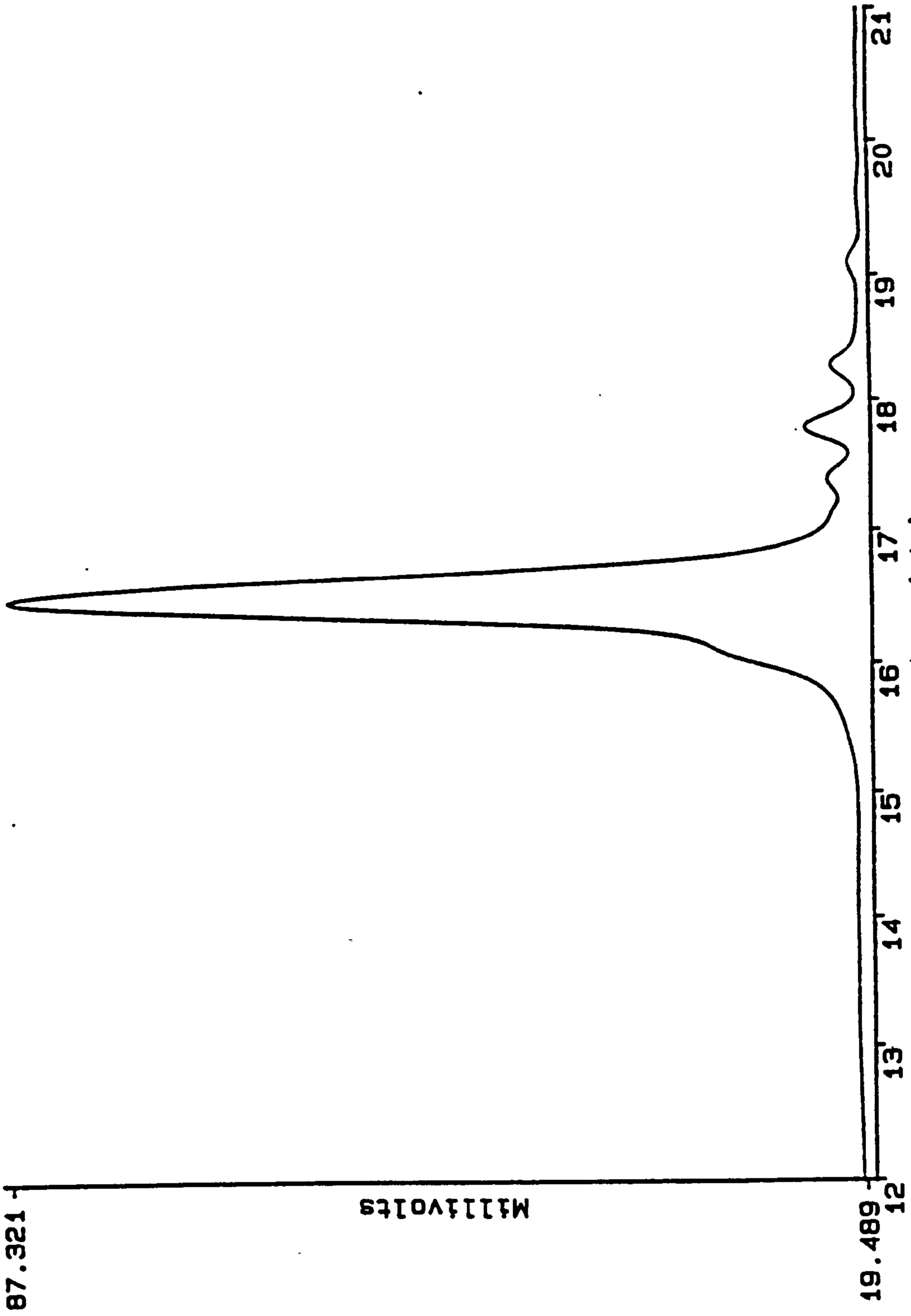

Figure 5.2 GPC chromatogram of the product of the reaction of T_8 + $HOSiMe_2(OSiMe_2)_3CH_3$.

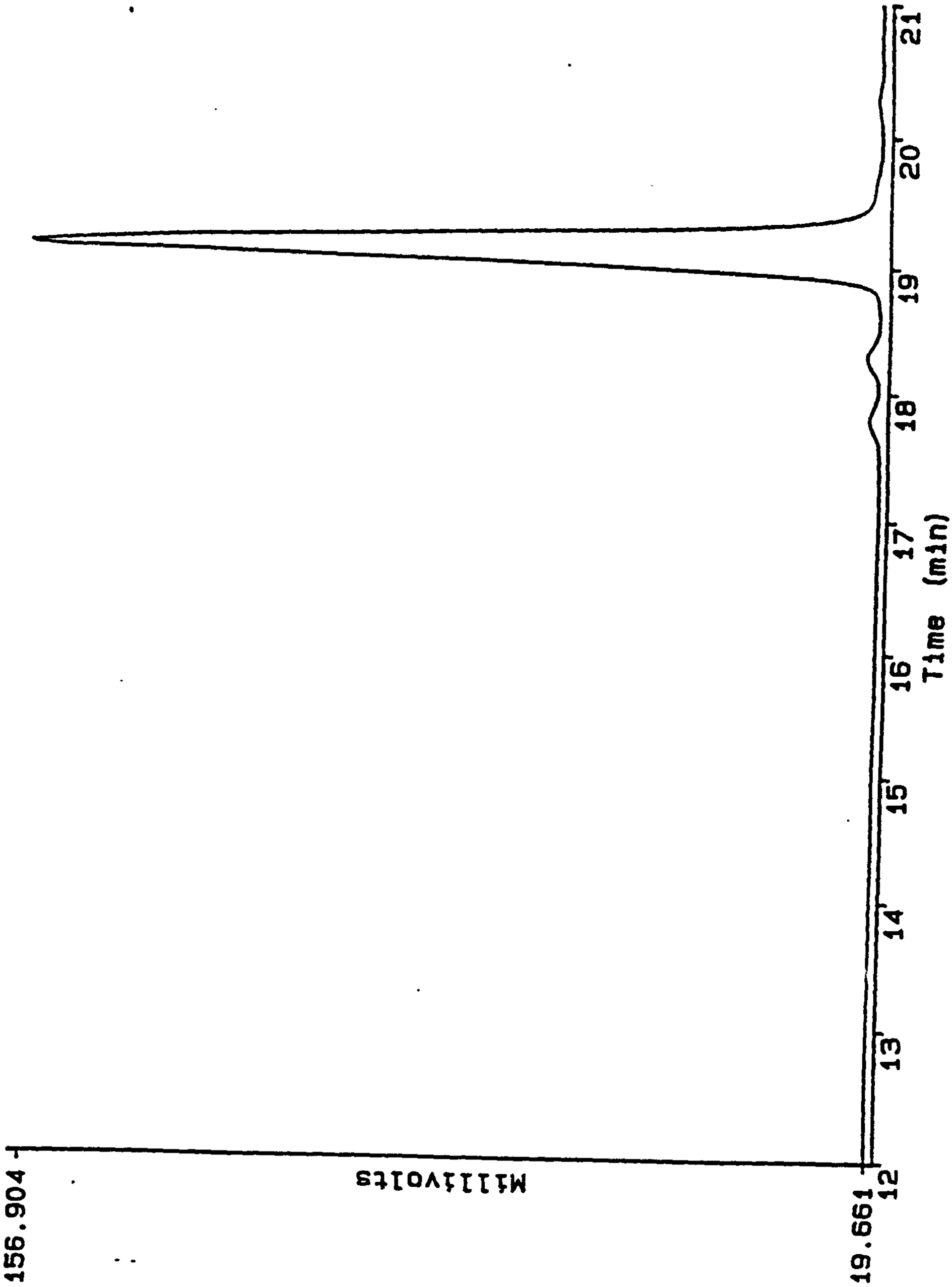

Figure 5.3 GPC chromatogram of $HOSiMe_2(OSiMe_2)_3CH_3$.

5.1.2 Hydrocarbon Octopus Molecule via Condensation Reaction

Similar to the reaction shown in reaction scheme 5.1, hydrocarbon functional molecules with a Si-O-C linkage of the hydrocarbon arms to the core were made using simple alcohols (e.g., $CH_3(CH_2)_5OH$).

As the ^{29}Si NMR spectrum (Figure 5.4) shows there are only Q-Si peaks as would be expected in the reaction. However, the Q-Si region has more than the one expected peak that would occur if the reaction resulted in the single expected product. Although there is one major peak at δ -102.70, there are many smaller not entirely resolved peaks, a group of which are between -94.0 and -95.2 ppm, another between -110.5 and -101.5 ppm, several on both sides of the main peak between -102.0 and -103.5, and finally some very small peaks between -109.5 and -110.0 ppm. Although the peaks around the main peak are not entirely resolved an estimate of the area of these other peaks relative to the total area is 40%. One possible explanation is again the SiH to SiH coupling (hydrolysis of SiH to SiOH followed by SiH + SiOH condensation) that is known to occur in the presence of any moisture[1-3] especially in the presence of an amine catalyst[4-5]. Mathias and Carothers[1] reported that an SiH functional dendrimer made from the polymerization of $CH_2=CHCH_2Si(OSiMe_2H)_3$ in CH_3CN and Et_2O catalyzed by H_2PCl_6 gradually became insoluble due to coupling of SiH bonds through Si-O-Si formation[1].

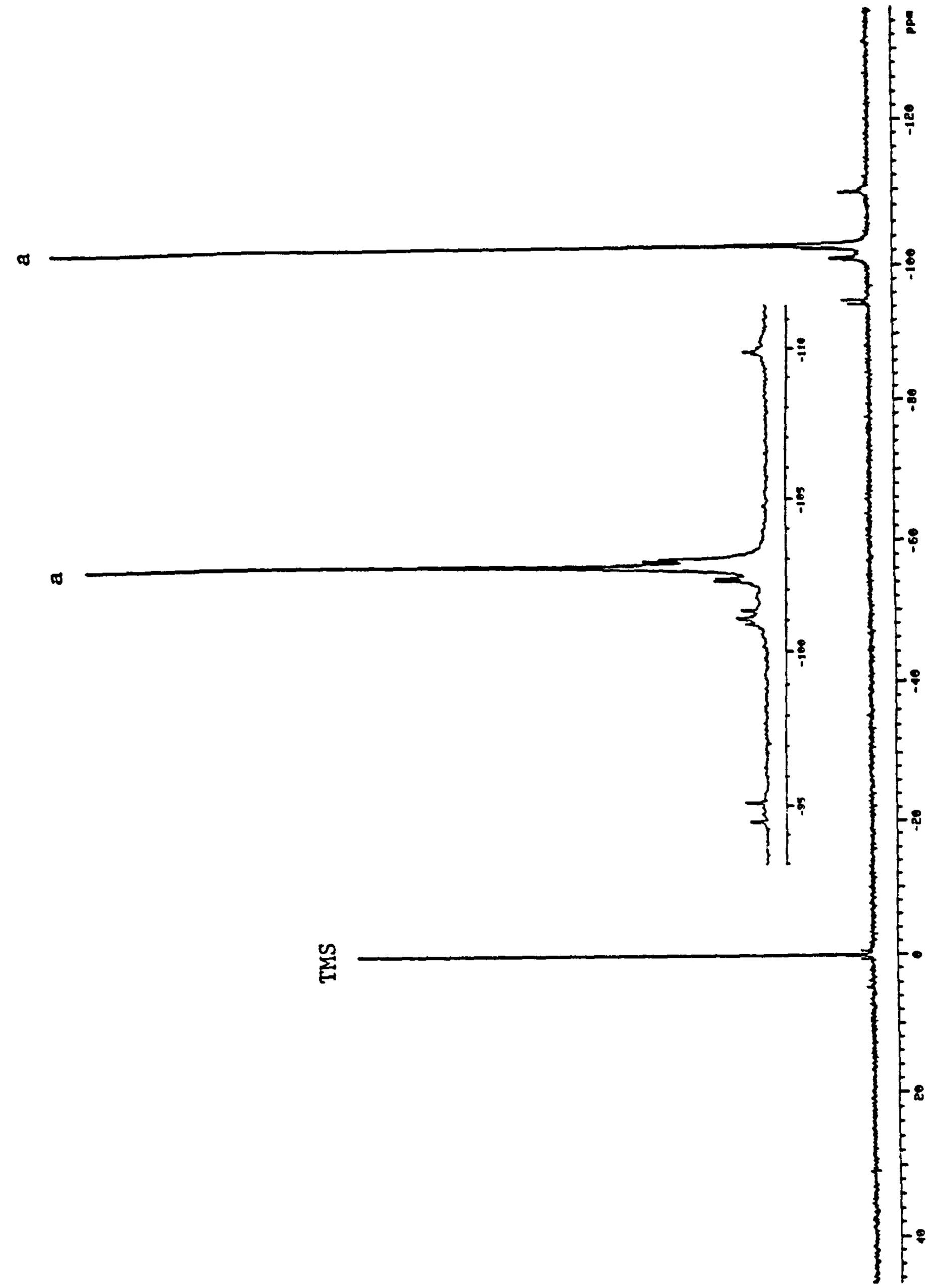

Figure 5.4 ^{29}Si NMR spectrum for the product of the reaction of $T_8 + HO(CH_2)_5CH_3$.

The GPC chromatogram of the product of the reaction of T_8 and hexyl alcohol (Figure 5.5) suggests that this SiH coupling leading to linking of cages together is occurring. A peak at retention time 17.26 is most likely the expected product, the hydrocarbon functional octopus with Si-O-C linkages of the eight carbon chains to a single T_8 core. There are additional peaks that are quite large in comparison. The peak at retention time 16.76 minutes could be two cages linked at one corner through a Si-O-Si bond each cage then having the remaining 7 corners functionalized with the hexyl chains. There are at least two other GPC peaks although not very well resolved at approximately 16.4 and 16.2 minutes that are most likely the result of linkage of three and four cages through Si-O-Si bonds.

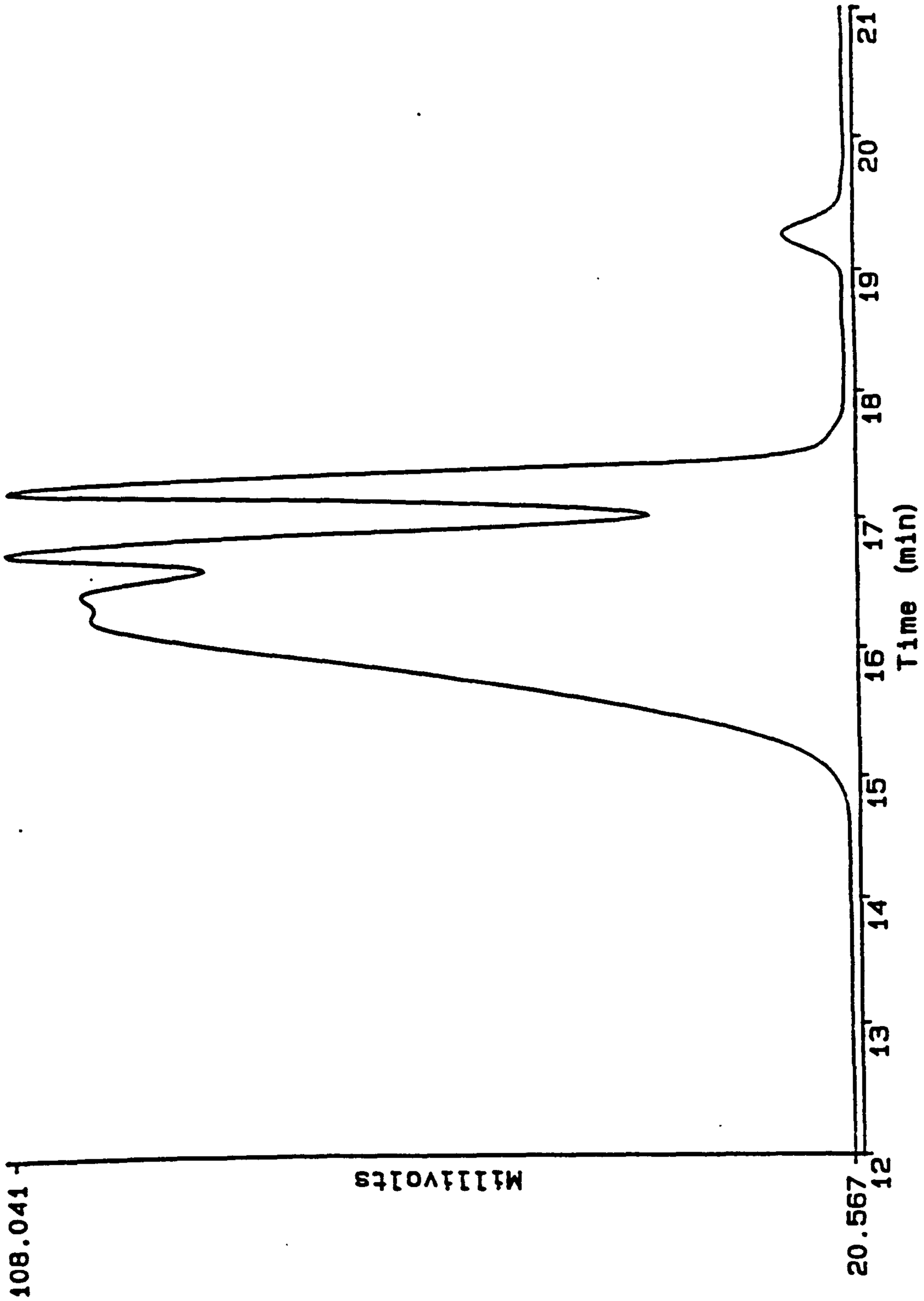

Figure 5.5 GPC chromatogram of the product of the reaction of $T_8 + HO(CH_2)_5CH_3$.

5.2 Conclusions

The work presented in this chapter serves to illustrate a route other than the previously described hydrosilylation route to forming octopus molecules. The use of condensation reactions involving the SiH of $(HSiO_{3/2})_8$ with R-OH and Si-OH functional materials was investigated and it was found that it is possible to make octopus molecules using this route and that the linkage of the pendant groups was through Si-O-Si and Si-O-C bonds, respectively. However, the characterization data demonstrates the difficulties that can occur in using this route when any moisture is present. Although great care was taken to eliminate all moisture during reaction, the resulting products still contained significant by-products due to coupling of SiH of cages leading to octopus dimers, trimers, and higher analogues.

5.3 Experimental

5.3.1 General

A Varian VRX200s NMR spectrometer fitted with a 5 mm probe and operating at 39 MHz was used to obtain ^{29}Si NMR spectra. GPC and FTIR analyses were accomplished using the techniques described in Chapter Two, Section 2.4.7.

5.3.2 Synthesis of $(HSiO_{3/2})_8$

The procedure for obtaining T_8 hydrogen silsesquioxane outlined in Chapter Two, Section 2.4.1, was used.

5.3.3 Synthesis of $HOSiMe_2(OSiMe_2)_3CH_3$

$HOSiMe_2(OSiMe_2)_3CH_3$ was made by first synthesizing $ClSiMe_2(OSiMe_2)_3CH_3$ followed by its hydrolysis to obtain $HOSiMe_2(OSiMe_2)_3CH_3$ as previously reported[6].

Hexamethylcyclotrisiloxane (D_3, 100.0 grams, 0.45 mol), Me_3SiCl (48.84 grams, 0.45 mol), CH_3CN (30.55 grams), and $Me_2NC(O)CH_3$ (3.12 grams) were placed in a 500 ml, 1-neck, round bottom flask with stir bar. The reaction mixture was heated to 40 °C to melt/dissolve the D_3. The mixture remained at 40 °C for approximately 3 hours at which time the desired $ClSiMe_2(OSiMe_2)_3CH_3$ was present at about 24% by GC analysis. The reaction mixture was cooled to room temperature and was stirred overnight. After stirring overnight and with one hour of additional heating at 40 °C GC analysis indicated the presence of 58.3% desired product. The reaction mixture was cooled and filtered to remove any unreacted D_3 solid. The liquid product, $ClSiMe_2(OSiMe_2)_3CH_3$, was obtained in higher purity (98.1% by GC) by distillation at reduced pressure (0.20 mm Hg) and pot temperature of 60 °C.

A portion of the purified $ClSiMe_2(OSiMe_2)_3CH_3$ was hydrolyzed to obtain the desired end product $HOSiMe_2(OSiMe_2)_3CH_3$. In a 500 ml separatory funnel, 41.3 grams of crushed ice (distilled, deionized H_2O), 38.51 grams of Et_2O, and 3.40 grams of concentrated NH_4OH (28-30% NH_3 in water) were placed. An addition flask containing 14.14 grams of the purified $ClSiMe_2(OSiMe_2)_3CH_3$ was connected to the separatory funnel.

The $ClSiMe_2(OSiMe_2)_3CH_3$ was added in small increments with swirling and venting of the funnel. After adding all the $ClSiMe_2(OSiMe_2)_3CH_3$, the aqueous phase was drained from the funnel and 29 ml of hexane was added. The organic phase was then washed with 100 ml aliquots of deionized distilled H_2O, followed by draining of the aqueous phase after each wash. Eight water washes were done before the aqueous phase was free of Cl by $AgNO_3$ test. One additional wash was then done and the aqueous wash drained off. Na_2SO_4 (11.78 grams) was then added to the funnel and the organic phase was left to dry for three days. After filtering and stripping of the volatiles, 7.30 grams of the desired final product, $HOSiMe_2(OSiMe_2)_3CH_3$, which was a liquid was obtained. A silylated sample (4 drops of MeCN, 5 drops Et_2O, 5 drops $Me_3SiNHSiMe_3$, 4 drops product, trace F_3CCOOH) was 98.5% pure by GC analysis. A ^{29}Si NMR spectrum of the $HOSiMe_2(OSiMe_2)_3CH_3$ is shown in Figure 5.6. There are four peaks at δ 7.78 ppm (M-Si of $SiMe_3$ terminus), δ -11.03 (M-Si of $SiMe_2OH$ terminus), and δ -20.88 and -21.01 ppm (the two D-Si). The integrated areas of the four peaks were 1:1:1:1. The GPC chromatogram of the product was shown in Figure 5.3. The main product peak had a retention time of 19.11 minutes and looked mondispersed. There were two very small peaks (<2% total area) at 18.27 and 17.79 minutes. Only GC data for $HOSiMe_2(OSiMe_2)_3CH_3$ were described in the previous report of this compound[6].

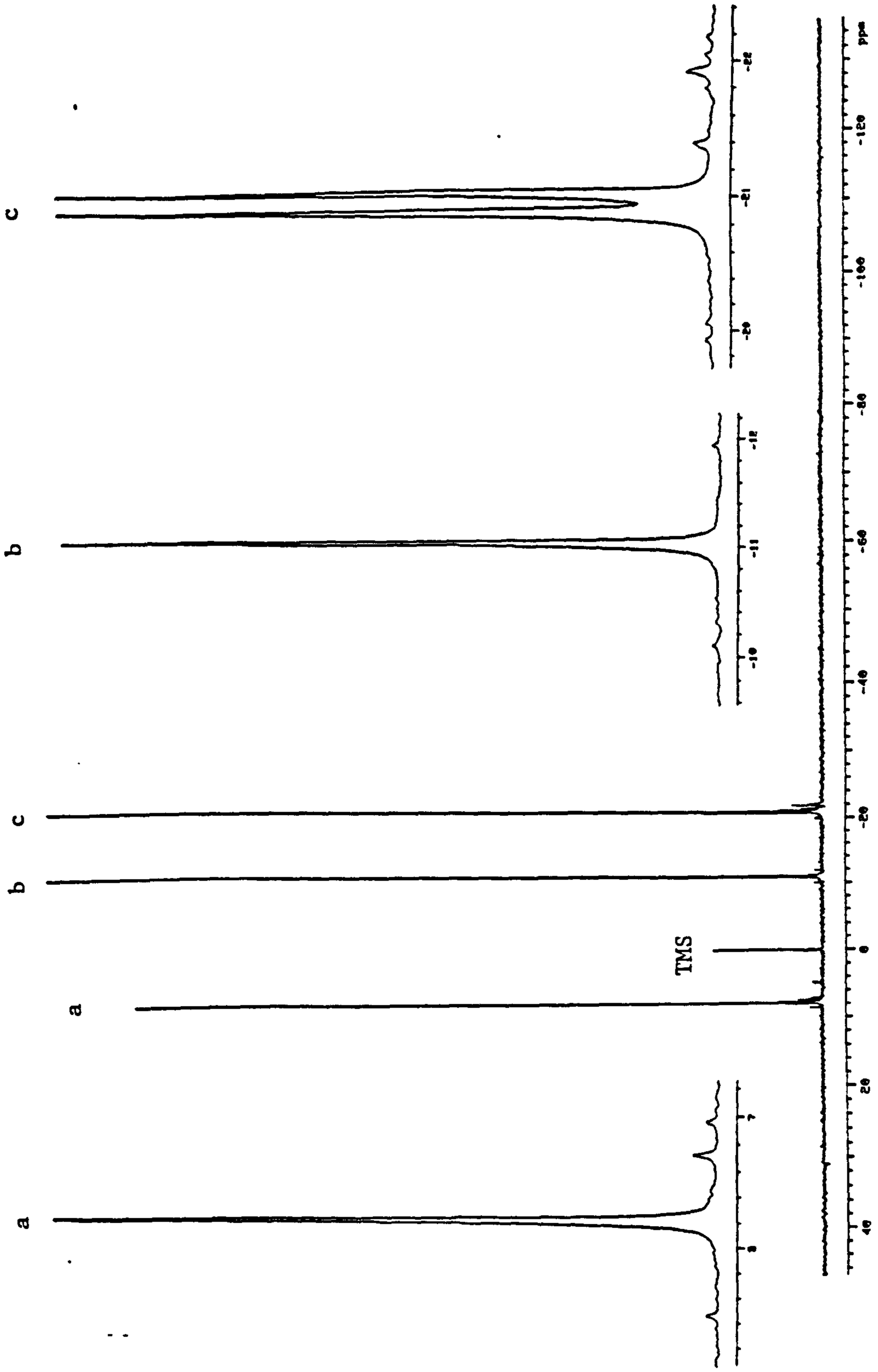

Figure 5.6 ^{29}Si NMR spectrum of $HOSiMe_2(OSiMe_2)_3CH_3$.

5.3.4 Synthesis of $[SiO_{3/2}]_8[OSiMe_2(OSiMe_2)_3CH_3]_8$

T_8 (0.50 grams, 1.2 mmol), excess $Me_3Si(OSiMe_2)_3OH$ (3.35 grams, 10.7 mmol), and 10 µl Et_2NOH (used as supplied from Aldrich Chemical Co.) were placed in a 50 ml 3-neck, round bottom flask equipped with a thermometer, H_2O condenser, and stir bar. The reaction mixture was stirred and a light flow of dry N_2 was maintained while the reaction mixture was heated to 89 °C over a 80 minute period at which time all the SiH appeared to be gone by FTIR.

The ^{29}Si NMR spectrum of the product was shown in Figure 5.1. There is a main peak at δ -110.16 ppm (Q-Si, $O_{3/2}\underline{Si}$-O of the cage) referenced to TMS at 0.0 ppm. There are possibly a couple of very small peaks that are not very well resolved from the noise around the peak at -110.16 ppm that were postulated to be the result of any SiH to SiH coupling (hydrolysis and condensation) leading to cage to cage condensation. There was a single peak for the M-Si of each appendage terminus ($O\underline{Si}Me_3$) at δ 7.24 ppm. There were at least 6 D-Si peaks between δ -19 and -22 ppm. Three of these peaks D-Si peaks can be assigned to the D-silicons of the siloxane chain appendages off the core (D-Si closest to the Si of the cage, the next D-Si along the siloxane chain, and the third along the chain nearest the M-Si at the chain terminus). The additional D-Si peaks were postulated to be the result of some silanol condensation reactions of the $HOSiMe_2(OSiMe_2)_3CH_3$ with itself although this was not proven.

The GPC chromatogram of the reaction product was shown in Figure 5.2. The main product peak was seen at a retention time of 16.50 minutes. There was a slight broadening of the product peak on the high molecular weight side which was postulated to be the result of cage to cage condensation that would result in an octopus dimer. In addition to the product peak in the GPC there appeared to be lower molecular weight impurities. A small peak at 19.11 minutes was found to be residual $HOSiMe_2(OSiMe_2)_3CH_3$ as confirmed by the GPC of the starting material itself (Figure 5.3). There were three other low molecular weight peaks at 18.27 minutes, 17.79 minutes, and 17.39 minutes that were proposed to be the result of silanol condensation reactions of the $HOSiMe_2(OSiMe_2)_3CH_3$ with itself.

5.3.5 Synthesis of $[SiO_{3/2}]_8[O(CH_2)_5CH_3]_8$

Into a 15 ml 3-neck round bottom flask equipped with stir bar, H_2O condenser, thermometer, and gas inlet tube was placed 0.52 grams of T_8 (1.2 mmol), and 1.05 grams of $CH_3(CH_2)_5OH$ (10.3 mmol, 98% used as supplied from Aldrich Chemical Co.). The reaction mixture was stirred while a flow of dry N_2 was maintained over it. Upon addition of 20 µl Et_2NOH (used as supplied from Aldrich Chemical Co.) gas starting evolving very vigorously and an exotherm to a maximum temperature of 71 °C took place within five minutes after the catalyst was added. The reaction mixture was allowed to cool to room temperature at which time no solid T_8 was visible and FTIR analysis indicated that no SiH was observable at 2260 cm^{-1}.

The ^{29}Si NMR spectrum of the product of the reaction was previously shown in Figure 5.4. The Q-Si region had more than the one expected peak that would occur if the reaction resulted in the single expected product. There was one major peak at δ -102.70 and many smaller not entirely resolved peaks, a group of which were between -94.0 and -95.2 ppm, another between -110.5 and -101.5 ppm, several on both sides of the main peak between -102.0 and -103.5, and finally some very small peaks between -109.5 and -110.0 ppm. Although the peaks around the main peak were not entirely resolved, the area of these other peaks relative to the total area was estimated to be approximately 40%. It was proposed that SiH to SiH coupling (hydrolysis and condensation) between cages with octopus dimer, trimer and higher oligomers resulting were the cause of these additional Q-Si peaks in the ^{29}Si NMR spectrum.

The GPC chromatogram of the product was previously shown in Figure 5.5. A peak at retention time 17.26 minutes was assigned to the expected product, the hydrocarbon functional octopus with Si-O-C linkages of the eight carbon chains to a single T_8 core. The peak at retention time 16.76 minutes was postulated to be two cages linked at one corner through a Si-O-Si bond with each cage then having the remaining 7 corners functionalized with the hexyl chains. There were at least two other GPC peaks although not very well resolved at approximately 16.4 and 16.2 minutes that were thought to be the result of linkage of three and four cages through Si-O-Si bonds.

5.4 References

1. Mathias, L.J.; Carothers, T.W. *J. Am. Chem. Soc.* **1991**, 113, 4043-4044.

2. Bazant, V.; Chvalovsky, V.; Rathousky, J. Organosilicon Compounds; Academic Press: New York, 1965; p. 137.

3. Noll, W. Chemistry and Technology of Silicones, Academic Press: New York, 1968; pg. 397.

4. Baney, R.H.; Bilgrien, C.J.; Broderick, D.W.; Carpenter, L.E. U.S. Patent 5,116,637.

5. Eaborn, C. Organosilicon Compounds, Butterworths Scientific Publications: London, 1960; pg. 200.

6. Chu, H-K.; Cross, R.P.; Crossan, D.J. *J. of Organomet. Chem.* **1992**, 425, 9-17.

Chapter Six

Dendrimers with Silsesquioxane Cores

6.0 Introduction

Having shown in the last two chapters that a variety of functionalities could be place on T_8 including dual functional chains, it appeared possible to expand into dendrimers with silsesquioxane cores. In this chapter, several approaches were used with varying degrees of success to make dendrimer molecules based on silsesquioxanes. Convergent (in which the arms or branches were constructed and then connected to the core) and divergent (in which the macromolecule was built from the core outward) approaches were attempted. Each attempted synthesis will be discussed to point out difficulties in preparing monodispersed molecules of this size. Finally a successful means of making a very pure, well characterized dendrimer will be presented.

6.1 Results

6.1.1 Attempted Divergent Synthesis of a 16-Armed Dendrimer: $[SiO_{3/2}]_8$-$[OSiMe_2(OSiMe_2)_3CH_2CH_2Si(Me)(OSiMe_3)_2]_8$

Dual functional chains were reacted with T_8 with the aim of reacting one functionality with the SiH of $(HSiO_{3/2})_8$ and leaving the other functionality available for subsequent reaction to form dendrimer molecules. For instance, using a condensation reaction similar to that shown in reaction scheme 5.1, a siloxane that had OH functionality at one end and vinyl functionality at the other was reacted with T_8 hydrogen silsesquioxane as shown

in reaction scheme 6.1. Because amines are known to inhibit the hydrosilylation of unsaturated substrates by SiH functional materials[1,2] while catalyzing the reaction of SiH with SiOH functional materials[3], the diethyl hydroxyl amine catalyst was used.

$$(HSiO_{3/2})_8 + 8\ HOSiMe_2(OSiMe_2)_3CH{=}CH_2 \rightarrow$$
$$[SiO_{3/2}]_8[OSiMe_2(OSiMe_2)_3CH{=}CH_2]_8 + H_2 \qquad (6.1)$$

The vinyl functionality at the end of each of the eight arms of the octopus formed in reaction scheme 6.1 was then available for hydrosilylation by an SiH containing material such as bis(trimethylsiloxy)methylsilane, $Me_3SiOSi(Me)(H)OSiMe_3$, to form a 16-armed dendrimer molecule as shown in reaction scheme 6.2.

$$[SiO_{3/2}]_8[OSiMe_2(OSiMe_2)_3CH{=}CH_2]_8 + 8\ Me_3SiOSi(Me)(H)OSiMe_3 \rightarrow$$
$$[SiO_{3/2}]_8[OSiMe_2(OSiMe_2)_3CH_2CH_2Si(Me)(OSiMe_3)_2]_8 \qquad (6.2)$$

The dendrimer was characterized at each step of its construction. The ^{29}Si NMR of the reaction product of T_8 and $HOSiMe_2(OSiMe_2)_3CH{=}CH_2$ catalyzed by the hydroxyl amine (Figure 6.1) shows no T-Si peak which was a good indication that the OH end of the dual functional $HOSiMe_2(OSiMe_2)_3CH{=}CH_2$ could be reacted without the vinyl end participating. However, as the ^{29}Si NMR shows there is more than the one expected Q-Si peak around δ -110 ppm. As was seen in the last chapter where this catalyst was used for condensation of SiOH and ROH functional chains with SiH of T_8, SiH to SiH coupling can occur and this may

be occurring in this reaction. The ratio of M:D:Q peak areas in the ^{29}Si NMR spectrum was found to be 1.3:5.6:1.0 instead of the expected 1:3:1 ratio if the reaction had gone cleanly. If the multiple peaks in the ^{29}Si NMR was simply due to cage to cage coupling reactions, one would expect to see a reduction in the areas for the M-Si and D-Si instead of the increase. The increase in M-Si and D-Si is suggestive of SiOH to SiOH condensations of the $HOSiMe_2(OSiMe_2)_3CH{=}CH_2$ starting material. The multiple peaks in the M-Si and D-Si regions of the ^{29}Si NMR spectrum would also support this.

The GPC chromatogram of the reaction product of the first step of the dendrimer construction (Figure 6.2) indicates that significant cage to cage coupling is occurring leading to large amounts of dimer, trimer and higher species. In addition to what is presumably the octopus molecule at retention time 16.70 minutes, there are higher molecular weight peaks at 16.16 and 15.91 minutes that are proposed to be the dimer and trimer. In addition to the large amount of high molecular weight impurities, there is a rather large lower molecular weight peak at retention time 17.97 minutes that is suggestive of the reaction product of SiOH to SiOH condensations of the $HOSiMe_2(OSiMe_2)_3CH{=}CH_2$ starting material proposed from the ^{29}Si NMR results.

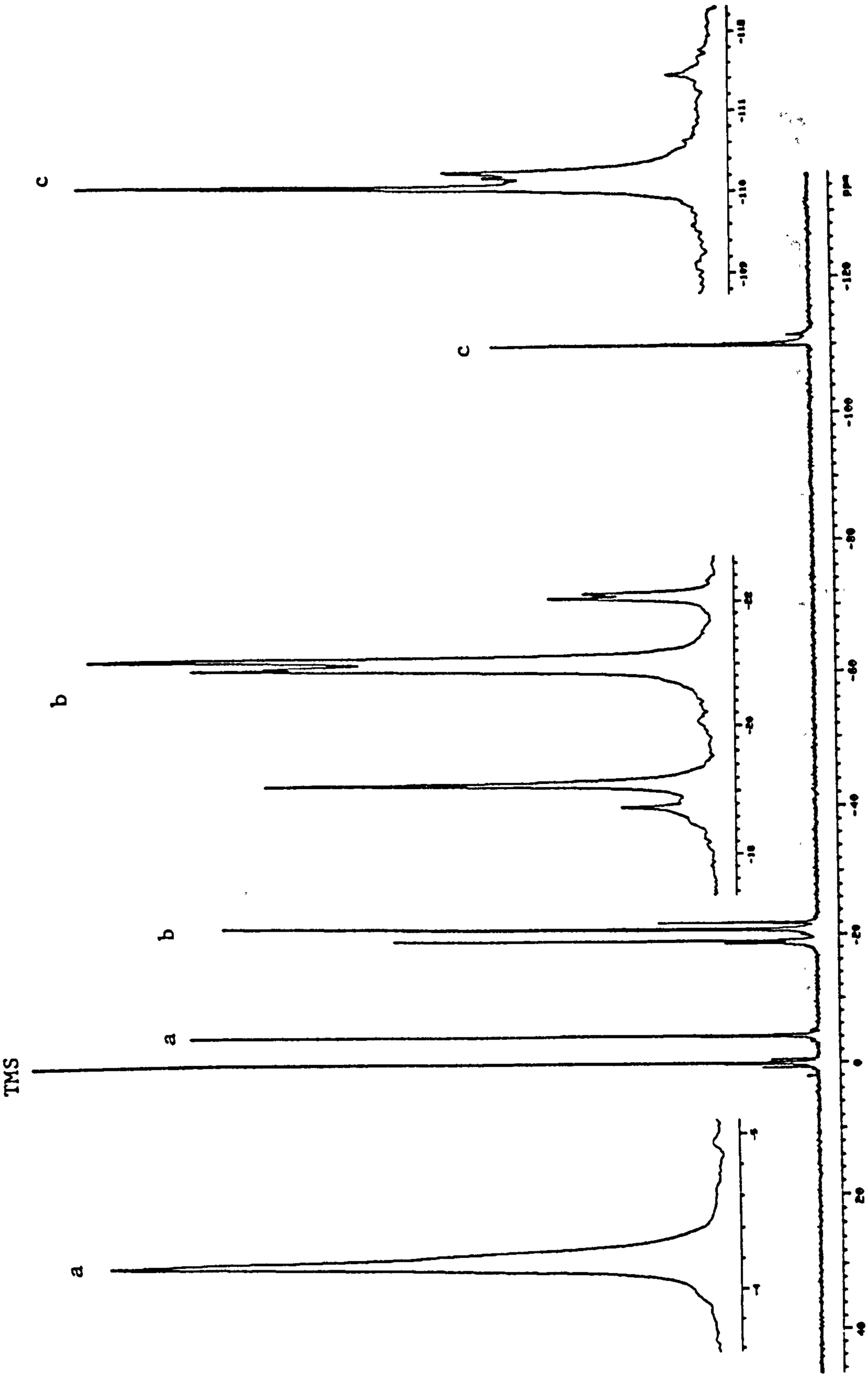

Figure 6.1 ^{29}Si NMR spectrum for the product of the reaction of T_8 + $HOSiMe_2(OSiMe_2)_3CH{=}CH_2$.

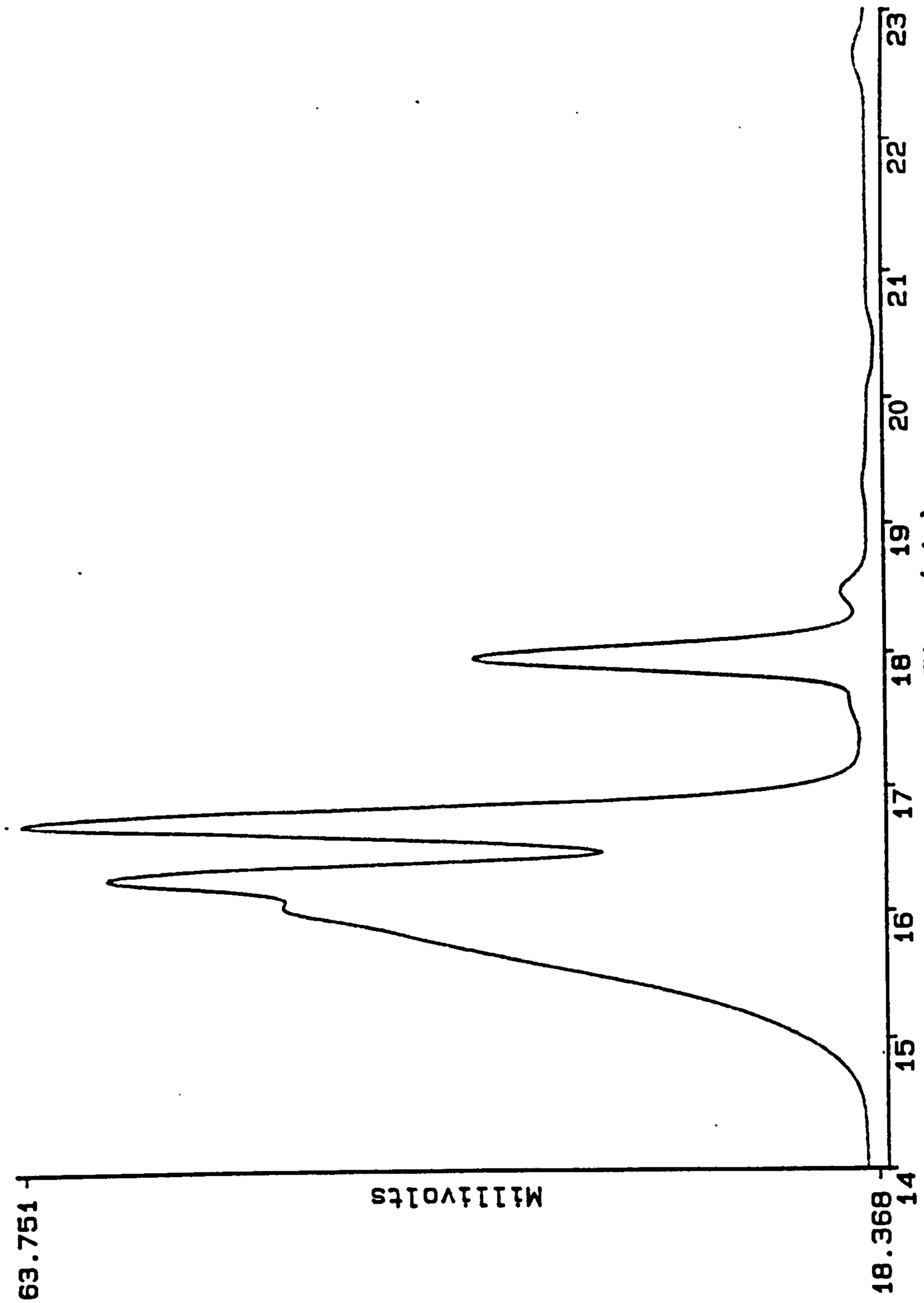

Figure 6.2 GPC chromatogram of the product of the reaction of T_8 + $HOSiMe_2(OSiMe_2)_3CH=CH_2$.

The GPC chromatogram of the $HOSiMe_2(OSiMe_2)_3CH=CH_2$ starting material (Figure 6.3) contains this same impurity but at a lower level. It appears that with heat and other reaction conditions (catalyst, possibly H_2O) this impurity increase significantly which is also suggestive of a condensation reaction product.

The second step of the dendrimer formation, the hydrosilylation of the unsaturated functional groups at the end of each appendage of the cage by Bis(trimethylsiloxy)methylsilane or $Me_3SiOSi(Me)(H)OSiMe_3$ was done before realizing the extent of high molecular weight impurities (dimer, trimer, etc.) and other by-products that had formed in the first step. And as would be expected the presence of the higher oligomers resulted in the same type of distribution of species in the final dendrimer reaction mixture as shown by the GPC chromatogram (Figure 6.3). The ^{29}Si NMR spectrum of this reaction product (Figure 6.4) was found to not surprisingly have the multiple peaks in the Q-Si region as well as the multiple peaks in the M-Si and D-Si regions.

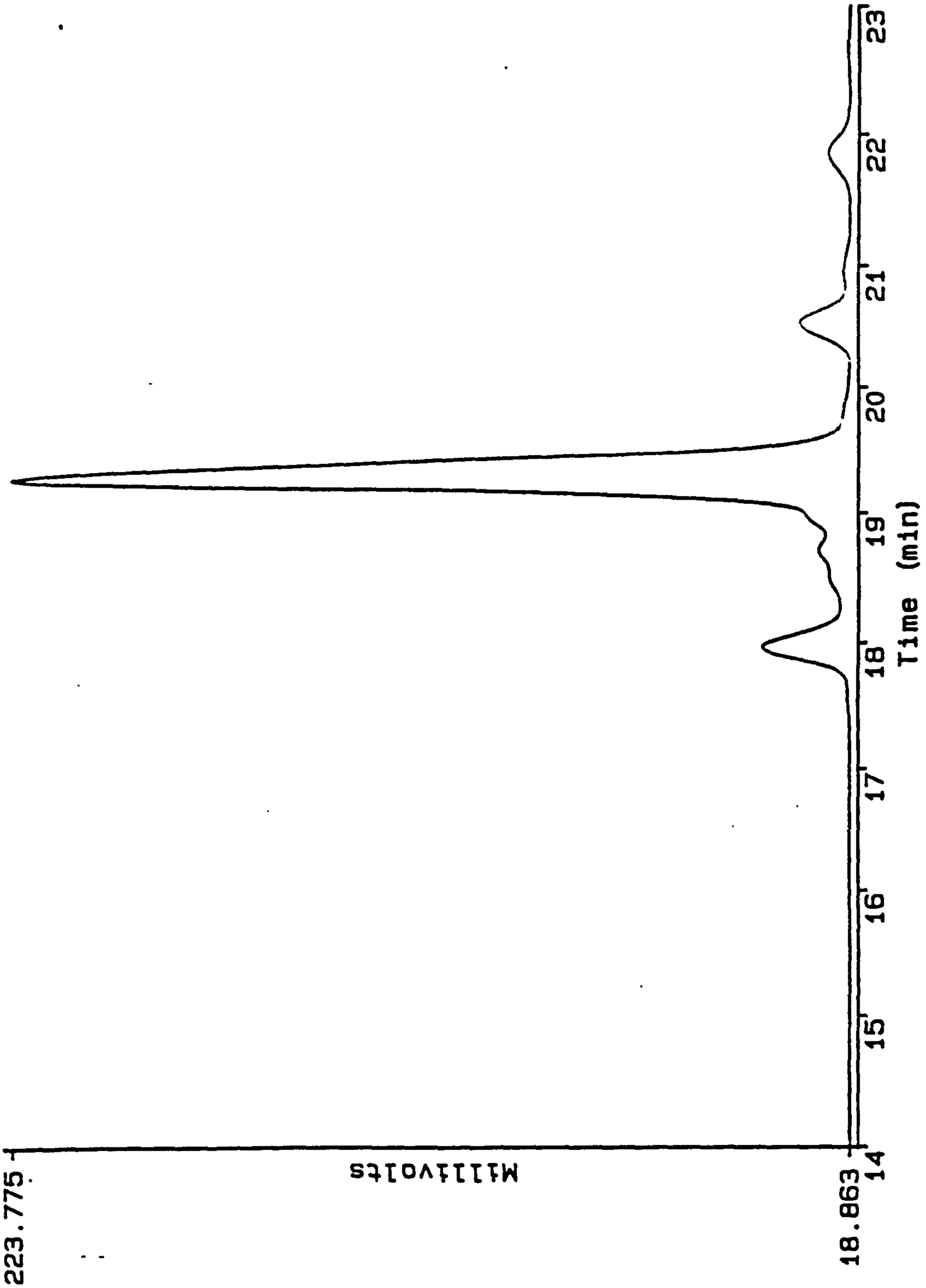

Figure 6.3 GPC chromatogram of $HOSiMe_2(OSiMe_2)_3CH=CH_2$.

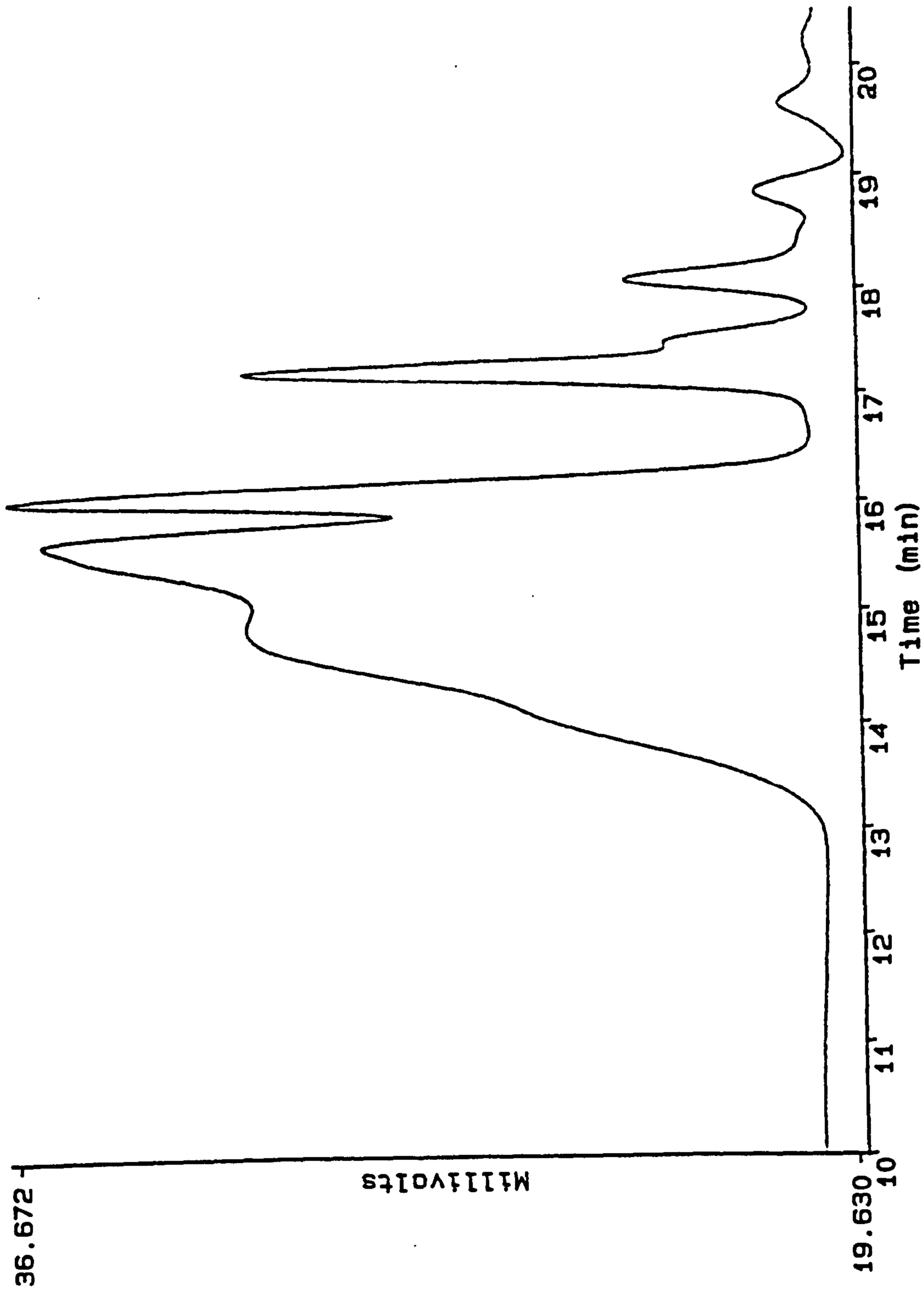

Figure 6.4 GPC chromatogram of the product of the reaction of T_8 + $HOSiMe_2(OSiMe_2)_3CH=CH_2$ subsequently reacted with $Me_3SiOSi(Me)(H)OSiMe_3$.

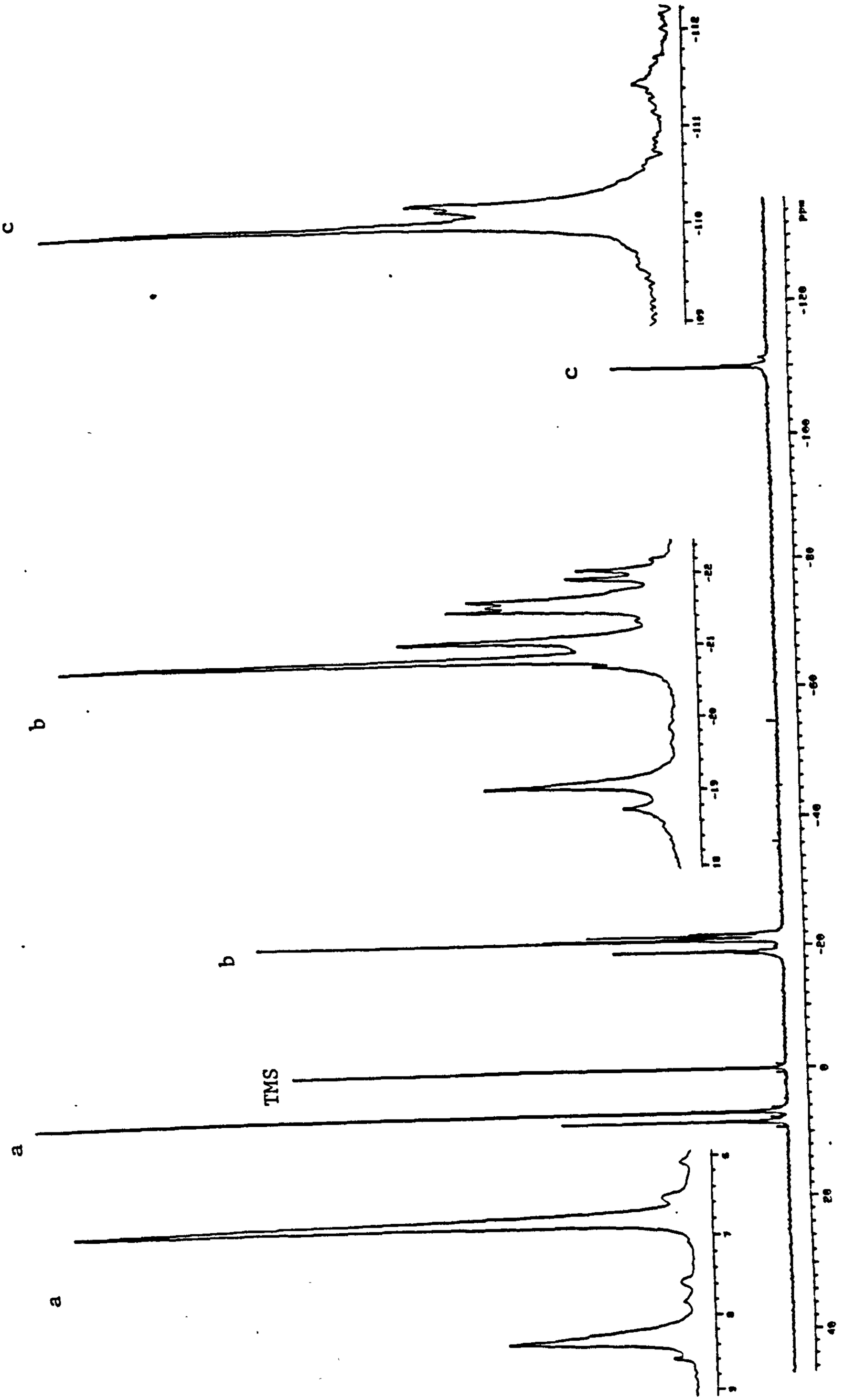

Figure 6.5 ^{29}Si NMR spectrum for the product of the reaction of T_8 + $HOSiMe_2(OSiMe_2)_3CH=CH_2$ subsequently reacted with $Me_3SiOSi(Me)(H)OSiMe_3$.

6.1.2 Attempted Convergent Synthesis of a 48-Armed Dendrimer: $(SiO_{3/2})_8$-$[OCH_2C[CH_2OCH_2CH_2CH_2Si(Me)(OSiMe_3)_2]_3]_8$

A convergent approach involving hydrosilylation of a compound with multiple unsaturated functionality by an SiH functional siloxane was done to make branched dendrons that were then placed on the T_8 core using a condensation reaction.

Bis(trimethylsiloxy)methylsilane or $Me_3SiOSi(Me)(H)OSiMe_3$ was reacted first with pentaerythritol triallylether, $HOCH_2C(CH_2OCH_2CH{=}CH_2)_3$, to make $HOCH_2C[CH_2OCH_2CH_2CH_2Si(Me)(OSiMe_3)_2]_3$, a six branched material, as shown in the first reaction of Figure 6.6. The product of this first reaction was then used in a condensation reaction with T_8 to make the 48-armed dendrimer as depicted in the second reaction in Figure 6.6.

As with the previous attempted dendrimer synthesis characterization of the product at each step of the synthesis was done. The ^{29}Si NMR spectrum of the product of the reaction of $Me_3SiOSi(Me)(H)OSiMe_3$ with pentaerythritol triallylether [PETAE, $HOCH_2C(CH_2OCH_2CH{=}CH_2)_3$] is shown in Figure 6.7. As the spectrum shows there is the expected D-Si peak {δ -21.55 ppm, $(HOCH_2C[CH_2OCH_2CH_2CH_2\underline{Si}(Me)(OSiMe_3)_2]_3$} and the M-Si peak {δ 7.17 ppm, $HOCH_2C[CH_2OCH_2CH_2CH_2Si(Me)(O\underline{Si}Me_3)_2]_3$} in approximately the expected M:D ratio of 2:1. However, both the D-Si and M-Si peaks have smaller not entirely resolved peaks around them.

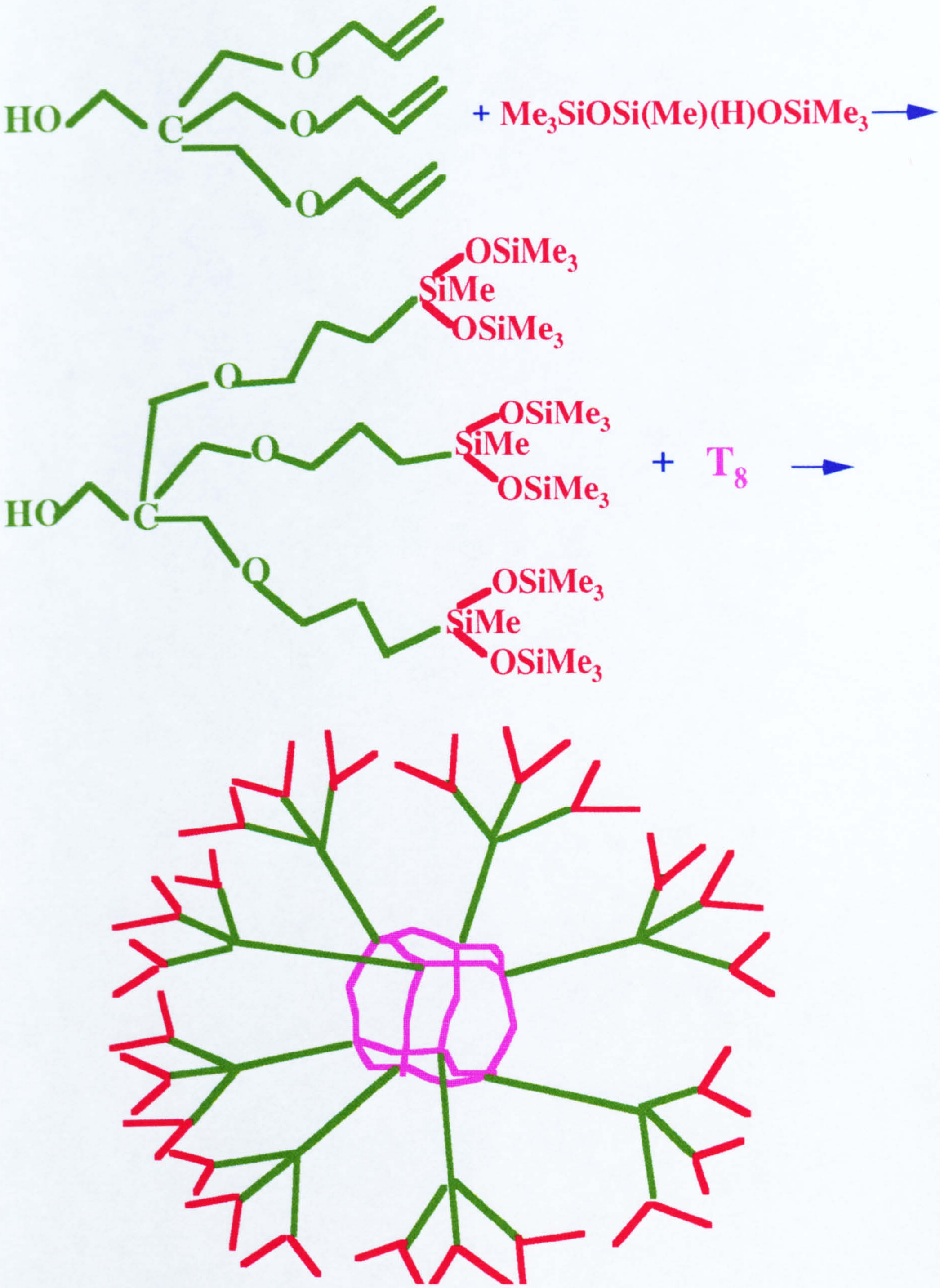

Figure 6.6. Schematic of reaction steps involved in making a 48-armed dendrimer with silsesquioxane core.

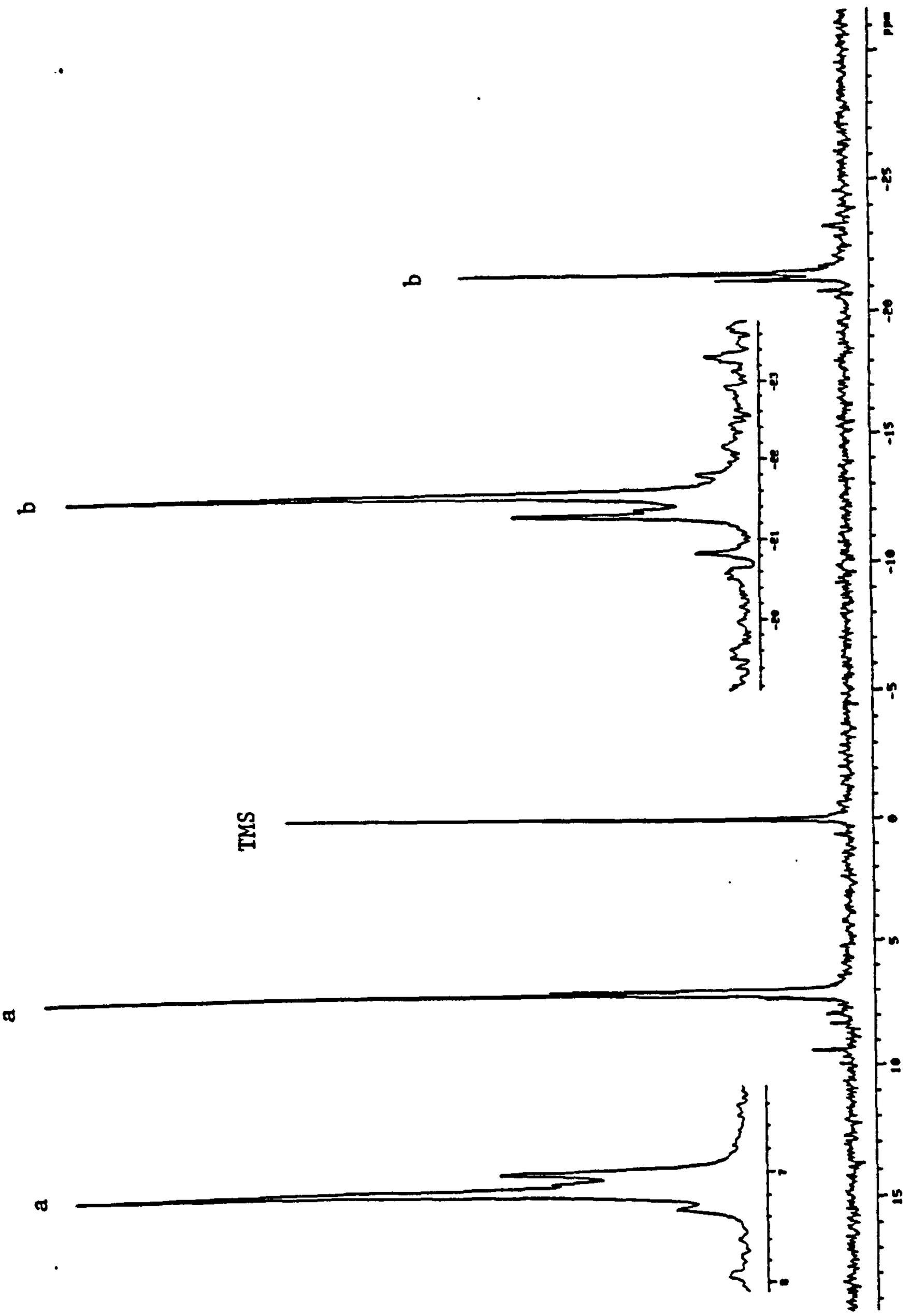

Figure 6.7 ^{29}Si NMR spectrum for the product of the reaction of $Me_3SiOSi(Me)(H)OSiMe_3$ with $HOCH_2C(CH_2OCH_2CH{=}CH_2)_3$.

The GPC chromatogram of the the product of the reaction of $Me_3SiOSi(Me)(H)OSiMe_3$ with $HOCH_2C(CH_2OCH_2CH{=}CH_2)_3$ (Figure 6.8) shows the main product peak at retention time 17.85 minutes. There appears to be a significant amount of higher molecular weight impurities, one with retention time 17.35 minutes and another with retention time 16.95 minutes. It is unclear the source of these higher molecular weight impurities until one looks at the GPC chromatogram of the $HOCH_2C(CH_2OCH_2CH{=}CH_2)_3$ starting material (Figure 6.9). The $HOCH_2C(CH_2OCH_2CH{=}CH_2)_3$ has a retention time of 20.30 minutes and there is another higher molecular weight peak at 19.17 minutes that is quite significant in size (~25% of the total area). This higher molecular weight impurity appears to have reacted with the $Me_3SiOSi(Me)(H)OSiMe_3$ to make the high molecular weight shoulder of the main product peak in Figure 6.8.

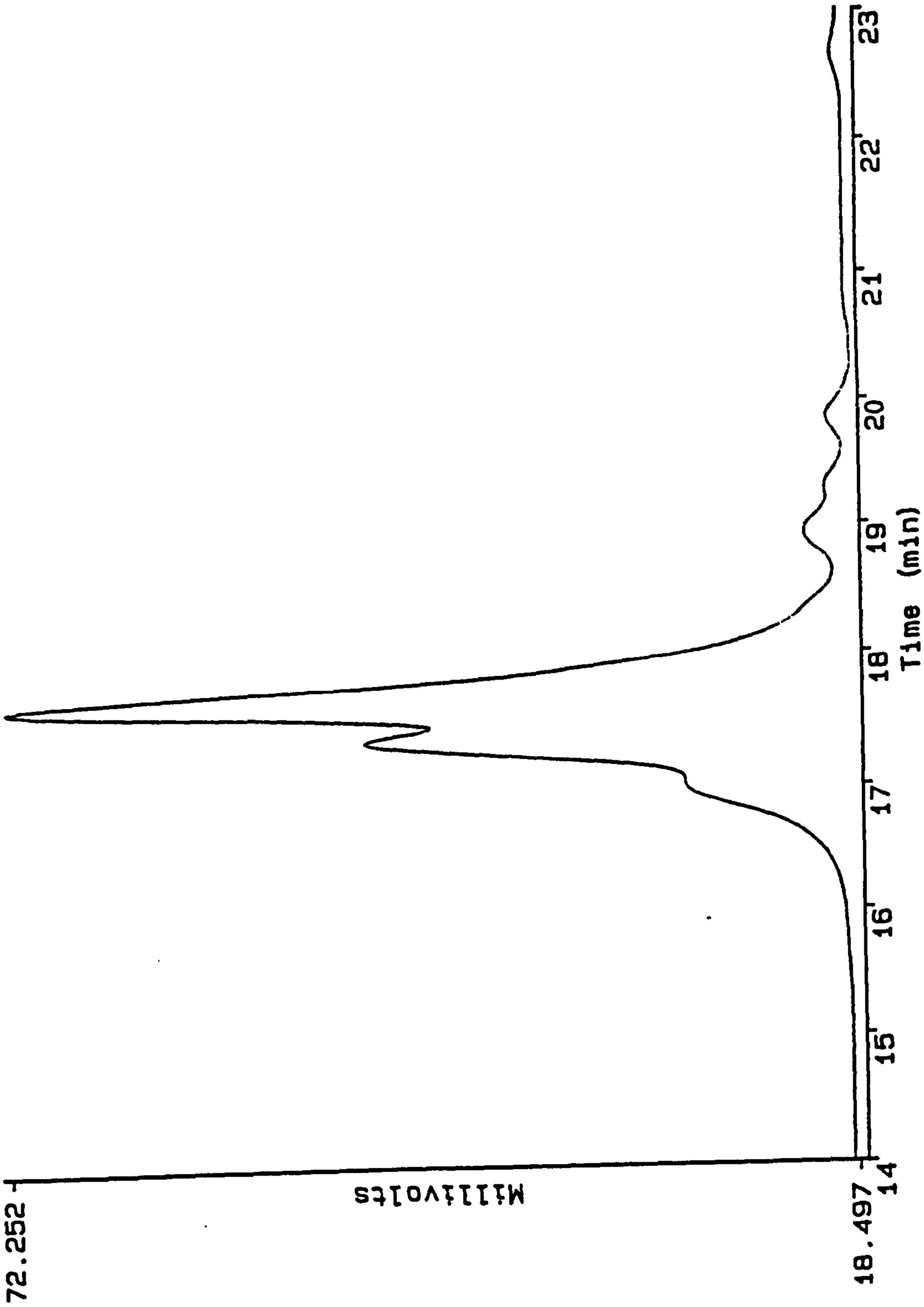

Figure 6.8 GPC chromatogram of the product of the reaction of $Me_3SiOSi(Me)(H)OSiMe_3$ with $HOCH_2C(CH_2OCH_2CH{=}CH_2)_3$.

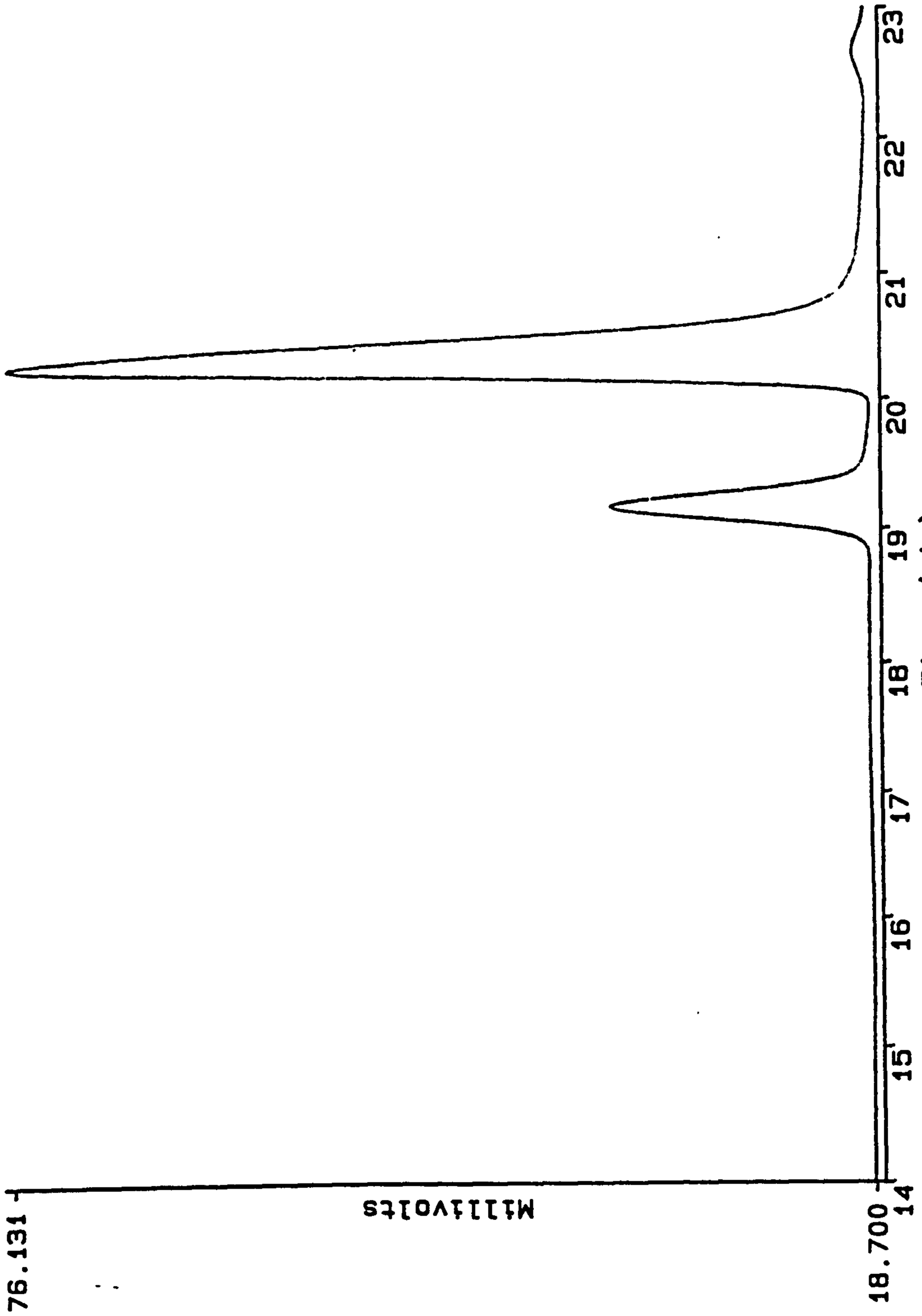

Figure 6.9 GPC chromatogram of $HOCH_2C(CH_2OCH_2CH{=}CH_2)_3$.

Continuation of the dendrimer construction by attachment of the unpure branches to the T_8 core, of course, resulted in a reaction mixture containing the desired dendrimer and significant amounts of other higher molecular weight materials as shown by the GPC chromatogram of the reaction mixture (Figure 6.10). The GPC also indicates that a large excess of starting material [previous reaction product of $Me_3SiOSi(Me)(H)OSiMe_3$ with $HOCH_2C(CH_2OCH_2CH{=}CH_2)_3$] was used in this final step of dendrimer construction.

The ^{29}Si NMR spectrum also shows a great excess of starting material as judged by the low ratio of Q-Si peak area to M-Si and D-Si peak areas. The M, D, and Q-Si peaks are all multiple peaks indicative of a mixture of reaction products as confirmed by the GPC chromatogram discussed above.

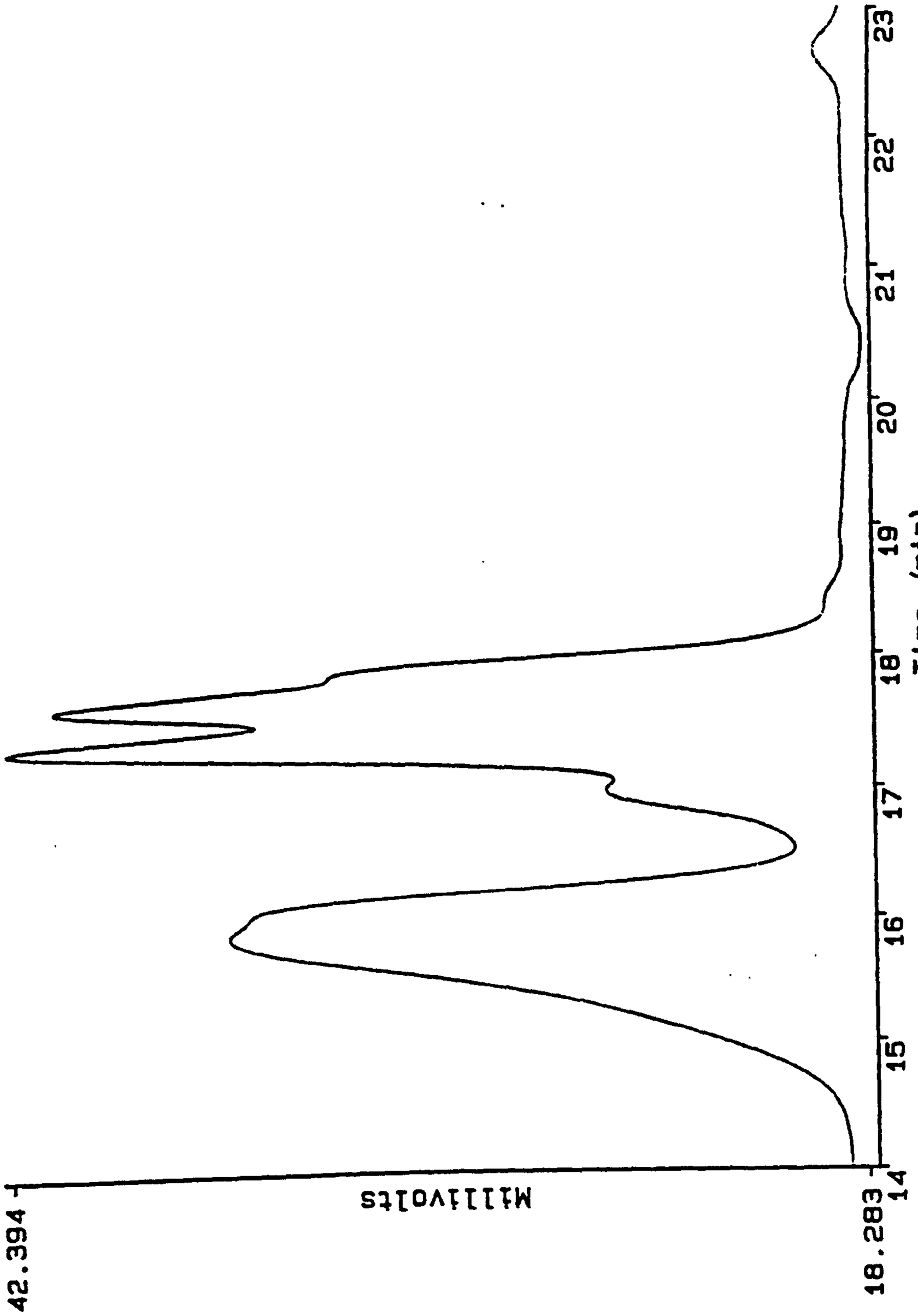

Figure 6.10 GPC chromatogram of the dendrimer made from reaction of $Me_3SiOSi(Me)(H)OSiMe_3$ with $HOCH_2C(CH_2OCH_2CH{=}CH_2)_3$ followed by its reaction with T_8.

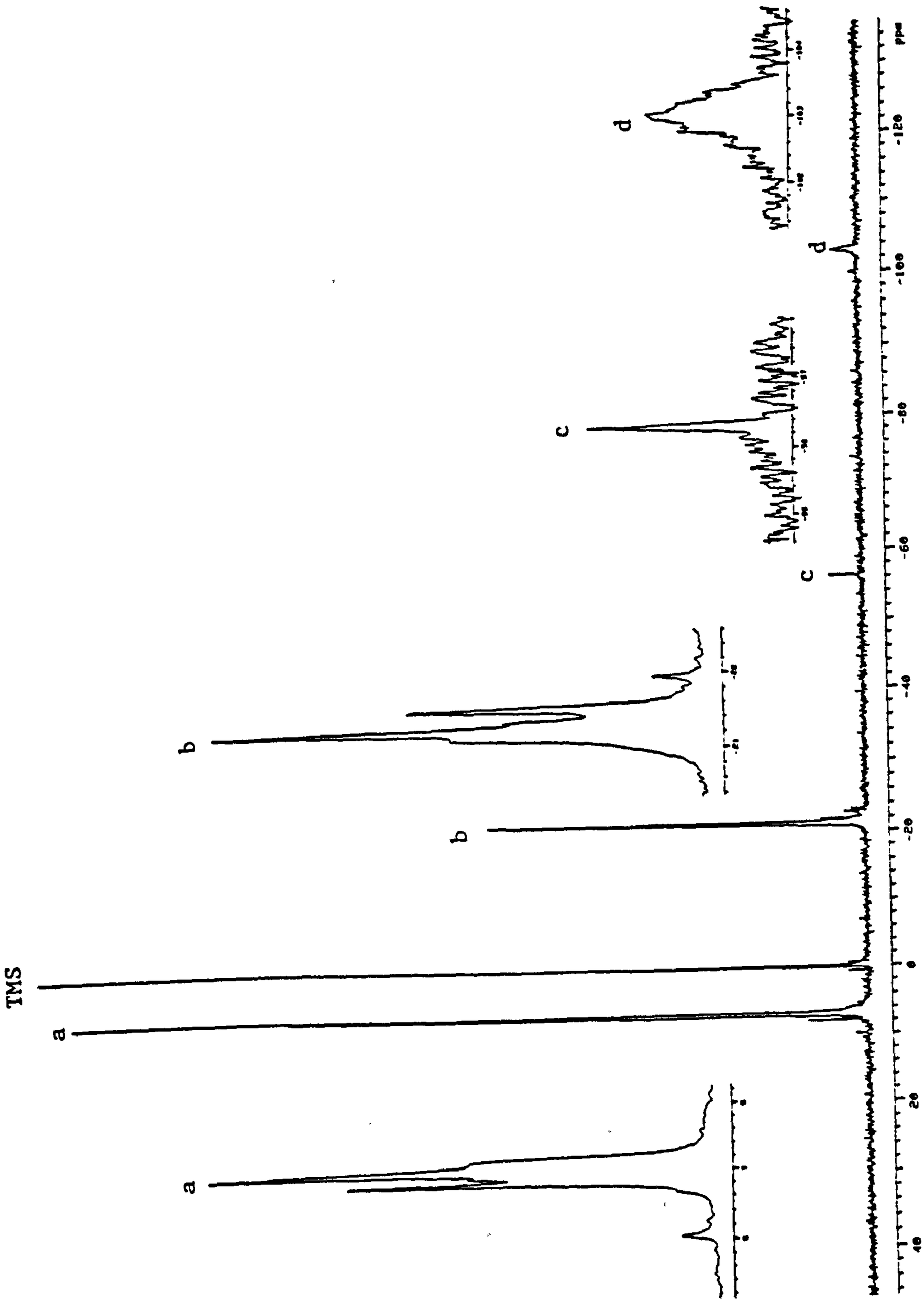

Figure 6.11 ^{29}Si NMR spectrum for the dendrimer made from reaction of $Me_3SiOSi(Me)(H)OSiMe_3$ with $HOCH_2C(CH_2OCH_2CH{=}CH_2)_3$ followed by its reaction with T_8.

6.1.3 Silsesquioxane Dendrimers

In view of the by-products and impurities obtained in the above synthetic routes that are difficult to remove by standard purification techniques due to their size and high molecular weight, it was thought that perhaps it would be better to build appendages of the dendrimer that could be distilled to high purity first and then attach these to the silsesquioxane core to obtain pure, monodispersed dendrimers.

6.1.3.1 Synthesis of Pure 16-armed Dendrimer: $(SiO_{3/2})_8$-$[(CH_2)_5OSi(Me)(OSiMe_3)_2]_8$

A process for obtaining a pure 16-armed dendrimer, $(SiO_{3/2})_8$-$[(CH_2)_5OSi(Me)(OSiMe_3)_2]_8$, was developed. The process involved the synthesis of the "arms" of the dendrimer, $CH_2=CH(CH_2)_3OSi(Me)(OSiMe_3)_2$, which were purified by distillation, and then attaching these arms to the silsesquixoane core via hydrosilylation.

The synthesis of the $CH_2=CH(CH_2)_3OSi(Me)(OSiMe_3)_2$ arms involved a condensation reaction of 4-penten-1-ol and $Me_3SiOSi(Me)(H)OSiMe_3$ as shown in reaction scheme 6.3.

$$CH_2=CH(CH_2)_3OH + Me_3SiOSi(Me)(H)OSiMe_3 \rightarrow CH_2=CH(CH_2)_3OSi(Me)(OSiMe_3)_2 \quad (6.3)$$

As with the previous condensation reactions, especially those involving starting materials containing both unsaturation and hydroxyl functionality, the hydroxyl amine catalyst, Et_2NOH, was employed in this reaction. And as previously suggested with this catalyst, the proposed SiH to SiH coupling was confirmed in this case. The SiH to SiH coupling in this case resulted in the formation of $(Me_3SiO)_2Si(Me)OSi(Me)(OSiMe_3)_2$ which was positively identified in the reaction mixture by GC/MS Another major impurity was $[CH_2=CH(CH_2)_3O]_2(Me)SiOSiMe_3$ or the molecule resulting from the -$SiMe_3$ group of one of the branches of the trisiloxane starting material also participating in the condensation reaction with the alcohol. By purification techniques however, the pure $CH_2=CH(CH_2)_3OSi(Me)(OSiMe_3)_2$ was obtained. The ^{29}Si NMR spectrum of the purified $CH_2=CH(CH_2)_3OSi(Me)(OSiMe_3)_2$ is shown in Figure 6.12. As expected for pure $CH_2=CH(CH_2)_3OSi(Me)(OSiMe_3)_2$, there is a M-Si peak ($\delta$ 8.14, O<u>Si</u>M e$_3$) and a T-Si peak [δ -57.00 ppm, -O<u>Si</u>$(Me)(OSiMe_3)_2$] and the areas of these peaks are in the expected 2:1 ratio. The GPC of the purified $CH_2=CH(CH_2)_3OSi(Me)(OSiMe_3)_2$ (Figure 6.13) shows the distilled product to be monodispersed with retention 18.66 minutes.

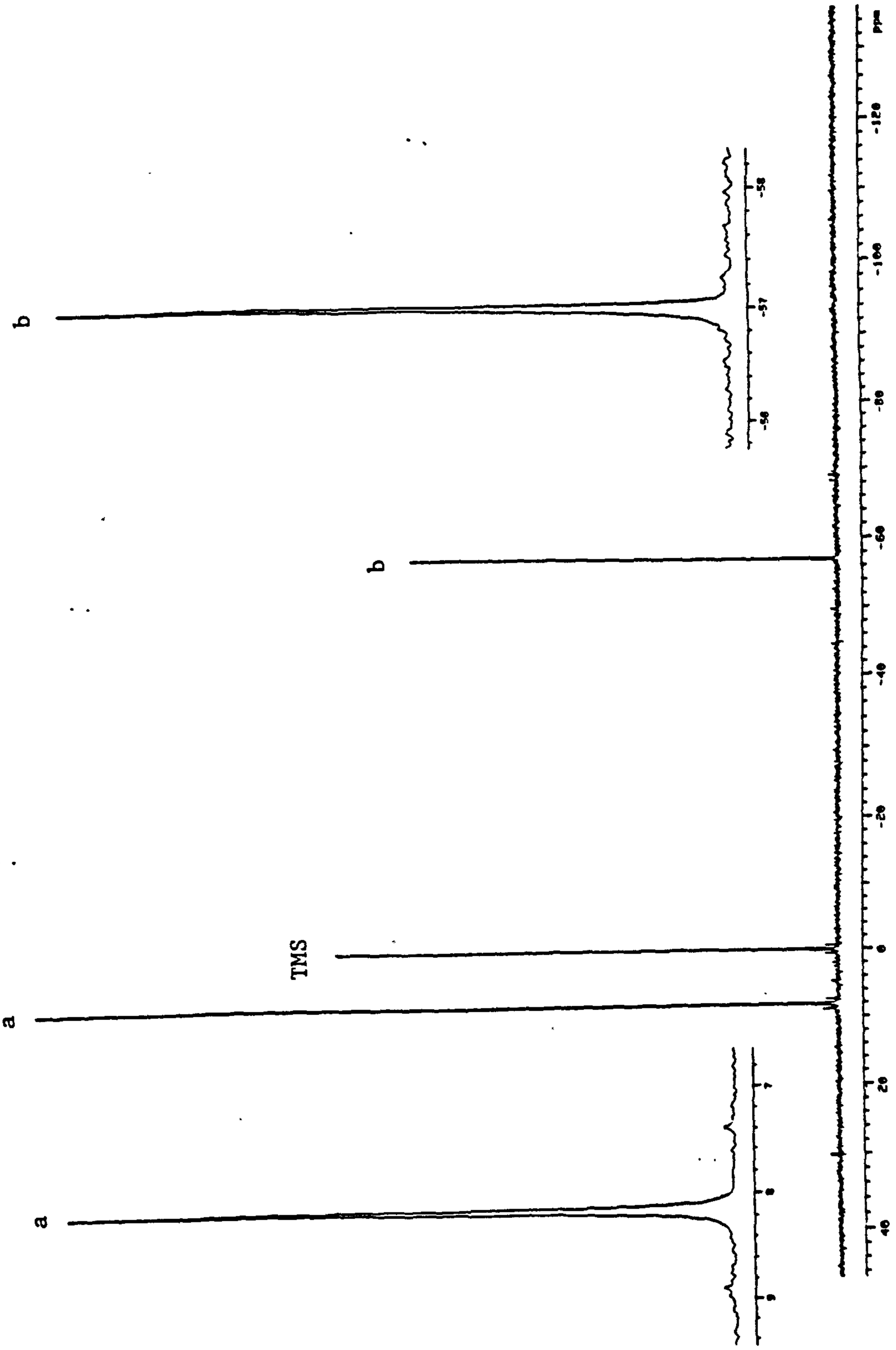

Figure 6.12 ^{29}Si NMR spectrum for purified $CH_2=CH(CH_2)_3OSi(Me)(OSiMe_3)_2$.

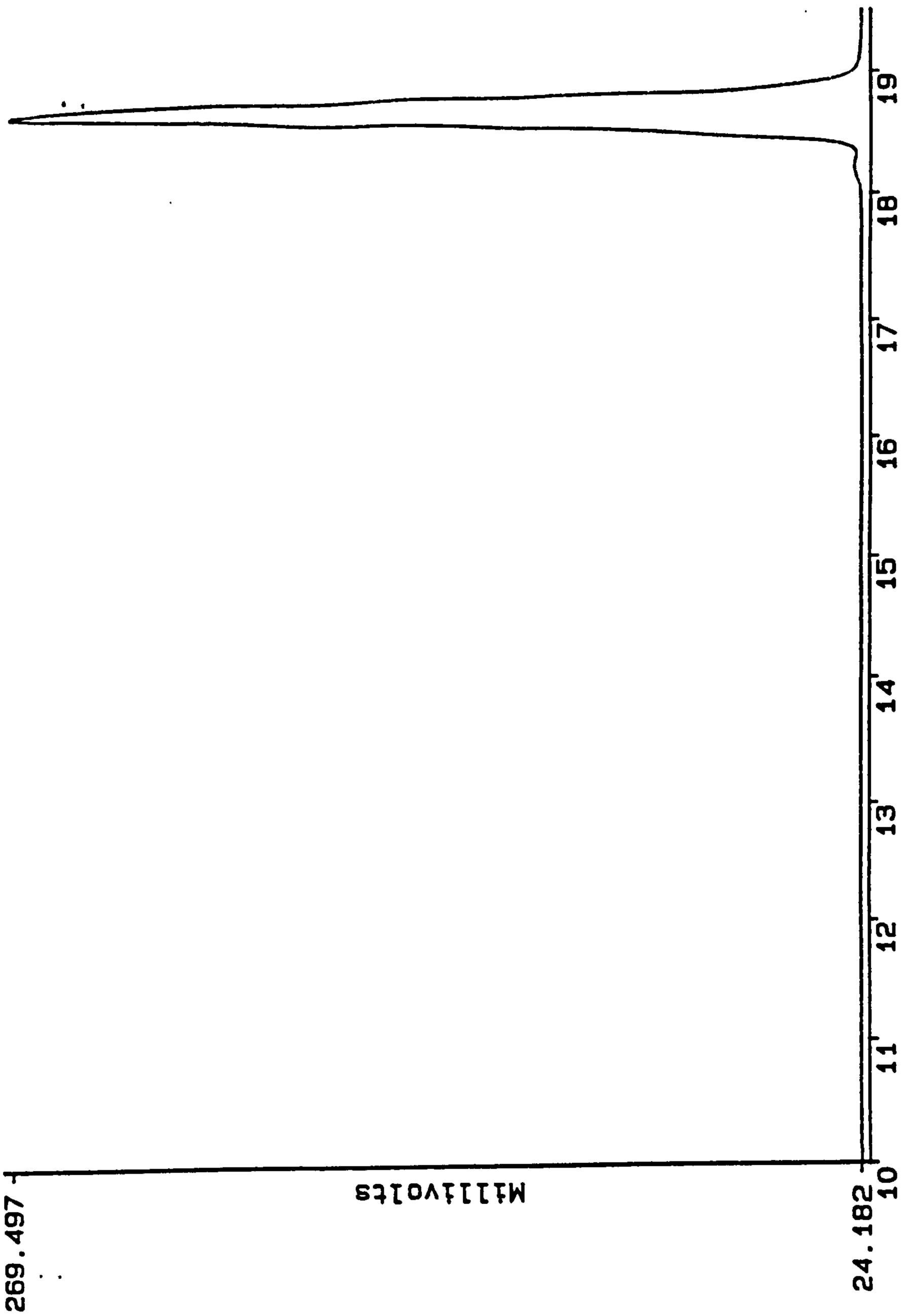

Figure 6.13 GPC chromatogram of purified $CH_2=CH(CH_2)_3OSi(Me)(OSiMe_3)_2$.

The purified $CH_2=CH(CH_2)_3OSi(Me)(OSiMe_3)_2$ was then hydrosilylated by T_8 hydrogen silsesquioxane to form the 16-armed dendrimer as the final product as indicated in reaction scheme 6.4 and as depicted in the model shown in Figure 6.14.

$$(HSiO_{3/2})_8 + CH_2=CH(CH_2)_3OSi(Me)(OSiMe_3)_2 \rightarrow (SiO_{3/2})_8\text{-}[(CH_2)_5OSi(Me)(OSiMe_3)_2]_8 \quad (6.4)$$

The ^{29}Si NMR of the final product is shown in Figure 6.15. The NMR indicates the presence of a single sharp M-Si peak at δ 7.08 ppm for the -O<u>Si</u>M e_3 branch termini; a single sharp T-Si peak at δ -57.06 ppm for the silicon at the branch point of each appendage $[CH_2O\underline{Si}(Me)(OSiMe_3)_2]$; and a T-Si peak at δ -66.74 ppm for the silicon of the cage $(O_{3/2}\underline{Si}CH_2)$. The ratio of the area of the M:T:T peaks was found to be 2.0:1.0:1.0 as expected if the reaction went cleanly. The GPC chromatogram (Figure 6.16) of the reaction product confirms that the reaction resulted in a pure product as indicated by the monodispersed peak at retention time 16.53 minutes.

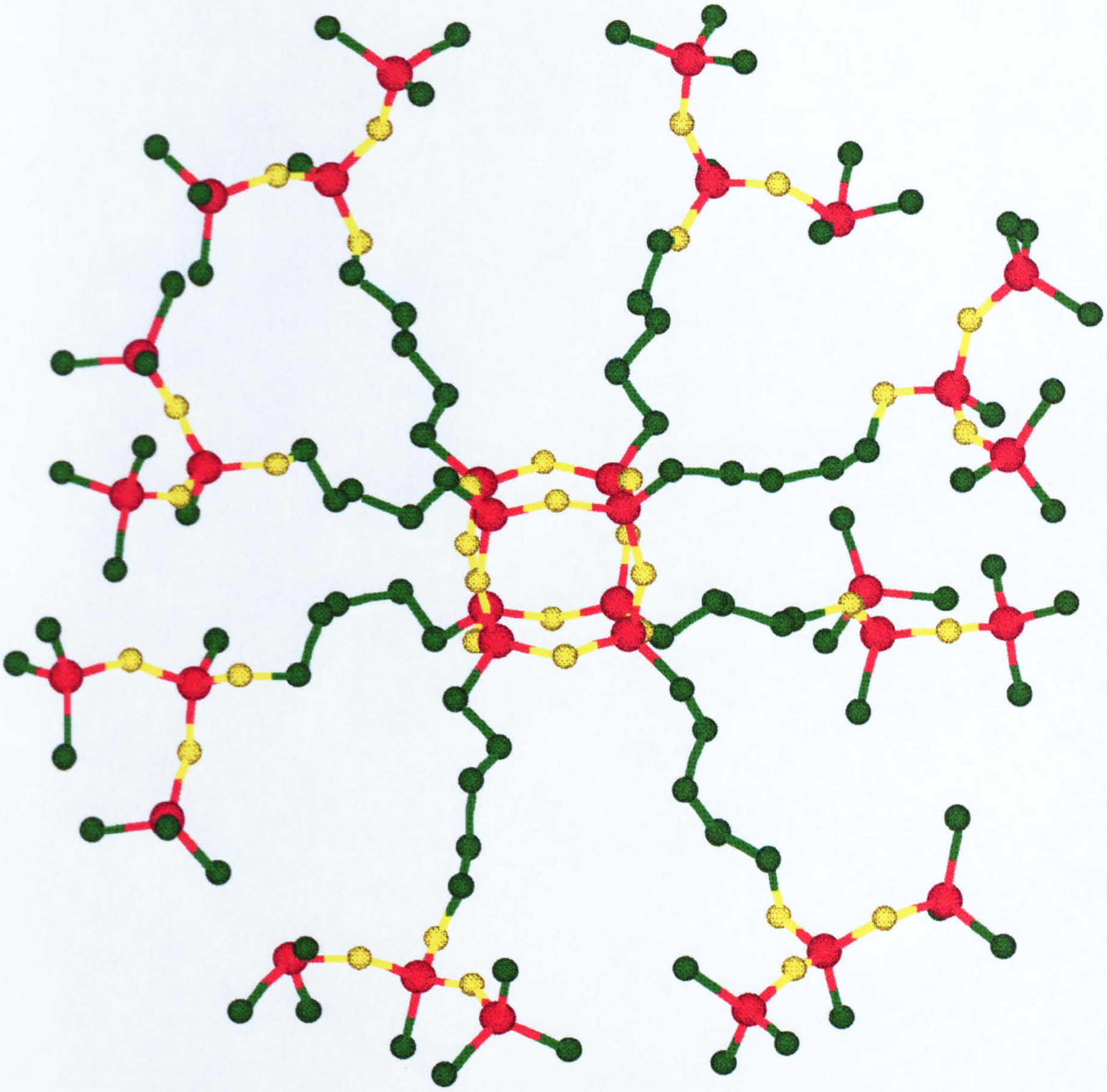

Figure 6.14 Model of the dendrimer made from the reaction of T_8 + CH_2=$CH(CH_2)_3OSi(Me)(OSiMe_3)_2$.
Red=Silicon, Yellow=Oxygen, Green=Carbon
(Hydrogens are hidden).

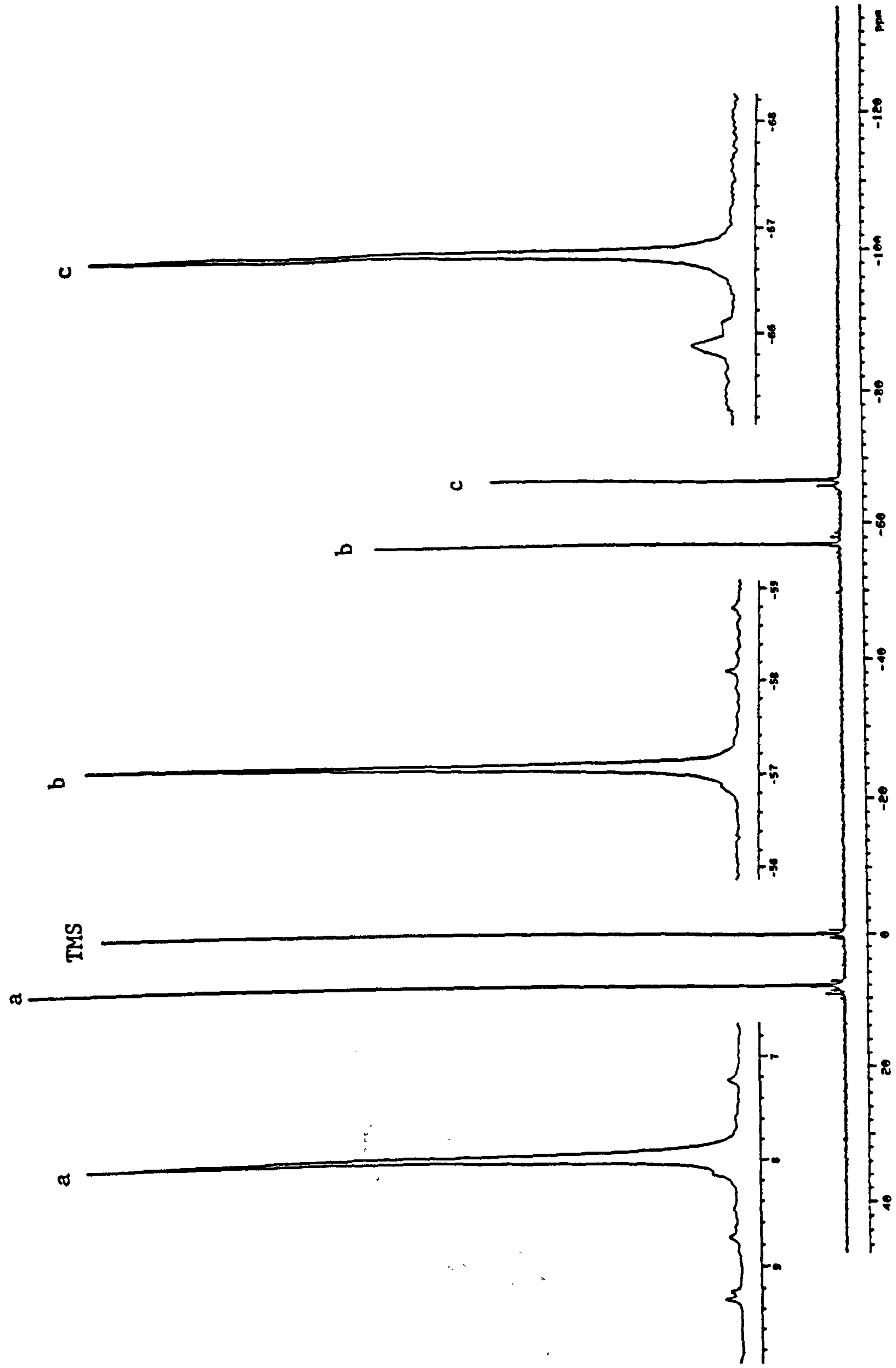

Figure 6.15 ^{29}Si NMR spectrum for the dendrimer made from the reaction of $T_8 + CH_2{=}CH(CH_2)_3OSi(Me)(OSiMe_3)_2$.

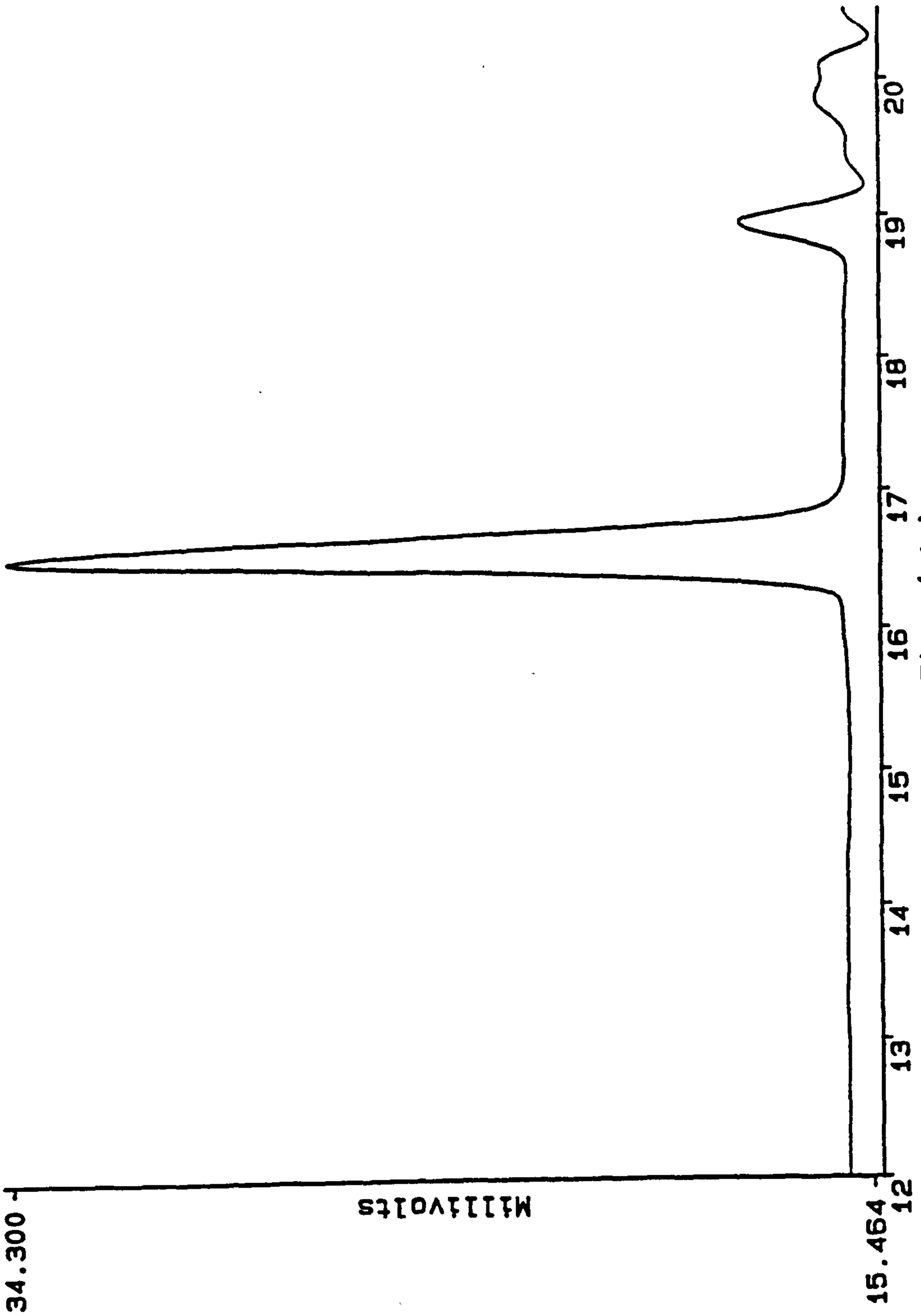

Figure 6.16 GPC chromatogram of the dendrimer made from the reaction of T_8 + CH_2=CH(CH_2)$_3$OSi(Me)(OSiMe$_3$)$_2$.

6.1.3.2 Another 16-armed Dendrimer: $(SiO_{3/2})_8$-$[O(CH_2)_5Si(Me)(OSiMe_3)_2]_8$

Similar to the last process in which the "arms" of the dendrimer were made and purified before attachment to the silsesquixoane core, another 16-armed dendrimer synthesis was attempted. This synthesis involved the use of all the same starting materials as the last one, 4-penten-1-ol, $Me_3SiOSi(Me)(H)OSiMe_3$, and eventually T_8, but a reversal of the sequence of the reaction types was done. In this case, 4-penten-1-ol was reacted with $Me_3SiOSi(Me)(H)OSiMe_3$ to make the arms but hydrosilylation was used as shown in reaction scheme 6.5 rather than the condensation reaction (reaction scheme 6.3) done for the arms of the last dendrimer.

$$CH_2=CH(CH_2)_3OH + Me_3SiOSi(Me)(H)OSiMe_3 \rightarrow HO(CH_2)_5Si(Me)(OSiMe_3)_2 \quad (6.5)$$

The resulting branched arms were OH functional and therefore a condensation reaction of the arms with the SiH of the core was used for attachment of the branched arms to the core as shown in reaction scheme 6.6 to obtain the dendrimer depicted in Figure 6.17.

$$(HSiO_{3/2})_8 + HO(CH_2)_5Si(Me)(OSiMe_3)_2 \rightarrow (SiO_{3/2})_8\text{-}[O(CH_2)_5Si(Me)(OSiMe_3)_2]_8 \quad (6.6)$$

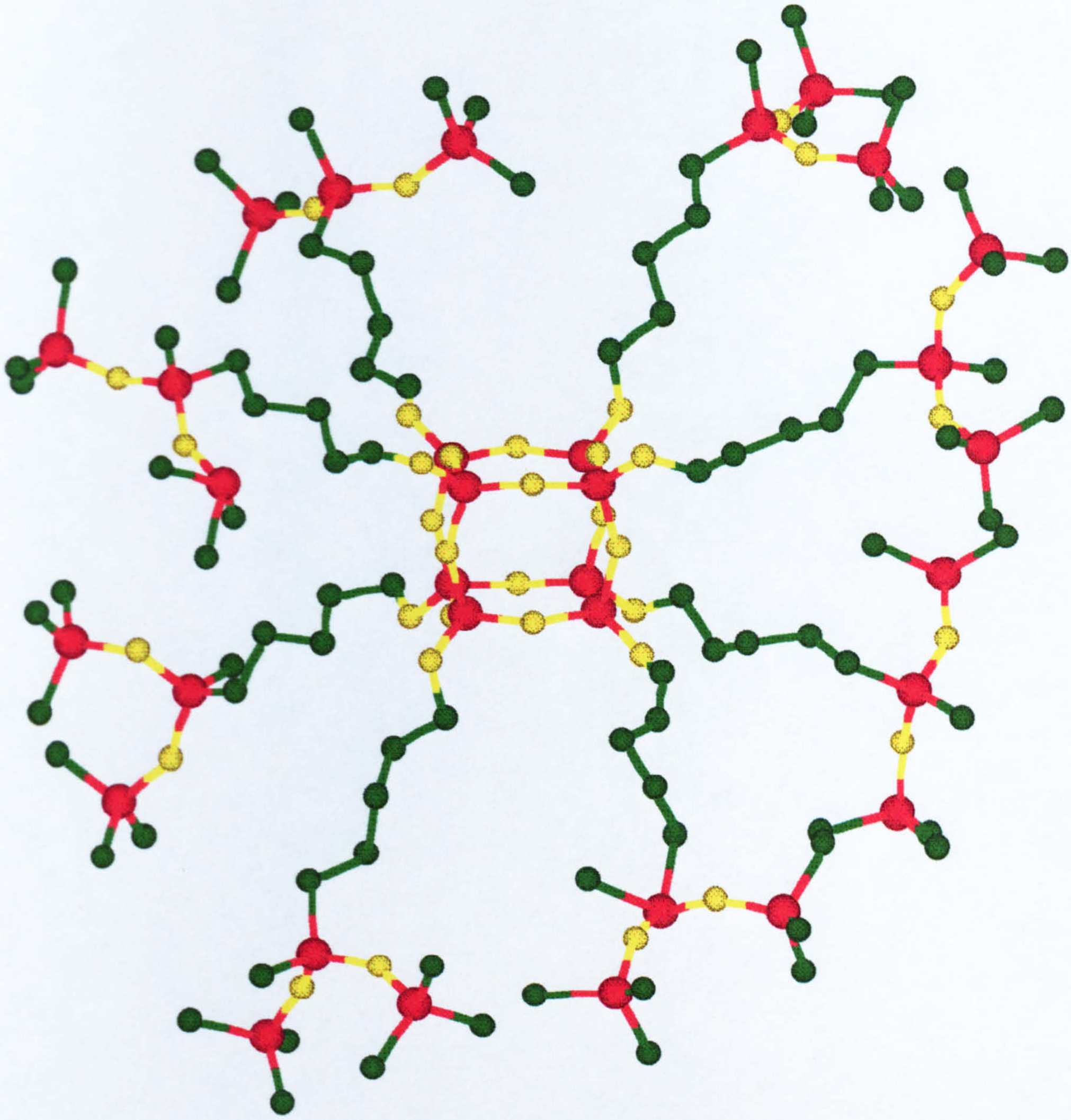

Figure 6.17 Model of the dendrimer obtained by the reaction of $T_8 + HO(CH_2)_5Si(Me)(OSiMe_3)_2$.

The hydrosilylation of 4-penten-1-ol by $Me_3SiOSi(Me)(H)OSiMe_3$ resulted in the desired product, $HO(CH_2)_5Si(Me)(OSiMe_3)_2$, as well as a number of by-products. Distillation of the reaction mixture, however, was used to obtain a pure sample of $HO(CH_2)_5Si(Me)(OSiMe_3)_2$. The ^{29}Si NMR of the purified $HO(CH_2)_5Si(Me)(OSiMe_3)_2$ is shown in Figure 6.18. The spectrum shows a single M-Si peak ($OSiMe_3$ branch termini) at δ 6.92 ppm and a single D-Si peak [$-CH_2-Si(Me)(OSiMe_3)_2$] at δ -21.42 ppm. The ratio of the areas of the M:D peaks is 2.0:1.0 as expected for a pure sample. The GPC chromatogram of the purified $HO(CH_2)_5Si(Me)(OSiMe_3)_2$ is shown in Figure 6.19. The chromatogram indicates the presence of the product peak at retention time 19.51 minutes. There are two other very small (<3% total area) higher molecular weight impurities as well.

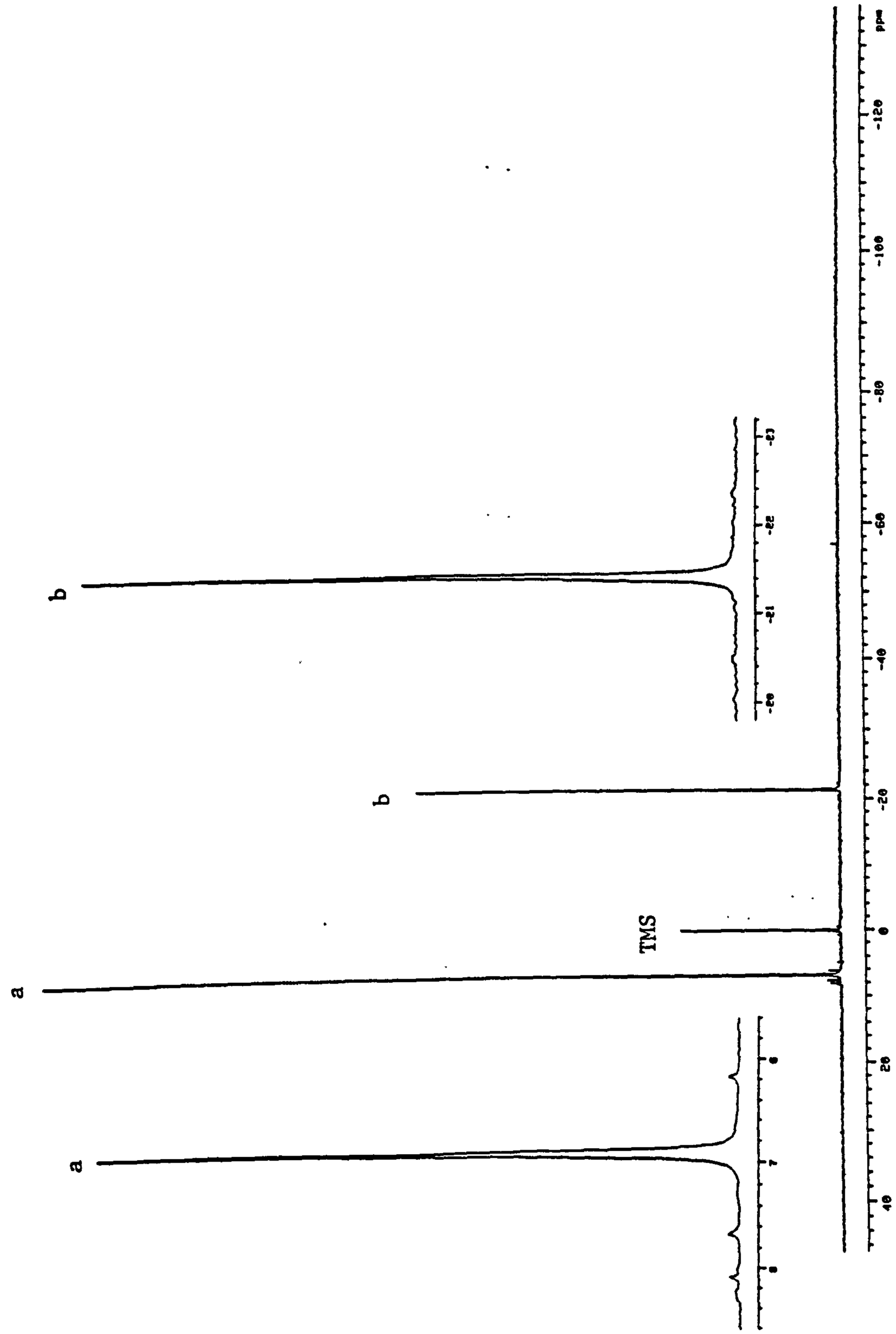

Figure 6.18 ^{29}Si NMR spectrum for purified $HO(CH_2)_5Si(Me)(OSiMe_3)_2$.

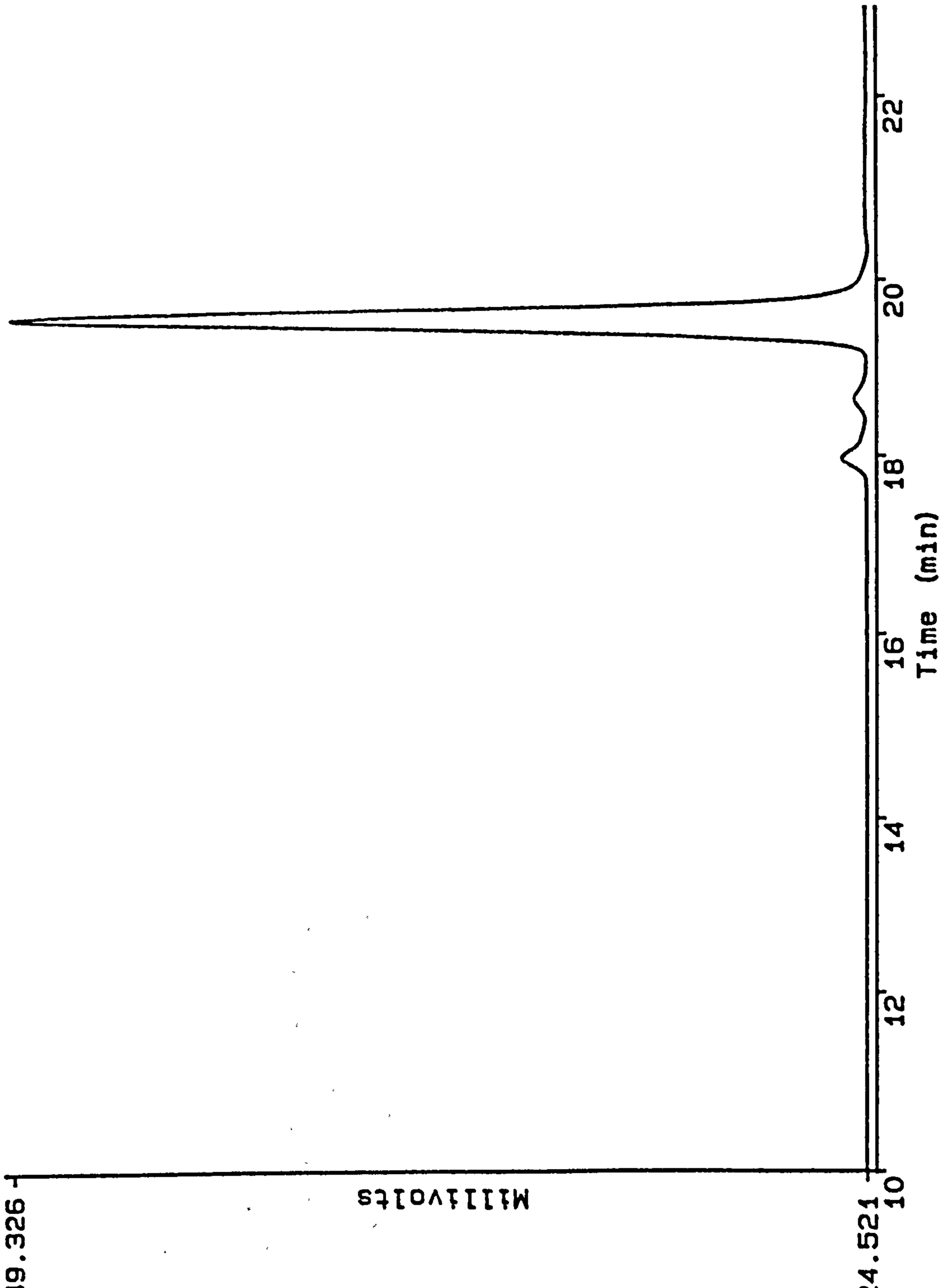

Figure 6.19 GPC chromatogram of purified $HO(CH_2)_5Si(Me)(OSiMe_3)_2$.

The purified $HO(CH_2)_5Si(Me)(OSiMe_3)_2$ was then reacted in a condensation reaction with T_8 to form the final dendrimer product, $(SiO_{3/2})_8$-$[O(CH_2)_5Si(Me)(OSiMe_3)_2]_8$. The hydroxyl amine catalyst, Et_2NOH, was again used for this condensation reaction. The ^{29}Si NMR of the reaction product shown in Figure 6.20 indicates that there is the expected M-Si peak for the $OSiMe_3$ branch termini at δ 7.04 ppm, D-Si peak at δ -21.10 ppm for the branch point silicon $[-CH_2Si(Me)(OSiMe_3)_2]$ and the Q-Si peak at approximately δ -102.02 ppm. The Q-peak is actually a grouping of at least four not entirely resolved peaks between δ -102 and -102.6 ppm. It is most likely that as seen previously with the hydroxyl amine catalyst that some cage to cage condensation took place resulting in the multiple Q-Si environments. The ratio of M:D:Q peak areas was found to be 3.1:1.6:1.0 instead of the expected 2:1:1 ratio. However, this difference can be explained by the large excess of $HO(CH_2)_5Si(Me)(OSiMe_3)_2$ starting material used in the dendrimer synthesis.

The GPC chromatogram of the dendrimer reaction product (Figure 6.21) also indicates that a large excess of $HO(CH_2)_5Si(Me)(OSiMe_3)_2$ is present in the final product. In addition to the peak at 19.53 minutes corresponding to the excess $HO(CH_2)_5Si(Me)(OSiMe_3)_2$, there are at least two peaks corresponding to the dendrimer reaction product. It is very evident that this reaction resulted in a large amount of high molecular weight impurity most likely the result of the cage to cage condensations proposed earlier.

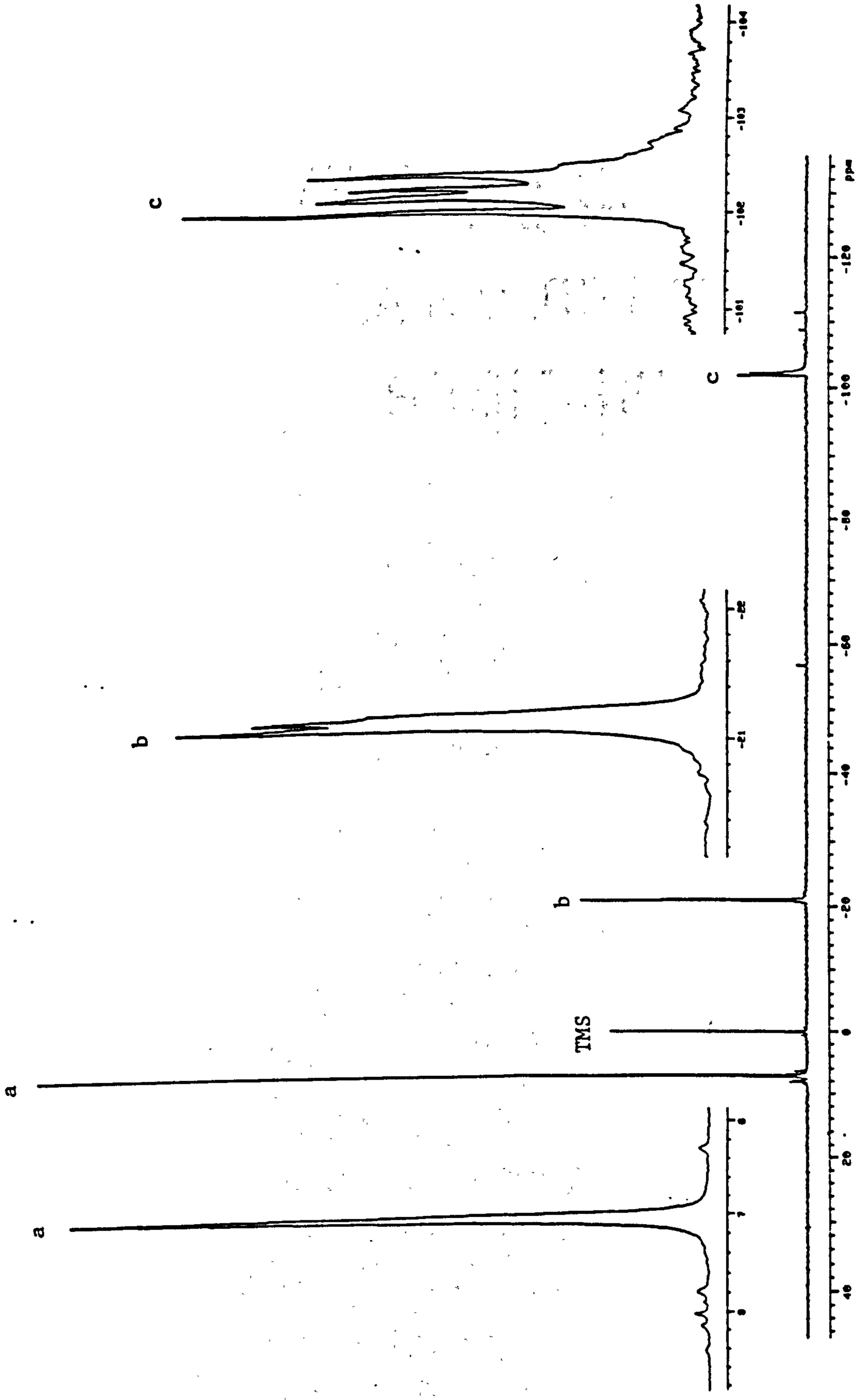

Figure 6.20 ^{29}Si NMR spectrum for the product of the reaction $T_8 + HO(CH_2)_5Si(Me)(OSiMe_3)_2$.

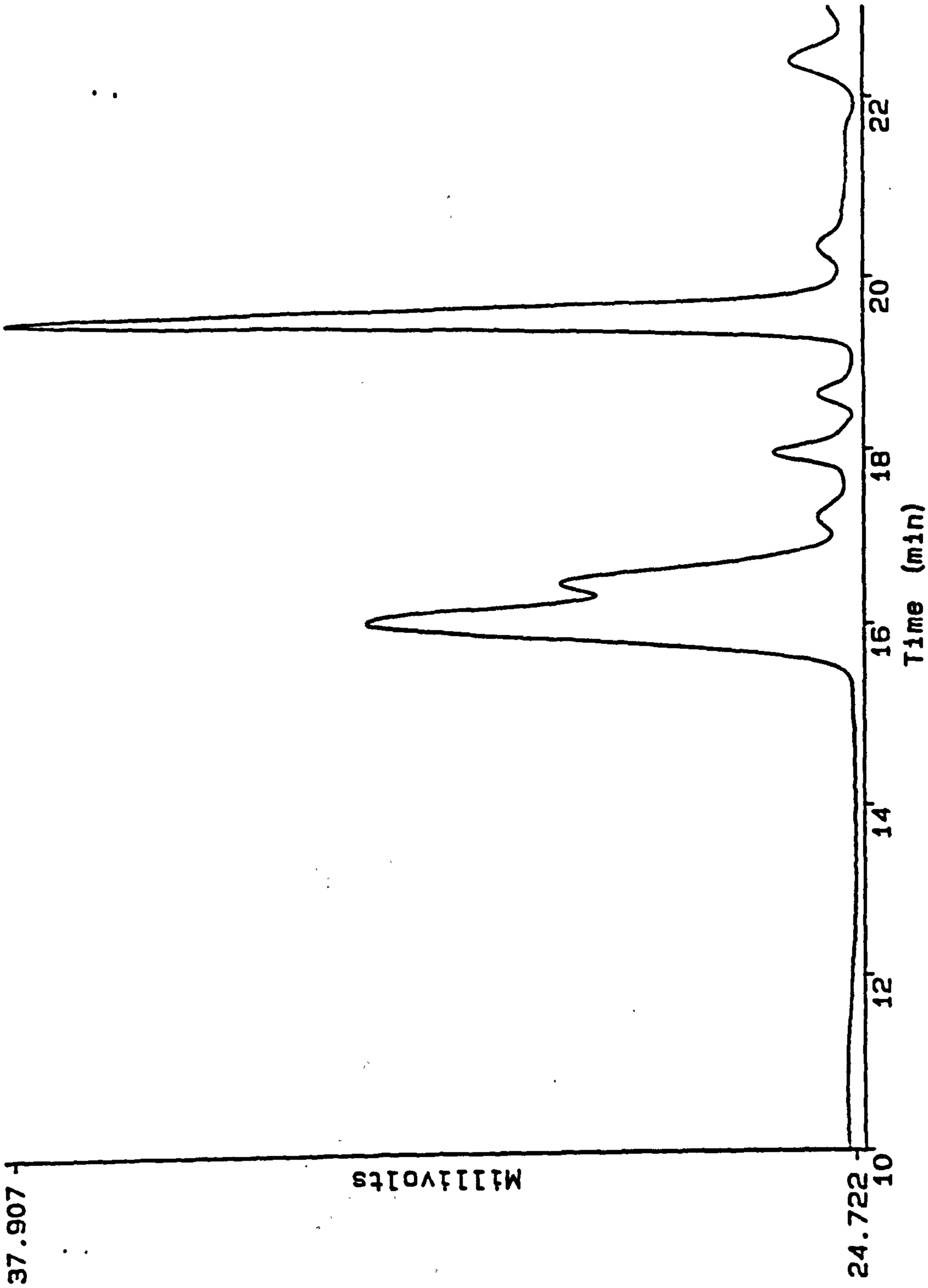

Figure 6.21 GPC chromatogram of the product of the reaction T_8 + $HO(CH_2)_5Si(Me)(OSiMe_3)_2$.

This example of dendrimer synthesis illustrates that even when the branches are made and purified that the final attachment of the branches to the cage must be done using a reaction that goes to completion and that has no side reactions possible.

6.2 Conclusions

As the examples of dendrimer molecules with silsesquioxane cores illustrate, the use of a highly functional core such as T_8 hydrogen silsesquioxane can lead to a highly branched dendrimer in a very limited number of reaction steps. As with any dendrimer synthesis, side reactions must be avoided otherwise even a minor by-product can cause substantial impurities in the final step as shown by the many attempted syntheses discussed in this chapter. Even with these difficulties with unwanted side reactions and by-products, it was found that it is feasible to make a pure dendrimer based on the silsesquioxane core as was the intention of this body of work. The successfully made dendrimer, $(SiO_{3/2})_8$-$[(CH_2)_5OSi(Me)(OSiMe_3)_2]_8$, serves as an example of a first generation dendrimer. Future work will involve the expansion of silsesquioxane dendrimers beyond this first generation. One such example involves the use of the trimethoxysilyl functional octopus molecule discussed in Chapter 4. Work is currently underway to use the trimethoxysilyl functionality as branch sites. The transesterification reaction of unsaturated alcohols with the alkoxy functionality will result in a dendrimer with branches that are terminally unsaturated. The unsaturation allows for the next generation to be built onto the dendrimer, for

instance, through hydrosilylation reactions. In this way, it should be possible to build dendrimers with only steric constraints limiting the size. Characterization and applications testing of silsesquioxane based dendrimers is also planned for the future.

6.3 Experimental

6.3.1 General

A Varian VRX200s NMR spectrometer fitted with a 5 mm probe and operating at 39 MHz was used to obtain ^{29}Si NMR spectra. GPC and FTIR analyses were accomplished using the techniques described in Chapter Two, Section 2.4.1.

6.3.2 Synthesis of $(HSiO_{3/2})_8$

The procedure for obtaining T_8 hydrogen silsesquioxane outlined in Chapter Two, Section 2.4.2, was used.

6.3.3 Synthesis of $HOSiMe_2(OSiMe_2)_3CH=CH_2$

The previously reported compound, $HOSiMe_2(OSiMe_2)_3CH=CH_2$, was made using a technique similar to the reported route[4-6]. Hexamethylcyclotrisiloxane (D_3, 200.0 grams, 0.9 mol), vinyldimethylchlorosilane (108.5 grams, 0.9 mol), N,N-dimethylacetamide (6.1 grams), and acetonitrile (93.3 grams) were placed in a 2-litre, three neck, round bottom flask equipped with a thermometer, and a blanket of N_2. The reaction

mixture was heated to 65 °C for 90 minutes. After heating, the reaction mixture was stirred at room temperature for 21 hours at which time, solvents were stripped at 109-111 °C. Pure (97.5% by GC) $ClSiMe_2(OSiMe_2)_3CH=CH_2$ was obtained via distillation using a spinning band column under reduced pressure (1.8 mm Hg) with heating at 98-100 °C. The purified $ClSiMe_2(OSiMe_2)_3CH=CH_2$ (50.9 grams) which was a liquid was then added a small amount at a time, from an addition funnel, with swirling and venting to a separatory flask containing diethyl ether (143.7 grams), ice (160.6 grams), and ammonium hydroxide (13.75 grams). After addition of the $ClSiMe_2(OSiMe_2)_3CH=CH_2$ was complete, the aqueous phase was drained and 100.5 grams of hexane was added. The organic phase was then washed (swirled) with deionized, distilled water and the aqueous phase drained off. The washing process was repeated 7 more times before the aqueous phase was free of Cl by a $AgNO_3$ test. Then two additional washes with water were done. The organic phase was stored over Na_2SO_4 (33.2 grams) overnight to dry the product. After filtration of the organic phase to remove the Na_2SO_4, volatiles were stripped using a rotary evaporator with reduced pressure and heating up to 76 °C to obtain the product, $HOSiMe_2(OSiMe_2)_3CH=CH_2$.

The ^{29}Si NMR spectrum for $HOSiMe_2(OSiMe_2)_3CH=CH_2$ is shown in Figure 6.22. There is a M-Si peak at δ -3.65 ($-O\underline{Si}(Me_2)CH=CH_2$), a peak at δ -11.04 ppm ($HO\underline{Si}Me_2$), and two main D-Si peaks at δ -20.43 and -20.99 ppm [$HOSiMe_2(O\underline{Si}Me_2)_2OSi(Me_2)CH=CH_2$]. ^{29}Si NMR analysis was not given in the previous reports of $HOSiMe_2(OSiMe_2)_2OSi(Me_2)CH=CH_2$[4-6].

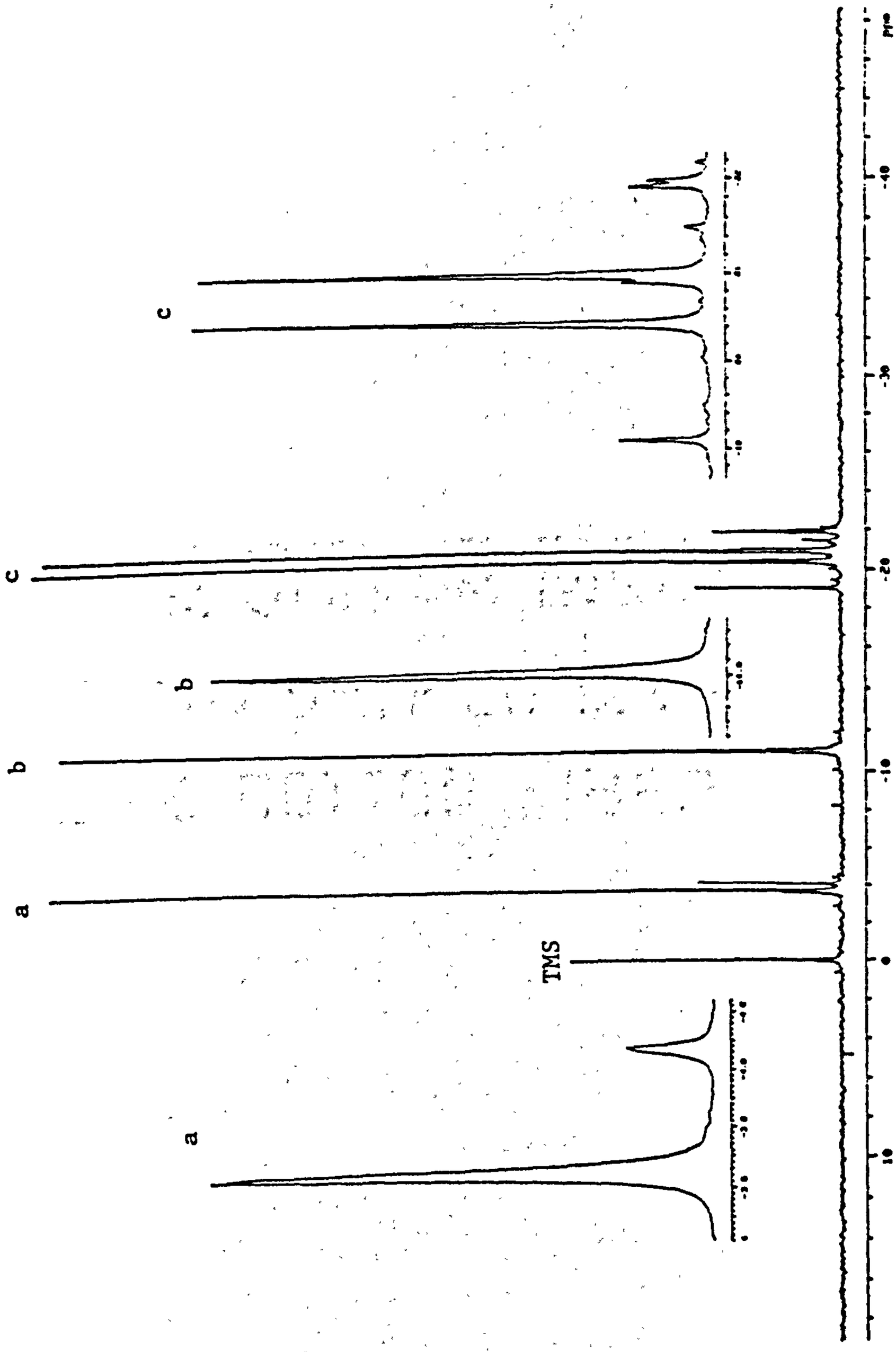

Figure 6.22 ^{29}Si NMR spectrum for $HOSiMe_2(OSiMe_2)_2OSi(Me_2)CH=CH_2$

The GPC chromatogram of the product, $HOSiMe_2(OSiMe_2)_3CH=CH_2$, was shown previously in Figure 6.3. The main product peak was seen at retention time 19.29 minutes. Some minor amounts of lower molecular weight impurity (retention time 20.52 minutes) and higher molecular weight impurity (retention time 17.97 minutes) were also present. Confirmation of the $HOSiMe_2(OSiMe_2)_2OSi(Me_2)CH=CH_2$ structure was obtained by GC/MS. A molecular ion of mass 324 was seen.

6.3.4 Synthesis of $[SiO_{3/2}]_8[OSiMe_2(OSiMe_2)_3CH=CH_2]_8$

T_8 (1.50 grams, 3.6 mmol), 11.00 grams hexane solvent, 20 µl Et_2NOH (used as supplied from Aldrich Chemical Co.) were placed in a 50 ml 3-neck, round bottom flask equipped with a thermometer, H_2O condenser, stir bar, and an addition flask containing 9.45 grams of $HOSiMe_2(OSiMe_2)_3CH=CH_2$ (29.2 mmol). The reaction mixture was stirred and a light flow of dry N_2 was maintained over the reaction while addition of the $HOSiMe_2(OSiMe_2)_3CH=CH_2$ occurred at room temperature over a five minute period. The reaction mixture was then heated to 70 °C for approximately 45 minutes at which time all the SiH appeared to be gone by FTIR. The hexane solvent was then stripped from the reaction under vacuum (0.35 mm Hg) and heating (76 °C).

The ^{29}Si NMR spectrum of the reaction product was previously shown in Figure 6.1. The spectrum showed a M-Si peak ($O\underline{Si}Me_2Bu$) at δ -4.18 ppm, a D-Si grouping of peaks (3 D-Si along

the pendant siloxane chains) between d -19.10 and -22.10 ppm, and a grouping of Q-Si peaks (silicon of the cube, $O_{3/2}\underline{Si}OSiMe_2$-) between -110.02 and -110.22 ppm. The multiple peaks in the Q-Si region were attributed to cage to cage condensation. The ratio of M:D:Q peak areas in the ^{29}Si NMR spectrum was found to be 1.3:5.6:1.0. The increase in M-Si and D-Si was proposed to be due to SiOH to SiOH condensations of the $HOSiMe_2(OSiMe_2)_3CH=CH_2$ starting material. The multiple peaks in the M-Si and D-Si regions of the ^{29}Si NMR spectrum were thought to be due to this as well.

The GPC chromatogram of the reaction product was shown in Figure 6.2. The peak at retention time 16.70 minutes was assigned to the desired product, $[SiO_{3/2}]_8[OSiMe_2(OSiMe_2)_3CH=CH_2]_8$. There were also higher molecular weight peaks at 16.16 and 15.91 minutes that were proposed to be the dimer and trimer resulting from cage to cage condensation reactions. There was a rather large lower molecular weight peak at retention time 17.97 minutes that was proposed to be the reaction product of SiOH to SiOH condensations of the $HOSiMe_2(OSiMe_2)_3CH=CH_2$ starting material.

6.3.5 Synthesis of $[SiO_{3/2}]_8$-$[OSiMe_2(OSiMe_2)_3CH_2CH_2Si(Me)(OSiMe_3)_2]_8$

To 5.00 grams of the above reaction product, 3.46 grams (excess) $Me_3SiOSi(Me)(H)OSiMe_3$ and 50 µl of the tetramethyldivinyldisiloxane complex of Pt diluted in toluene to 1.0% Pt was added. The reaction mixture was then heated to

between 80-100 °C for 4 hours. Any unreacted $Me_3SiOSi(Me)(H)OSiMe_3$ (excess) was removed using vacuum (~0.5 mm Hg) and heat (45 °C) to obtain product.

The ^{29}Si NMR of the reaction product was shown in Figure 6.5. Multiple peaks were seen in the M-Si region {δ 8.36 and 6.82, $[SiO_{3/2}]_8$-$[OSiMe_2(OSiMe_2)_3CH_2CH_2Si(Me)(O\underline{Si}Me_3)_2]_8$}, in the D-Si region {δ -19.07, -20.82, -21.08, -21.51, -21.58, -21.65 ppm, $[SiO_{3/2}]_8$-$[O\underline{Si}Me_2(O\underline{Si}Me_2)_3CH_2CH_2\underline{Si}(Me)(OSiMe_3)_2]_8$}, and in the Q-Si region {δ -110.0 to 110.4 ppm, $[\underline{Si}O_{3/2}]_8$-$[O\underline{Si}Me_2(O\underline{Si}Me_2)_3CH_2CH_2\underline{Si}(Me)(OSiMe_3)_2]_8$}.

The GPC chromatogram (previously shown in Figure 6.4) indicated the presence of the desired product at retention time 16.05 minutes as well as a number of higher molecular weight by-products assigned as the dimer, trimer and higher species resulting from cage to cage condensations. Some lower molecular weight by-products were also found to be present.

6.3.6 Synthesis of $HOCH_2C[CH_2OCH_2CH_2CH_2Si(Me)(OSiMe_3)_2]_3$

Bis(trimethylsiloxy)methylsilane or $Me_3SiOSi(Me)(H)OSiMe_3$ (26.23 grams, distilled to 98% purity by GC) and 200 µl of 0.02M H_2PtCl_6 in isopropanol were placed in a 3-neck, round bottom flask equipped with H_2O condenser, thermometer, and an addition flask containing 9.95 grams of pentaerythritol triallylether (PETAE, used as supplied by M&P). A dry air blanket was maintain over the contents of the flask while the

contents were heated to 80 °C and the PETAE was added over a 80 minute period. To ensure complete reaction, an additional 10.0 grams of bis(trimethylsiloxy)methylsilane and 100 µl of 0.02M H_2PtCl_6 in isopropanol was added to the flask and the reaction mixture heated to approximately 120 °C for a total of 7 hours at which time a vacuum strip (2.5 mm Hg, temperature up to 140 °C) of excess bis(trimethylsiloxy)methylsilane and other volatiles was done to obtain the product $HOCH_2C[CH_2OCH_2CH_2CH_2Si(Me)(OSiMe_3)_2]_3$. The product was then used for the second step of the dendrimer synthesis as described in the section 6.3.7.

The ^{29}Si NMR was previously shown in Figure 6.7. The spectrum showed the presence of a main M-Si peak at δ 7.17 ppm $\{HOCH_2C[CH_2OCH_2CH_2CH_2Si(Me)(O\underline{Si}Me_3)_2]_3\}$ and a main D-Si peak at δ -21.55 ppm $\{HOCH_2C[CH_2OCH_2CH_2CH_2\underline{Si}(Me)(OSiMe_3)_2]_3\}$. The M-Si and D-Si peaks had other minor peaks surrounding them due to impurities. The ratio of the areas of the M:D peaks was 2.2:1.0.

The GPC chromatogram of the reaction product was shown in Figure 6.8. The main product peak was seen at retention time 17.85 minutes. There appeared to be a significant amount of higher molecular weight impurities, one with retention time 17.35 minutes and another with retention time 16.95 minutes. These higher molecular weight impurities were proposed to be the result of high molecular weight impurities found in the $HOCH_2C(CH_2OCH_2CH{=}CH_2)_3$ starting material. These impurities were quite significant in the $HOCH_2C(CH_2OCH_2CH{=}CH_2)_3$ (~25% of

the total area). The higher molecular weight impurity was proposed to have reacted with the $Me_3SiOSi(Me)(H)OSiMe_3$ to make the high molecular weight shoulder of the main product peak in the GPC chromatogram.

6.3.7 Synthesis of $(SiO_{3/2})_8$-$[OCH_2C[CH_2OCH_2CH_2CH_2Si(Me)(OSiMe_3)_2]_3]_8$

The $HOCH_2C[CH_2OCH_2CH_2CH_2Si(Me)(OSiMe_3)_2]_3$ produced in the reaction above was then reacted with T_8 in an attempt to produce a 48-armed dendrimer. T_8 (0.50 grams, 1.18 mmol), 9.3 grams hexane solvent, and 10 µl of Et_2NOH catalyst were placed in a 3-neck, round bottom flask equipped with a thermometer, stir bar, H_2O condenser, and an addition flask containing 8.80 grams of $HOCH_2C[CH_2OCH_2CH_2CH_2Si(Me)(OSiMe_3)_2]_3$ (9.54 mmol). The $HOCH_2C[CH_2OCH_2CH_2CH_2Si(Me)(OSiMe_3)_2]_3$ was added to the stirring contents of the flask at room temperature over a 5 minute period while maintaining a dry N_2 blanket. The reaction mixture was then heated to 61 °C for approximately 1 hour. FTIR analysis showed the presence of SiH indicating the reaction was not complete. The hexane solvent was then stripped under vacuum (4.5 mm Hg, 60-104 °C) after which an additional 0.90 grams of $HOCH_2C[CH_2OCH_2CH_2CH_2Si(Me)(OSiMe_3)_2]_3$ and 20 µl Et_2NOH catalyst were added and the reaction mixture heated to approximately 140 °C under vacuum (3.5 mm Hg) for an additional 2.5 hours. At this point, SiH was no longer apparent by FTIR analysis and the reaction was stopped.

The ^{29}Si NMR spectrum was previously shown in Figure 6.11. The M, D, and Q-Si peaks were all multiple peaks indicative of a mixture of reaction products as expected from the impure $HOCH_2C[CH_2OCH_2CH_2CH_2Si(Me)(OSiMe_3)_2]_3$ produced in the previous reaction. There also appeared to be a great excess of starting material as judged by the low ratio of Q-Si peak area to M-Si and D-Si peak areas. The GPC chromatogram previously shown in Figure 6.10 also confirmed the product was a mixture of materials as judge by the polydispersed peak between retention times 14.5 and 16.6 minutes and that a great excess of the $HOCH_2C[CH_2OCH_2CH_2CH_2Si(Me)(OSiMe_3)_2]_3$ starting material was present (retention times 16.6 to 18.3 minutes).

6.3.8 Synthesis of $CH_2=CH(CH_2)_3OSi(Me)(OSiMe_3)_2$

Bis(trimethylsiloxy)methylsilane $[(H)Si(Me)(OSiMe_3)_2$, 12.9 grams, 58.1 mmol, 98% pure by GC) and 5.0 grams of 4-penten-1-ol (58.1 mmol, 99% available from Aldrich Chemical Co., stored over molecular sieves) were placed in a 100 ml 3-neck, round bottom flask equipped with a thermometer, H_2O condenser, and stir bar. The reaction mixture was stirred and a light flow of dry N_2 was maintained over the reaction while addition of an initial aliquot of 20 µl of N,N diethylhydroxylamine (Et_2NOH, 99%, used as supplied by Aldrich Chemical Co.) catalyst was added. The reaction mixture was then heated to approximately 50 °C for 30 minutes. GC analysis indicated that the reaction had not yet taken place to any extent so 90 µl additional catalyst was added and the heat increased to between 100 and 118 °C over a 3 hour period. At the end of this period, GC analysis indicated that

59.8% product had formed with the major impurity being a higher molecular weight by-product. The product was obtained in higher purity (97.8% by GC) using standard distillation techniques at reduced pressure (16 mm Hg, 93 °C).

The ^{29}Si NMR spectrum of the purified $CH_2=CH(CH_2)_3OSi(Me)(OSiMe_3)_2$ was previously shown in Figure 6.12. As expected for pure $CH_2=CH(CH_2)_3OSi(Me)(OSiMe_3)_2$, there is a M-Si peak (δ 8.14, O<u>Si</u>M e$_3$) and a T-Si peak [δ -57.00 ppm, -O<u>Si</u>(Me)$(OSiMe_3)_2$] and the areas of these peaks are in the expected 2:1 ratio. The GPC of the purified $CH_2=CH(CH_2)_3OSi(Me)(OSiMe_3)_2$ (previously shown in Figure 6.13) shows the distilled product to be monodispersed with retention 18.66 minutes. GC/MS was also done and a molecular ion with mass 306 was found which confirmed the structure.

6.3.9 Synthesis of $(SiO_{3/2})_8$-$[(CH_2)_5OSi(Me)(OSiMe_3)_2]_8$

Into a 25 ml 3-neck, round bottom flask equipped with a thermometer, H_2O condenser, stir bar, and gas inlet tube to provide an air flow over the reaction mixture, 2.19 grams of $CH_2=CH(CH_2)_3OSi(Me)(OSiMe_3)_2$ (product from above synthesis, 7.2 mmol) and 0.30 grams of T_8 hydrogen silsesquioxane (0.7 mmol) were placed. An initial 20 µl of the tetramethyldivinyldisiloxane complex of Pt diluted in toluene to 1.0% Pt was added before heating the reaction mixture. The reaction mixture was heated to between 100 and 120 °C for approximately four hours during which time additional catalyst

solution (total of 100 µl) was added. The progress of the reaction was monitored by observation of the reduction of SiH via FTIR analysis. When the SiH peak at 2260 cm^{-1} was no longer observable, the reaction mixture was considered complete. The product was a viscous clear liquid with a yellow-brown color from the Pt catalyst.

The ^{29}Si NMR of the final product was previously shown in Figure 6.14. The NMR indicated the presence of a single sharp M-Si peak at δ 7.08 ppm for the -O<u>Si</u>M e_3 branch termini; a single sharp T-Si peak at δ -57.06 ppm for the silicon at the branch point of each appendage [CH_2O<u>Si</u>(Me)$(OSiMe_3)_2$]; and a T-Si peak at δ -66.74 ppm for the silicon of the cage ($O_{3/2}$<u>Si</u>CH_2). The ratio of the area of the M:T:T peaks was found to be 2:1:1 as expected if the reaction went cleanly. The GPC chromatogram (Figure 6.14) of the reaction product confirmed that the reaction resulted in a pure product as indicated by the monodispersed peak at retention time 16.53 minutes. Some residual CH_2=CH$(CH_2)_3OSi(Me)(OSiMe_3)_2$ was present in the chromatogram at approximately 18.7 minutes.

6.3.10 Synthesis of $HO(CH_2)_5Si(Me)(OSiMe_3)_2$

Bis(trimethylsiloxy)methylsilane [(H)Si(Me)$(OSiMe_3)_2$, 12.9 grams, 58.1 mmol, 98% pure by GC) and 5.0 grams of 4-penten-1-ol (58.1 mmol, 99% available from Aldrich Chemical Co., stored over molecular sieves) were placed in a 100 ml 3-neck, round bottom flask equipped with a thermometer, H_2O condenser, stir bar and gas inlet tube to provide an air flow over the reaction

mixture. An initial 20 µl of the tetramethyldivinyldisiloxane complex of Pt diluted in toluene to 1.0% Pt was added before heating the reaction mixture. The reaction mixture was heated to between 60 and 80 °C for approximately three and one-half hours during which time an additional 20 µl of catalyst solution (total of 40 µl) was added. The disappearance of the SiH peak at 2250 cm^{-1} in the FTIR spectrum was used to indicate the reaction was complete. GC analysis indicated the reaction mixture contained 70.0% product and a number of by-products. Vacuum distillation (135 °C, 2.5 mm Hg) was used to obtain a fraction that was 97.4% (by GC) desired product.

The ^{29}Si NMR of the purified $HO(CH_2)_5Si(Me)(OSiMe_3)_2$ was previously shown in Figure 6.18. The spectrum shows a single M-Si peak ($OSiMe_3$ branch termini) at δ 6.92 ppm and a single D-Si peak [$-CH_2-Si(Me)(OSiMe_3)_2$] at δ -21.42 ppm. The ratio of the areas of the M:D peaks is 2.0:1.0 as expected for a pure sample. The GPC chromatogram of the purified $HO(CH_2)_5Si(Me)(OSiMe_3)_2$ was shown in Figure 6.19. The chromatogram indicated the presence of the product peak at retention time 19.51 minutes. There were two other very small (<3% total area) higher molecular weight impurities as well. GC/MS was also done and a molecular ion with mass 308 was found which was consistent with the proposed structure.

6.3.11 Synthesis of $(SiO_{3/2})_8$-$[O(CH_2)_5Si(Me)(OSiMe_3)_2]_8$

The purified reaction product above ($HO(CH_2)_5Si(Me)(OSiMe_3)_2$, 1.77 grams, 5.7 mmol) and T_8 (0.30 grams, 0.7 mmol) were place in a 50 ml 3-neck, round bottom flask equipped with a thermometer, H_2O condenser, stir bar, and gas inlet tube. The reaction mixture was stirred and a light flow of dry N_2 was maintained over the reaction while 10 µl of N,N-diethylhydroxylamine (Et_2NOH, 99%, used as supplied by Aldrich Chemical Co.) catalyst was added. Vigorous gas evolution was observed immediately and an exotherm to a maximum temperature of 42 °C occurred within 6 minutes of adding the catalyst. Shortly after the exotherm, FTIR analysis indicated the absence of an SiH peak at 2260 cm^{-1}.

The ^{29}Si NMR of the reaction product previously shown in Figure 6.20 indicated that there was a M-Si peak for the O<u>Si</u>M e_3 branch termini at δ 7.04 ppm, a D-Si peak at δ -21.10 ppm for the branch point silicon [$-CH_2\underline{Si}(Me)(OSiMe_3)_2$] and a Q-Si peak at approximately δ -102.02 ppm assigned to the cage silicon ($O_{3/2}\underline{Si}OC$-). The Q-peak was actually a grouping of at least four not entirely resolved peaks between δ-102 and -102.6 ppm proposed to be due to some cage to cage condensation. The ratio of M:D:Q peak areas was found to be 3.1:1.6:1.0 instead of the expected 2:1:1 ratio due to a large excess of $HO(CH_2)_5Si(Me)(OSiMe_3)_2$ starting material used in the dendrimer synthesis.

The GPC chromatogram of the dendrimer reaction product (previously shown in Figure 6.21) also indicated that a large excess of $HO(CH_2)_5Si(Me)(OSiMe_3)_2$ was present in the final product. In addition to the peak at 19.53 minutes corresponding to the excess $HO(CH_2)_5Si(Me)(OSiMe_3)_2$, there were at least two peaks corresponding to the dendrimer reaction product due to a large amount of high molecular weight impurity most likely the result of the cage to cage condensations proposed earlier.

6.4 References

1. Gauthier, L.A.; Legrow, G.E. US Patent 4,239,867; December 3, 1980.

2. Janik, G.; Lo, P. US Patent 4,584,361; April 22, 1986.

3. Noll, W. Chemistry and Technology of Silicones, Academic Press: New York, 1968; pg. 397.

4. Suzuki, T.; Okawa, Tadashi *Polymer Communications* **1988**, 29, 225.

5. Suzuki, T. *Polymer* **1989**, 30, 333.

6. Bontems, S.L.; Stein, J.; Zumbrum, M.A. *J. of Polym. Sci., Part A: Polym. Chem.* **1993**, 31, 2697-2710.

APPENDIX A

Molecular Model Generation

In this thesis all colored molecular model figures were generated by the author on an Apple Macintosh computer using Chem3D Plus (version 3.1.2) software. The structural error for each model was minimized.

Colored Schematics

The colored schematics (4.16, Schematic of surface tension measurement technique, pg. 162; 4.17, A schematic of the bulk and surface behavior of a 'typical' or linear surfactant in aqueous solution, pg. 164; 4.18, An "idealized" plot of surface tension versus surfactant concentration showing the proposed behavior of a linear surfactant in each region, pg. 167) were drawn by the author on an Apple Macintosh computer using Canvas (version 3.5) software.

Plotted Data

Data was plotted by the author to generate graphs on an Apple Macintosh computer using Cricket Graph (version 1.3.2).